Università degli Studi di Ferrara

UCA Universidad de Cádiz

INTERNATIONAL DOCTORAL COURSE IN
EARTH AND MARINE SCIENCE
Cycle XXXIV
Coordinator Prof. Massimo COLTORTI

COMMON PLASTICS DEGRADATION IN COASTAL ENVIRONMENTS

Scientific Disciplinary Sector (SDS) GEO/09

Ph.D. Candidate:
Marzia RIZZO

Supervisor:
Prof. Carmela VACCARO

Years 2018/2022

Abstract

According to recent studies, only 9% of plastic waste is recycled, 12% incinerated and 79% is accumulated in landfills and dumps or littered in the environment. Once in the environment, plastic waste is degraded through factors working together or in sequence. They cause degradation, defined as a process that causes the material to lose its original properties and fragmentation.

In the environment, the main factors influencing the degradation of plastics are the type of polymer, abiotic processes, and biotic factors. Photodegradation, thermal degradation, oxidative degradation, hydrolytic degradation, and mechanical disintegration contribute to abiotic degradation; while biodegradation is a degradation process initiated or propagated by microorganisms such as bacteria, fungi, protozoa, algae, which act by mechanical, chemical and / or enzymatic means.

According to the literature reviewed, the environment where plastic waste from anthropogenic sources is subjected to environmental conditions that favor its degradation and the production of microplastics seems to be the coastal one.

In order to increase knowledge on the degradation of plastics in this environment, in situ experiments were conducted in sub coastal environments to test the degradation of six commonly used types of plastics and the possible factors responsible for the degradation were investigated. The degradation in the urban air environment has also been studied and compared with that in the coastal environment.

The types of plastic used were polystyrene (PS), polypropylene (PP), high density polyethylene (HDPE), low density polyethylene (LDPE), polyethylene terephthalate (PET) and polyvinyl chloride (PVC).

The sub-environments selected were a) a lagoon, a natural coastal environment with low hydrodynamic energy, b) a port environment, a heavily anthropized coastal environment with low hydrodynamic energy, and c) a fluvial environment near the mouth, a natural transition environment with low hydrodynamic energy. They have been identified in Italy, in Goro (Ferrara) and in the area of Siracusa.

Before proceeding with the experiment that forms the basis of this thesis, I participated in a similar but smaller scale experiment already started along the southern shore of the Choptank River, a tidal sub-estuary of the Chesapeake Bay, Maryland (USA). This experiment was performed using two types of plastics, HDPE and PS, to test how intertidal and subtidal exposure regimes under contrasting hydrodynamic, erosive versus depositional conditions, affected their fragmentation and degradation. Plastics were collected after environmental exposures at 4, 8, and 43 weeks and analyzed for change in mass, algal biofilm growth, and imaged by petrographic and electron microscopy (SEM-EDS). Significant surface erosion was evident on both polymers and was more rapid and more extensive with PS. Degradation of PS was responsive to intensity of hydrodynamic activity, and was greater at intertidal depths, highlighting the critical role played by photo-oxidation in the coastal zone, and suggesting that algal biofilms may slow degradation by playing a photo-protective role.

To proceed with the experiment, testing racks were built to allow the exposure of all types of plastics in the form of strips, so that they were individually traceable and equally exposed for each selected environment.

Once built, the testing racks were suitably installed in the Goro lagoon and in the “Porto Piccolo” of Siracusa at intertidal and subtidal depths, at the Ciane River in Siracusa, in semi-floating and submerged conditions, and on a terrace of a building at Siracusa.

Sampling of the plastic strips was performed after 4, 8, 12, 16, 20, 28 and 36 weeks of exposure in each environment.

At each sampling time point, total mass change and mass change after washing with hydrochloric acid were measured; from week 4 to week 28 samples chlorophyll *a* accumulation were measured. The 12- and 28-week exposure samples were also observed using the scanning electron microscope (SEM) and were subjected to leaching testing. Moreover, plastic strips exposed for 28 weeks in the lagoon and port environments were subjected to dissolution by acid attacks.

Subsequently, factorial ANOVA was performed individually for each environment to assess the influence of plastic type, depth zonation, and deployment time, on apparent plastic mass change, biofilm mass accumulation, and Chla accumulation. Furthermore,

ANOVA was performed for the data of apparent mass change, fouling mass and chlorophyll *a*, considering the factors of location, zonation, deployment time and plastic type for the port, lagoon and river environments.

The study showed that the rate of degradation and the type of degradation strongly depend on the environment to which the plastics were exposed. Greater UV radiation, higher temperatures and the absence of fouling are the causes that have led to greater degradation in the air environment than in the aquatic environment.

Among the aquatic environments tested in this study, the one that caused the greatest degradation is the port one, followed by the lagoon one and finally the river one. In the latter, however, no significant degradation was found.

The agents that contributed to the degradation are many: exposure to UV rays, environmental temperature, water salinity, accumulation of fouling, oxygen availability, hydrodynamic energy.

Beyond UV radiation, considered the most influential factor on degradation, fouling also played an important effect. In fact, it mainly carried out a role by shielding the plastic from UV radiation.

It was also seen how the degradation was influenced by the depth of deployment. In intertidal/semi-floating conditions, in fact, due to the greater UV radiation, the greater thermal stress and the greater hydrodynamic energy, the plastic strips have undergone greater degradation compared to the subtidal/submerged conditions.

The type of plastic also affected the rate of degradation. PS was the one most subject to degradation in all environments, showing mostly fragmentation. In the air environment, there was a greater degradation for PP, PET and PVC plastics and minimal degradation for LDPE and HDPE. In the lagoon and port environment, on the other hand, there was a greater degradation for PET and PVC and gradually decreasing for LDPE, HDPE, and PP. In the river environment, even if it was present differentiated by type of plastic, the degradation was not found significantly.

Leaching test and dissolutions did not produce relevant results.

Keywords: PS, PP, HDPE, LDPE, PVC, PET, plastic degradation, coastal environment, in situ experiment, environmental factors, UV radiation, fouling, zonation.

Riassunto

Secondo recenti studi, soltanto il 9% dei rifiuti plastici viene riciclato, il 12% incenerito e ben il 79% è accumulato in discariche o disseminato nell'ambiente. Una volta nell'ambiente, i rifiuti di plastica si degradano attraverso fattori che agiscono contemporaneamente o in sequenza. Essi causano degrado, definito come un processo che induce nel materiale perdita delle originarie proprietà e frammentazione.
Nell'ambiente, i principali fattori che influenzano il degrado della plastica sono il tipo di polimero, i processi abiotici e i fattori biotici. La fotodegradazione, la degradazione termica, la degradazione ossidativa, la degradazione idrolitica e la disintegrazione meccanica contribuiscono alla degradazione abiotica; mentre la biodegradazione è un processo di degradazione avviato o propagato da microrganismi come batteri, funghi, protozoi, alghe, che agiscono con mezzi meccanici, chimici e/o enzimatici.
Secondo la letteratura esaminata, l'ambiente in cui i rifiuti di plastica di origine antropica sono soggetti a condizioni ambientali che ne favoriscono il degrado e la produzione di microplastiche sembra essere quello costiero.

Al fine di incrementare la conoscenza sulla degradazione di plastiche in questo ambiente, sono stati condotti esperimenti in situ in sub ambienti costieri per testare la degradazione di sei tipologie di plastica comunemente usate e sono stati indagati i possibili fattori responsabili del degrado. È stato anche studiato il degrado in ambiente aereo urbano e messo a confronto con quello in ambiente costiero.
Le tipologie di plastica impiegate sono state polistirene (PS), polipropilene (PP), polietilene ad alta densità (HDPE), polietilene a bassa densità (LDPE), polietilene tereftalato (PET) e polivinilcloruro (PVC).
I sub ambienti selezionati sono stati a) uno lagunare, ambiente costiero naturale a bassa energia idrodinamica, b) uno portuale, ambiente costiero fortemente antropizzato a bassa energia idrodinamica e c) uno fluviale in prossimità della foce, ambiente naturale di transizione a bassa energia idrodinamica. Essi sono stati individuati in Italia, a Goro (Ferrara) e nell'area di Siracusa.

Prima di procedere con l'esperimento che sta alla base di questa tesi, ho partecipato a un esperimento simile ma su scala ridotta già iniziato lungo la sponda meridionale del fiume Choptank, un subestuario di marea della baia di Chesapeake, Maryland (USA). Questo esperimento è stato eseguito utilizzando due tipi di plastica, HDPE e PS, per testare in che modo i regimi di esposizione intertidale e subtidale in condizioni idrodinamiche contrastanti, erosive e deposizionali, influenzassero la loro frammentazione e degradazione. Le plastiche sono state raccolte dopo esposizioni ambientali a 4, 8 e 43 settimane e analizzate per il cambiamento di massa, crescita del biofilm algale e osservate mediante microscopia petrografica ed elettronica (SEM-EDS). Una significativa erosione superficiale era evidente su entrambi i polimeri ed era più rapida e più estesa su PS. La degradazione del PS rispondeva all'intensità dell'attività idrodinamica ed era maggiore alle profondità intertidali, evidenziando il ruolo critico svolto dalla foto-ossidazione nella zona costiera e suggerendo che i biofilm algali possono rallentare il degrado svolgendo un ruolo foto protettivo.

Per procedere con l'esperimento, sono stati costruiti "testing rack" per permettere l'esposizione di tutte le tipologie di plastica sotto forma di strisce, in modo che fossero identificabili singolarmente ed ugualmente esposte per ogni ambiente selezionato. Una volta costruiti, i testing rack sono stati adeguatamente installati nella laguna di Goro e nel Porto Piccolo di Siracusa a profondità intertidali e subtidali, presso il Fiume Ciane a Siracusa, in condizioni semi-galleggianti e sommersi, e su una terrazza di un palazzo a Siracusa.

Il campionamento delle strisce di plastica è stato effettuato dopo 4, 8, 12, 16, 20, 28 e 36 settimane di esposizione in ogni ambiente.

Per ogni intervallo di campionamento sono state misurate la variazione di massa totale e la variazione di massa dopo il lavaggio con acido cloridrico; per gli intervalli tra le 4 e le 28 settimane è stato misurato l'accumulo di clorofilla *a* sui campioni. I campioni che sono stati esposti per 12 e 28 settimane sono stati osservati anche utilizzando il microscopio elettronico a scansione (SEM) e sono stati sottoposti a test di lisciviazione. Inoltre, i campioni esposti per 28 settimane negli ambienti lagunari e portuali sono stati soggetti a dissoluzione con attacchi acidi.

Successivamente, è stata eseguita l'ANOVA fattoriale individualmente per ciascun ambiente per valutare l'influenza del tipo di plastica, della zonazione e del tempo di dispiegamento, sul cambiamento apparente di massa della plastica, sulla massa di fouling e sull'accumulo di clorofilla *a*. Inoltre, l'ANOVA è stata eseguita per i dati di cambiamento di massa apparente, massa del fouling e clorofilla *a*, considerando i fattori di posizione, zonazione, tempo di dispiegamento e tipo di plastica per gli ambienti portuale, lagunare e fluviale.

Lo studio ha dimostrato che il tasso di degrado e il tipo di degrado dipendono fortemente dall'ambiente in cui la plastica è stata esposta. Un maggiore irraggiamento UV, temperature più elevate e l'assenza di fouling sono le cause che hanno comportato un maggior degrado nell'ambiente aereo rispetto agli ambienti acquatici.

Tra gli ambienti acquatici testati in questo studio, quello che ha causato il maggior degrado è quello portuale, seguito da quello lagunare ed infine quello fluviale. In quest'ultimo non si è comunque riscontrato un degrado significativo.

Gli agenti che hanno contribuito al degrado in ambiente acquatico sono stati molteplici: esposizione ai raggi UV, temperatura ambientale, salinità dell'acqua, accumulo di fouling, disponibilità di ossigeno, energia idrodinamica.

Oltre la radiazione UV, considerato il fattore più influente sul degrado, anche il fouling ha svolto un importante effetto. Esso, infatti, ha svolto principalmente un'azione protettiva nei confronti della plastica verso le radiazioni UV.

Si è visto inoltre come la degradazione è stata influenzata dalla profondità di dispiegamento. In condizioni intertidali/semi-galleggianti, infatti, a causa del maggiore irraggiamento UV, del maggior stress termico e della maggiore energia idrodinamica le strisce di plastica hanno subito maggior degrado rispetto alle condizioni subtidali/sommerse.

Anche il tipo di plastica ha influenzato il tasso di degrado. Il PS è stato quello più soggetto a degrado in tutti gli ambienti, mostrando per lo più frammentazione. In ambiente aereo è risultato un maggiore degrado per le plastiche PP, PET e PVC e minimo per LDPE e HDPE. In ambiente lagunare e portuale invece è risultato un degrado maggiore per PET e PVC e via via decrescente per LDPE, HDPE e PP. In ambiente fluviale, seppur era

presente differenziato per tipologia di plastica, il degrado non è stato riscontrato in modo significativo.

I test di lisciviazione e le dissoluzioni, invece, non hanno prodotto risultati rilevanti.

Parole chiave: PS, PP, HDPE, LDPE, PVC, PET, degradazione della plastica, ambiente costiero, esperimento in situ, fattori ambientali, irraggiamento UV, fouling, zonazione.

Contents

List of tables

List of figures

Introduction

What are plastics?

The term “Plastics” is commonly used to describe a wide range of synthetic or semi-synthetic materials that are used in a huge and growing range of applications. Plastics are derived from natural materials such as cellulose, coal, natural gas, salt and crude oil. The production of plastics begins with the distillation of crude oil, through which the heavy crude oil is separated into groups of lighter components, called fractions. One of these fractions (mixture of hydrocarbon chains), naphtha, is the fundamental compound to produce plastics. (PlasticsEurope.org)

There are many different types of plastics, but they can be grouped into two main polymer families: thermoplastics and thermosets.

Thermoplastics are defined as polymers that can be melted and remelted almost indefinitely. They are melted when heated and harden upon cooling. When frozen, however, a thermoplastic becomes glass-like and prone to fracture. These characteristics, which give the material its name, are reversible, so the material can be heated, reshaped and frozen repeatedly. Consequently, thermoplastics are mechanically recyclable. Some of the more common types of thermoplastics are polypropylene, polyethylene, polyvinyl chloride, polystyrene, polyethylene terephthalate, and polycarbonate. (PlasticsEurope.org)

Thermosets are defined as polymers created by a crosslinking reaction, which promotes chemical bonding between macromolecular chains and creates a three-dimensional network (Marques, 2011). After their processing by means of heat and pressure, thermosets undergo variations that permanently modify their nature. Once the object is made with the designed shape, the material, if heated again, chars, unable to burn or change shape. Examples of thermosets are polyurethane (PUR), epoxy resins, unsaturated polyester, acrylic resins, vinyl ester, urea-formaldehyde, phenol-formaldehyde, phenolic resins, melamine resin, silicone.

A further classification of the main polymers, published by Rodriguez et al. (2016) and reported here, is based on the composition of their backbones, the chains of linked repeating units that make up the macromolecules, according to which they are distinguished in carbon-chain polymers or heterochain polymers (Figure 1). In carbon-chain polymers, the backbones are composed of linkages between carbon atoms; in heterochain polymers a number of other elements are linked together in the backbones, including oxygen, nitrogen, sulfur, and silicon. Among the carbon chain polymers are polyethylene (PE), polypropylene (PP), polystyrene (PS), polyvinyl chloride (PVC) and acrylic polymers. The information below has also been integrated with what is contained in the PlasticsEurope (2016) report.

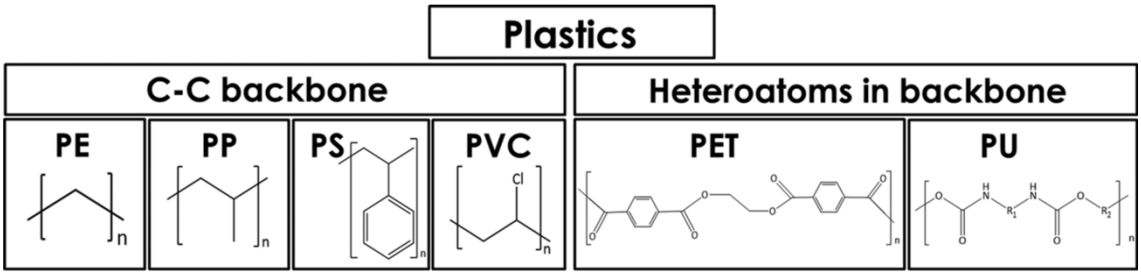

Figure 1: Structures of polymer types (modified from Gewert et al., 2015).

Polyethylene (PE)

Ethylene, produced by the cracking[1] of ethane gas, forms the basis for the largest single class of plastics, the polyethylenes. The ethylene monomer has the chemical composition $CH_2=CH_2$. This simple structure can be produced in linear or branched forms. Branched versions are known as low-density polyethylene (LDPE) and linear low-density polyethylene (LLDPE); the linear versions are known as high-density polyethylene (HDPE) and ultrahigh molecular weight polyethylene (UHMWPE).

LDPE is prepared from gaseous ethylene under very high pressures (up to 350 MP) and high temperatures (up to 350° C) in the presence of peroxide initiators. These processes yield a polymer structure with both long and short branches. As a result, LDPE is only partly crystalline, yielding a material of high flexibility. Its principal uses are in packaging

[1] Cracking is a petrochemical process in which saturated hydrocarbons are broken down into smaller hydrocarbons and it is the principal industrial method for producing ethylene and propylene.

film, trash and grocery bags, agricultural mulch, wire and cable insulation, squeeze bottles, toys, and housewares.

LLDPE is structurally similar to LDPE. It is made by copolymerizing ethylene with 1-butene and smaller amounts of 1-hexene and 1-octene. The resulting structure has a linear backbone, but it has short, uniform branches that, like the longer branches of LDPE, prevent the polymer chains from packing closely together. The main advantages of LLDPE are that the polymerization conditions are less energy-intensive and that the polymer's properties may be altered by varying the type and amount of comonomer. Overall, LLDPE has similar properties to LDPE and competes for the same markets.

HDPE is manufactured at low temperatures and pressures. The lack of branches allows the polymer chains to pack closely together, resulting in a dense, highly crystalline material of high strength and moderate stiffness. Uses include blow-molded bottles for milk and household cleaners and injection-molded pails, bottle caps, appliance housings, and toys.

UHMWPE is made with molecular weights of 3 million to 6 million atomic units, as opposed to 500,000 atomic units for HDPE. These polymers can be spun into fibers and drawn, or stretched, into a highly crystalline state, resulting in high stiffness and a tensile strength many times greater that of steel.

Polypropylene (PP)

Polypropylene is a highly crystalline thermoplastic resin built up by the chain-growth polymerization of propylene (CH_2=$CHCH_3$), a gaseous compound obtained by the thermal cracking of ethane, propane, butane, or the naphtha fraction of petroleum.

Only the isotactic form of polypropylene, where all the methyl (CH_3) groups are arranged along the same side of the polymer chain, is marketed in significant quantities. It is produced at low temperatures and pressures.

Polypropylene shares some of the properties of polyethylene, but it is stiffer, has a higher melting temperature, and is slightly more oxidation sensitive. A large proportion goes into fibers, where it is a major constituent in fabrics for home furnishings, rope and cordage, disposable nonwoven fabrics for diapers and medical applications, and

nonwoven fabrics for ground stabilization and reinforcement in construction and road paving.

Moreover, polypropylene is blow-molded into bottles for foods, shampoos, and other household liquids and it is also injection-molded into many products, such as appliance housings, dishwasher-proof food containers, toys, automobile battery casings, and outdoor furniture.

Polystyrene (PS)

This rigid, relatively brittle thermoplastic resin is polymerized from styrene (CH_2=CHC_6H_5). Styrene is obtained by reacting ethylene with benzene in the presence of aluminum chloride to yield ethylbenzene, which is then dehydrogenated to yield clear, liquid styrene. The presence of the pendant phenyl (C_6H_5) groups is key to the properties of polystyrene. These large, ring-shaped groups prevent the polymer chains from packing into close, crystalline arrangements, so that solid polystyrene is transparent. In addition, the phenyl rings restrict rotation of the chains around the carbon-carbon bonds, thus lending the polymer its noted rigidity.

Foamed polystyrene is made into insulation, packaging, and food containers. Solid polystyrene products include injection-molded eating utensils, audiocassette holders, and cases for packaging compact discs.

More than half of all polystyrene produced is blended with 5 to 10 percent polybutadiene to reduce brittleness and improve impact strength.

Polyvinyl chloride (PVC)

Second only to PE in production and consumption, PVC is manufactured by bulk, solution, suspension, and emulsion polymerization of vinyl chloride monomer. Vinyl chloride (CH_2=$CHCl$) is most often obtained by reacting ethylene with oxygen and hydrogen chloride.

Pure PVC finds application in the construction trades, where its rigidity and low flammability are useful in pipe, conduit, siding, window frames, and door frames. In combination with plasticizer (sometimes in concentrations as high as 50 percent), it is familiar to consumers as floor tile, garden hose, imitation leather upholstery, and shower curtains.

Acrylic polymers

Acrylic is a generic term denoting derivatives of acrylic and methacrylic acid, including acrylic esters and compounds containing nitrile and amide groups. Examples of acrylic polymers are polyacrylonitrile (PAN), employed in acrylic fibers, also used as precursors to produce carbon and graphite fibers, as replacements for asbestos in cement, and in industrial filters and battery separators; and the polymethyl methacrylate (PMMA), a substitute for glass, used in internally lighted signs, swimming pool enclosures, aircraft canopies, instrument panels, and luminous ceilings.

There are also fluoropolymers, fluorocarbon-based polymers with multiple carbon – fluorine bonds, dienes, compounds whose molecules contain two carbon-carbon double bonds separated by a single bond, and copolymers, polymers derived from more than one species of monomer.

A wide variety of heterochain polymers, that is polymers in which the backbone contains elements such as oxygen, nitrogen, sulfur, or silicon in addition to carbon, are in commercial use. Many of these compounds are complex in structure. The major heterochain polymer families are:

- Aldehyde condensation polymers: compounds produced by the reaction of formaldehyde with phenol, urea, or melamine. The polymerization reactions of these monomers produce complex, thermosetting network polymers.
- Cellulosics: cellulose ($C_6H_7O_2[OH]_3$) is a naturally occurring polymer made up of repeating glucose units. In its natural state (known as native cellulose), it has long been harvested as a commercial fiber - as in cotton, flax, hemp, kapok, sisal, jute, and ramie. Although it is a linear polymer, cellulose is thermosetting; that is, it forms permanent, bonded structures that cannot be loosened by heat or solvents without causing chemical decomposition.
- Polyamides: a polyamide is a polymer that contains recurring amide groups (R—CO—NH—R') as integral parts of the main polymer chain. Synthetic polyamides are produced by a condensation reaction between monomers, in which the linkage of the molecules occurs through the formation of the amide

groups. The most important amide polymers are the nylons, an extremely versatile class of material that is an indispensable fiber and plastic, and aramids.

- Polyesters: polymers made by a condensation reaction taking place between monomers in which the linkage between the molecules occurs through the formation of ester groups. The major industrial polyesters include polyethylene terephthalate, polycarbonate, degradable polyesters, alkyds, and unsaturated polyesters.

  Polyethylene terephthalate (PET)

  PET is produced by the step-growth polymerization of ethylene glycol and terephthalic acid. The presence of the benzene rings in the repeating units gives the polymer stiffness and strength. In the semicrystalline form, PET is made into a high-strength textile fiber. The stiffness of PET fibers makes them highly resistant to deformation, so that they impart excellent resistance to wrinkling in fabrics. PET is also made into fiber filling for insulated clothing and for furniture and pillows. It is used in artificial silk and in carpets. Among the industrial applications of PET are automobile tire yarns, conveyor belts and drive belts, reinforcement for fire and garden hoses, seat belts, nonwoven fabrics for stabilizing drainage ditches, culverts, and railroad beds, and nonwovens for use as diaper top sheets and disposable medical garments. PET is the most important of the man-made fibers in weight produced and in value. At a slightly higher molecular weight, PET is made into a high-strength plastic that can be shaped by all the common methods employed with other thermoplastics. Molten PET can be blow-molded into a transparent container of high strength and rigidity that also possesses good impermeability to gas and liquid. In this form PET has become widely used in carbonated-beverage bottles and in jars for food processed at low temperatures. It is the most widely recycled plastic.

- Polyethers: polymers that are formed by the joining of monomers through ether linkages - i.e., two carbon atoms connected to an oxygen atom. A variety of polyethers are manufactured, ranging from engineering plastics to elastomers. Among them are polyacetal and epoxy resins.

- Polyimides: polymers that usually consist of aromatic rings coupled by imide linkages, that is, linkages in which two carbonyl (CO) groups are attached to the same nitrogen (N) atom. They are used in aircraft components, sporting goods, electronics components, plastic films, and adhesives.
- Polysiloxanes (silicones): polymers whose backbones consist of alternating atoms of silicon and oxygen. They can exist as elastomers, greases, resins, liquids, and adhesives.
- Polysulfides: polymers that contain one or more groups of sulfur atoms in their backbones. They fall into two types: compounds containing a single sulfur atom per repeating unit and compounds containing two or more.
- Polyurethanes: polymers that are transformed into flexible and rigid foams, fibers, elastomers, and surface coatings with a variety of uses. They are used in upholstery, insulation, packaging, for garments with high elasticity requirements, for automobile parts and industrial tools.

The history of plastic

Humans have already been using real natural polymers such as amber, tortoise shell or horn since prehistoric times. The modern history of plastic is traced back to the 19th century (1861-62) (Painter and Coleman, 2008), when the Englishman Alexander Parkes isolated and patented the first semi-synthetic plastic material, which he named Parkesine (UK Patent office, 1865), better known as Xylonite.[2]

The first real affirmation of the new material occurred when, in 1870, the Hyatt Brothers patented a process of making a "horn-like material" with the inclusion of cellulose nitrate and camphor (Staudinger, 1920; Jensen, 2008). This material was unsuitable for being worked with high temperature molding techniques, as it was highly flammable. Therefore, the addition of camphor led to the first modified thermoplastic polymer, which was used for celluloid films.

In the early 1900s, the Belgian chemist Leo Baekeland obtained, by condensation between phenol and formaldehyde, the first thermosetting resin of synthetic origin which he patented in 1910 with the name of Bakelite: the new material quickly became the most and used plastic material for many years (Bowden, 1997; Amato, 1999).

Used as the basis for Bakelite, phenol formaldehyde resins (PF) or phenolic resins were the first commercial synthetic resins (plastics). The successful use of PF resin catalyzed the development of other polycondensation products based on formaldehyde with urea and melamine, known as amino resins, aminoplasts or aminoplastics (Feldman, 2008).

[2] Polymers are the basis of important industrial goods. Their rapid growth is caused, in addition to social factors, by the need to replace classic materials. The term was coined in 1833 by Jöns Jacob Berzelius, though with a definition distinct from the modern IUPAC definition. (Jensen, 2008)
The modern concept of polymers as covalently bonded macromolecular structures was proposed in 1920 by Hermann Staudinger, who demonstrated the existence of macromolecules, which he characterized as polymers (Staudinger, 1920). For this work he received the 1953 Nobel Prize in Chemistry.
Many examples of synthetic polymers can be cited, some everyday, such as polyester or nylon stockings, others less known as those used for medical applications, for organs, sutures, degradable, etc.
Polymers initially tended to be seen as a chemical specialty, but now they are strongly associated as plastics, fibers and elastomers also with engineering through the design, manufacture and testing of products.
The last few decades have shown increasing importance in the polymer industry: it is the rapid development and introduction of new and improved products.

After a few years, in 1912, it was the turn of the first flexible, transparent, and waterproof material, Cellophane (Carlisle, 2004), which immediately found application in the field of packaging, being a cellulose-based material produced in very thin and flexible sheets.

In the 1930s, we moved on to the "adulthood" of plastic with the creation of a real modern industry with new production techniques such as molding and with a new raw material, oil (Corepla.it).

Another creation of the period is Nylon, a polyamide synthesized by Wallace Carothers (Acs.org; Sciencehistory.org), a material that will find several applications thanks to its characteristics that make it absolutely functional for the textile industry: the rise of "synthetic fibers" begins.

Polystyrene terephthalate (PET) is then patented by John Rex Whinfield and James Tennant Dickson at the Calico Printers' Association in Manchester (Whinfield and Dickson, 1941). This polyester is still widely used today in the production of artificial textile fiber, fleece, and has been used to patent PET bottles as carbonated beverage containers, still used today for its impact resistance and transparency, for the packaging of mineral waters and soft drinks (Wyeth and Roseveare, 1973).

At the beginning of the Second World War, to find substitutes for natural products, polyurethanes were developed to replace rubber and the first chloride-vinyl acetate (PVC) copolymers were industrialized (Seymour and Kauffman, 1992).

The original discovery leading to the world-wide interest in all classes of polyurethanes (PU) was made by Bayer and his co-workers in 1937; years later he published an impressive account of the synthesis of PU and polyureas (Feldman, 2008).

In the 1950s the basic technology used polyesters to obtain the flexible foams (Oertel, 1985). Later on, PUs were found to be useful for the production of plastics, elastomers, foams, adhesives, fibers and corrosion-resistant coatings (Klempner and Frish, 1991; Hepburn, 1992).

These are the years that saw the discovery of melamine-formaldehyde resins, known on the market as Formica, which enabled the production of laminates for furnishings and low-priced crockery and the first boom of "synthetic fibers" (polyester, nylon), valid alternative to natural fibers. Also, in this period Polyethylene is on the rise, one of the most widely used plastic materials in the world thanks to its higher melting point which allows applications previously unthinkable, and Giulio Natta, in 1954, discovers isotactic Polypropylene following its studies on ethylene polymerization catalysts that earned him the Nobel Prize in 1963 together with the German Karl Ziegler, who had isolated the polyethylene. Polypropylene will be industrially produced under the "Moplen" brand (Corepla.it).

It is from here on that plastic established itself as a "new frontier" in all fields of fashion, design, art, helping to create the modern lifestyle.

The following decades are those of the great technological growth, of the progressive affirmation for increasingly sophisticated and unthinkable applications, thanks to the development of the so-called "engineering plastic". Each engineering plastic usually has a unique combination of properties that may make it the material of choice for some application, for example highly resistant to impact, highly resistant to abrasion, heat resistance, mechanical strength, rigidity, chemical stability, self-lubrication (International Association of Plastics Distributors).

According to an analysis by Geyer et al. (2017), nowadays the most common resins and fibers are: high density polyethylene (HDPE), low density polyethylene (LDPE), polypropylene (PP), polystyrene (PS), polyvinyl chloride (PVC), polyethylene terephthalate (PET) and PUR resins (Figure 2).

The most widely used plastics in total nonfiber plastics production are PE (36%), PP (21%), and PVC (12%), followed by PET, PUR, and PS (<10% each) (Geyer et al., 2017). Polyester, most of which is PET, accounts for 70% of all PP&A fiber production. Together, these seven groups account for 92% of all plastics ever made. Approximately 42% of all nonfiber plastics have been used for packaging, which is predominantly composed of

PE, PP, and PET. The building and construction sector, which has used 69% of all PVC, is the next largest consuming sector, using 19% of all nonfiber plastics.

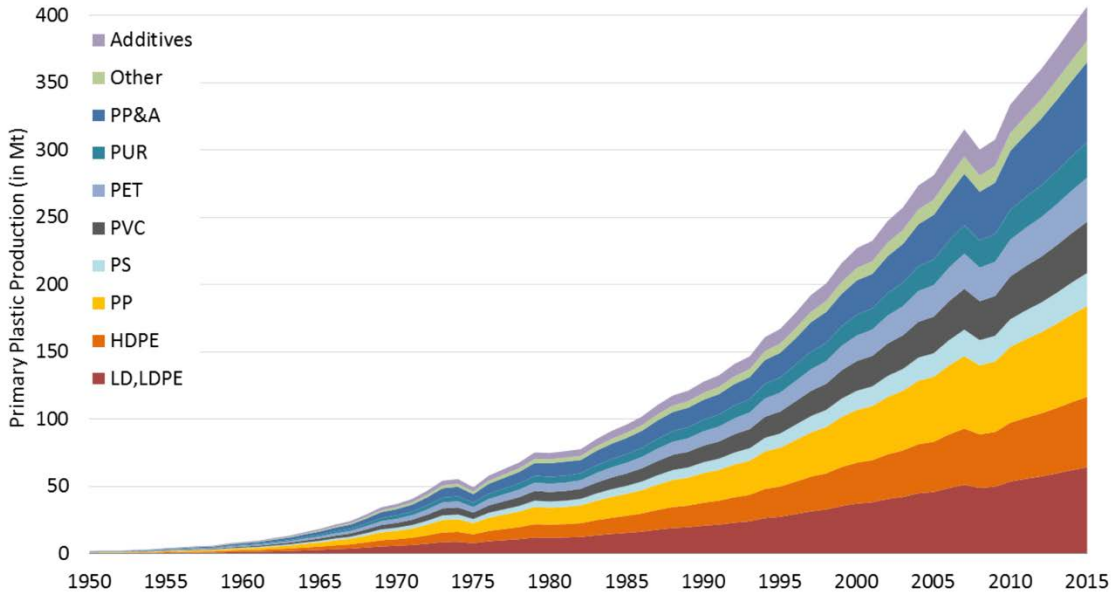

Figure 2: Global primary plastics production (in million metric tons) according to polymer type from 1950 to 2015 (from Geyer et al., 2017).

In recent years, a very current topic in the field of plastics are so-called bioplastics, however an ambiguous term. According to European Bioplastic, a plastic material is defined as a bioplastic if it is either biobased, biodegradable, or features both properties (European-bioplastics.org, Figure 3). This means that a bioplastic can derive:

- from biomass, partially or entirely, and not be biodegradable (for example: bio-PE, bio-PP, bio-PET),
- from non-renewable raw materials, entirely, and be biodegradable (for example: polybutylene adipate terephthalate (PBAT), polycaprolactone (PCL), polybutylene succinate (PBS)),
- from biomass, partially or entirely, and be biodegradable (for example: PLA, PHA, PHB, starch-based plastics).

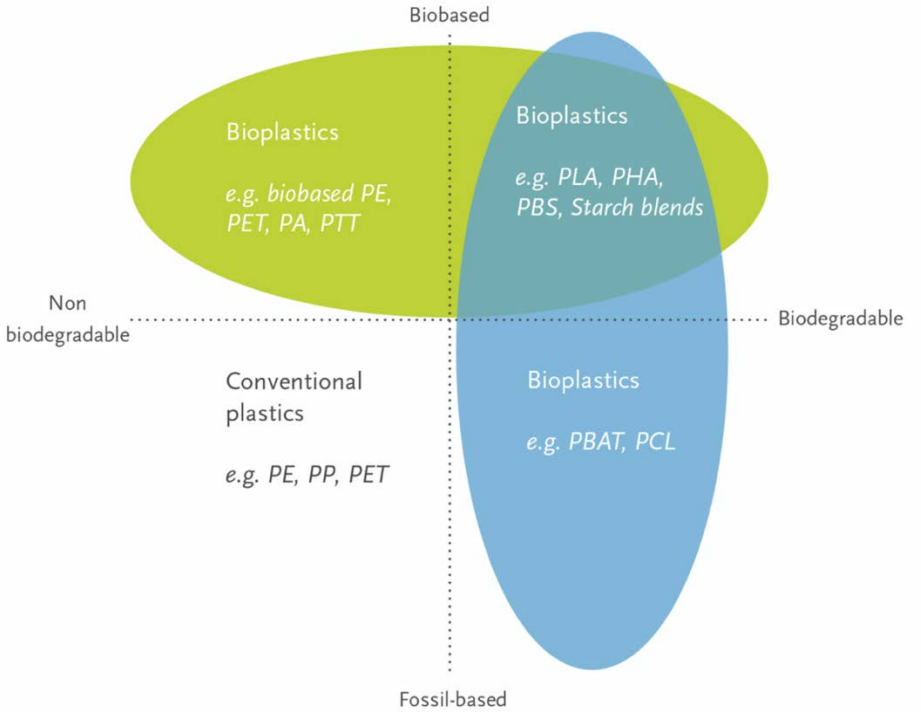

Figure 3: Definition of bioplastics according to European Bioplastic (from https://www.european-bioplastics.org/bioplastics/).

In contrast, according to the definition given by Assobioplastiche, bioplastics are those materials and manufactured products, both from renewable and fossil-based sources, which have the characteristic of being biodegradable and compostable. Therefore, Assobioplastiche suggests not to include in bioplastics those deriving (partially or entirely) from biomass which are not biodegradable and compostable, rather indicating them with the name "vegetable plastics" (Assobioplastiche.org).

Currently, the only European standard that specifies what is meant by "biodegradable plastic" is EN 13432:2000, dedicated to compostable packaging, adopted in Italy with the name of UNI EN 13432:2002, which determines the criteria for compostability of a given bioplastic in an industrial composting plant, at temperatures of about 55-60 °C, with a certain level of humidity and in the presence of oxygen: conditions much more suitable for biodegradation than natural biodegradation conditions in the soil, in freshwater or in a marine environment.

Degradation of plastics

According to Geyer et al. (2017), as of 2015, approximately 6300 Mt of plastic waste had been generated, around 9% of which had been recycled, 12% was incinerated, and 79% was accumulated in landfills and dumps or littered in the environment (Figure 4).

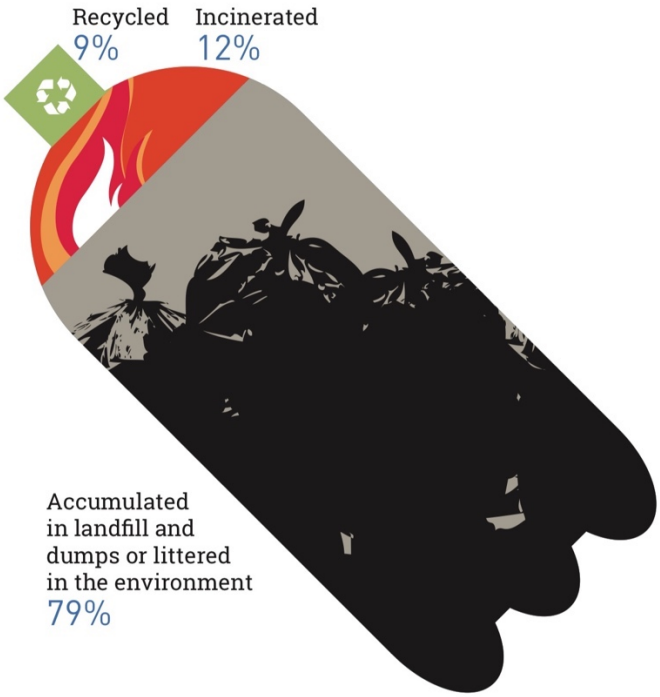

Figure 4: Disposal of all plastic waste ever generated, as of 2015 (from UNEP, 2018).

Once in the environment plastic waste is degraded through abiotic or biotic factors working together or in sequence; these processes cause the disintegration of the polymer matrix, with the consequent formation of fragmented particles of various sizes (Lambert et al., 2014).

The American Society for Testing and Materials (ASTM) and the International Organization for Standardization (ISO) define degradation as ‘‘an irreversible process leading to a significant change of the structure of a material, typically characterized by a loss of properties (e.g. integrity, molecular weight, structure or mechanical strength) and/or fragmentation. Degradation is affected by environmental conditions and proceeds over a period of time comprising one or more steps’’ (ISO, 2013; ASTM, 2019). When plastics are exposed to an energetic environment characterized by an energy level

comparable to the energy values of the chemical bonds of the atoms constituting the polymer, the macromolecular architecture collapses with consequent fragmentation and the onset of degradation (Krzan et al., 2006).

The plastic degradation process includes two phases, disintegration, and mineralization (Figure 5); disintegration, the first stage that intervenes, is associated with the deterioration of physical properties, such as discoloration, embrittlement and fragmentation. The second stage is defined as the conversion of the plastics (whole or fragments) into CO_2 and water under aerobic conditions or into CH_4 under anaerobic conditions (Krzan et al., 2006). A small fraction of the plastic carbon may additionally be incorporated into microbes as biomass.

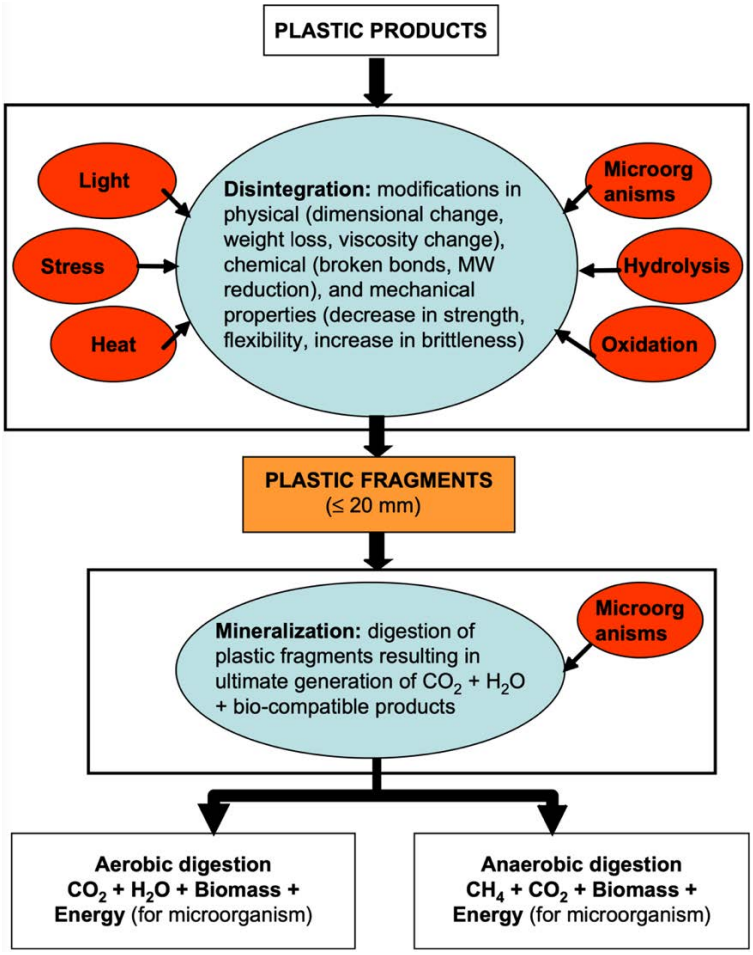

Figure 5: Schematic representation of plastics degradation processes in the environment (from Krzan et al., 2006).

In the environment, the main factors influencing the degradation of plastics are the type of polymer, abiotic processes, and biotic factors. Polymer characteristics play an important role in the degradation rate of plastics (Lambert et al., 2014). Molecular composition also affects the hydrophobicity of the polymer surface, which affects the ease with which microorganisms can attach themselves (Albertsson and Karlsson, 1993). The complexity of a specific polymer structure and composition can affect the overall degradability by directly affecting the accessibility of enzymes (Artham and Doble, 2008). The composition also affects the sensitivity of a polymer to photodegradation (Kaczmarek et al., 2007).

Photodegradation, thermal degradation, oxidative degradation, hydrolytic degradation, and mechanical disintegration contribute to abiotic degradation. Photodegradation involves a gradual reaction with atmospheric oxygen in the presence of light for most polymers. The photodegradation mechanism provides for the absorption of UV light with consequent generation of free radicals. An auto-oxidation process then occurs which leads to the possible disintegration of the plastic (Ammala et al., 2011). Under conditions typically encountered by plastics that have escaped the waste stream, photodegradation is one of the most important parameters (Lucas et al., 2008). The photooxidative degradation caused by UV radiation causes the breakdown of the polymer chains, produces free radicals, and reduces the molecular weight, causing the deterioration of the mechanical properties (Yousif and Haddad, 2013). Thermal degradation is the molecular deterioration of a polymer because of over-heating, which causes bond scissions of the main polymer chain (Lambert et al., 2014). Chiellini et al. (2006), experimenting the degradation at temperatures of 55°C and 70°C, demonstrate that the rate of thermal degradation depends upon the temperature, with higher values achievable at higher temperatures. The rate of thermal oxidation is slow at ambient temperatures (Ammala et al., 2011). The oxidation process consists in the reaction of the oxygen present in the air with the polymer. The incorporation of oxygen, which attacks covalent bonds, into the carbon chain polymer backbone leads to the formation of hydroxyl and carbonyl functional groups, which aid subsequent breakdown by biotic processes (Lambert et al., 2014). The oxidation of the carbon backbone of the polymer

results in the formation of smaller molecular fragments. The oxidative degradation depends on the polymer structure and involves changing the hydrophobic to hydrophilic behavior of the plastic allowing the fragmented polymer to absorb water (Lucas et al., 2008). Hydrolysis consists in the breaking of the bonds present in the polymer chains of the plastic due to the effect of a water molecule, but to be split by H_2O, the polymer must contain hydrolysable covalent bonds, and it depends on parameters such as temperature, pH, water activity and time (Lucas et al., 2008). Mechanical disintegration involves the application of shear forces to break the plastics apart. This process differs from degradation as the molecular bonds of the materials remain unchanged (Lambert et al., 2014). Mechanical disintegration is due, for example, to cycles of freezing and thawing, pressure following burial, water or wind turbulence, damage caused by animals.

Abiotic processes act as a first step in the degradation of plastics as they involve a loss of mechanical properties and structural changes in the molecular bonds of materials that promote greater accessibility to moisture and oxygen and greater susceptibility to microbial activity (Roy et al. 2008; Kijchavengkul et al., 2010; Lambert et al., 2014).

Biodegradation is a degradation process initiated or propagated by microorganisms such as bacteria, fungi, protozoa, algae (Wallström et al., 2005), which act by mechanical, chemical and / or enzymatic means (Gu, 2003). During the biodegradation phase, most of the abiotic oxidation products (low molecular weight compounds) are used by microorganisms (Ammala et al., 2011). The biodegradation process is strongly influenced by the constitution and the properties of polymer materials, the quantities, and available types of microorganisms and their microbial activities, which are sensitive to environmental parameters such as temperature, humidity, pH, C/N ratio and amount of oxygen available (Lugauskas et al., 2003; Krzan et al., 2006; Lucas et al., 2008).

Environmental degradability of plastics is a multifaceted complex process that is strongly influenced by the nature of the plastics as well as biotic and abiotic conditions to which they are exposed (Krzan et al., 2006).

Degradation of plastics can be assessed by measuring changes in physical appearance, molecular weight, amount of carbon-dioxide evolved and by enumeration of microbial growth on polymer surface after exposure to natural environments such as soil, compost, fresh water/seawater and sewage-sludge (Ammala et al, 2011).

Plastic debris in the environment and negative impacts

The countless uses and low degradation rates of plastics have resulted in the accumulation of plastics of various sizes in the environment. The first articles reporting the presence of plastic debris in the marine environment were Carpenter and Smith (1972), Carpenter et al., (1972) and Colton et al. (1974) published in the early 1970s. The last decade has seen an annual increase in publications attesting to the increase in environmental contamination by plastic. Plastic fragments and microplastics are globally distributed, and by now can be found in potentially all earth surface habitats, including polar regions (Barnes et al., 2010; Waller et al., 2017; Anfuso et al., 2020), ice (Peeken et al., 2018), soil (Nizzetto et al., 2016; Bläsing and Amelung, 2018), lakes (Zbyszewski and Corcoran, 2011; Zbyszewski et al., 2014; Eriksen et al., 2013; Free et al., 2014), rivers (Gasperi et al., 2014; Lechner et al., 2014; Sadri and Thompson, 2014), ocean gyres (Thiel et al., 2018; Bouhroum et al., 2019), deep sea (Van Cauwenberghe et al., 2013), beaches (Costa et al., 2010; Lee et al., 2013; Garcés-Ordóñez et al., 2020), nearshore environments (Ho and Not, 2019; Compa et al., 2020), water column (Rowley et al., 2020), seafloor (Woodall et al., 2014; Courtene-Jones et al., 2020), and surface waters (Pojar et al., 2020; Zhang et al., 2020).

Use of single-use plastic products and improper waste management are the two main causes of the release of plastic debris into the environment. Due to degradation and weathering, macroplastics produce so-called secondary microplastics and nanoplastics. The term microplastics defines plastic particles with a diameter of less than 5 mm (Andrady 2011; GESAMP, 2015). It includes both primary microplastics, manufactured as microplastics, and secondary microplastics, a consequence of degradation (Cole et al. 2011). The term nanoplastics, instead, defines particles unintentionally produced and presenting a colloidal behavior, within the size range from 1 to 1000 nm (Gigault et al., 2018).

Plastic debris can cause injuries to a wide range of marine vertebrate species and represent an ecotoxicology threat to food webs, as well as to human health, in particular in aquatic environments (Sharma and Chatterjee, 2017; Wright and Kelly, 2017; Akdogan

and Guven, 2019; Mancia et al., 2020). The injuries are due both to the fact that the animals become entangled in the debris, resulting in lacerations, ulcers, reduced ability to move, suffocation or drowning and to ingestion, which in turn causes both internal lacerations and toxicological effects. Because of their shape and color, plastic debris is often mistaken for food and ingested by marine organisms, such as turtles (Petri et al., 2021), whales (Im et al., 2020), sharks (Bernardini et al., 2021), marine birds (Zhu et al., 2019), fishes (Kühn et al., 2020), etc.

It has been shown that some zooplankton are also able to filter microplastic particles from the water column and ingest them (Katija et al., 2017). Once ingested, microplastics can also move and remain trapped in the tissues, causing accumulation over their lifetimes (Moore et al., 2001). The accumulation of plastics in animals can also increase up the food pyramid, as animals with microplastic loads are consumed by other animals which retain these particles (Chae et al., 2018; Athey et al., 2020).

A consequence of ingesting plastic is the leaching of toxic chemicals into organisms. These chemicals can be contained directly in the plastic because of production processes or can be absorbed during the period of stay in the environment. In fact, given the high capacity of the plastics to sorb contaminants, plastics may be an important vehicle for transporting contaminants to organisms (Teuten et al., 2007). Furthermore, according to a research by Bakir et al. (2014), chemicals absorbed by plastic particles are released much faster in intestinal conditions than in seawater, due to a more acidic pH and higher temperature environment.

EU directives and law decrees

Among the reasons why the institutions push for the separate collection of plastic it is possible to include its slow degradability, due to which there is an increasing accumulation of plastic waste in the environment. Objects made of polyethylene or polyvinyl chloride abandoned in the environment, then exposed to environmental conditions, for example, take between hundreds and thousands of years to degrade. The disposal of plastic can be done through its recovery or recycling, from which it is possible to obtain new products, even if of lower quality than the original ones, energy, heat, and electricity.

In Europe, a series of regulations that aim to incentivize plastic recovery and recycling practices regulate the recycling of plastic. These have the objective of saving resources, limiting emissions of polluting gases, safeguarding the environment, and protecting public health.

European regulations on plastic recycling aim to reduce CO_2 emissions and limit the production of single-use plastic products. The European Union aims both to reduce the amount of waste produced and to encourage their recycling, to allow the plastic eliminated to have a second life. Achieving these objectives would move from a linear economy, based on the extraction of raw materials, the production of goods, the consumption of products and finally the disposal of waste, to a circular economy, in which waste become a raw material for further production cycles. The European directives on waste management and plastic recycling were approved on 30 May 2018 and the main ones are 2018/850/EU, 2018/851/EU, 2018/852/EU, respectively concerning landfills, treatment of waste and packaging. Regarding plastics, these regulations establish that all European states must recycle at least 65% of packaging by 2025 and 70% by 2030. Other regulations, approved in 2019, stipulate that by 2021 the production of some disposable plastic products such as plates, cutlery and straws must be stopped; plastic bottles must be collected separately from other types of plastic waste; from 2025, all plastic bottles will have to contain at least 25% recycled plastic and by 2030 at least 30%.

The Italian laws on plastic recycling refer to European regulations. From 2006 to 2020, the Legislative Decree 152/2006 called "Environmental Code" was in force which, in the part relating to waste management, established that the approach to waste must focus on its correct management and recycling and not only on processes disposal in landfills and that it is necessary to aim at the prevention of waste production, preparation for reuse, recycling, energy recovery and, ultimately, disposal. In September 2020, the New Environmental Code was approved, Legislative Decree 116/2020, which indicates the recycling objectives that Italy aims to achieve within the next few years, including the recycling of 50% of plastic packaging by 2025 and 55% by 2030. Furthermore, this Code discourages the use of plastics and other non-recyclable materials, provides tax relief for companies that purchase products made with recycled plastic, paper or aluminum and encourages the purchase of biodegradable and compostable packaging. Italian companies are also invited to limit the use of single-use products and to adopt separate collection systems.

In addition to national laws, there are also regulations drawn up by the UNIPLAST technical commission, which deals with the development of projects to be sent to UNI for control and subsequent publication as Technical Standards, Technical Specifications and Technical Reports. These standards have the purpose of classifying plastics obtained from the recovery and recycling of waste, called primary-secondary plastics, and establish the requirements that these materials must have, the methods for their recycling and the possible uses after recycling.

Aims and objectives

As early as 1972, just a century after the patent for the process of making a "horn-like material", Carpenter and Smith predicted that the increase in plastic production combined with waste disposal practices at the time would increasingly sharpen the problem of the presence of plastic waste in the marine environment. The forecast was unfortunately confirmed by reality. Furthermore, according to the literature reviewed, including Biber et al. (2019), the marine environment where plastic waste from anthropogenic sources is subjected to environmental conditions that favor its degradation and the production of microplastics seems to be the coastal one.

The study aims to advance current knowledge on the degradation of plastics in the coastal environment by testing their degradation and providing a comparison, with isochronous exposure, between coastal sub-environments, a lagoon environment (natural coastal environment with low hydrodynamics), a port environment (coastal environment strongly anthropized environment with low hydrodynamics), a fluvial environment near the river mouth (natural transition environment with very low hydrodynamics), contrasting them with an urban air environment and investigating the possible responsible factors.

This PhD thesis therefore proposes to analyze and quantify the degradation of six types of commonly used plastics, polystyrene (PS), polypropylene (PP), high-density polyethylene (HDPE), low-density polyethylene (LDPE), polyethylene terephthalate (PET) and polyvinyl chloride (PVC), in different coastal environments and at different deployment depths.

For this purpose, testing racks were built to allow the exposure of all types of plastics, in the form of strips, so that they were individually traceable and equally exposed for each selected environment.

The following hypotheses were therefore tested:

1) the rate of degradation during environmental exposure differs between different environments (river vs lagoon vs port vs air);

2) the degradation rate during environmental exposure differs between types of plastics (PS vs PP vs HDPE vs LDPE vs PVC vs PET);
3) the degree of degradation of the plastic is influenced by the exposure time;
4) the rate of plastic degradation is affected by water depth (subtidal/submerged vs intertidal/semi-floating);
5) the fouling that accumulates on the plastic affects the deterioration of the polymers.

Furthermore, through leaching and dissolution tests, an attempt was made to evaluate whether the plastics with the relative accumulated fouling could adsorb any inorganic compounds from the surrounding environment, as happens with organic pollutants, and if, in case of imbalance with a new environment, they could release them again.

Test sites

Plastic pollution mainly affects the coastal environment. However, it has not been clarified how the boundary conditions of the sub-environments affect the degradation of plastics. I therefore chose coastal sub-environments (river, lagoon, port) with different characteristics (energy, salinity, UV radiation, anthropic impact) to study the degradation of commonly used plastics simultaneously and compare it with the degradation in the air environment.

The sub-environments chosen were identified in the Goro Lagoon in Ferrara and in the Porto Piccolo and in the Ciane River in Siracusa (Figure 6). Due to the availability and accessibility of spaces, the air environment has also been identified in Siracusa.

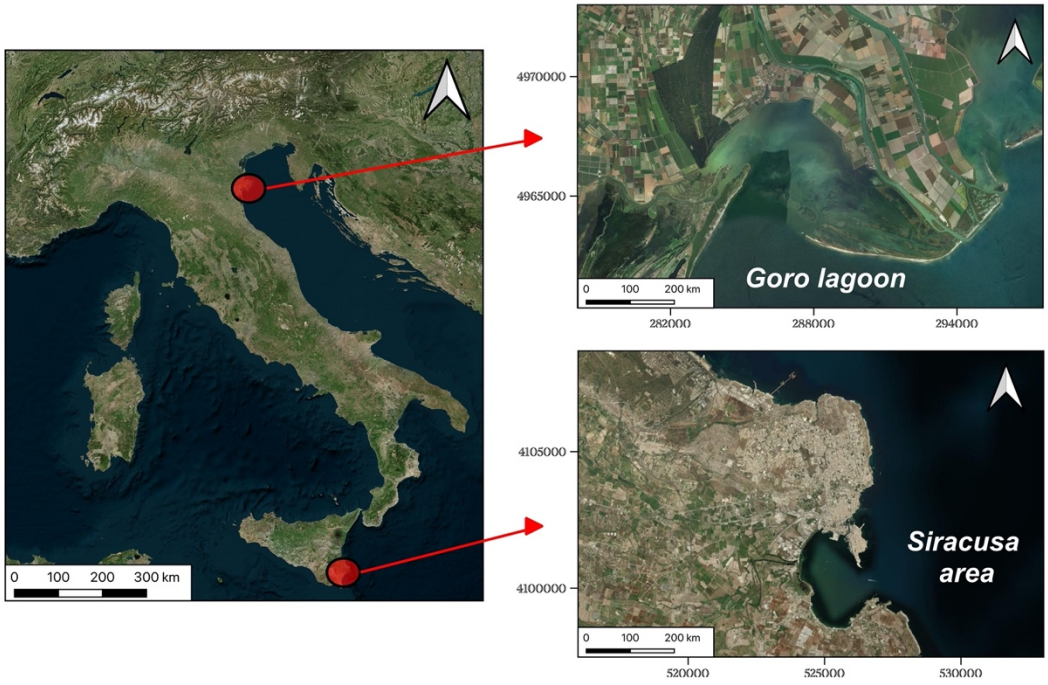

Figure 6: Location of the areas identified to carry out the experiment.

Siracusa framework

Geographical setting

Siracusa is located in the coastal area of southeastern Sicily, and it extends for about 2110 km^2 (Regione Siciliana, 1998). It is bordered to the north by the plain of Catania, to the east and south by the Ionian Sea and to the west by the natural barrier of the Hyblean mountains.

As for topographic cartography, the city of Siracusa is represented in foglio n.274 (Figure 7) and n.277 of the Carta d'Italia, published on a scale of 1:100,000 by the Istituto Geografico Militare. More precisely, the area affected by the study falls on the tavoletta "Siracusa", quadrante II S.O. of foglio n.274.

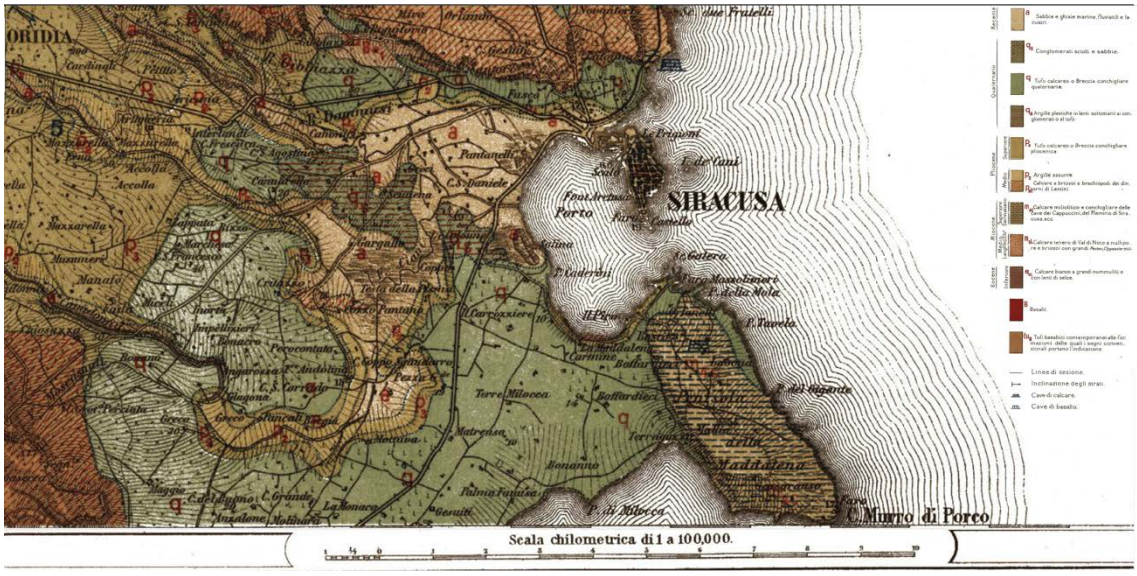

Figure 7: Shred of Foglio 274 of the Carta d'Italia.

The Syracusan territory has many areas of significant environmental and naturalistic value, the protected areas are currently five: the Ciane river and the salt pans of Syracuse, the oasis of Vendicari, Cava Grande del Cassibile, the island of Capo Passero, Pantalica and Anapo Valley.

Climatic setting

For the climatological characterization of Syracuse, reference is made to the report "Climatology of Sicily" of the Regione Siciliana (1998) which used the data of the Hydrographic Service of the Civil Engineers of the thirty-year historical series (1965-1994), relating to the meteorological parameters, temperature, and precipitation.

From the climatic point of view, it presents a territory with marked variability, linked to different zonal contexts. It is possible to distinguish: the coastal plain of the Ionian side; the hilly transition belt, which separates the coastal plain from the Hyblaean plateau; the inland area of the Hyblaean Mountains.

The analysis of the average annual values of temperatures shows that Syracuse has temperate climate conditions from October to March and arid from April to September. The average annual temperature is 18-19 °C, with annual maximums that normally reach 40 °C (in July/August).

The average annual rainfall in the province of Siracusa (615 mm) is slightly lower (-3%) than the regional average, equal to 633 mm.
The monthly distribution of rainfall in the individual stations is typically Mediterranean, with a concentration of rainy events in the autumn-winter period and a scarce presence of the same in spring and summer.

Geological setting

The Hyblean region, in southeastern Sicily, represents the emerged portion of the NE-SW-oriented continental bulge of the African foreland (Lentini et al., 1994) that buttressed the thrust front of the eastern Sicily collision belt (Roure et al., 1990), during the post-Tortonian NW-SE-oriented Africa-Europe convergence (Dewey et al., 1989; Romagnoli et al., 2015).

In the Hyblean Foreland, two distinct tectonic domains, separated by the Tellaro River Valley, can be recognized: the Siracusa Plateau, to the east, and the Ragusa Plateau, to the west, (Ghisetti and Vezzani, 1980; Grasso and Lentini, 1982; Pedley et al., 1992; Romagnoli et al., 2015; Figure 8). In particular, the Siracusa Plateau is mainly composed

of a Late Cretaceous-Late Tortonian shallow-water carbonate succession, resting on Early Cretaceous volcanic edifices, gradually replaced to the west by carbonate ramp deposits, representing the transition to basinal sequences (Romagnoli et al., 2015).

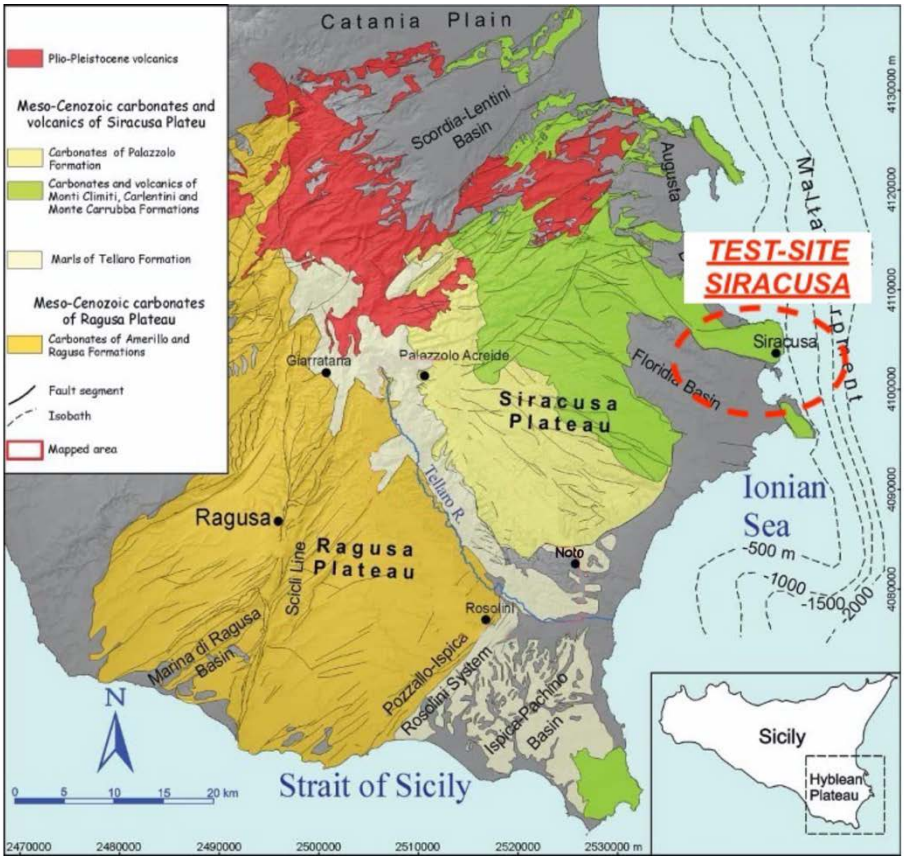

Figure 8: Geological and structural sketch map of the Hyblean region (modified from Romagnoli et al., 2015).

During the Quaternary, the Hyblean region was fragmented by tectonic features that developed during two distinct extensional episodes (Romagnoli et al., 2015). The former, governed by a NW-SE-oriented extension, consisted of the widespread reactivation of the NE-SW trending faults of the bulge, coincident with the dextral remobilization of the Scicli Line, inherited from a Late Cretaceous tectonic lineament, dissecting the Ragusa Plateau (Grasso and Reuther, 1988; Catalano et al., 2008; Romagnoli et al., 2015). This caused the propagation of a fault belt across the entire region, from the northern border of the Siracusa Plateau (Scordia-Lentini Basin) to the southern edge of the Ragusa Plateau (Marina di Ragusa and Ispica-Pachino Basins),

associated with the deposition of 1.5 to 0.9 ka syn-tectonic deposits (Pedley et al., 2001; Romagnoli et al., 2015).

The second extensional episode, governed by a NE-SW-oriented crustal stretching, affected, since about 850 ka (Catalano et al., 2010), only the Siracusa Plateau where the collapse of the Floridia and Augusta Basins occurred (Romagnoli et al., 2015).

Stratigraphic succession of the Siracusa Plateau

The stratigraphic succession of the Siracusa Plateau is exposed along the eastern flank of the Tellaro River Valley (Romagnoli et al., 2015). The basal levels consist of the upper Serravallian – Early Tortonian (Musumeci, 1959; Romeo and Sciuto, 1987; Di Stefano, 1995) marls of the Tellaro Formation (Rigo and Barberi, 1959), also described as Castelluccio Marls Member (Pedley, 1981; Romagnoli et al., 2015). This pelagic units gradually passes to the Tortonian carbonate sequence (Musumeci, 1959; Di Grande et al., 1982; Romeo and Sciuto, 1987; Di Stefano, 1995) of upward coarsening clastic (Palazzolo Formation; Rigo and Barbieri, 1959), that deposited at the front of the westward prograding carbonate ramp (Pedley et al., 1992), fed by the eastern sectors of the Hyblean region (Romagnoli et al., 2015). The transition from the pelagic to the detritic levels is heralded by lenses of a thin-bedded alternation of marls and limestones that are interleaved in the top levels of the Tellaro Formation, showing several slumped horizons (Romagnoli et al., 2015). The clastic sequence, capping the pelagic levels, varies from lower fine-grained horizons, hosting lens of calcarenites, (Gaetanì Member) to calcarenitic upper levels (Buscemi Member; Di Grande et al., 1982; Romagnoli et al., 2015).

In the Siracusa area, the substratum outlines a horst structure formed by a Meso-Cenozoic carbonate sequence with interbedded volcanics (Grasso and Lentini, 1982) cropping out in the northern part of the town (Figure 9; Panzera et al., 2016). The Cretaceous volcanic locally represents the deepest term which is unconformably covered by a sub-horizontal carbonate sequence that stands for the lithotype more frequently cropping out in the Siracusa town (Panzera et al., 2016). This sequence is distinguished in two main units, Mt. Climiti and Mt. Carruba formations. The former,

having thickness ranging between 20 and 80 m, lies on the Cretaceous volcanic and consists of compact and well-cemented calcarenites (Panzera et al., 2016). The latter, with an average thickness of about 20 m, is characterized by alternating calcarenites and marlstones (Panzera et al., 2016). Alluvial deposits fill out the graben of the Pantanelli plain, while detritus, having thickness of about 6–8 m, due to anthropic activity and historical ruins, is mainly outcropping in the Ortigia peninsula, the historical part of the town (Panzera et al., 2016; Figure 9).

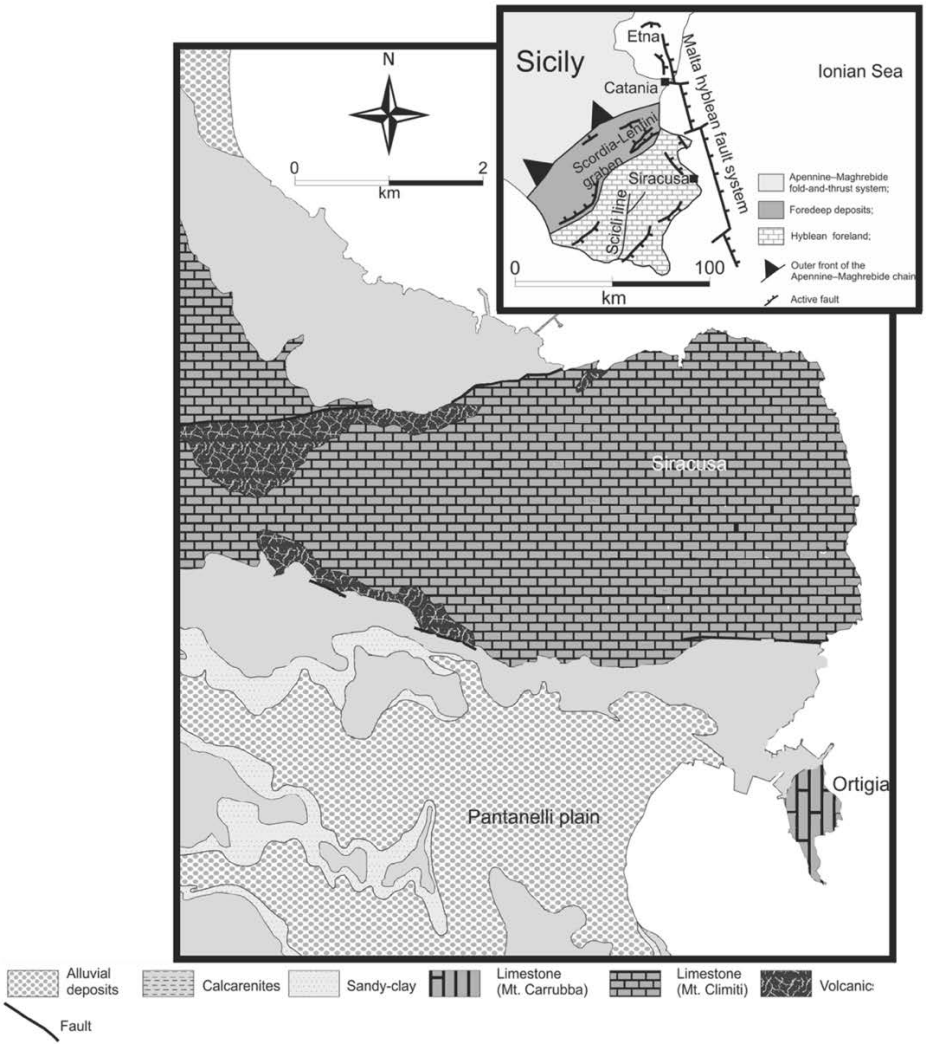

Figure 9: Geolithologic map of Siracusa area (modified from Panzera et al., 2016).

Geomorphological setting

The territory is characterized by the succession of plateaus generally corresponding to tectonic horst and tectonic plain corresponding to graben. This morphological

monotony is locally marked by morphological slopes, testifying to the tectonic events and uplift phenomena that have affected this area. (Regione Siciliana, 2013).

The morphology of the area is strongly influenced by the nature of the outcropping lithotypes and by their degree of erodibility; surface hydrology, meteoric precipitations and acclivity are among the main causes that have determined a differentiated modelling of the slopes.

The coastal area of Syracuse is characterized by the Bay of Syracuse (Porto Grande) which is limited to the north by the island of Ortigia and has the northern closure in the Punta di Castelluccio, while to the south it is limited by the Maddalena Peninsula between Punta Castelluccio to the North and Capo Murro di Porco to the South (Figure 10).

To the north of this system there is another small funnel-shaped bay, called Porto Piccolo (or Porto Marmoreo), limited, in the innermost part, by the Scoglio Pizzo and the system of minor rocks that surround it, while to the south it is closed by Punta Scogliera and the structure therein. The area in the center of which there is the Porto Piccolo is limited to the north by Punta Spuntone and to the south by Punta di Castello Maniace (Figure 10).

The island of Ortigia, which extends in the direction of the N-S, divides the two aforementioned ports, the Porto Piccolo to the north and the Porto Grande to the south. The rocky coast located in this sector is modified by the port works and the ancient Spanish walls.

The northern sector of the coastal area of Siracusa is characterized by high and rocky coasts, exclusively carbonate. The cliffs are characterized by the horizontal succession, with intense fracturing systems and deep cavities. (Regione Siciliana, 2013)

Approximately in the center of the tract is the Porto Piccolo which intrudes towards the interior, penetrating the urban fabric of the city of Siracusa which borders the entire area. Inside the Porto Piccolo, a canal opens that connects the Porto Piccolo with the Porto Grande (Figure 10).

The Porto Grande is occupied to the north by the urban settlement of Siracusa, while in the SW it is limited by the mouths of the Ciane river and the Anapo river where there is a rather articulated coastline, along which beaches and rocky coasts extend above the sea (Regione Siciliana, 2013).

Between the mouth of the Ciane and Anapo rivers there is also the area of the salt pans, a Nature Reserve aimed at preserving the environmental values of wetlands. The salt pans extend for about 50 - 60 hectares, bordered towards the sea by a sandy coastal strip and a low cliff and to the north by the Mammaiabica canal, which flows into the mouth of Ciane and Anapo (Regione Siciliana, 2013, Figure 10).

Figure 10: Coastal conformation of the Siracusa area.

As regards the coastal area of Siracusa area, so as the entire coastal area of southeastern Sicily, is characterized by the occurrence of several strands of marine terraces formed by wave-cut surfaces and/or thin depositional platforms (Di Grande and Raimondo, 1982; Bianca et al., 1999; Scicchitano et al., 2008). These morphological forms develop from the current coastline up to several kilometers from it, as well as from the presence of various morphological slopes which, presenting various types of sea level indicators

(leaf grooves, vermetid platforms, lithodome holes), have been interpreted as paleo-lines of coastline linked to sea level settlements during the late Quaternary (Carbone et al., 1982; Di Grande and Raimondo, 1982; Bianca et al., 1999; Scicchitano and Monaco, 2006).

Hydrogeological setting

From a hydrogeological point of view, the north-eastern sector of the Hyblaean Mountains is divided into four water bodies: the Lentinese basin, the north-eastern Siracusa area, the southern Siracusa area and the Augusta-Priolo plain. Water bodies have different geochemical characteristics in relation to the directions of groundwater flow. In particular, in the northern portion, from Monte Lauro to the Piana di Lentini, the groundwater circulates mainly in the Plio-Pleistocene volcanic deposits with an outflow direction towards N-NE. The semipermeable substrate of the aforementioned aquifer is locally made up of Miocene vulcanites, often altered by argillification processes, on the top. A structural high along the NE-SW alignment separates this water body from the adjacent mixed aquifer (Augusta basin).

The carbonate basin of Siracusa area extends even further to the west bordered to the north by the graben Melilli - Monti Climiti, a structural high with ONO-ESE direction.

In particular, the waterways (Tellaro, Anapo) that descend from the top of the Hyblaean Mountains towards the coast are short and torrential. In their middle course they appear recessed due to the action of water.

Ciane River and Saline of Siracusa

The site of community importance (SCI) Ciane River and Saline of Siracusa (Figure 11) develops in the SSW-NNE direction with an area of 3.6 km^2 and includes the Saline of Siracusa and the Ciane River which, together with the Anapo river and the Mammaiabica canal, has, in fact, a single focal apparatus that overlooks the Porto Grande of Siracusa.

The perimeter of the SCI, of about 16.5 km, follows the course of the Ciane from the sources of Cozzo Pantano in the east to its mouth in the west, enclosing the areas of the

salt pans. In the Regional Technical Cartography, the area falls within Sections 646110, 646120, 646150, 646160 on a scale of 1: 10,000.

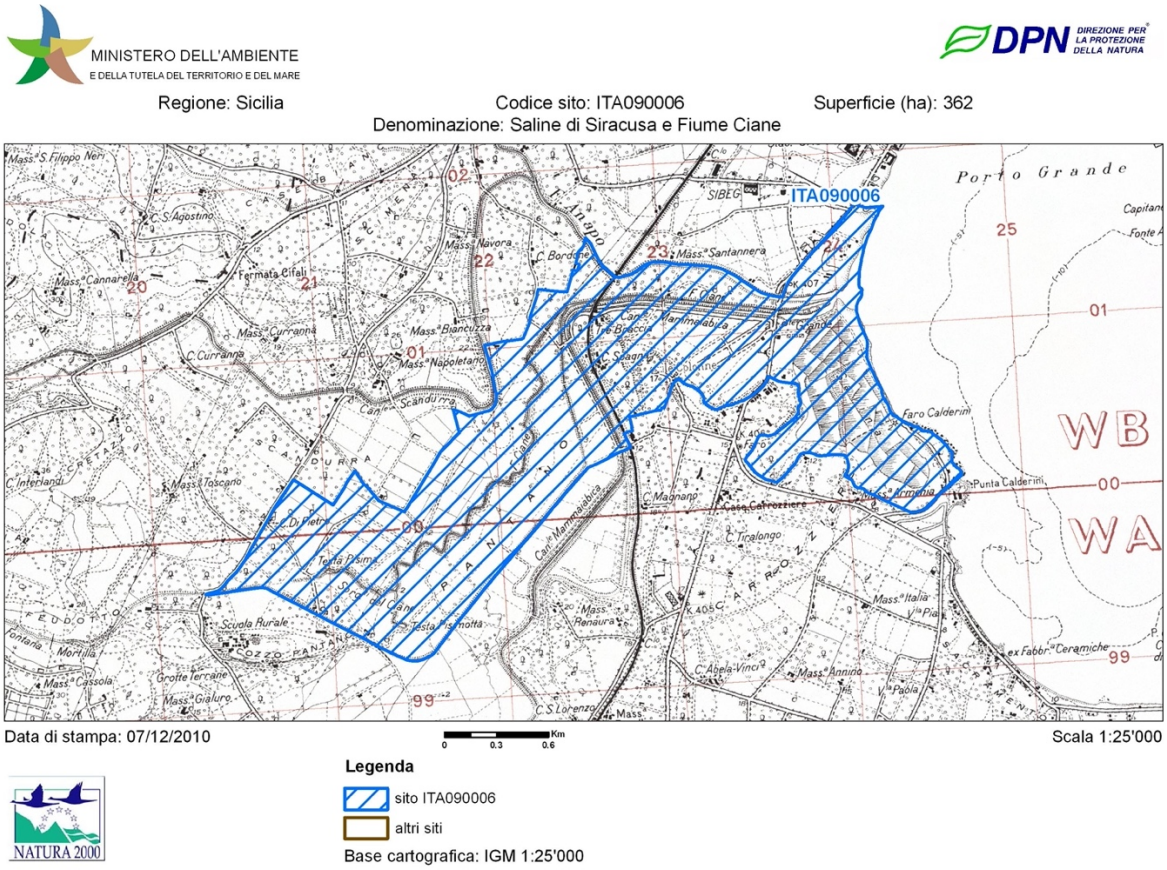

Figure 11: Map of the site of community importance ITA090006 River Ciane and the Saline of Siracusa (from minambiente.it)

From a morphological point of view, the area on which the Ciane river and the Saline of Siracusa stand, represents a plain of alluvial origin consisting largely of the deposits of the Anapo, bordered by hilly reliefs and terraces of calcarenite and clayey nature.

The silty-clayey nature of the substratum soils has allowed the creation of the Saline with the now abandoned saliculture activity, so the environment that has been created, with dense reeds and glasswort, offers aspects of high naturalistic interest in a little far from the city center. The coastal pillow that currently protects the salt pans is exposed to the action of the storms that have led to its retreat.

Geological aspects

From a geological point of view, the stratigraphic succession in the SCI area is given, from top to bottom, by:

- Calcarenites and sands, characterized by frequent facies heteropies, that is by lateral-vertical passages from hard and compact calcarenitic levels to sandy and conglomeratic lens levels. The age refers to the middle-upper Pleistocene.

- Infrapleistocene blue clays, with little evident stratification, of a fresh cut blue color and yellowish if altered, constitute the substrate of the salt pans and emerge in Contrada Tre Braccia.

- Calcarenites with algae and bryozoans, outcropping in Cozzo Pantano, are made up of a succession of bryozoan calcarenites and algal biolithites in banks of 4-5 m thick, crumbly or hard and compact. Referable to the Formation of the Climiti Mountains - Member of the Limestone of Siracusa, they are from the Miocene age.

From a tectonic point of view, at the base of Cozzo Pantano a fault with an E-W direction puts the Miocene limestones in contact with the Pleistocene clays, giving rise to the group of springs that feed the River Ciane.

Hydrology and hydrogeological conditions

The courses of Anapo, Ciane and Mammaiabica mainly develop within the hydrographic basin, with joint focal systems in the port of Siracusa.

The Anapo river originates from Monte Lauro at 986 m a.s.l. and flows inside deep canyons with a basin of 302 km^2 and a course of 60 km.

The Ciane river originates from the springs of Testa Pisima and Testa Pisimotta at the base of Cozzo Pantano and flows over a large flat area with a basin of 16 km^2, within which it collects the waters of the Fontana Mortella stream.

The Mammaiabica stream originates from Monte Cardinale (560 m a.s.l.), with a basin of about 131 km^2 and a course of 33 km.

The hydrological characteristics refer to the Anapo river which, with an average annual flow of 3.6 m^3/sec, constitutes the most important water resource of the Hyblaean Mountains.

Goro framework

Geographical setting

The Goro lagoon is the southernmost of the lagoons of the Po delta, which is characterized by five main distributary channels: Po di Maistra, Po di Pila, Po di Tolle, Po di Gnocca (or Po di Donzella) and Po di Goro (Figure 12). The lagoon of Goro developed in the 19th century westward to the last branch, and today covers about 26 km², with an average depth of 1.5 m and contains about 40 million cubic meters of water (Simeoni et al., 2000; Bezzi et al., 2019). It is located almost entirely within the territory of the Municipality of Goro, in the Province of Ferrara in the Italian region Emilia-Romagna, except to S-E where both the Municipality of Codigoro, in the part of the Po di Volano outlet, and the Municipality of Comacchio, for the part bordering the sea - Lido di Volano, overlook. The lagoon is bounded to N by the town of Goro and by defense embankments up to Gorino and continuing eastwards it is bounded by the Po di Goro bank, to N-W by the levees of Valle Goara and Valle Pioppa and Gran Bosco Della Mesola; to S, the Scanno di Goro, an 8 km long spit, separates the lagoon from the open sea.

Figure 12: Po Delta and location of the Goro Lagoon.

The Lagoon of Goro is an environment of particular natural value and is included within the SPA (Special Protection Area) - SCI (Site of Community Importance) - SAC (Special Area of Conservation) IT4060005, called "Sacca di Goro, Po di Goro, Valle Dindona, Foce del Po di Volano" (minambiente.it).

Evolution of the lagoon

From a morphological point of view, the area under study is very complex, due to the evolution that has taken place over the years. The salient points of the main changes that occurred in the Goro Lagoon area (Fontolan et al., 2000) are summarized in Figure 13.

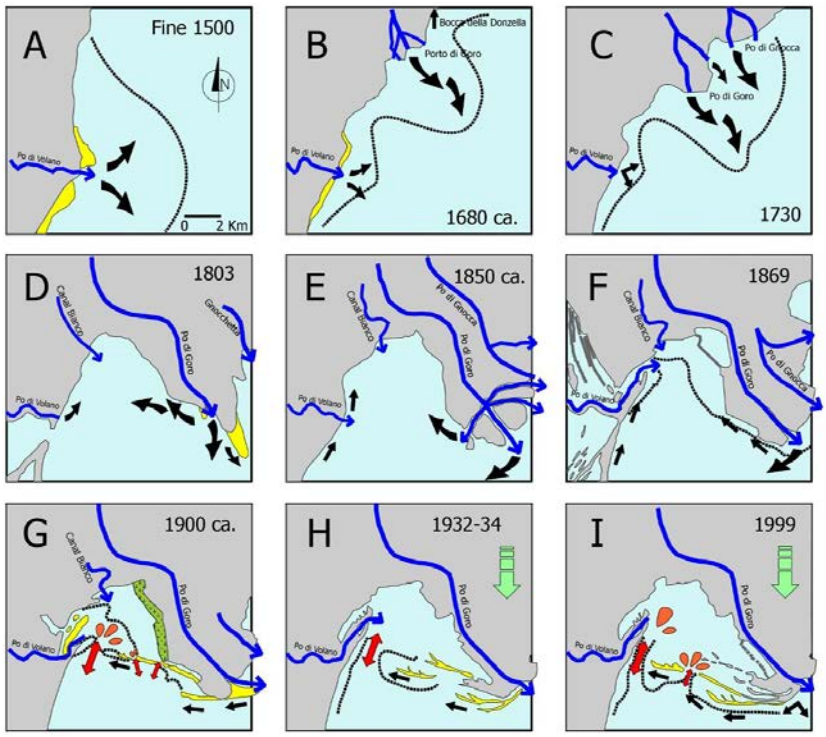

Figure 13: Evolution of the Po di Goro area from the end of the XVI century to the present time (from Fontolan et al., 2000). The boxes in the figures always refer to the same area; the bathymetric configurations of the shallow depths, around one meter, are shown in dashed lines.

These profound changes in the environmental characteristics of the area have transformed the Po mouth apparatus from a delta dominated by fluvial inputs to a delta dominated by wave motion (Dal Cin, 1983).

The current Goro Lagoon (Figure 14) represents a very articulated environment not only for the diachronic interacting between marine and terrestrial components, but also for the contemporary and, sometimes, intense conditioning action exerted by man.

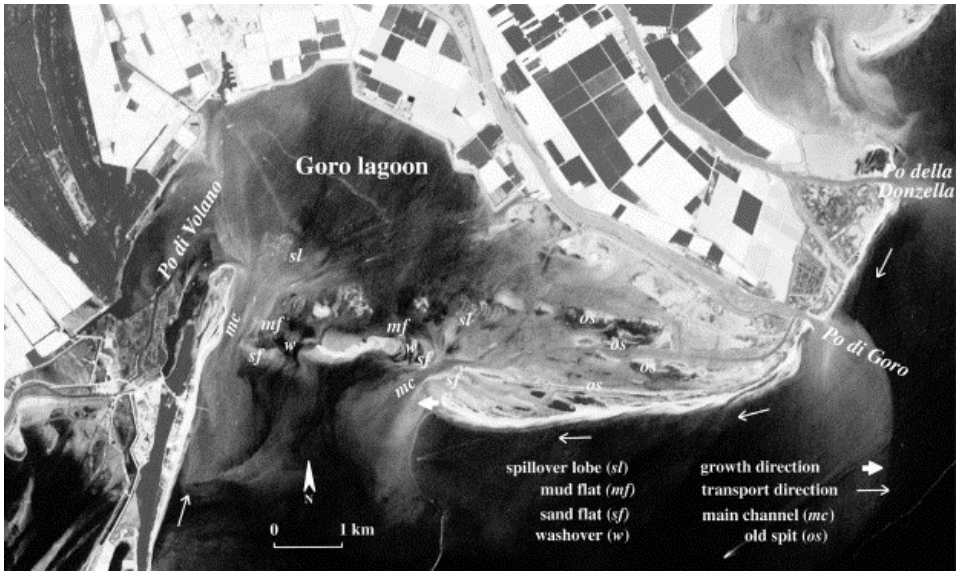

Figure 14: Satellite image of the Goro Lagoon showing the main morphologies of the lagoon mouth (from Simeoni et al., 2007).

Meteo-marine setting

Meteorological regime

The Delta area belongs to the Po Valley which falls within the cold temperate climate zone. These conditions are locally very accentuated by the presence of the sea, which tends to give the area more Mediterranean climatic characteristics.

In the Delta area the temperature drops below 2°C in January and exceeds 23°C in July; the average temperature ranges are generally below 22°C. The average annual precipitation values are less than 600 millimeters per year (Ciavola et al., 2000).

In the entire eastern Po Valley, relative humidity is very high, falling below 60% only in July and August, while it is very high in the period between November and February.

Anemological regime

In the study on the anemological regime in the Po Delta and at the mouth of the Adige, Calderoni (1982) analyzed the data collected by the anemograph positioned on the Punta Maistra lighthouse in the period from 1929 to 1943, and by those provided by anemograph positioned on the Rosolina Mare coast in the period between 1974 and 1977. This study shows that in the average year the N-E wind (Bora) is the most frequent wind (155.3 ‰), followed by the S-E wind (Scirocco, 123.0 ‰) and from E (Levante, 116.4 ‰).

In the period considered and in the average year, the most frequent and fastest wind is the Bora (8.36 m/s), which is therefore considered the dominant wind in the area.

According to IDROSER (1996) the expansions of the high-pressure areas near the coast have a great influence on the state of the weather in the central-northern Adriatic, so the prevailing winds are those included between N-NE and E (Bora), between E-SE (Scirocco) and those of NW (Mistral), in agreement with the previous observations.

Wave regime and exposure

A recent study (Simeoni et al., 2008) studied the marine climate starting from the recordings made from the wave buoy RON located off Ancona for the period 1999-2006. The data, transposed off the Goro Lagoon (Figure 15), show how the whole sector between 60° N and 120° N presents waves with heights greater than 3 m, while in terms of frequency the two sectors of 30° and 120° are approximately the same, although the former is characterized by lower waves since it is more protected by the presence of the delta and in any case characterized by a shorter fetch length (Simeoni et al., 2008).

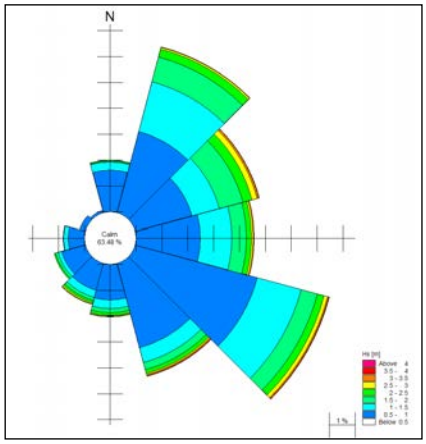

Figure 15: Wave rose obtained from the transposition of the waves recorded by the Ancona buoy to a point close to the Goro Lagoon (Simeoni et al., 2008).

The Emilia-Romagna Region, through the study of Osservatorio clima di Arpae, 2020, confirms, for the period 2007-2018, that the prevailing waves (those with the highest frequency) come from the eastern directions (ENE-E-ESE), while the dominant waves (those with greater intensity) come from the north-eastern directions (NE-ENE), associated with the strong Bora winds, which are those to which the Emilia-Romagna coast is most exposed and vulnerable (Figure 16).

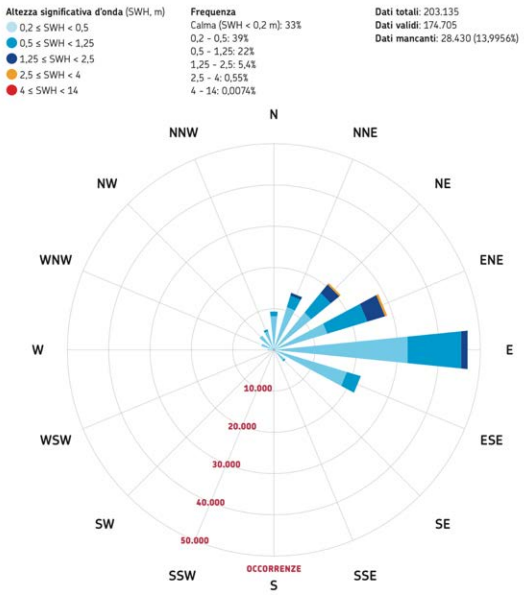

Figure 16: Rose of the waves recorded by the wave buoy of Cesenatico in the period 2007 – 2018 (Osservatorio clima di Arpae, 2020).

During storm surges, the average direction of origin of the waves was found to be E-NE, with an average wave height of 1.82 m. The monthly analysis of the number of storm surges in the period considered (June 2007-December 2019) highlighted that the months with the highest number of storm surges recorded (therefore more energetic) are those from October to March (Osservatorio clima di Arpae, 2020).

Characterization of tidal flows

The tidal variations on the Goro Lagoon are mainly semi-daytime: there are normally two high and two low tides per day, although diurnal tides can occur, with a single high and low tide within 24 hours, mainly when in the full or new moon phase. In addition, the tides are also affected by meteorological phenomena, such as the action of the wind and the differences in air pressure over the sea, during the transit of atmospheric disturbances.

The tidal regime that characterizes the Goro Lagoon, with a tidal interval of less than 1 m (on average 0.60 m), varies from 0.40 m during the neap tide to 1.20 m during the spring tide (Simeoni et al., 2007).

In the Lagoon, the tidal delay between the secondary inlet and the eastern end of the lagoon is of the order of 30 minutes, while between the eastern internal area of the lagoon and the mouth of the Po di Goro there is a delay of about 1 hour (Simeoni et al., 2007).

Furthermore, by analyzing the tide values recorded at the Porto Garibaldi station (source Arpae) in the 2011-2019 interval, the oscillations between high and low tide in the Goro Lagoon range on average between a maximum of 89.9 cm and a minimum of -88.3 cm.

Geomorphological setting

The lagoon of Goro is an environment of transition from internal (fresh) to external (salty) waters and subject to the phenomenon of subsidence (LIFE13 NAT/IT/000115, 2021; Gabbianelli et al., 2000). The shallow seabed and the limited exchange from the mouths determine a strong environmental risk mainly linked to the proliferation of macroalgae and the corresponding risk of water anoxia (LIFE13 NAT/IT/000115, 2021).

The quality of the water in the lagoon is guaranteed by a network of sub-lagoon canals that favor interchange with the sea and an increase in internal circulation, and by various hydraulic structures that control the introduction of fresh water (LIFE13 NAT/IT/000115, 2021). The fresh waters from the Po di Volano to W, the Canal Bianco and Po di Goro to E flow into it, while to S, through the mouths, the salty waters converge for hydrodynamic lagoon-sea exchanges (LIFE13 NAT/IT/000115, 2021).

Geomorphologically, the Goro Lagoon is characterized by three main units (Gabbianelli et al., 2000):

- emerged territories, consisting mostly of areas of recent hydraulic reclamation and characterized by altitudes below sea level;
- the brackish lagoon with shallow bottoms (1.5 - 2 m maximum);
- the system of coastal arrows and sandy bars that give it its lagoon characteristics.

All three units have been characterized, during their evolution, by a differentiated development in time and space due to the continuous interaction between anthropic interventions and physical-natural phenomena (river efficiency, sedimentary inputs, wave motion, currents, etc.).

The current morphological and altimetric structure has been strongly influenced by human intervention (Gabbianelli et al., 2000).

The mouth of the Po di Goro has a clearly asymmetrical morphology due to the erosive retreat of the left bank and the presence of a well-developed bar with an elongated mouth on the overcurrent side, elements that suggest a strong wave control system (Del Grande et al., 1997; Simeoni et al., 1998). The latter, which prevails over the efficiency of picnalic flows directed on shallow and shallow seabeds, generates coastal drift currents capable of sorting, mainly towards the west, the sandy sediments, thus feeding the system of coastal arrows (IDROSER, 1984; Dal Cin, 1994; Lambetti, 1998).

The direction of transport of materials is linked to the absolute prevalence of the Scirocco and Levante seas compared to the others which, in this area, are instead affected by the shadow effect generated by the morphology of the Delta.

The sedimentary contributions, which arrive from the Lagoon, come mainly from the solid contributions of the Po di Goro and to a lesser extent from the Po di Gnocca and Tolle and from the reworking of the deposits of the northernmost beaches.

Sedimentologically, the study carried out in the Goro Lagoon by Dal Cin and Pambianchi (1991) highlighted how the granulometric characteristics varied continuously going from the mouth of the Lagoon towards the inside (Figure 17). The study by Simeoni et al. (2000) highlighted the presence of sandy or predominantly sandy sediments concentrated on the emerged part of the Scanno and the barrier island, on the seabed in front up to the isobath of about 2 m, and in correspondence with the main mouth. The presence of predominantly muddy sediments distinguishes some less extensive but more complex areas at the mouth of the Po di Goro and the maximum depths of the seabed in front of the Scanno (Simeoni et al., 2000).

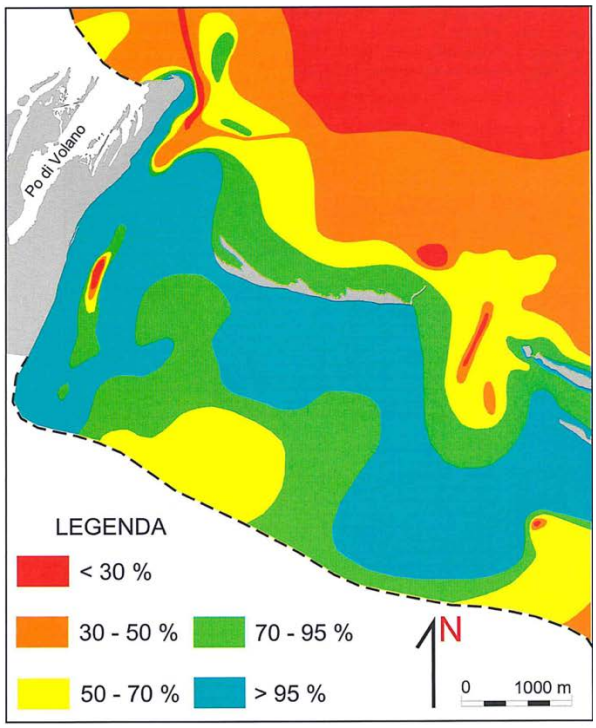

Figure 17: Distribution of the percentage of sand on the bottoms of the lagoon mouths of the Goro Lagoon (from Simeoni et al., 2000).

Methods

The experiment carried out with the methodologies used is summarized schematically in the figure where all the steps of the study are represented, from the choice of plastics to the statistical treatment of the data (Figure 18).

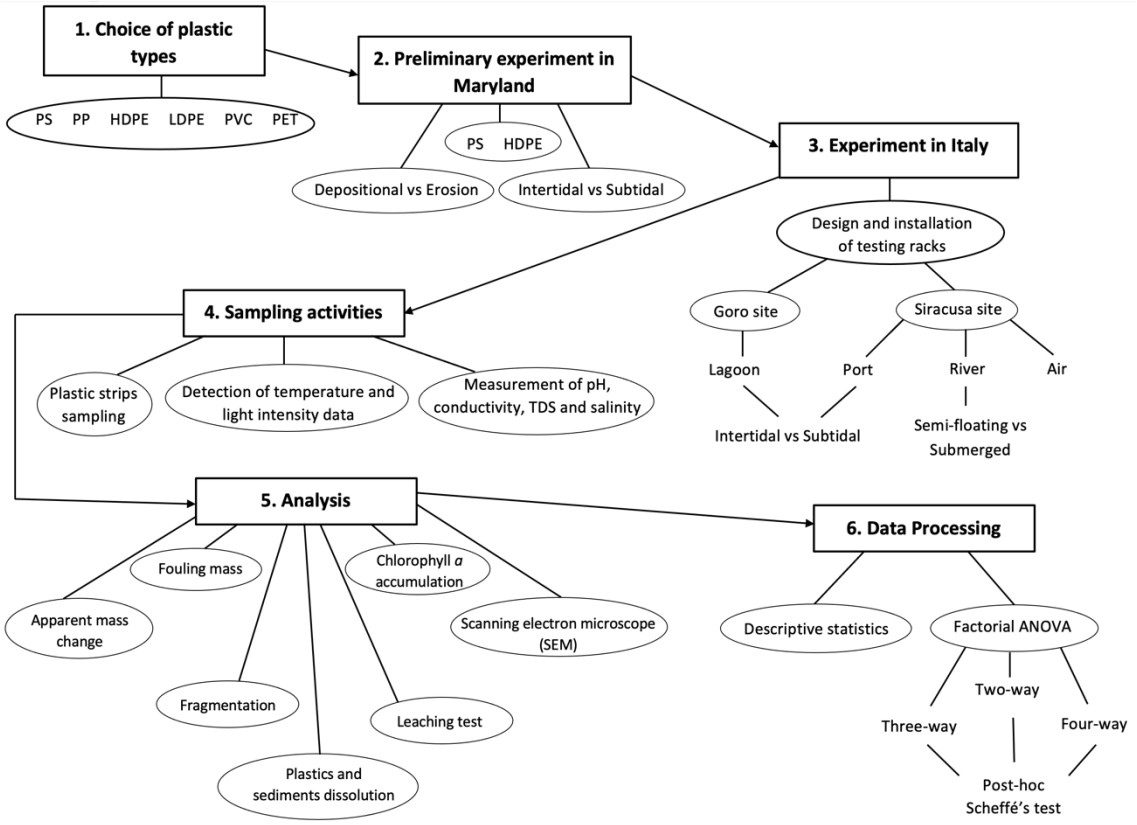

Figure 18: Summary scheme of the experiment with the steps of the study.

Choice of types of plastics

From the results shown by the study by Geyer et al. (2017) on the most commonly used types of plastics and considering the prices of the materials, I decided to use PS, PP, HDPE, LDPE, PVC and PET for the experiment.

PS strips were cut and drilled from Isap Packaging S.p.A. flat plates (20.5 cm diameter, thickness 0.3 mm, color white, density 0.83 g/cm^3). PP strips were cut and drilled from Plastotecnica Emiliana s.r.l. extruded rigid slams (size 100 cm x 200 cm, thickness 1 mm, color natural (semi-transparent white), density 0.83 g/cm^3). HDPE strips were cut and

drilled from Plastotecnica Emiliana s.r.l. extruded rigid slams (size 100 cm x 200 cm, thickness 1 mm, color natural (white), density 1.07 g/cm^3). LDPE strips were cut and drilled from Plastotecnica Emiliana s.r.l. soft sheet (size 100 cm x 500 cm, thickness 0.5 mm, color natural (semi-transparent white), density 1.04 g/cm^3). PVC strips were cut and drilled from Plastotecnica Emiliana s.r.l. extruded rigid slams (size 100 cm x 200 cm, thickness 1 mm, color natural (avory), density 1.64 g/cm^3). PET strips were cut and drilled from Plastotecnica Emiliana s.r.l. extruded rigid slams (size 100 cm x 200 cm, thickness 2 mm, color natural (white), density 1.41 g/cm^3). Table 1 summarizes the characteristics of the plastics used for the experiment.

Table 1: Characteristics of the plastics used for the experiment.

Plastic type	Thickness	Density	Color	Source
PS	0.3 mm	0.83 g/cm^3	white	Isap Packaging S.p.A. flat plates
PP	1 mm	0.93 g/cm^3	natural (semi-transparent white)	Plastotecnica Emiliana s.r.l. extruded rigid slams
HDPE	2 mm	1.07 g/cm^3	natural (white)	Plastotecnica Emiliana s.r.l. extruded rigid slams
LDPE	0.5 mm	1.04 g/cm^3	natural (semi-transparent white)	Plastotecnica Emiliana s.r.l. soft sheet
PVC	1 mm	1.64 g/cm^3	natural (avory)	Plastotecnica Emiliana s.r.l. extruded rigid slams
PET	2 mm	1.41 g/cm^3	natural (white)	Plastotecnica Emiliana s.r.l. extruded rigid slams

Preliminary experiment in Maryland

Before proceeding with the experiment that forms the basis of this thesis, I participated in a similar but smaller scale experiment already started along the southern shore of the Choptank River, a tidal sub-estuary of the Chesapeake Bay, along the shoreline at Lakes Cove at UMCES Horn Point Laboratory (Figure 19). This experiment was performed using two types of plastics, HDPE and PS, to test how intertidal and subtidal exposure regimes under contrasting hydrodynamic, erosive versus depositional conditions, affected their fragmentation and degradation.

We sampled plastic strips at 4, 8, and 43 weeks after deployment. At each sampling time point, the following metrics were measured: total mass change, mass change after washing with peroxide, and chlorophyll *a* accumulation, as well as observations using petrographic microscope and scanning electron microscope (SEM).

My original plan was to conduct the experiment described above in the Chesapeake Bay as well, examining a larger number of plastic types, and examining the influence of

hydrodynamic and exposure regimes. However, due to travel restrictions imposed following the COVID-19 pandemic, the experiment was only carried out at sites located in Italy.

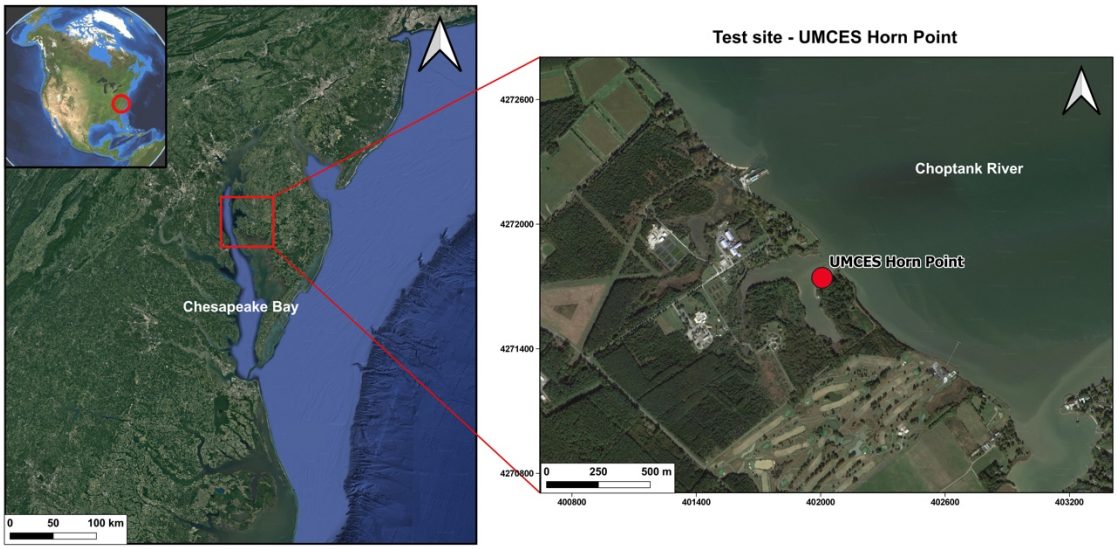

Figure 19: Localization of the preliminary experiment site.

Design

The experimental approach was to expose strips of plastic to different environmental conditions. To allow the plastics to be exposed to environmental conditions, I decided to cut the materials into strips all the same with dimensions of 15 cm x 2.5 cm and to drill a hole of 0.2 cm in diameter on each strip at a distance of 1.5 cm, as illustrated in Figure 20.

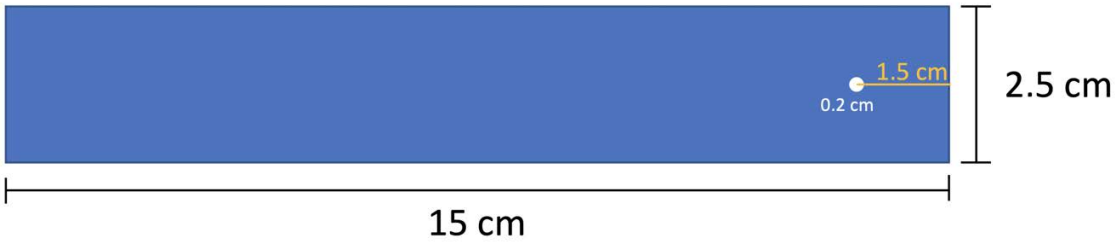

Figure 20: Schematic design of the plastic strips.

Each strip was anchored in the middle of two slats of raw fir wood (2 m x 4 cm x 3 cm, length, width, height) by means of steel nails (dimension: 1.9 mm diameter x 5 cm

length) (Figure 21), so that the strip was anchored on one side and free to move on the other (Figure 22).

Figure 21: a) Assembly phase of the plastic strips on the wooden slats. b) Detail.

Figure 22: Slats with plastic strips.

Once the slats with the anchored strips were ready, they were mounted in a galvanized iron frame to group them into 10 frame strips by means of galvanized bolts and nuts (Figure 23).

Figure 23: Frame assembled with strips.

The result was 7 testing racks, where in each were mounted 10 slats containing 60 identical plastic strips each, 10 for each plastic type selected, while 10 strips of each plastic type were left unattached and served as control strips. All plastic strips were numbered and weighed before deployment.

Installation

There were four test sites: one in Goro, province of Ferrara, Emilia-Romagna in a lagoon environment, and the other three in Siracusa, Sicily, respectively in a port, in a river and in an air environment (Figure 24).

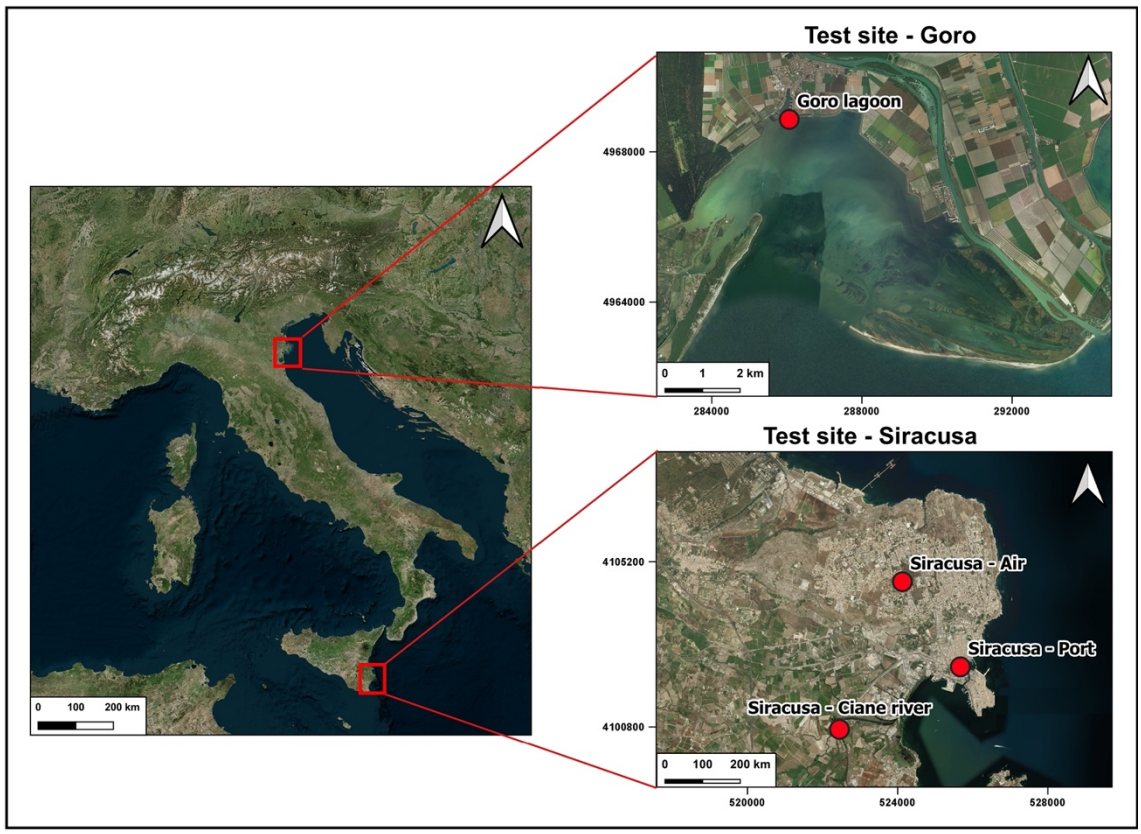

Figure 24: Localization of test sites.

The first site of Siracusa (37°04'03.0"N 15°17'19.5"E) was located inside the Porto Piccolo, a small funnel-shaped bay, head of many nautical clubs, therefore heavily anthropized. In this place, there were two testing racks in the water placed side by side (Figure 25). One rack was in the intertidal zone (herein, Port-IT) so that it was inundated for approximately 12 hours per day, and the other in the subtidal zone (Port-ST) on average about 1.5 meters deep. The racks were anchored to the wharf granted in concession by the Lega Navale Italiana – Sezione di Siracusa by means of nautical ropes and ballasted in order to keep the established depth and make periodic sampling possible.

Figure 25: Testing racks deployed in the port of Siracusa and anchored to the wharf.

Another rack was installed on a terrace of a building in Siracusa (Air) (Figure 26) (37°5'16.90"N 15°16'17.43"E), exposed to the air in an urban area, subject only to weather conditions. It was raised about 15 cm above the ground so that the strips, while moving, did not touch the supporting surface. These three racks were first lined up on June 10, 2020.

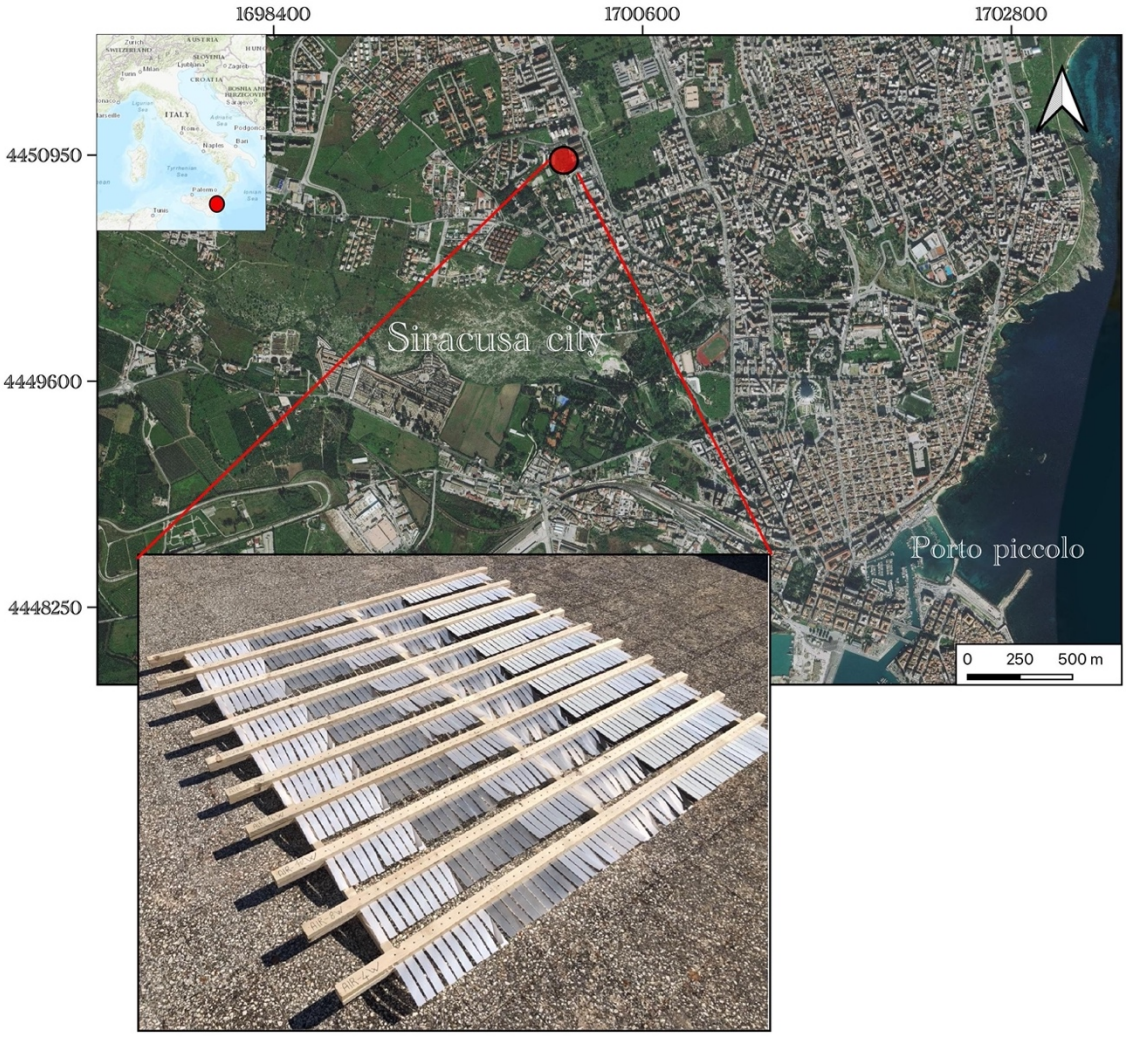

Figure 26: Testing rack installed on a terrace of a building in Siracusa.

Two testing racks were installed on July 9, 2020, in the Goro lagoon. One was deployed in the intertidal zone (Lagoon-IT) (Figure 27) (44°50'26.0"N 12°17'37.0"E) so that it was inundated for approximately 12 hours per day. The other was secured in the subtidal zone (Lagoon-ST) (44°50'25.6"N 12°17'37.7"E) at a depth of 30 cm in low tide conditions. The fastening of the racks was carried out by means of wooden poles stuck into the sediment with the help of a high-pressure water jet machine to which the racks were fixed by nautical ropes with the support of the Istituto Delta Ecologia Applicata Srl.

Figure 27: Testing rack deployed in the Goro Lagoon in intertidal condition.

The river environment was located within the Site of Community Importance (SCI) called "Ciane River and Saline of Siracusa". In the Ciane river (37°04'03.0"N 15°17'19.5"E) the test racks were placed so that one always remained submerged at a depth of about 70 cm (Riv-S) (Figure 28) and one always submerged but on the surface of the water, in semi-floating condition (Riv-F) (Figure 29). The installation was performed on August 6, 2020. Both the installation and the subsequent samplings were authorized by the Director of the “Riserva Naturale Orientata Fiume Ciane e Saline di Siracusa”.

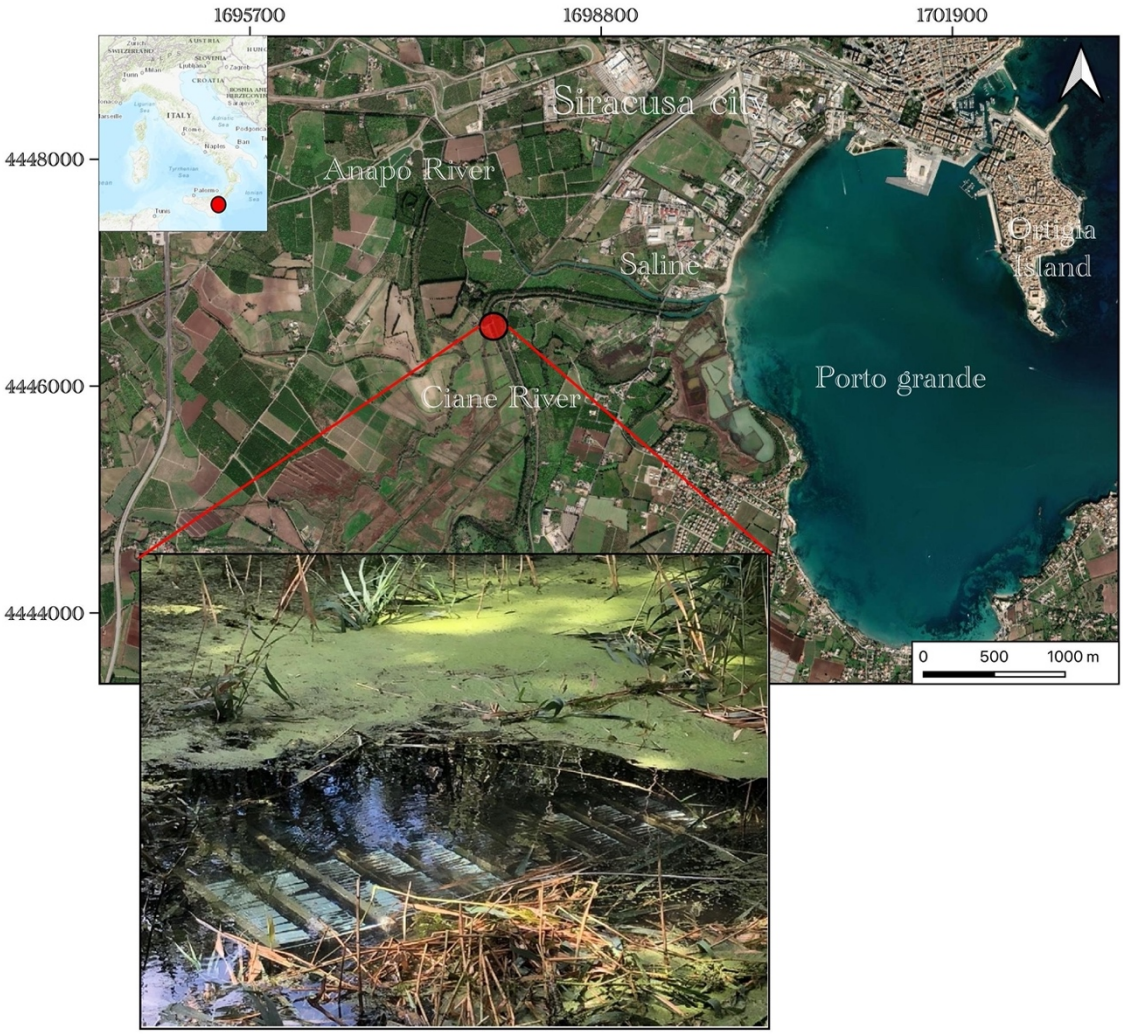

Figure 28: Testing rack deployed in the Ciane river in submerged condition.

Figure 29: Installation of the slats in the Ciane river in semi-floating condition.

Simultaneously with the installation, where possible, sediment and water samples were taken in order to characterize the environment.

Light intensity (150 to 1200 nm) and temperature were measured in each rack, using factory calibrated HOBO sensors (HOBO Pendant, UA-002-64), logging every 30 min and cleaned during each sampling (Figure 30).

Figure 30: HOBO Pendant, UA-002-64.

Sampling and processing

The plastic strips samplings were scheduled at 4, 8, 12, 16, 20, 28, 36, 44, 52 and 60 weeks after deployment. Unfortunately, however, they stopped after the 36-week sampling due to the complete degradation of the wooden slats which caused the plastic samples to be lost.

Each sampling consisted of taking a plank with plastic strips from each testing rack (Figure 31), of a sample of water in which the plastic samples were immersed (Figure 32), in the measurement of pH, conductivity, and salinity by means of a portable logging multiparameter meter equipped with a multi-sensor probe (Hanna Instruments HI98195) (Figure 33), and in the detection of the temperature and light intensity data recorded by HOBO sensors (Figure 34).

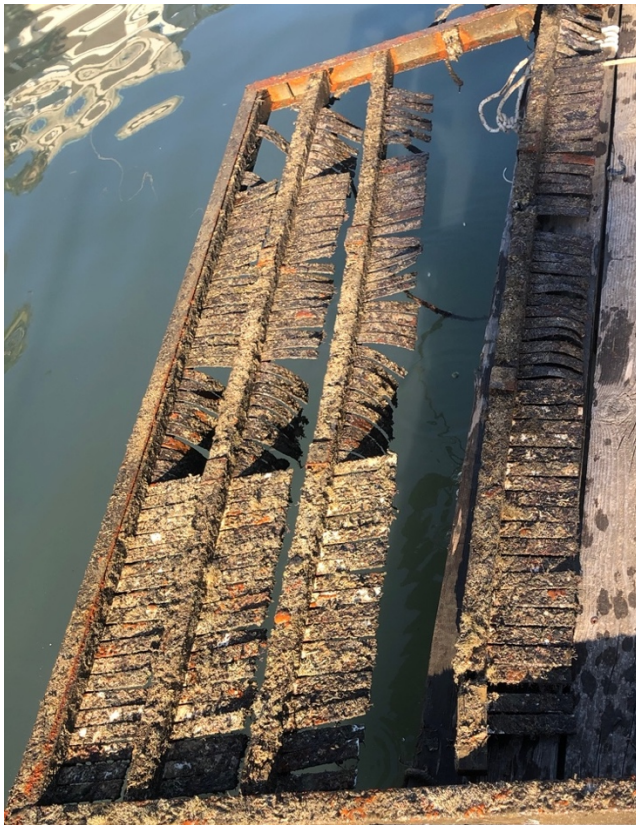

Figure 31: Example of a sampling phase of a plank deployed in the subtidal port environment.

Figure 32: Rudimentary sampler by means of which water samples were taken from the bottom of the port.

Figure 33: Measurement of chemical-physical parameters with portable logging multiparameter meter equipped with a multi-sensor probe.

Figure 34: HOBO sensor in the intertidal lagoon environment. The light intensity data in the lagoon environment were not reliable as the strong and sudden colonization of the sensors by the biofouling, associated with logistical difficulties in cleaning the HOBO sensors, did not allow the recording in an optimal and continuous way.

At each sampling time point, total mass change and mass change after washing with hydrochloric acid (Figure 35) were measured; from week 4 to week 28 samples chlorophyll *a* accumulation were measured (Figure 36).

Figure 35: Example of plastic strips exposed for 12 weeks in port areas, before (left) and after (right) washing with hydrochloric acid.

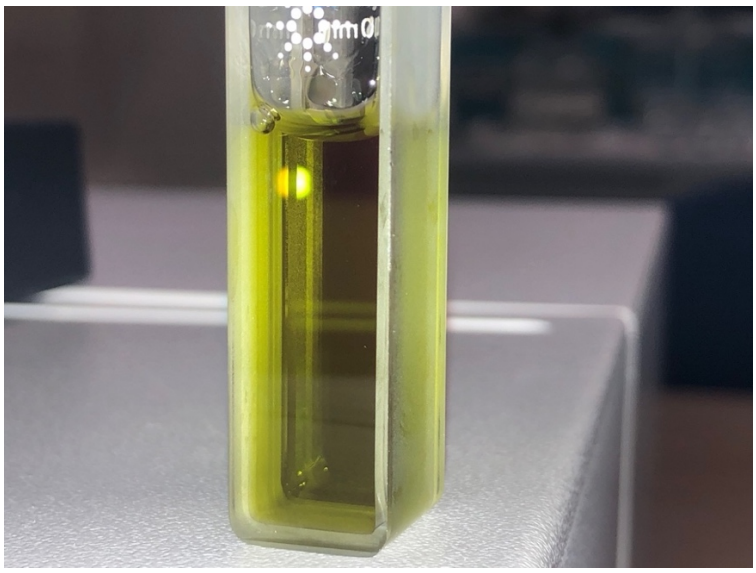

Figure 36: Solution obtained from the extraction of chlorophyll with acetone to measure the accumulation of Chl *a* on the plastic strips.

The 12- and 28-week exposure samples were also observed using a scanning electron microscope (SEM) and were subjected to leaching test. To accomplish this, at each time point, ten strips of each type of plastic from each treatment were collected. Of these, three were weighed after drying in a natural circulation oven (Argo Lab TCN 50) at 50°C for 24 hours. This estimate yielded the total mass gain and reflected the net balance between accumulation of dry mass associated with a developing fouling and any mass loss of plastic. These same strips were subsequently soaked in hydrochloric acid (5%) for 24 h at room temperature. After soaking in acid, the plastic strips were gently wiped with a kimwipe to remove any residual debris, then rinsed with ultrapure water and oven dried (50°C for 24 h) to remove any water trapped in the plastic, and reweighed. Among control samples, this procedure did not cause a detectable change in mass or appearance under SEM.

Change in apparent plastic mass was calculated for the samples of each treatment as follows:

$$\%\ apparent\ mass\ change = \frac{m_w - m_0}{m_0}\ x\ 100$$

where m_w is the mass after acid-washing and m_0 is the initial mass before environmental exposure.

Fouling mass, referred to accumulated mass consisting of biofilm and sediment, per surface area for each strip in contact with water was calculated as follows:

$$fouling\ mass = \frac{m_e - m_w}{s}$$

where fouling mass is expressed in units of mg/cm^2, m_e is the total mass after environmental exposure, m_w is the mass after acid-washing and s is the surface area of each plastic strip. Plastic strips were weighed using a Denver Instrument SI-234 Summit Series analytical balance.

Three plastic strips, except those exposed only to air, were analyzed for chlorophyll *a* (Chl *a*) accumulation at each time point. These plastic strips were kept in the dark and frozen (-20°C) until analysis. Chl *a* attached to plastic strips was extracted in a 90% acetone solution in the dark at -20°C for 24 h. The pigment concentration was measured by spectrophotometry (Agilent Cary 3500 UV-Vis double-beam spectrophotometer),

using a 1 cm pathlength cuvette, and employing the empirical equations of Lorenzen (1967). Chl *a* concentrations were normalized to the upper surface area.

For microstructural characterization and for determining element compositions, a Scanning Electron Microscope (SEM) model ZEISS EVO MA 15, coupled with an Energy Dispersive X-Ray Spectroscopy (EDS) system (Aztec Oxford apparatus, SDD detector, WD 8.5 mm, EHT 20 kV) provided with a LaB6 filament as electron source was used. A total of 81 plastic strips were analyzed by SEM, representing control (i.e. unexposed) samples, and those collected after 12 and 28 weeks of environmental exposure. The strips were examined following the acid washing step to remove fouling, as described above.

Leaching tests were performed on control plastic strips and plastic strips that had been exposed to aquatic environments for 12 and 28 weeks to assess the potential for accumulation and release of contaminants. A section of a plastic strip, measuring 11 cm x 2.5 cm, was cut and placed in 100 mL of ultrapure water inside a glass bottle and stirred for 24 hours using an orbital oscillator (VDRL 711/CT) at 25°C and speed 5 (corresponding to approximately 125 oscillations per minute) (Figure 37). Ultrapure water was chosen as a solvent to investigate any inorganic compounds leached from the plastic strips with the relative accumulated fouling, as indicated by the European legislation on the leaching of granular waste and sludge (EN 12457). A total of 73 leaching tests were performed. The solutions obtained were filtered through a vacuum filter system and paper filters (Whatman quantitative filter paper, ashless, Grade 40) (Figure 38 and Figure 39). Conductivity and total alkalinity (via alkalinity test kit HI3811) were measured in the solutions, which were then analyzed for F^-, Cl^-, NO_2^-, Br^-, NO_3^-, PO_4^{3-} and SO_4^{2-} by anion chromatography (Thermo Scientific Dionex ICS-1000) and for lithium, beryllium, boron, sodium, magnesium, aluminum, phosphorus, potassium, calcium, scandium, titanium, vanadium, chromium, manganese, iron, cobalt, nickel, copper, zinc, gallium, arsenic, selenium, rubidium, strontium, molybdenum, silver, cadmium, tin, antimony, tellurium, barium, mercury, thallium, lead, bismuth and uranium ions by inductively coupled plasma-mass spectrometry (Thermo Scientific iCAP TQ ICP-MS).

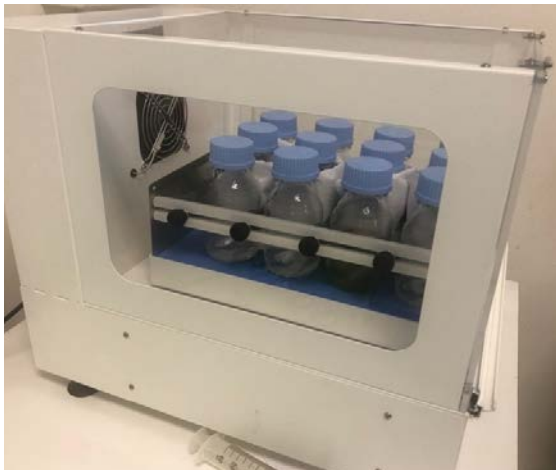

Figure 37: Glass bottles with sections of the plastic strips in agitation for performing leaching tests.

Figure 38: Vacuum filter system for the extraction of the solution obtained by shaking the plastic strips.

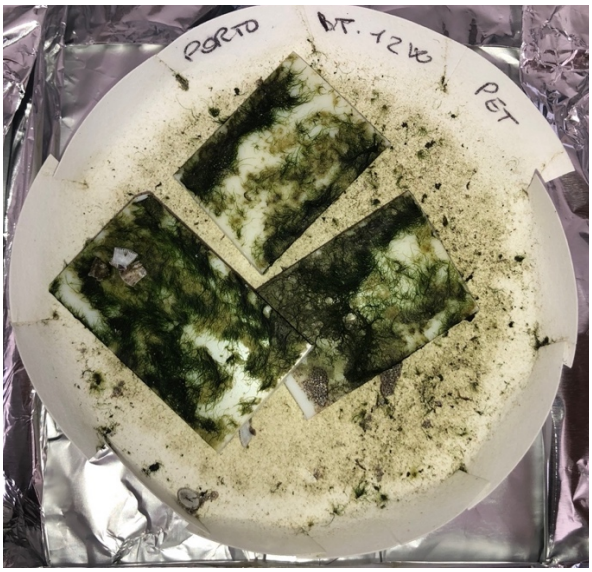

Figure 39: Filter paper with sections of the plastic strip obtained from the leaching test on which the dissolution was then carried out.

The filters of the lagoon and port environments after 28 weeks of exposure, with all the filtered material, obtained following the leaching tests, in addition to the control samples, were subjected to dissolution by attacks with hydrofluoric acid, nitric acid and hydrogen peroxide. The 27 solutions obtained were analyzed for lithium, beryllium, boron, sodium, magnesium, aluminum, phosphorus, potassium, calcium, scandium, titanium, vanadium, chromium, manganese, iron, cobalt, nickel, copper, zinc, gallium, arsenic, selenium, rubidium, strontium, molybdenum, silver, cadmium, tin, antimony, tellurium, barium, mercury, thallium, lead, bismuth and uranium ions by inductively coupled plasma-mass spectrometry (Thermo Scientific iCAP TQ ICP-MS).

The sediments below the testing racks sampled during the installations were subjected to grain size analysis using ASTM sieves, Giuliani Quadridimensional Sieveshaker IG/1 and Micromeritics Sedigraph 5100 and dissolution by attacks with hydrofluoric acid, nitric acid and hydrogen peroxide for subsequent analysis by inductively coupled plasma-mass spectrometry (Thermo Scientific iCAP TQ ICP-MS). The water samples collected both during installation and during subsequent sampling were analyzed with anion chromatography (Thermo Scientific Dionex ICS-1000) and inductively coupled plasma-mass spectrometry (Thermo Scientific iCAP TQ ICP-MS).

Statistical methods

Statistical analyzes were performed using Microsoft Excel (Microsoft 365) and Statistica 10 (Statisoft). With Excel, a first processing was carried out using descriptive statistics to determine the mean, median, minimum value, maximum value, and standard deviation of the available data. The descriptive statistics concerned the geochemical data of the sediments and water, the data of temperature and light intensity, the data of fouling mass, chlorophyll *a* accumulation, and apparent mass change in plastic strips. All this was associated with graphic processing with scatter and bar graphs.

Subsequently, factorial ANOVA (analysis of variance) was performed, individually for each environment, to assess the influence of plastic type (PS, PP, LDPE, HDPE, PVC or PET), depth zonation (intertidal or subtidal / submerged or semi-floating), and deployment time (4w, 8w, 12w, 16w, 20w or 28w), on apparent plastic mass change,

fouling mass, and Chl *a* accumulation. All analyzes were performed in Statistica 10. Three-way ANOVA were performed on data obtained from port, lagoon and river experiments. A two-way ANOVA was performed on data from the air experiment, to examine the effects of deployment time and plastic type.

Furthermore, to get an overview, four-way ANOVA was performed for the data of apparent mass change, fouling mass and chlorophyll *a*, considering the factors of location (environments), zonation, deployment time and plastic type for the port, lagoon and river environments. The air environment was not taken into consideration for this analysis as the data matrix is incomplete compared to the matrices of the other environments.

Factors and interaction terms that were not significant at $\alpha = 0.05$ were removed sequentially, and each model was re-analyzed. After the analysis of variance, a post-hoc test, Scheffé's test, was carried out for all the results obtained, which made possible to find out which pairs of means are significant.

Results

Summary of preliminary experiment in Maryland

The preliminary experiment in Maryland, published by Rizzo et al. (2021), demonstrated significant surface weathering of HDPE within 4 weeks of environmental exposure of the plastic strips deployed at subtidal and intertidal depths in contrasting conditions of hydrodynamic activity (erosional and depositional). While the mass change of HPDE was only marginal, extensive surface degradation was observed by SEM imaging, with the development of numerous grooves and pittings on the polymer surface. The PS strips degraded more rapidly than HDPE strips in all deployment locations, as determined by mass loss at 4 weeks, and by examination of the polymer surface (petrographic and SEM microscopy). Hydrodynamic conditions influenced the rate of surface weathering and fragmentation of PS, with larger cavity formation and significantly greater PS mass loss observed at the erosional site relative to the depositional site. While formation of fractures and cavities were evident by SEM among all PS strips retrieved after environmental exposure, cavities developing on the strips were larger (oblong) and appeared earlier at the erosional site (first appearance at 4 weeks), than at the depositional site (first appearance at 8 weeks). Given the similarity in light exposure, temperature, and oxygen conditions between the two sites, the greater degradation was most likely due to the greater mechanical weathering, either by direct abrasion and/or by inhibiting the formation of a biofilm, which tend to protect plastics from weathering. The effects of depth (intertidal versus subtidal) on plastic weathering were somewhat more complex, potentially due to non-linear interactions associated with fouling formation. Generally, PS strips exhibited greater weathering at intertidal depths than subtidal depths. This was most clearly seen at the erosional site at week 4, based on mass changes (i.e., among peroxide-washed samples), and was supported by microscopy, with PS strips at both erosional and depositional sites exhibiting signs of greater surface weathering including more cracking and pitting among intertidal samples.

Plastic strips of both types developed a fouling. Biofilms were detected as an increase in Chl *a* and a directly proportional increase in mass (as measured prior to peroxide-washing) and observed by microscopy. In the experiment, regardless of plastic type, greater fouling development occurred at subtidal depths.

Characterization of test sites

Sediment analysis

Grain size analyzes and ICP-MS analyzes were carried out for the grain size and geochemical characterization of the sediments present in the environments in which the plastic strips were exposed.

According to the Wentworth classification, the river environment was mainly composed of silt (almost 67%) and clay (almost 33%); the lagoon environment of fine sand (almost 61%), very find sand (almost 20%) and for the remainder of medium sand, clay and silt; the port environment, on the other hand, has a heterogeneous particle size, in fact there was the presence of all the particle size classes in a variable percentage between 20% and 3% (Table 2, Figure 40).

Table 2: Percentage of the respective grain size class for river, lagoon and port sediments according to the Wentworth classification.

(%)	River	Lagoon	Port
Gravel	0	0	20.15
Very coarse sand	0	0	12.54
Coarse sand	0	0	16.46
Medium sand	0	7.63	14.45
Fine sand	0	60.85	7.35
Very find sand	0.68	19.74	3.09
Silt	66.62	5.44	13.44
Clay	32.71	6.35	12.51

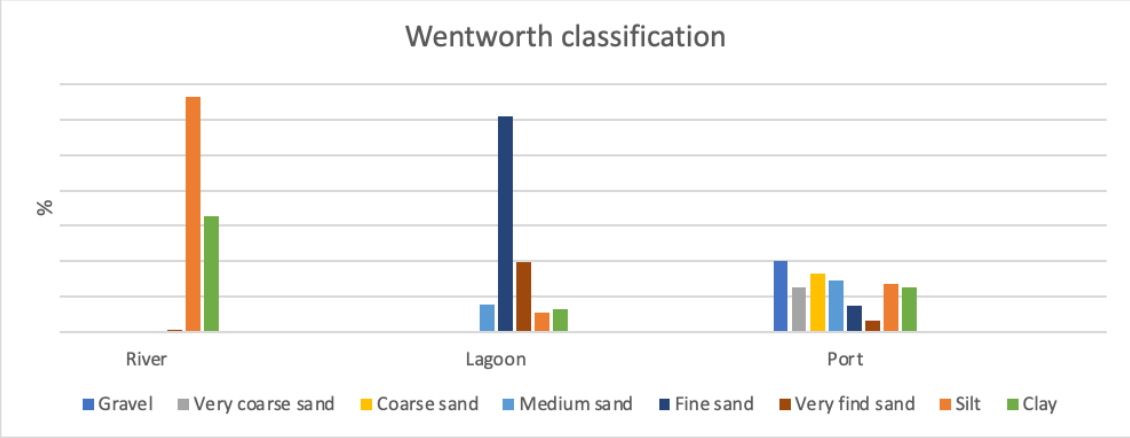

Figure 40: Graph with the percentages of the granulometric classes in accordance with the Wentworth classification of the sediments of the environments in which the plastic strips have been exposed.

It was also added that the sample coming from the river had a prevalence of organic substance which was removed by dissolution by means of hydrogen peroxide (35%). Figure 41 shows the trend of the cumulative curves of the sediment samples.

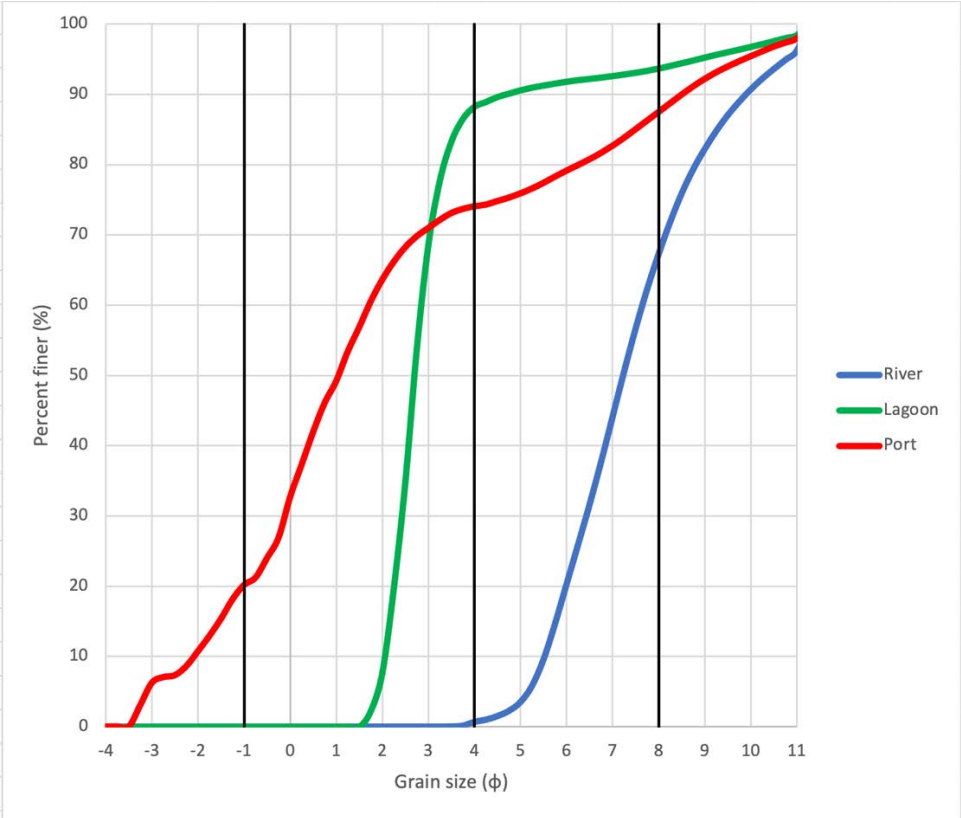

Figure 41: Cumulative curves of the sediment samples.

The concentrations of the cations present in the solutions obtained by acid attack of the sediment samples are shown in Table 3.

Table 3: Results, expressed in ppm, of multi-element analysis in sediments by inductively coupled plasma-mass spectrometry.

(ppm)	River	Lagoon	Port
Li	43.1	28.0	10.2
Be	2.0	1.8	0.8
B	39.2	30.8	42.2
Na	4043.5	17020.4	11427.0
Mg	8004.3	10140.4	10311.5
Al	47459.3	40721.5	13948.0
P	1563.9	684.4	1742.9
K	9754.6	16607.1	5042.9
Ca	120224.0	62540.2	241997.7
Sc	9.4	6.8	4.3
Ti	3140.3	1598.9	1566.2
V	115.7	59.3	56.0
Cr	120.4	147.9	81.2
Mn	312.0	906.3	377.0
Fe	32155.2	19523.4	23931.6
Co	12.1	12.2	7.7
Ni	35.5	74.6	28.5
Cu	33.8	9.4	815.4
Zn	96.2	48.2	451.4
Ga	16.9	11.3	4.9
As	12.2	4.5	10.7
Se	2.2	0.1	0.2
Rb	58.1	51.7	14.5
Sr	223.1	261.3	675.3
Mo	1.2	0.2	4.4
Ag	0.3	0.0	0.6
Cd	0.4	0.1	0.3
Sn	1.7	1.5	7.3
Sb	0.4	0.3	1.0
Te	0.1	0.0	0.0
Ba	149.2	200.9	183.5
Hg	0.1	0.1	0.0
Tl	0.4	0.3	0.2
Pb	21.4	9.1	116.1
Bi	0.2	0.1	0.2
U	1.9	0.9	1.5

Water chemical characterization

For the geochemical characterization and monitoring of the waters in which the plastic strips were immersed, measurements of the chemical-physical parameters and analysis of the ions present in solution were carried out. The pH, electrical conductivity (EC), total dissolved solids (TDS) and salinity values and the concentration of anions and cations in the water during the entire exposure period were then determined.

The values of pH, EC, TDS and salinity (Table 4) and the concentrations of anions and cations (Table 5, Table 6, Table 7, Table 8) obtained from the measurements and analyzes have been studied by means of the descriptive statistics.

Table 4: Descriptive statistic of the chemical-physical parameters of the water measured by the HI98195 probe.

	Mean	Median	Minimum	Maximum	Std.Dev.
River					
pH	7.19	7.22	7.00	7.30	0.11
EC (ms/cm)	2.93	2.97	2.51	3.18	0.21
TDS (ppt)	1.47	1.49	1.25	1.59	0.10
Sal (psu)	1.53	1.56	1.30	1.67	0.11
Lagoon					
pH	8.05	8.16	7.78	8.22	0.19
EC (ms/cm)	32.52	27.09	23.07	44.44	8.82
TDS (ppt)	16.69	16.23	11.83	22.22	4.19
Sal (psu)	20.45	16.69	14.49	28.67	5.96
Port (bottom)					
pH	8.15	8.17	8.03	8.24	0.07
EC (ms/cm)	58.32	57.93	57.59	59.09	0.65
TDS (ppt)	29.16	28.96	28.79	29.54	0.33
Sal (psu)	38.93	38.67	38.41	39.61	0.55
Port (surface)					
pH	8.14	8.15	7.93	8.24	0.10
EC (ms/cm)	54.25	55.21	47.73	58.59	3.87
TDS (ppt)	27.12	27.60	23.86	29.29	1.93
Sal (psu)	35.90	36.60	31.15	39.21	2.85

Table 5: Descriptive statistic of the concentration of ions present in the river water in which the plastic strips have been immersed.

River					
(ppm)	Mean	Median	Minimum	Maximum	Std.Dev.
F^-	0.20	0.18	0.16	0.26	0.04
Cl^-	1006.67	1040.41	726.76	1081.31	125.43
NO_2^-	n.d.				
Br^-	2.37	2.38	1.65	2.73	0.35
NO_3^-	19.10	20.09	13.36	20.85	2.62
PO_4^{3-}	n.d.				
SO_4^{2-}	119.20	117.70	115.97	125.15	3.34
Li	0.01	0.01	0.01	0.01	0.00
Be	0.00	0.00	0.00	0.00	0.00
B	0.18	0.19	0.15	0.19	0.02
Na	134.42	134.86	126.06	140.78	5.39
Mg	44.65	48.59	29.75	50.52	8.19
Al	0.00	0.00	0.00	0.00	0.00
P	0.01	0.01	0.00	0.02	0.01
K	13.97	14.49	10.52	14.88	1.56
Ca	70.04	64.30	57.49	92.51	12.70
Sc	0.00	0.00	0.00	0.00	0.00
Ti	0.03	0.03	0.02	0.05	0.01
V	0.00	0.00	0.00	0.00	0.00
Cr	0.00	0.00	0.00	0.00	0.00
Mn	0.00	0.00	0.00	0.01	0.00
Fe	0.00	0.00	0.00	0.00	0.00
Co	0.00	0.00	0.00	0.00	0.00
Ni	0.00	0.00	0.00	0.00	0.00
Cu	0.00	0.00	0.00	0.00	0.00
Zn	0.00	0.00	0.00	0.01	0.00
Ga	0.00	0.00	0.00	0.00	0.00
As	0.00	0.00	0.00	0.00	0.00
Se	0.00	0.00	0.00	0.00	0.00
Rb	0.00	0.00	0.00	0.00	0.00
Sr	0.71	0.70	0.55	0.79	0.08
Mo	0.00	0.00	0.00	0.00	0.00
Ag	0.00	0.00	0.00	0.00	0.00
Cd	0.00	0.00	0.00	0.00	0.00
Sn	0.00	0.00	0.00	0.00	0.00
Sb	0.00	0.00	0.00	0.00	0.00
Te	0.00	0.00	0.00	0.00	0.00
Ba	0.01	0.01	0.01	0.02	0.00
Hg	0.00	0.00	0.00	0.00	0.00
Tl	0.00	0.00	0.00	0.00	0.00
Pb	0.00	0.00	0.00	0.00	0.00
Bi	0.00	0.00	0.00	0.00	0.00
U	0.00	0.00	0.00	0.00	0.00

Table 6: Descriptive statistic of the concentration of ions present in the lagoon water in which the plastic strips have been immersed.

Lagoon					
(ppm)	Mean	Median	Minimum	Maximum	Std.Dev.
F^-	0.85	0.81	0.38	1.46	0.36
Cl^-	14764.85	13777.90	9258.12	22008.58	4538.53
NO_2^-	n.d.				
Br^-	33.48	29.52	22.09	53.05	10.37
NO_3^-	2.76	2.76	2.34	3.17	0.58
PO_4^{3-}	n.d.				
SO_4^{2-}	1870.32	1797.25	1292.93	2743.89	534.99
Li	0.09	0.08	0.06	0.13	0.03
Be	0.00	0.00	0.00	0.00	0.00
B	2.40	2.28	1.53	3.44	0.77
Na	2293.05	2342.89	1948.08	2553.35	204.08
Mg	387.61	390.56	244.35	540.37	108.22
Al	0.04	0.00	0.00	0.15	0.06
P	0.06	0.08	0.00	0.15	0.06
K	184.47	176.48	118.42	268.03	58.64
Ca	204.25	192.94	136.28	293.00	59.68
Sc	0.00	0.00	0.00	0.00	0.00
Ti	0.11	0.11	0.06	0.16	0.04
V	0.00	0.00	0.00	0.00	0.00
Cr	0.00	0.00	0.00	0.00	0.00
Mn	0.01	0.01	0.00	0.04	0.01
Fe	0.07	0.05	0.00	0.22	0.08
Co	0.00	0.00	0.00	0.00	0.00
Ni	0.00	0.00	0.00	0.00	0.00
Cu	0.00	0.00	0.00	0.01	0.00
Zn	0.01	0.00	0.00	0.02	0.01
Ga	0.00	0.00	0.00	0.00	0.00
As	0.00	0.00	0.00	0.00	0.00
Se	0.00	0.00	0.00	0.00	0.00
Rb	0.05	0.05	0.03	0.07	0.02
Sr	3.81	3.80	2.26	5.32	1.22
Mo	0.00	0.00	0.00	0.00	0.00
Ag	0.00	0.00	0.00	0.00	0.00
Cd	0.00	0.00	0.00	0.00	0.00
Sn	0.00	0.00	0.00	0.00	0.00
Sb	0.00	0.00	0.00	0.00	0.00
Te	0.00	0.00	0.00	0.00	0.00
Ba	0.03	0.02	0.02	0.04	0.01
Hg	0.00	0.00	0.00	0.03	0.01
Tl	0.00	0.00	0.00	0.00	0.00
Pb	0.00	0.00	0.00	0.00	0.00
Bi	0.00	0.00	0.00	0.00	0.00
U	0.00	0.00	0.00	0.00	0.00

Table 7: Descriptive statistic of the concentration of ions present in the port bottom water in which the plastic strips have been immersed.

Port (bottom)					
(ppm)	Mean	Median	Minimum	Maximum	Std.Dev.
F^-	1.68	1.44	1.03	2.66	0.60
Cl^-	27148.26	27988.80	20712.83	30462.88	3272.65
NO_2^-	n.d.				
Br^-	60.58	63.08	47.23	68.11	7.59
NO_3^-	n.d.				
PO_4^{3-}	n.d.				
SO_4^{2-}	2967.37	3039.23	2299.15	3200.97	291.25
Li	0.18	0.18	0.14	0.20	0.02
Be	0.00	0.00	0.00	0.00	0.00
B	4.81	4.86	3.89	5.46	0.43
Na	3480.67	3496.56	3279.36	3622.23	105.87
Mg	1153.30	1179.64	931.67	1261.03	98.11
Al	0.92	0.56	0.21	3.68	1.15
P	4.66	2.19	0.17	24.37	8.13
K	379.51	387.26	308.95	413.65	31.09
Ca	383.07	392.02	302.62	426.10	35.49
Sc	0.00	0.00	0.00	0.00	0.00
Ti	0.19	0.19	0.14	0.22	0.02
V	0.00	0.00	0.00	0.00	0.00
Cr	0.00	0.00	0.00	0.01	0.00
Mn	0.01	0.01	0.00	0.05	0.02
Fe	0.25	0.12	0.01	1.26	0.42
Co	0.00	0.00	0.00	0.00	0.00
Ni	0.03	0.02	0.00	0.14	0.05
Cu	0.04	0.02	0.00	0.18	0.06
Zn	0.12	0.06	0.00	0.61	0.20
Ga	0.00	0.00	0.00	0.00	0.00
As	0.00	0.00	0.00	0.00	0.00
Se	0.00	0.00	0.00	0.00	0.00
Rb	0.11	0.11	0.09	0.12	0.01
Sr	8.36	8.63	6.60	8.79	0.73
Mo	0.01	0.01	0.01	0.02	0.00
Ag	0.00	0.00	0.00	0.00	0.00
Cd	0.00	0.00	0.00	0.00	0.00
Sn	0.01	0.01	0.00	0.06	0.02
Sb	0.00	0.00	0.00	0.02	0.01
Te	0.00	0.00	0.00	0.00	0.00
Ba	0.03	0.02	0.01	0.11	0.03
Hg	0.00	0.00	0.00	0.00	0.00
Tl	0.00	0.00	0.00	0.00	0.00
Pb	0.01	0.00	0.00	0.04	0.01
Bi	0.00	0.00	0.00	0.00	0.00
U	0.00	0.00	0.00	0.00	0.00

Table 8: Descriptive statistic of the concentration of ions present in the port surface water in which the plastic strips have been immersed.

Port (surface)					
(ppm)	Mean	Median	Minimum	Maximum	Std.Dev.
F^-	1.38	1.35	0.74	1.90	0.46
Cl^-	20838.56	19701.31	14729.78	31019.66	5905.76
NO_2^-	n.d.				
Br^-	46.72	45.27	33.64	66.85	11.98
NO_3^-	3.16	3.16	3.16	3.16	
PO_4^{3-}	n.d.				
SO_4^{2-}	2309.37	2120.82	1733.18	3347.24	578.85
Li	0.16	0.16	0.11	0.19	0.03
Be	0.00	0.00	0.00	0.00	0.00
B	4.17	4.23	3.15	4.86	0.60
Na	2859.76	2610.92	2483.86	3684.52	516.73
Mg	753.62	747.35	493.19	1072.06	189.90
Al	0.55	0.62	0.20	0.93	0.29
P	3.31	0.74	0.22	13.47	4.71
K	328.99	338.57	246.26	402.10	54.18
Ca	350.91	353.74	291.09	414.75	43.38
Sc	0.00	0.00	0.00	0.00	0.00
Ti	0.19	0.18	0.16	0.23	0.03
V	0.00	0.00	0.00	0.01	0.00
Cr	0.01	0.00	0.00	0.03	0.01
Mn	0.01	0.01	0.00	0.03	0.01
Fe	0.15	0.08	0.04	0.45	0.14
Co	0.00	0.00	0.00	0.00	0.00
Ni	0.02	0.01	0.00	0.07	0.02
Cu	0.03	0.01	0.00	0.10	0.03
Zn	0.10	0.09	0.02	0.29	0.09
Ga	0.00	0.00	0.00	0.00	0.00
As	0.00	0.00	0.00	0.01	0.00
Se	0.00	0.00	0.00	0.00	0.00
Rb	0.10	0.10	0.07	0.11	0.01
Sr	7.15	7.09	5.46	8.27	1.02
Mo	0.01	0.01	0.00	0.01	0.00
Ag	0.00	0.00	0.00	0.00	0.00
Cd	0.00	0.00	0.00	0.00	0.00
Sn	0.01	0.00	0.00	0.03	0.01
Sb	0.00	0.00	0.00	0.00	0.00
Te	0.00	0.00	0.00	0.00	0.00
Ba	0.03	0.02	0.01	0.08	0.02
Hg	0.00	0.00	0.00	0.00	0.00
Tl	0.00	0.00	0.00	0.00	0.00
Pb	0.01	0.00	0.00	0.02	0.01
Bi	0.00	0.00	0.00	0.00	0.00
U	0.00	0.00	0.00	0.00	0.00

Temperature and light intensity monitoring

The monitoring performed by hobo sensors made possible to determine the variations in temperature and light intensity during the 36 weeks of exposure in both aquatic and airborne environments.

Table 9, Table 10, Table 11, Table 12 show the monthly average values of temperature and light intensity recorded during exposure. The trends of the individual parameters recorded in each environment are also reported in Figure 42, Figure 43, Figure 44, Figure 45, Figure 46, Figure 47 and Figure 48.

The water temperature of the river presented a constant trend throughout the research period, both on the surface and in depth, with values ranging between 17°C and 18°C. The light intensity had very variable patterns due to the presence of vegetation along the banks of the river and on the surface of the water which hindered radiation (Figure 42 and Figure 43).

In the lagoon, the temperature varied according to the seasonal trend. In the subtidal zone it had more restricted ranges of variations as the sensor, and therefore the plastics, had always been immersed: during the hottest months it varied between 25°C and 30°C, while in the colder months between 5°C and 10°C. In the intertidal zone, on the other hand, a more marked oscillation was observed due to the cyclic emergence and immersion of the structure, with temperatures ranging between 20°C and 35°C in the warmer months and between 0°C and 10°C in the cold months.

The light intensity data were not reliable as the strong and sudden colonization of the sensors by the biofouling, associated with logistical difficulties in cleaning the HOBO sensors, did not allow the recording in an optimal and continuous way (Figure 44 and Figure 45).

In the port environment, the temperature had values that varied according to the seasonal trend. However, there were differences between the two zones. In the subtidal zone, the temperature had narrower ranges of variations as the sensor, and therefore the plastics, had always been immersed, with temperatures ranging between 25°C and 30°C in the warmer months, and around 15°C in the colder months. In the intertidal

zone, on the other hand, a more marked oscillation was observed due to the cyclic emergence and immersion of the structure, with temperatures ranging between 20°C and 50°C in the warmer months and between 5°C and 25°in the colder months.

In the intertidal zone, the light intensity followed the temperature trend with maximum values recorded in emergence of 200,000 Lux during the summer and values ranging between 50,000 Lux and 100,000 Lux in the winter. In the subtidal zone, the maximum values did not exceed 50 thousand Lux in the summer and 10 thousand Lux in the winter, as the water had a shielding effect.

Especially in the subtidal zone, a cyclical trend was observed with higher values of light intensity in conjunction with the sampling dates, which decreased over time, due to the cleaning of the sensor and the subsequent accumulation of fouling on the sensor. This phenomenon was more evident in the summer and less marked in the colder periods (Figure 46 and Figure 47).

In the air environment, the seasonal temperature oscillated from 20°C at night to 60°C during the day from June to September, and from 10°C at night to 30°C during the day from October to February. The light intensity followed the seasonal trend of temperature values with values above 150 thousand Lux between June and August, which decreased gradually between September and December with maximum values around 100 thousand Lux and then increased again in February (Figure 48).

Table 9: Monthly average values of temperature and light intensity recorded during exposure in the river environment, submerged on the left and semi-floating on the right.

River - S			River - F		
	Temperature (°C)	Intensity (Lux)		Temperature (°C)	Intensity (Lux)
2020			**2020**		
August	18.5	24	August	18.9	1873
September	18.2	409	September	18.5	4101
October	17.7	434	October	17.8	5738
November	17.4	685	November	17.4	2186
December	17.0	963	December	16.8	3494
2021			**2021**		
January	17.0	1172	January	16.9	1963
February	17.1	2277	February	17.0	1864
March	17.1	1399	March	17.1	4117
April	17.4	411	April	17.4	3261

Table 10: Monthly average values of temperature and light intensity recorded during exposure in the lagoon environment, subtidal on the left and intertidal on the right.

Lagoon - ST			Lagoon - IT		
	Temperature (°C)	Intensity (Lux)		Temperature (°C)	Intensity (Lux)
2020			**2020**		
July	28.1	3049	July	27.9	21577
August	28.8	286	August	28.1	2915
September	24.5	448	September	23.5	3521
October	17.4	209	October	17.1	1238
November	14.0	702	November	13.0	3238
December	9.3	198	December	8.9	817
2021			**2021**		
January	7.5	254	January	6.5	1733
February	9.4	227	February	9.3	14783
March	13.1	118	March	12.5	34377

Table 11: Monthly average values of temperature and light intensity recorded during exposure in the port environment, subtidal on the left and intertidal on the right.

Port - ST			Port - IT		
	Temperature (°C)	Intensity (Lux)		Temperature (°C)	Intensity (Lux)
2020			**2020**		
June	23.9	8579	June	27.8	48810
July	27.4	5104	July	31.0	54608
August	29.0	2889	August	30.2	45858
September	27.1	2710	September	27.3	30226
October	23.7	1602	October	22.5	18515
November	21.1	815	November	18.9	14065
December	18.5	471	December	16.9	8260
2021			**2021**		
January	16.2	623	January	14.5	10022
February	15.8	475	February	14.9	8195

Table 12: Monthly average values of temperature and light intensity recorded during exposure in the airborne environment.

Air		
	Temperature (°C)	Intensity (Lux)
2020		
June	31.5	69160
July	34.0	63922
August	34.4	52838
September	28.2	35217
October	22.5	25685
November	18.3	16881
December	14.0	12158
2021		
January	13.6	4250
February	15.1	19406

Figure 42: Trends of the temperature (top) and light intensity (bottom) parameters recorded by the HOBO sensor in the submerged river environment.

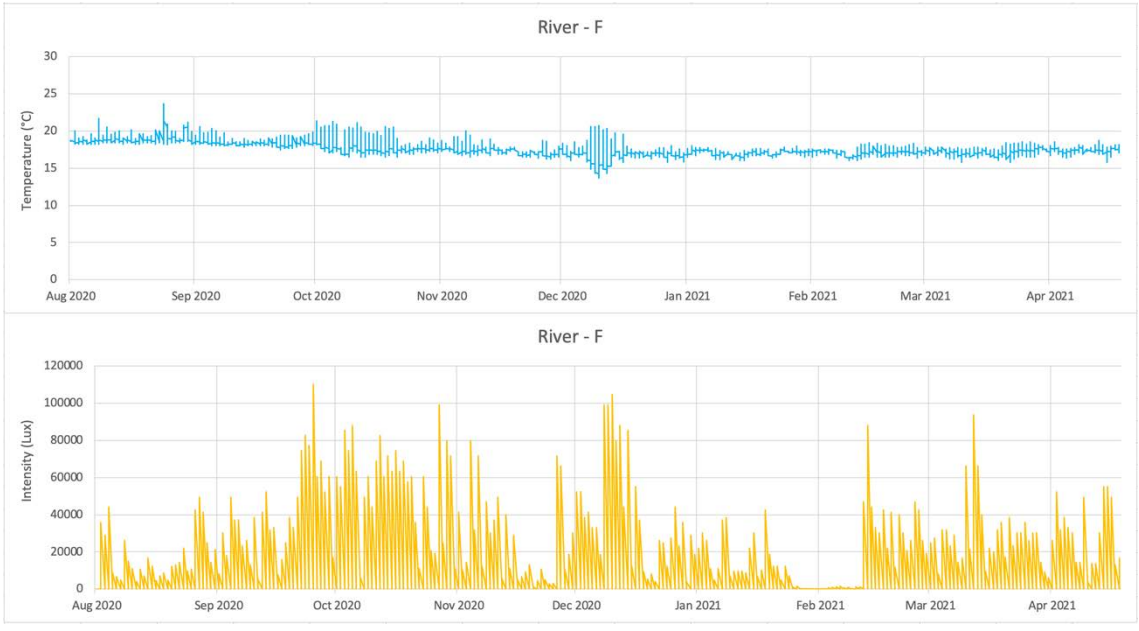

Figure 43: Trends of the temperature (top) and light intensity (bottom) parameters recorded by the HOBO sensor in the semi-floating river environment.

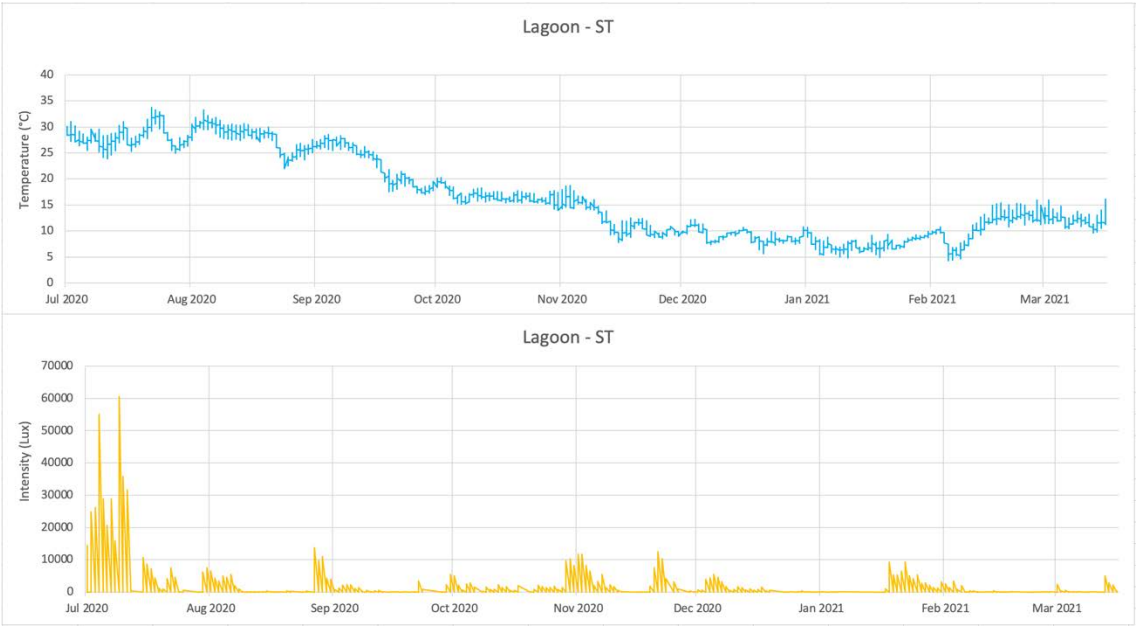

Figure 44: Trends of the temperature (top) and light intensity (bottom) parameters recorded by the HOBO sensor in the subtidal zone of the lagoon environment.

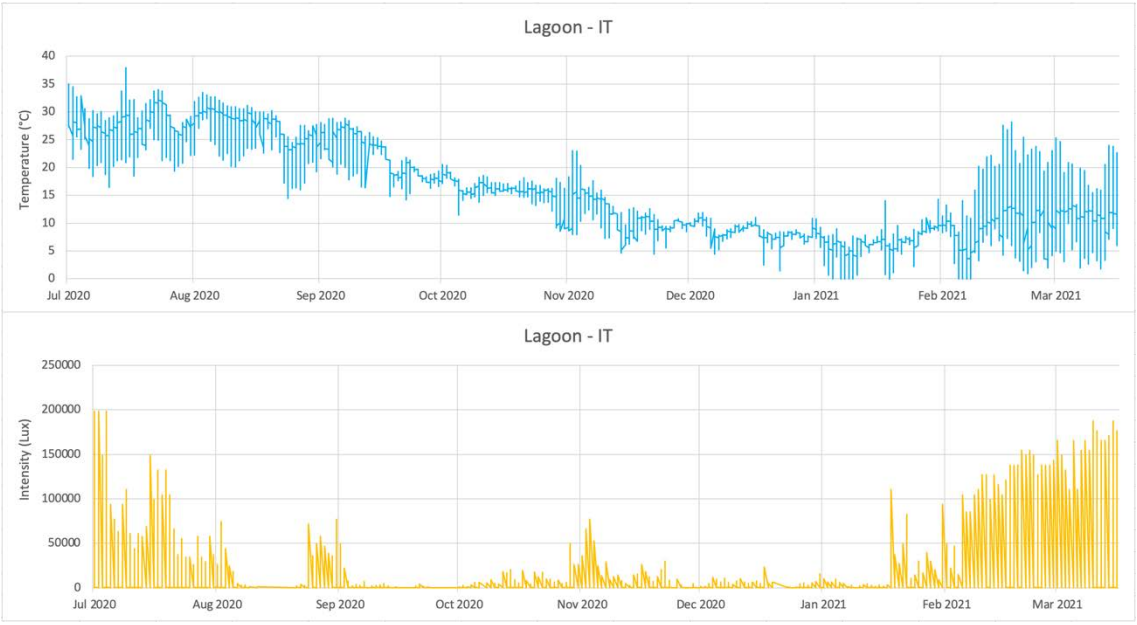

Figure 45: Trends of the temperature (top) and light intensity (bottom) parameters recorded by the HOBO sensor in the intertidal zone of the lagoon environment.

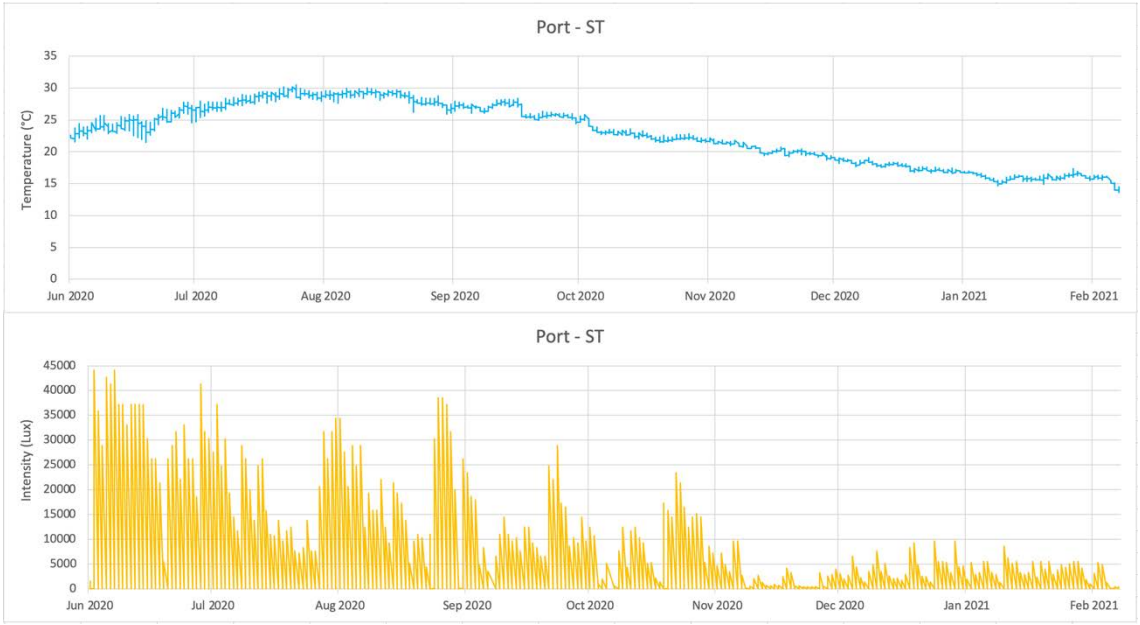

Figure 46: Trends of the temperature (top) and light intensity (bottom) parameters recorded by the HOBO sensor in the subtidal zone of the port environment.

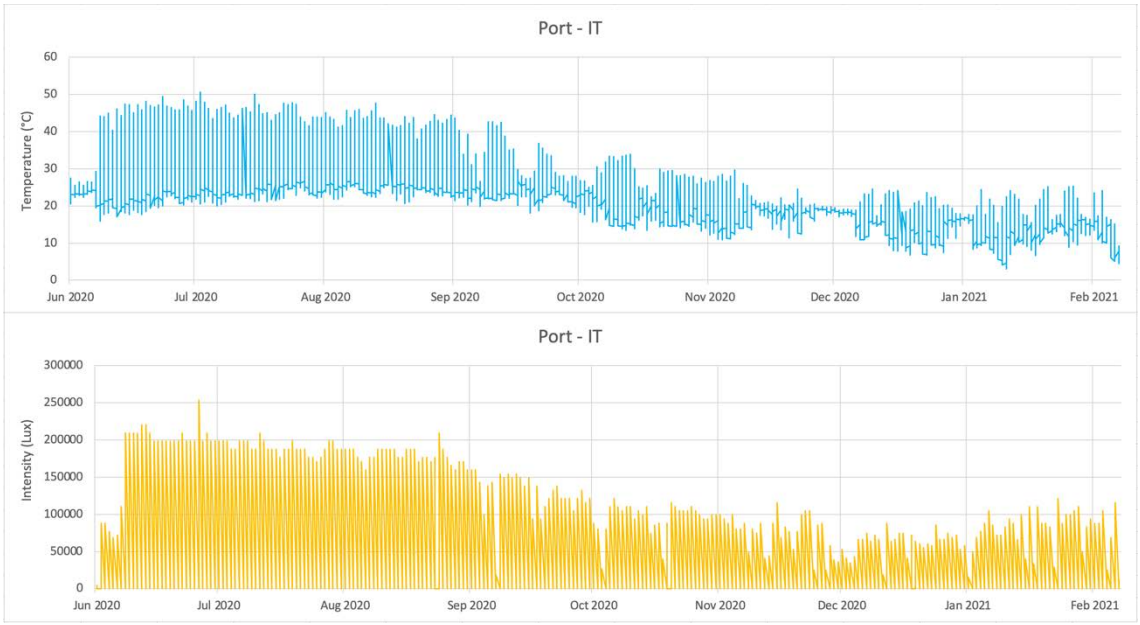

Figure 47: Trends of the temperature (top) and light intensity (bottom) parameters recorded by the HOBO sensor in the intertidal zone of the port environment.

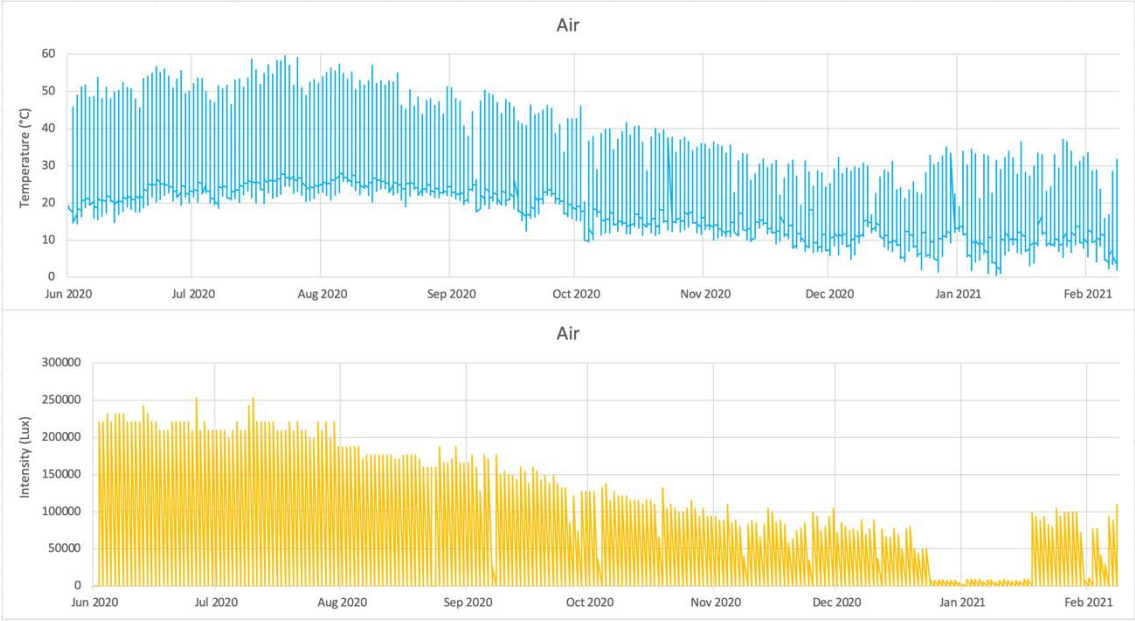

Figure 48: Trends of the temperature (top) and light intensity (bottom) parameters recorded by the HOBO sensor in the airborne environment.

Plastic strips recovery

There was no evidence of degradation of the plastics exposed in the river environment over the course of 36 weeks (Figure 49). The development of fouling on the surface was very mild. In the semi-floating strips, a change in color was found between 12 and 16 weeks of exposure with a slight accumulation of the biofilm after 20 weeks. Among the submerged strips, the color change occurred after 28 weeks of exposure, but to a lesser degree than in the semi-floating strips, in conjunction with a low development of biofilm, also less than in the semi-floating strips.

In the lagoon environment, by 4 weeks of exposure, the PS strips were no longer present. At both depths, subtidal and intertidal, there was a marked growth of biofouling from the beginning of exposure, which decreased over time (Figure 50). Macroscopically, there were no substantial differences between the types of plastic. Algae growth appeared greater in the intertidal environment than in the subtidal one. In the intertidal the algae were filamentous and branched, while in the subtidal they were mostly encrusting. In the subtidal environment there was a slight colonization by encrusting organisms (barnacles) of small dimensions in HDPE and LDPE and of larger dimensions in PVC and PET, while in the intertidal one, after 36 weeks of exposure, colonization by part of mussels.

In the port environment, a gradual development of the fouling was observed up to 20 or 28 weeks of exposure depending on the type of plastic, with a subsequent decrease in the quantity of fouling (Figure 51). In the subtidal environment, the biofilm appeared in the form of green encrustations while in the intertidal one it was mainly filamentous and branched. Both in the intertidal and in the subtidal, PS, PP, HDPE and LDPE had a more uniform growth of biofilm on the surface of the strip, while in PVC and PET the growth occurred in a less uniform manner, in spots. During the sampling at 20 weeks, the dispersion of the PS strips from the structure placed in the intertidal environment was noted. During the sampling after 36 weeks of exposure, all the plastics presented in the subtidal structure were covered with fine sediment.

In the strips of HDPE, LDPE, PVC and PET exposed to air, macroscopically, there were no significant changes during the entire period (Figure 52). The PP strips showed, after 28 weeks of exposure, the presence of fractures on the surface (Figure 53). The PS strips, on the other hand, already after 4 weeks of exposure, were dispersed into the environment.

The temporal evolution from 4 to 36 weeks of exposure of the different types of plastics for the different environments is reported below. The photo of a strip was randomly selected by type and for each sampling.

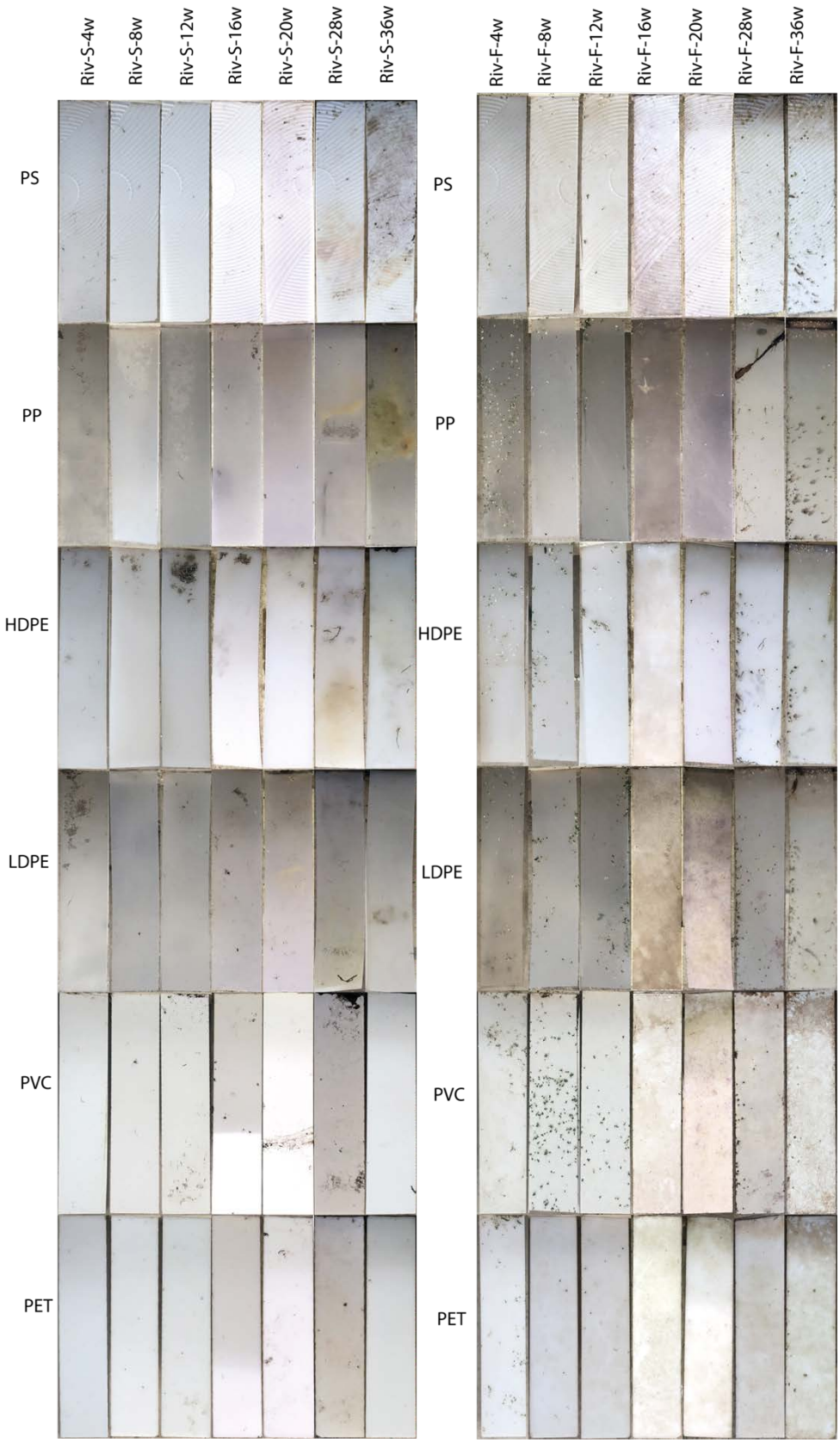

Figure 49: Temporal evolution of the different types of plastics exposed to river environments, submerged on the left, semi-floating on the right.

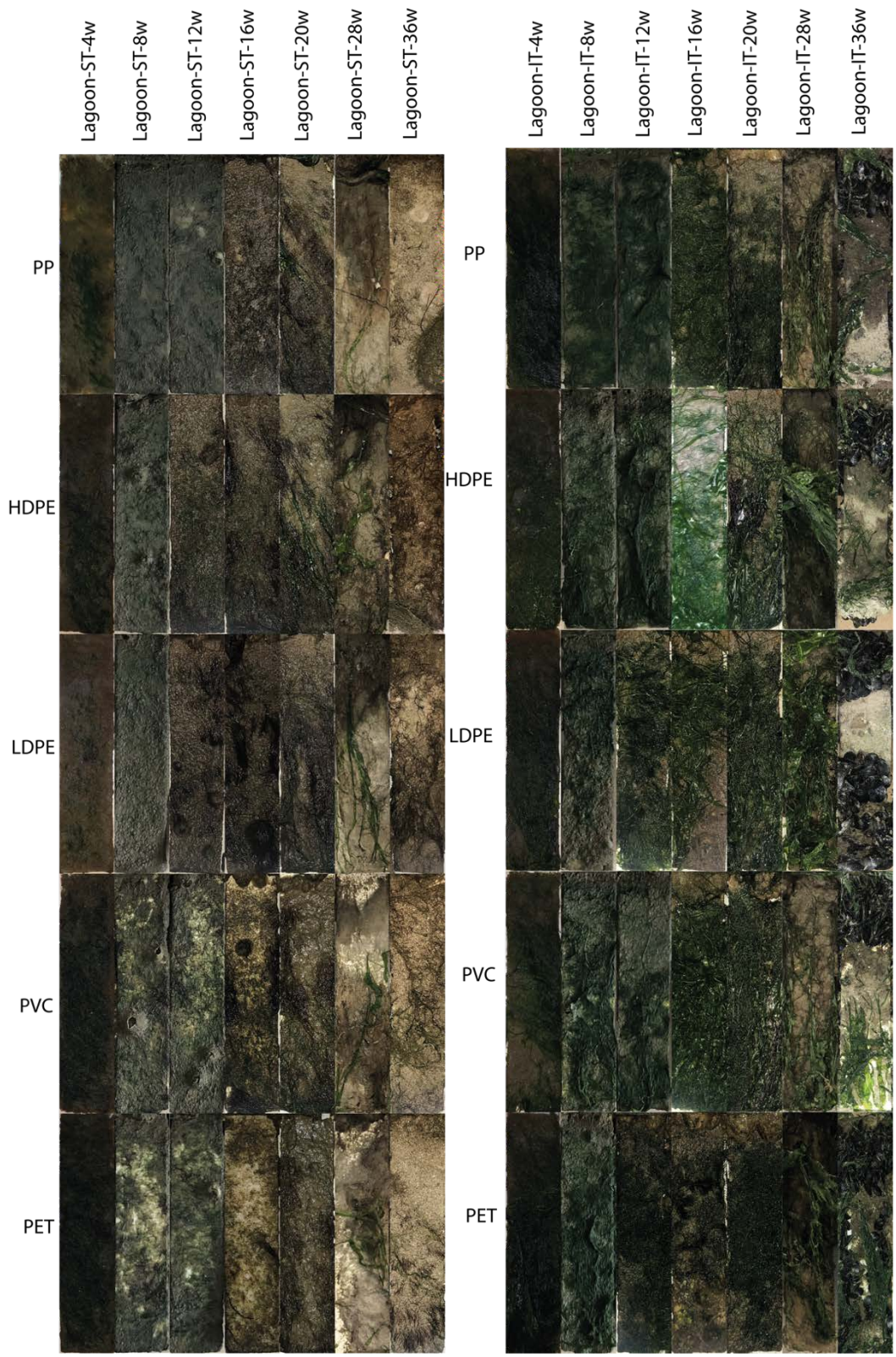

Figure 50: Temporal evolution of the different types of plastics exposed to lagoon environments, in subtidal and intertidal conditions on the left and right respectively.

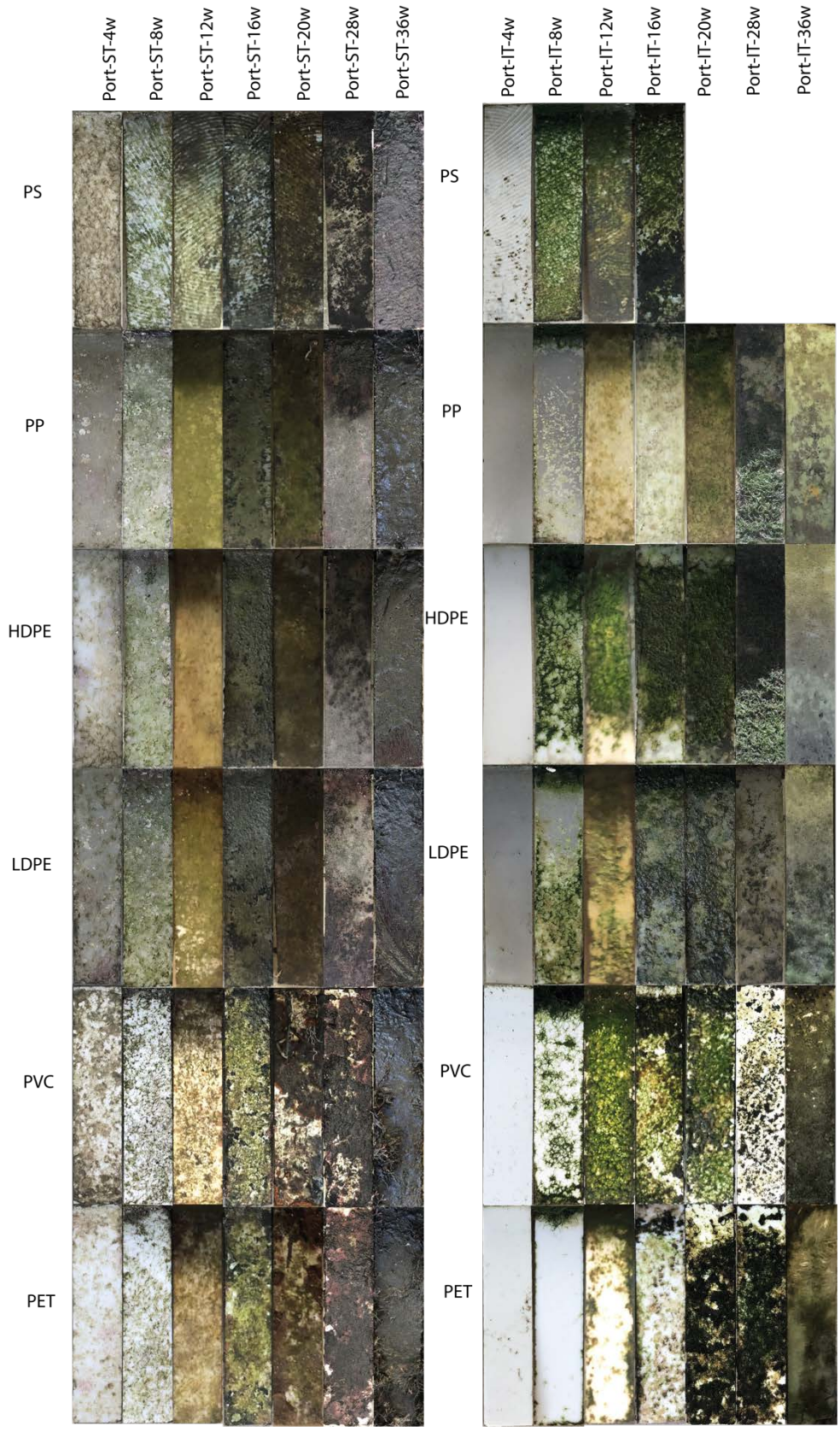

Figure 51: Temporal evolution of the different types of plastics exposed to port environments, in subtidal and intertidal conditions on the left and right respectively.

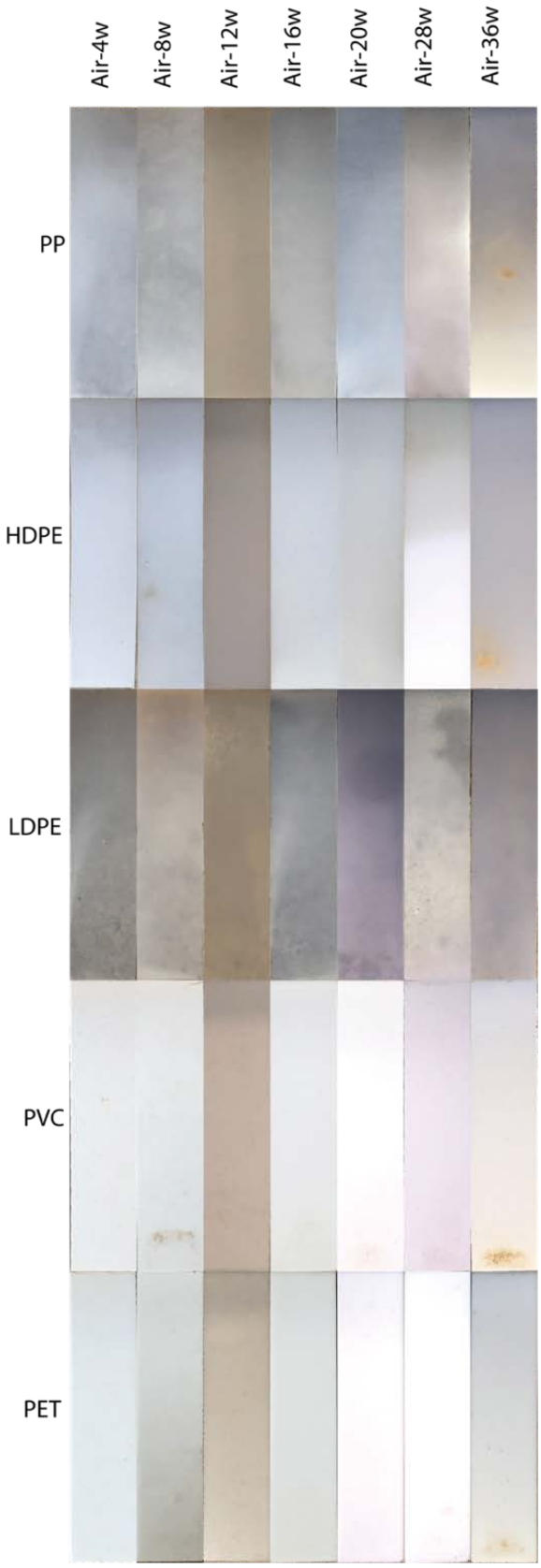

Figure 52: Temporal evolution of the different types of plastics exposed to airborne environment.

Figure 53: Fractures on the surface of the PP strips exposed in the air environment.

In Figure 54, some photos show, by way of example, the temporal evolution of the lower surface of the plastic strips exposed in the lagoon and port environment, that is, in those two environments where there was a greater development of fouling.

The underside of the plastic strips was not directly exposed to sunlight and, as a result, developed a completely different fouling than that which formed on the upper surface of the strips. A greater colonization was noted, in both environments, by encrusting organisms, more markedly in the lagoon environment than in the port one. By comparing the two exposure zones, in the subtidal one there was a greater development of organisms, both in quantity and in size. Comparing the types of plastic, the greatest development occurred on PVC and PET.

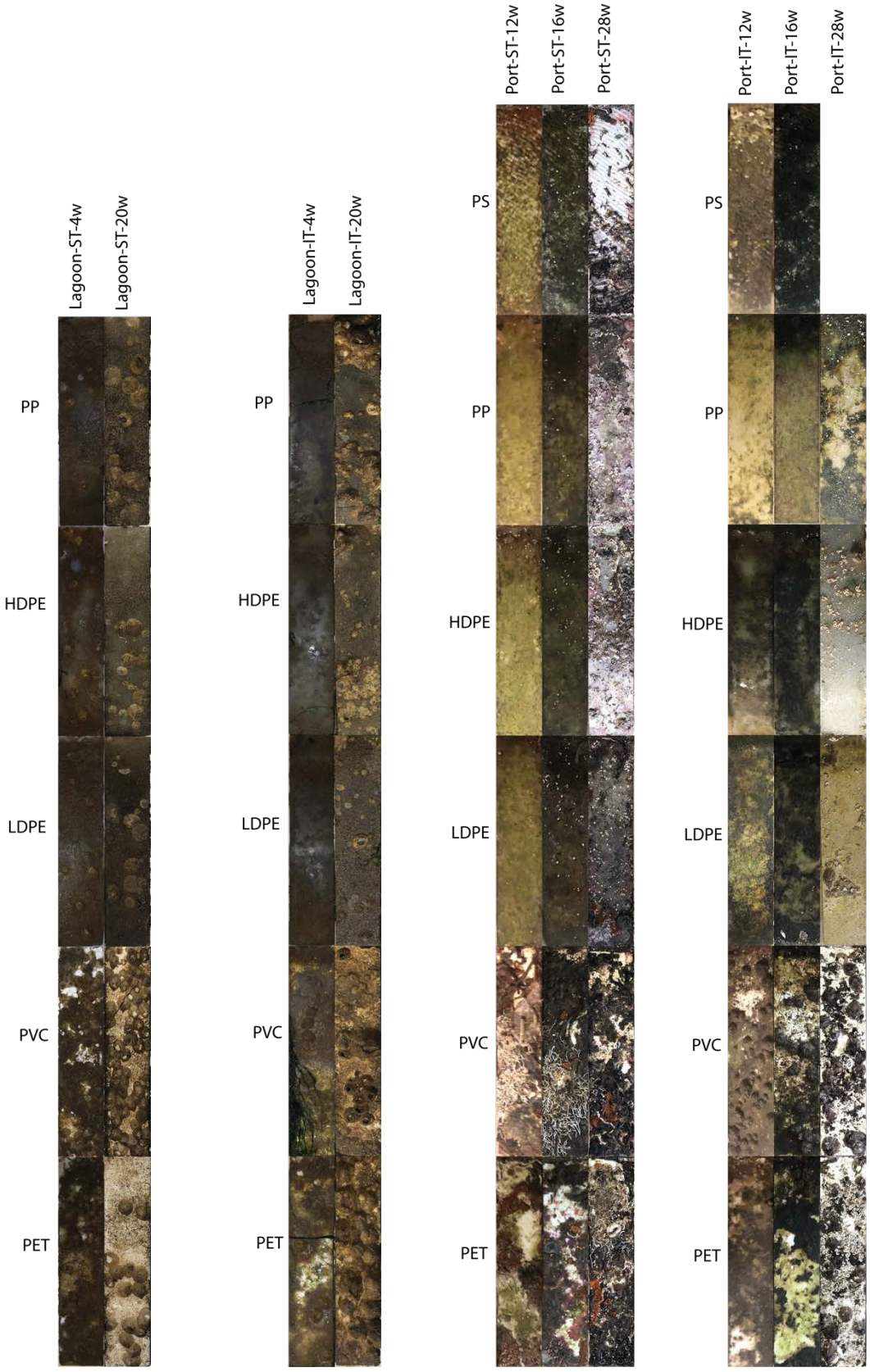

Figure 54: Photos of the lower surface of the plastic strips exposed in the lagoon and port environment.

Fragmentation

None of the HDPE, PVC and PET strips were visibly broken or fragmented at any sampling week. By contrast, the PS strips suffered breakage, with consequent total dispersion in the environment. In the lagoon environment, at both depths (intertidal and subtidal) and in air, all PS strips were detached and dispersed in the environment. In the intertidal port environment after 12 weeks of exposure 10% of the PS strips exhibited fragmentation, after 16 weeks 60% of plastic strips exhibited fragmentation, and after 20 weeks 100% of the PS strips exhibited fragmentation. In the subtidal port environment, 30% of the PS strips were broken after 36 weeks of exposure. In the river environment, both submerged and semi-floating, they had not suffered breakage (Figure 55, Table 13).

Some PP strips broke in the air environment after 36 weeks of exposure (2 out of 10), while in the other environments they were totally recovered.

In the air environment, 4 out of 20 strips of LDPE broke after 28 weeks of exposure and 3 out of 10 after 36 weeks.

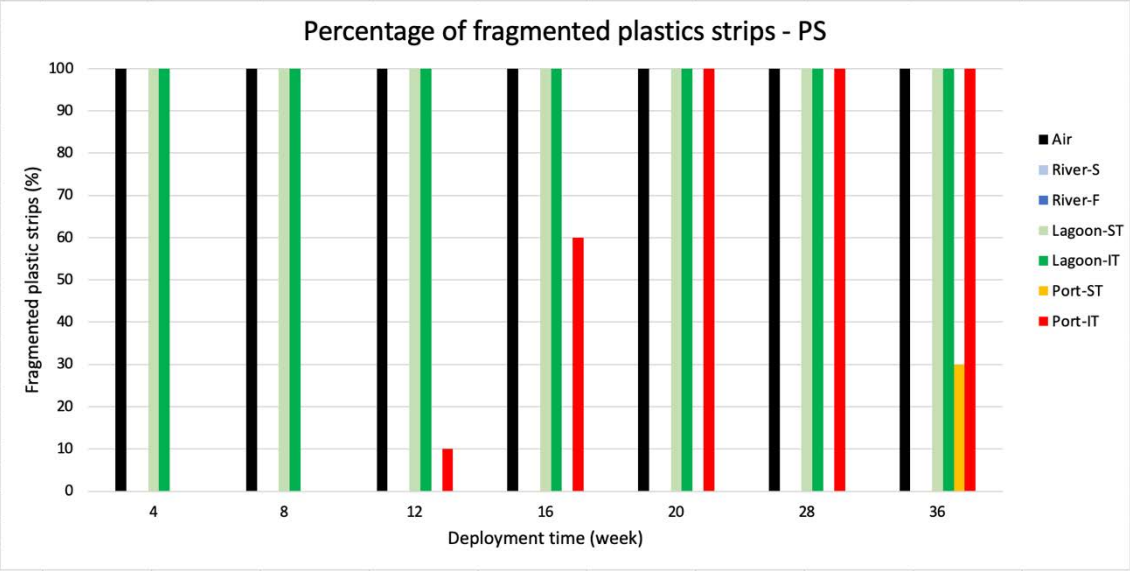

Figure 55: Percentage of fragmented PS strips after exposure in the different environments tested.

Table 13: Percentage of fragmented PS strips.

Sample code	Location	Zonation	Deployment time (week)	Plastic Type	Percentage of fragmented plastic strips
River-S-PS-4W	River	Submerged	4	PS	0
River-S-PS-8W	River	Submerged	8	PS	0
River-S-PS-12W	River	Submerged	12	PS	0
River-S-PS-16W	River	Submerged	16	PS	0
River-S-PS-20W	River	Submerged	20	PS	0
River-S-PS-28W	River	Submerged	28	PS	0
River-S-PS-36W	River	Submerged	36	PS	0
River-F-PS-4W	River	Semi-floating	4	PS	0
River-F-PS-8W	River	Semi-floating	8	PS	0
River-F-PS-12W	River	Semi-floating	12	PS	0
River-F-PS-16W	River	Semi-floating	16	PS	0
River-F-PS-20W	River	Semi-floating	20	PS	0
River-F-PS-28W	River	Semi-floating	28	PS	0
River-F-PS-36W	River	Semi-floating	36	PS	0
Port-ST-PS-4W	Port	Subtidal	4	PS	0
Port-ST-PS-8W	Port	Subtidal	8	PS	0
Port-ST-PS-12W	Port	Subtidal	12	PS	0
Port-ST-PS-16W	Port	Subtidal	16	PS	0
Port-ST-PS-20W	Port	Subtidal	20	PS	0
Port-ST-PS-28W	Port	Subtidal	28	PS	0
Port-ST-PS-36W	Port	Subtidal	36	PS	30
Port-IT-PS-4W	Port	Intertidal	4	PS	0
Port-IT-PS-8W	Port	Intertidal	8	PS	0
Port-IT-PS-12W	Port	Intertidal	12	PS	10
Port-IT-PS-16W	Port	Intertidal	16	PS	60
Port-IT-PS-20W	Port	Intertidal	20	PS	100
Port-IT-PS-28W	Port	Intertidal	28	PS	100
Port-IT-PS-36W	Port	Intertidal	36	PS	100
Lagoon-ST-PS-4W	Lagoon	Subtidal	4	PS	100
Lagoon-ST-PS-8W	Lagoon	Subtidal	8	PS	100
Lagoon-ST-PS-12W	Lagoon	Subtidal	12	PS	100
Lagoon-ST-PS-16W	Lagoon	Subtidal	16	PS	100
Lagoon-ST-PS-20W	Lagoon	Subtidal	20	PS	100
Lagoon-ST-PS-28W	Lagoon	Subtidal	28	PS	100
Lagoon-ST-PS-36W	Lagoon	Subtidal	36	PS	100
Lagoon-IT-PS-4W	Lagoon	Intertidal	4	PS	100
Lagoon-IT-PS-8W	Lagoon	Intertidal	8	PS	100
Lagoon-IT-PS-12W	Lagoon	Intertidal	12	PS	100
Lagoon-IT-PS-16W	Lagoon	Intertidal	16	PS	100
Lagoon-IT-PS-20W	Lagoon	Intertidal	20	PS	100
Lagoon-IT-PS-28W	Lagoon	Intertidal	28	PS	100
Lagoon-IT-PS-36W	Lagoon	Intertidal	36	PS	100
Air-PS-4W	Air		4	PS	100
Air-PS-8W	Air		8	PS	100
Air-PS-12W	Air		12	PS	100
Air-PS-16W	Air		16	PS	100
Air-PS-20W	Air		20	PS	100
Air-PS-28W	Air		28	PS	100
Air-PS-36W	Air		36	PS	100

Apparent change in plastic mass

The apparent change in mass calculated the mass loss of the plastic. This occurred in all types of plastics and in all environments in which the strips were exposed with an increase over time.

From the graphs regarding the river environment (Figure 56), the greatest loss occurred for PS in submerged condition, followed by LDPE, PVC, HDPE, PET and PP, while in semi-floating condition for PS, followed by LDPE, HDPE, PET, PVC and PP.

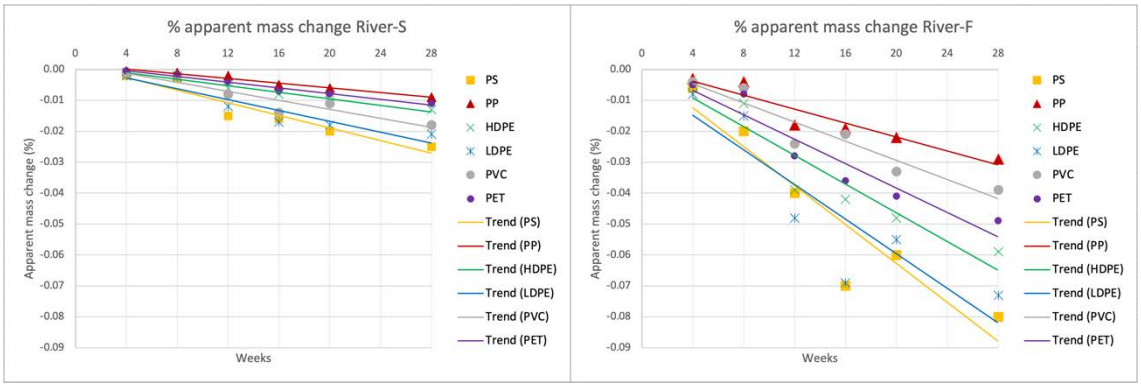

Figure 56: Trends over time of the apparent mass change of the plastic strips exposed in the river environment, in submerged (left) and semi-floating (right) condition.

The apparent percent mass change of the plastic strips in the river environment (i.e. after acid-washing) reached up to -0.025% ± 0.005% for PS in submerged condition, while -0.08% ± 0.06% for PS in semi-floating condition, where values below zero indicate apparent loss of plastic mass.

ANOVA, shown in Table 14, identified zonation (submerged or semi-floating; $F_{(1,88)}$ = 100.12, $p < 0.001$) and the deployment time (4w, 8w, 16w, 20w, 28w; $F_{(5,88)}$ = 18.50, $p < 0.001$) as significant predictors of differences in apparent mass change at river environment (Figure 57, Figure 58). The plastic type (PP, HDPE, LDPE, PVC, PET; $F_{(5,88)}$ = 8.59, $p < 0.001$), the interaction between zonation and deployment time ($F_{(5,88)}$ = 4.87, $p < 0.001$) and the interaction between zonation and plastic type ($F_{(5,88)}$ = 3.42, $p < 0.001$), albeit showing an increase in apparent mass loss with time and more marked for the semi-floating environment and for some types of plastics, the difference was not quite significant at $\alpha = 0.05$ (Figure 59, Figure 60, Figure 61). Table 15, Table 16 and Table 17

show the results of the Scheffè's test performed respectively for zonation, deployment time and plastic type to integrate the results obtained with ANOVA.

Table 14: Results of the three-way ANOVA analysis of variance for apparent mass change in the river environment.

	SS	Degr. Of Freedom	MS	F	p
Intercept	0.06	1.00	0.06	301.13	0.00
Zonation	0.02	1.00	0.02	100.12	0.00
Deployment time (week)	0.02	5.00	0.00	18.50	0.00
Plastic Type	0.01	5.00	0.00	8.59	0.00
Zonation*Deployment time (week)	0.00	5.00	0.00	4.87	0.00
Zonation*Plastic Type	0.00	5.00	0.00	3.42	0.01
Deployment time (week)*Plastic Type	0.00	25.00	0.00	0.59	0.93
Zonation*Deployment time (week)*Plastic Type	0.00	25.00	0.00	0.28	1.00
Error	0.02	88.00	0.00		

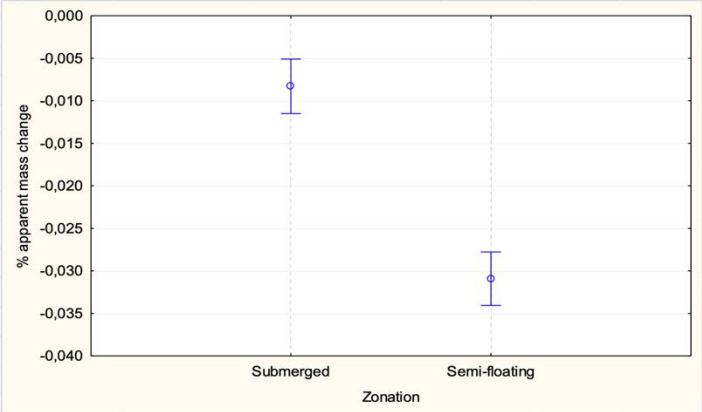

Figure 57: Graphical representation of the ANOVA results: comparison between the variability of the apparent mass change averages for zonation in the river environment.

Table 15: Results of the post-hoc test, Scheffé's test, of the apparent mass change for the zonation in the river environment.

Zonation	Mean apparent mass change (%)	1	2
Semi-floating	-0.031	****	
Submerged	-0.009		****

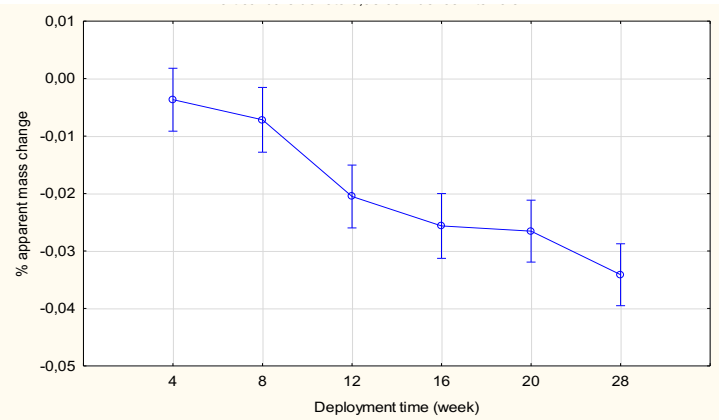

Figure 58: Graphical representation of the ANOVA results: comparison between the variability of the apparent mass change averages for deployment time in the river environment.

Table 16: Results of the post-hoc test, Scheffé's test, of the apparent mass change for the deployment time in the river environment.

Deployment time (week)	Mean apparent mass change (%)	1	2	3
28	-0.035	****		
20	-0.027	****	****	
16	-0.026	****	****	
12	-0.021		****	
8	-0.007			****
4	-0.004			****

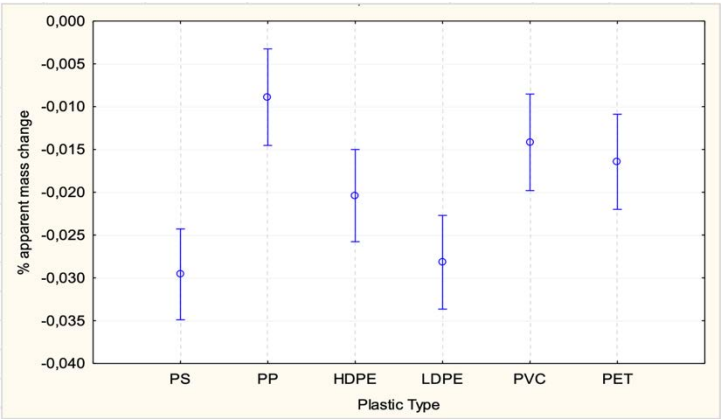

Figure 59: Graphical representation of the ANOVA results: comparison between the variability of the apparent mass change averages for plastic type in the river environment.

Table 17: Results of the post-hoc test, Scheffé's test, of the apparent mass change for the plastic type in the river environment.

Plastic Type	Mean apparent mass change (%)	1	2	3
PS	-0.030		****	
LDPE	-0.028		****	****
HDPE	-0.021	****	****	****
PET	-0.017	****		****
PVC	-0.014	****		
PP	-0.009	****		

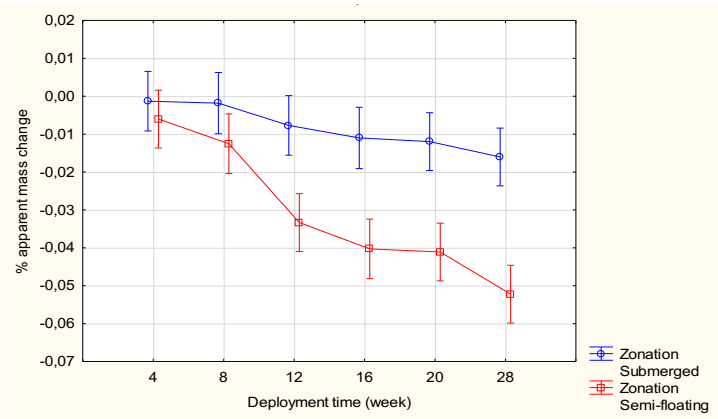

Figure 60: Graphical representation of the ANOVA results: comparison between the variability of the apparent mass change averages for zonation and deployment time in the river environment.

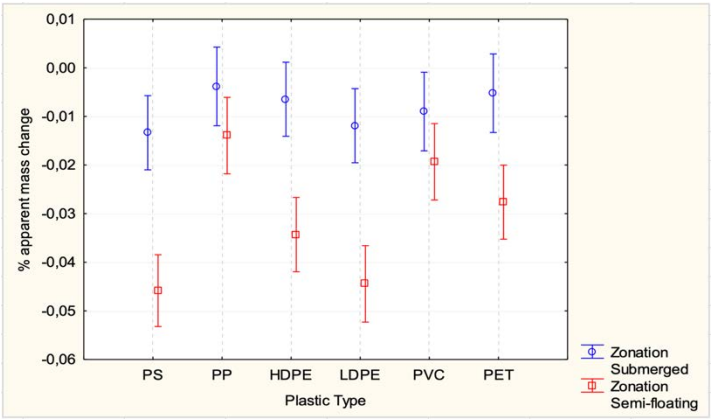

Figure 61: Graphical representation of the ANOVA results: comparison between the variability of the apparent mass change averages for zonation and plastic type in the river environment.

In the lagoon environment (Figure 62), remembering that in both areas there was the complete dispersion of PS, the greatest loss occurred for PET, followed by PVC, LDPE, HDPE, and PP both for the subtidal zone and for the intertidal zone.

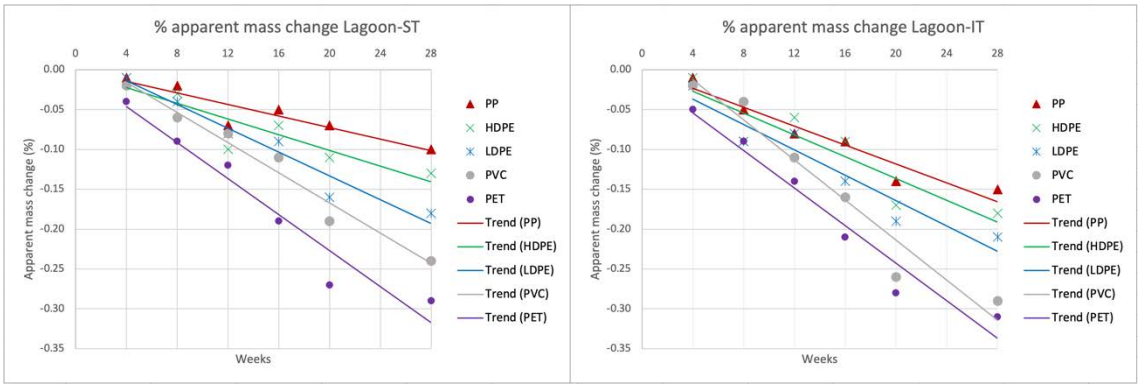

Figure 62: Trends over time of the apparent mass change of the plastic strips exposed in the lagoon environment, in subtidal (left) and intertidal (right) zones.

The apparent change in plastic mass reached up to -0.29% ± 0.01% and -0.31 % ± 0.01% for PET in lagoon environment in subtidal and intertidal condition respectively.

ANOVA, shown in Table 18, identified zonation (subtidal or intertidal; $F_{(1,81)}$= 15.89, p < 0.001), deployment time (4w, 8w, 16w, 20w, 28w; $F_{(5,81)}$ = 76.80, p < 0.001) and plastic type (PP, HDPE, LDPE, PVC, PET; $F_{(4,81)}$ = 28.86, p < 0.001) as significant predictors of differences in apparent mass change at lagoon environment (Figure 63, Figure 64, Figure 65). Table 19, Table 20 and Table 21 show the results of the Scheffè's test performed respectively for zonation, deployment time and plastic type to integrate the results obtained with ANOVA.

Table 18: Results of the three-way ANOVA analysis of variance for apparent mass change in the lagoon environment.

	SS	Degr. Of Freedom	MS	F	p
Intercept	1.73	1.00	1.73	1119.35	0.00
Zonation	0.02	1.00	0.02	15.89	0.00
Deployment time (week)	0.59	5.00	0.12	76.80	0.00
Plastic Type	0.18	4.00	0.04	28.86	0.00
Zonation*Deployment time (week)	0.01	5.00	0.00	1.15	0.34
Zonation*Plastic Type	0.00	4.00	0.00	0.30	0.88
Deployment time (week)*Plastic Type	0.07	20.00	0.00	2.36	0.00
Zonation*Deployment time (week)*Plastic Type	0.01	20.00	0.00	0.40	0.99
Error	0.12	81.00	0.00		

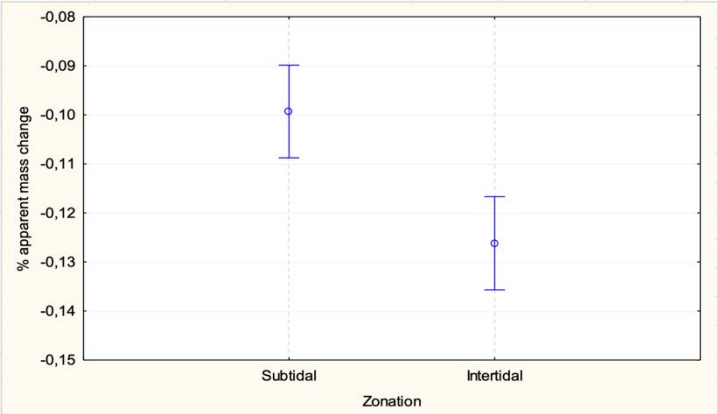

Figure 63: Graphical representation of the ANOVA results: comparison between the variability of the apparent mass change averages for zonation in the lagoon environment.

Table 19: Results of the post-hoc test, Scheffé's test, of the apparent mass change for the zonation in the lagoon environment.

Zonation	Mean apparent mass change (%)	1	2
Intertidal	-0.125	****	
Subtidal	-0.096		****

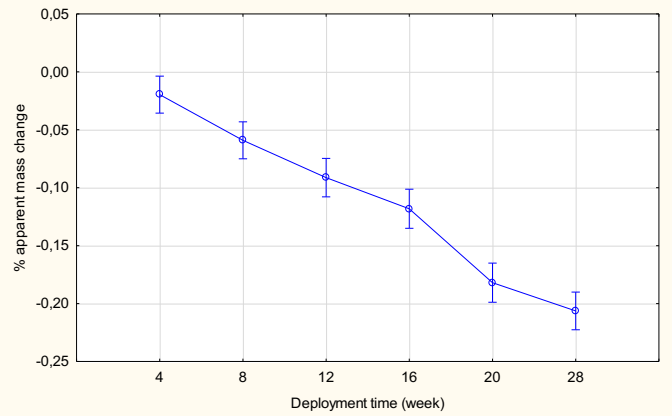

Figure 64: Graphical representation of the ANOVA results: comparison between the variability of the apparent mass change averages for deployment time in the lagoon environment.

Table 20: Results of the post-hoc test, Scheffé's test, of the apparent mass change for the deployment time in the lagoon environment.

Deployment time (week)	Mean apparent mass change (%)	1	2	3	4
28	-0.208	****			
20	-0.176	****			
16	-0.119		****		
12	-0.090		****	****	
8	-0.061			****	
4	-0.018				****

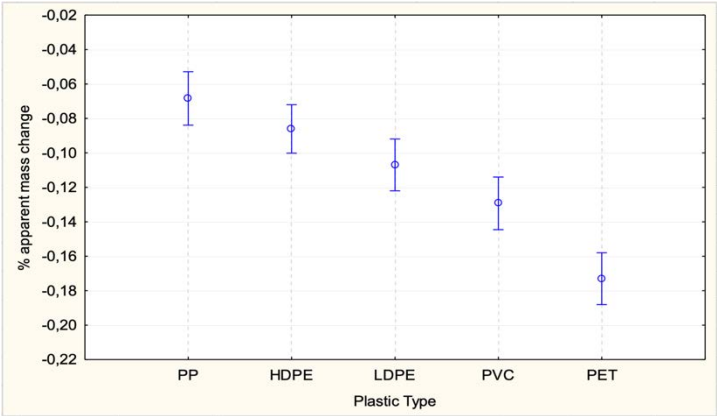

Figure 65: Graphical representation of the ANOVA results: comparison between the variability of the apparent mass change averages for plastic type in the lagoon environment.

Table 21: Results of the post-hoc test, Scheffé's test, of the apparent mass change for the plastic type in the lagoon environment.

Plastic Type	Mean apparent mass change (%)	1	2	3	4
PET	-0.173				****
PVC	-0.121	****			
LDPE	-0.110	****	****		
HDPE	-0.084		****	****	
PP	-0.066			****	

In the port environment (Figure 66), in the subtidal zone, the greatest loss occurred for PS, followed by PET, PVC, LDPE, HDPE and PP, while for the intertidal zone the greatest loss was recorded in PET, followed by PVC, LDPE, PP and HDPE.

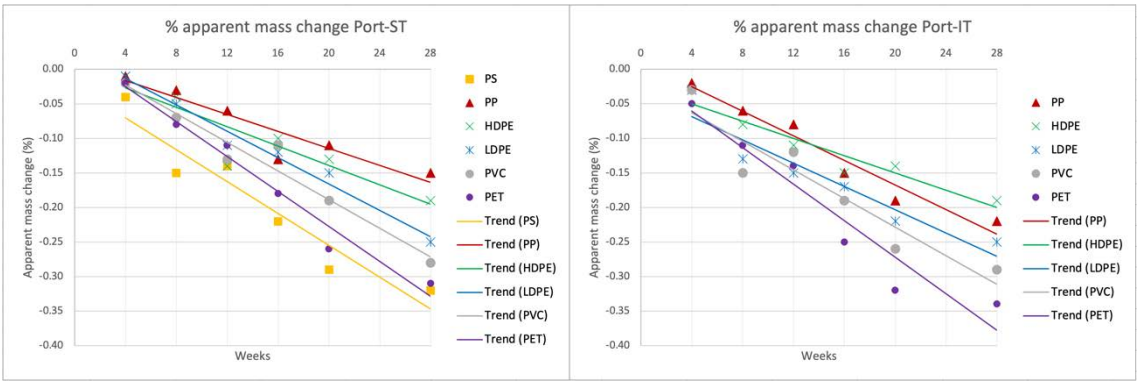

Figure 66: Trends over time of the apparent mass change of the plastic strips exposed in the port environment, in subtidal (left) and intertidal (right) zones.

In the port environment the apparent mass change reached up to -0.32% ± 0.09% for PS in subtidal condition and -0.34% ± 0.11% for PET in intertidal condition.

ANOVA, shown in Table 22, identified zonation (subtidal or intertidal; $F_{(1,84)}$= 17.93, p < 0.001), deployment time (4w, 8w, 16w, 20w, 28w; $F_{(5,84)}$ = 60.11, p < 0.001), and plastic type (PP, HDPE, LDPE, PVC, PET; $F_{(4,84)}$ = 12.52, p < 0.001) as significant predictors of differences in apparent mass change at port environment (Figure 67, Figure 68, Figure 69). Table 23, Table 24, and Table 25 show the results of the Scheffè's test performed respectively for zonation, deployment time and plastic type to integrate the results obtained with ANOVA.

Table 22: Results of the three-way ANOVA analysis of variance for apparent mass change in the port environment.

	SS	Degr. Of Freedom	MS	F	p
Intercept	2.52	1.00	2.52	1040.53	0.00
Zonation	0.04	1.00	0.04	17.93	0.00
Deployment time (week)	0.73	5.00	0.15	60.11	0.00
Plastic Type	0.12	4.00	0.03	12.52	0.00
Zonation*Deployment time (week)	0.01	5.00	0.00	1.07	0.38
Zonation*Plastic Type	0.00	4.00	0.00	0.42	0.80
Deployment time (week)*Plastic Type	0.07	20.00	0.00	1.51	0.10
Zonation*Deployment time (week)*Plastic Type	0.01	20.00	0.00	0.30	1.00
Error	0.20	84.00	0.00		

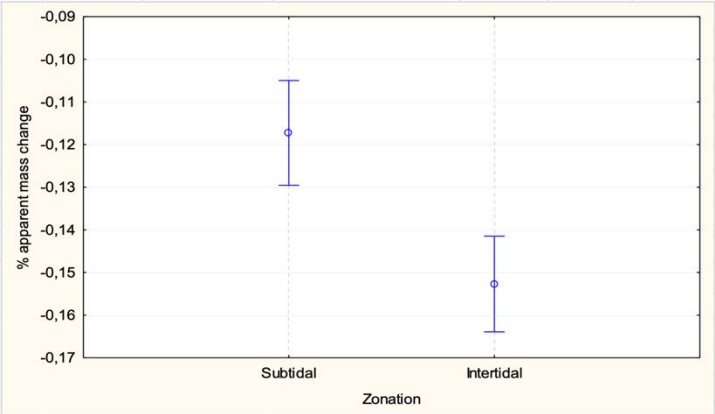

Figure 67: Graphical representation of the ANOVA results: comparison between the variability of the apparent mass change averages for zonation in the port environment.

Table 23: Results of the post-hoc test, Scheffé's test, of the apparent mass change for the zonation in the port environment.

Zonation	Mean apparent mass change (%)	1	2
Intertidal	-0.160	****	
Subtidal	-0.117		****

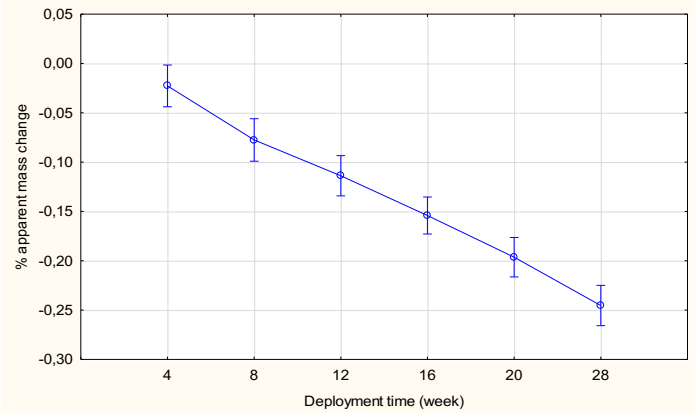

Figure 68: Graphical representation of the ANOVA results: comparison between the variability of the apparent mass change averages for deployment time in the port environment.

Table 24: Results of the post-hoc test, Scheffé's test, of the apparent mass change for the deployment time in the port environment.

Deployment time (week)	Mean apparent mass change (%)	1	2	3	4
28	-0.246	****			
20	-0.202	****			
16	-0.154		****		
12	-0.115		****	****	
8	-0.079			****	
4	-0.024				****

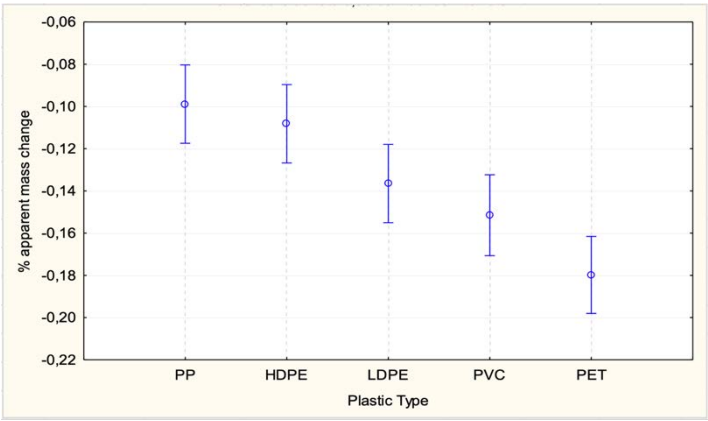

Figure 69: Graphical representation of the ANOVA results: comparison between the variability of the apparent mass change averages for plastic type in the port environment.

Table 25: Results of the post-hoc test, Scheffé's test, of the apparent mass change for the plastic type in the port environment.

Plastic Type	Mean apparent mass change (%)	1	2	4
PET	-0.184		****	
PVC	-0.155		****	****
LDPE	-0.141	****		****
HDPE	-0.113	****		
PP	-0.108	****		

In the air environment (Figure 70), remembering that here too there was the complete dispersion of PS, the most negative loss trend was that of PP, followed by PET, PVC, LDPE and HDPE.

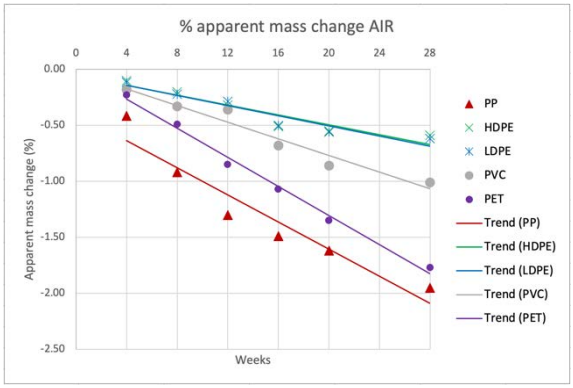

Figure 70: Trends over time of the apparent mass change of the plastic strips exposed in the airborne environment.

It reached up to -1.95% ± 0.49% for PP in the strips exposed to air environment.

Two-way ANOVA, shown in Table 26, highlighted how the deployment time (4w, 8w, 16w, 20w, 28w; $F_{(5,43)} = 2.77$, $p < 0.001$) and the plastic type ($F_{(4,43)} = 9.96$, $p < 0.001$), albeit showing an increase in apparent mass loss with time and more marked for some types of plastics, the difference was not quite significant at $\alpha = 0.05$ (Figure 71, Figure 72). Table 27 and Table 28 show the results of the Scheffè's test performed respectively for zonation, deployment time and plastic type to integrate the results obtained with ANOVA.

Table 26: Results of the two-way ANOVA analysis of variance for apparent mass change in the air environment.

	SS	Degr. Of Freedom	MS	F	p
Intercept	40.48	1.00	40.48	155.07	0.00
Deployment time (week)	3.62	5.00	0.72	2.77	0.03
Plastic Type	10.40	4.00	2.60	9.96	0.00
Deployment time (week)*Plastic Type	3.73	20.00	0.19	0.71	0.79
Error	11.22	43.00	0.26		

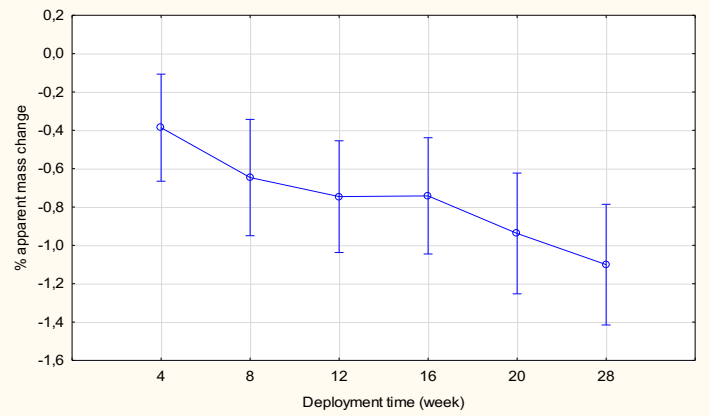

Figure 71: Graphical representation of the ANOVA results: comparison between the variability of the apparent mass change averages for deployment time in the air environment.

Table 27: Results of the post-hoc test, Scheffé's test, of the apparent mass change for the deployment time in the air environment.

Deployment time (week)	Mean apparent mass change (%)	1	2
28	-1.148	****	
20	-0.958	****	****
12	-0.702	****	****
16	-0.687	****	****
8	-0.600	****	****
4	-0.405		****

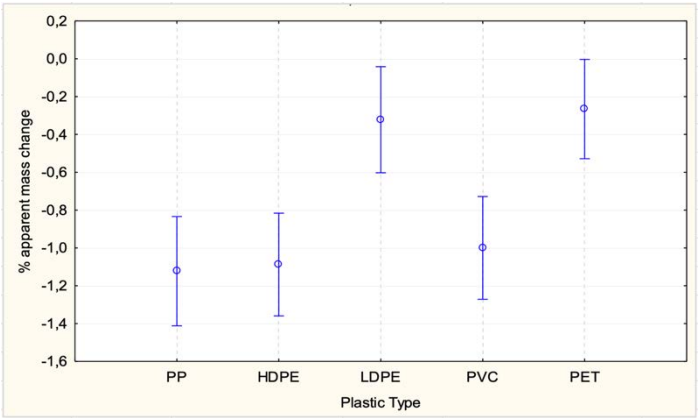

Figure 72: Graphical representation of the ANOVA results: comparison between the variability of the apparent mass change averages for plastic type in the air environment.

Table 28: Results of the post-hoc test, Scheffé's test, of the apparent mass change for the plastic type in the air environment.

Plastic Type	Mean apparent mass change (%)	1	2	4
HDPE	-1.122	****		
PP	-1.068	****		
PVC	-0.932	****	****	
LDPE	-0.332		****	****
PET	-0.254			****

SEM imaging

SEM images of the control strips revealed different surfaces depending on the type of plastic. PS had a grainy structure and had elongated cavities. PP had a compact structure with some scratches parallel to each other on the surface. HDPE had a compact texture, the surface was not perfectly smooth. LDPE had an uneven surface. PVC had a compact but granular structure. PET had a rough surface with ripples that followed a preferential direction on which there were some scratches.

Depending on the type of plastic and the exposure environment, the strips showed different signs of degradation.

Figure 73 shows the SEM images of the PS strips. On the PS strips exposed to air, fractures had formed, the width of which had dimensions between 2 µm and 6.5 µm and length up to 100 µm. In the sample deployed in the subtidal port environment, rounded holes were found, therefore different from the elongated cavities found in the control sample, with a diameter between 25 µm and 30 µm. In correspondence with the holes, the surface of the plastic was cracked, the cracks had a width between 0.2 µm and 2 µm. Furthermore, the cavities present had a greater depth. The appearance of the cavities was different from the control sample. No differences were found on the samples exposed in the river environment compared to the control sample.

In Figure 74 the SEM images of the PP strips can be observed. Parallel or quasi-parallel fractures were formed on the PP strips that were exposed in the air environment, up to 2.5 cm in length and width up to about 25 µm. On the strips deployed in the river environment there were no differences compared to the control strips, while on those positioned in both the lagoon and port environments there were scratches. These were in greater number in the port environment than in the lagoon and in the intertidal zone compared to the subtidal one.

SEM images of the HDPE strips are shown in Figure 75. Sub-rounded holes with an average diameter of about 40 µm were present on HDPE exposed to air. On the surface of the strips deployed in the river environment, chaps had formed, more prominent in

the strips in semi-floating conditions than submerged. In the lagoon and port environments, the surface of the strips appeared more rugged than that of the control and that of the strips that had been exposed in the river environment. In particular, it was more rugged in the port environment than in the lagoon, while there was no clear differentiation between the two areas.

LDPE, which already showed a rough surface in the control strip, showed a smoother surface as degradation increased (Figure 76). In the sample exposed in the air environment, a smoother surface was seen at lower magnification, while at higher magnification a micro-fractured surface. The fractures were approximately 2 μm in length and 0.5 μm in width. These microfractures were not visible in the aquatic environment, where a smoother surface was observed. The surface seemed to be smoother in the port environment than in the lagoon and in the lagoon environment compared to the river one; moreover, the surfaces that had been exposed in the intertidal / semi-floating zone were more rough than the respective ones exposed in the subtidal / submerged zone.

From the SEM images it was seen that the degradation of the PVC occurred with the removal of the granules of material from the surface and the formation of voids instead of the granules, the cavities had in fact the same size of the granules (Figure 77). This occurred in all environments, both in air and in water, but in different quantities. The greater number of voids formed was evident in the air environment, followed by the intertidal port and intertidal lagoon environment, between which there was no substantial difference, while in the semi-floating river environment the number of voids formed was small. The same sequence was evident for the subtidal zones, where however the overall quantity of voids was much lower. The examined sample exposed in submerged conditions in the river environment, on the other hand, did not show any difference with the control.

PET had undergone different types of degradation based on the environment in which it was exposed (Figure 78). On the surface of the strips deployed in the air environment, cracks formed a kind of mosaic pattern with no preferential propagation tendency. The

width of the fractures was approximately 0.3-0.4 µm. On the sample exposed in the intertidal port environment, rounded holes with an average diameter of about 2 µm were formed in considerable quantities, while on the strip exposed in the intertidal lagoon environment there were rare round furrows with dimensions of about 6 µm. In the subtidal zones, on the other hand, the surface was chapped, mostly in the port environment than in the lagoon. In the river environment, however, the surface did not appear to have undergone particular degradation.

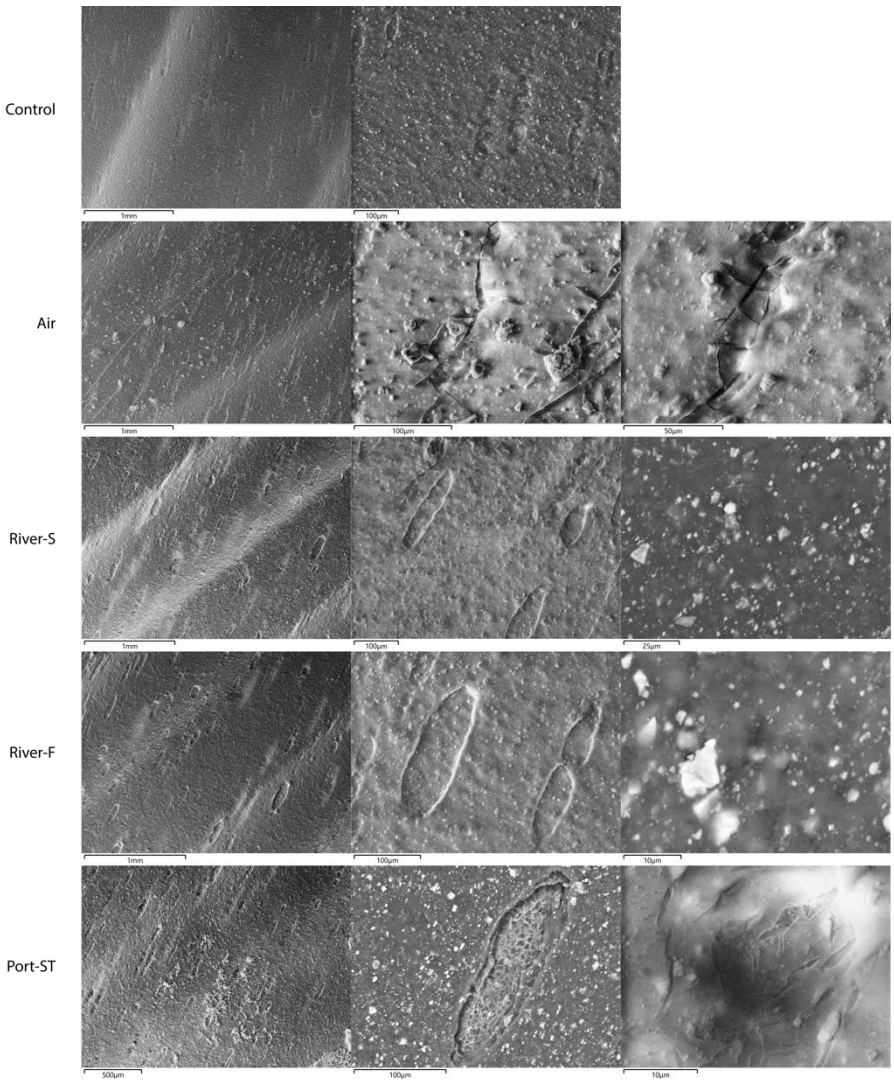

Figure 73: Example SEM images of PS strips. Control strip (row 1) and after environmental exposure of 28 weeks in air (row 2), submerged condition of the river environment (row 3), semi-floating condition of the river environment (row 4) and subtidal zone of the port environment (row 5).

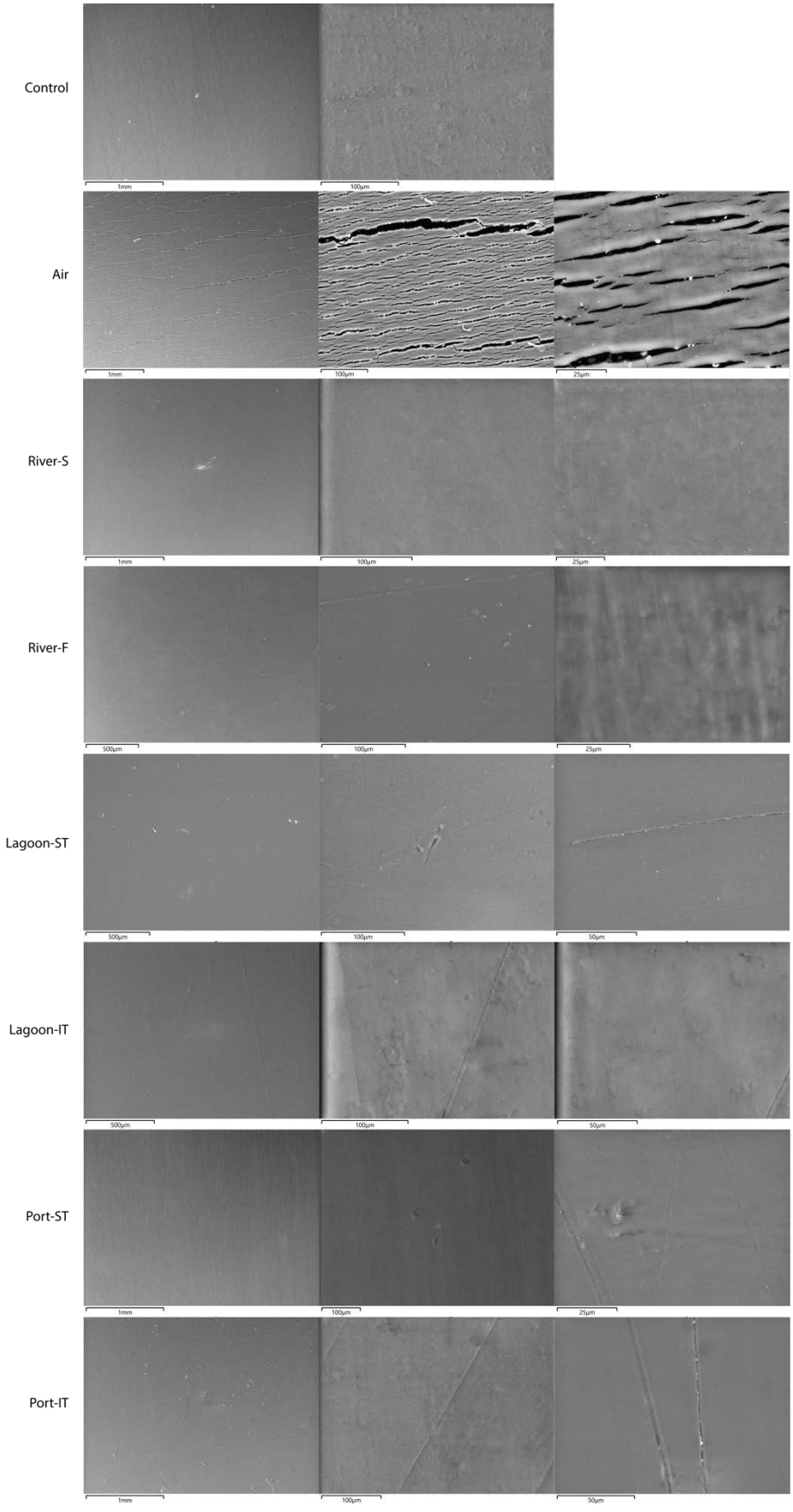
Control
1mm
100µm
Air
1mm
100µm
25µm
River-S
1mm
100µm
25µm
River-F
500µm
100µm
25µm
Lagoon-ST
500µm
100µm
50µm
Lagoon-IT
500µm
100µm
50µm
Port-ST
1mm
100µm
25µm
Port-IT
1mm
100µm
50µm

Figure 74: Example SEM images of PP strips. Control strip (row 1) and after environmental exposure of 28 weeks in air (row 2), submerged condition of the river environment (row 3), semi-floating condition of the river environment (row 4), subtidal zone of the lagoon environment (row 5), intertidal zone of the lagoon environment (row 6), subtidal zone of the port environment (row 7) and intertidal zone of the port environment (row 8).

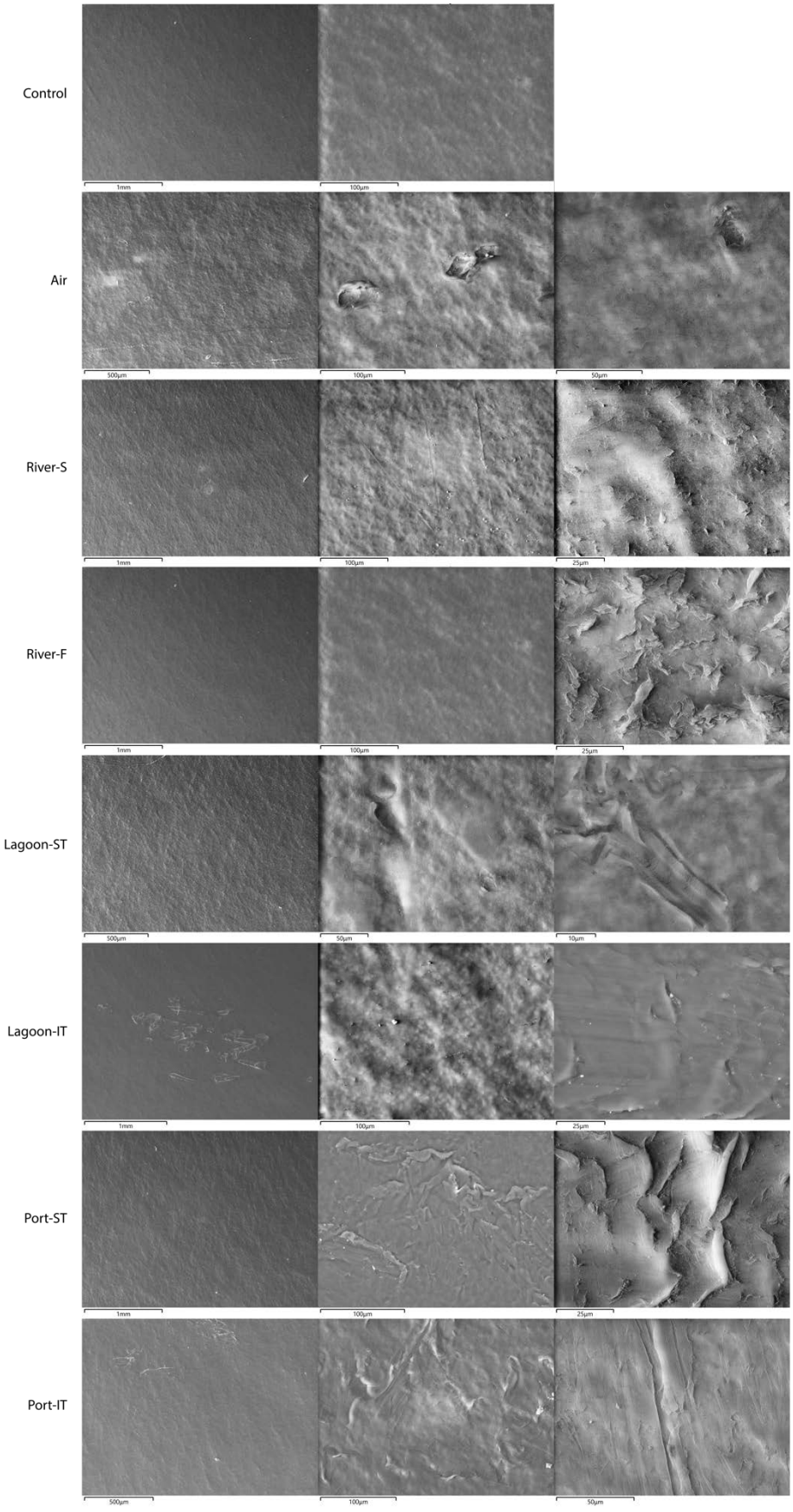
Control
1mm
100µm
Air
500µm
100µm
50µm
River-S
1mm
100µm
25µm
River-F
1mm
100µm
25µm
Lagoon-ST
500µm
50µm
10µm
Lagoon-IT
1mm
100µm
25µm
Port-ST
1mm
100µm
25µm
Port-IT
500µm
100µm
50µm

Figure 75: Example SEM images of HDPE strips. Control strip (row 1) and after environmental exposure of 28 weeks in air (row 2), submerged condition of the river environment (row 3), semi-floating condition of the river environment (row 4), subtidal zone of the lagoon environment (row 5), intertidal zone of the lagoon environment (row 6), subtidal zone of the port environment (row 7) and intertidal zone of the port environment (row 8).

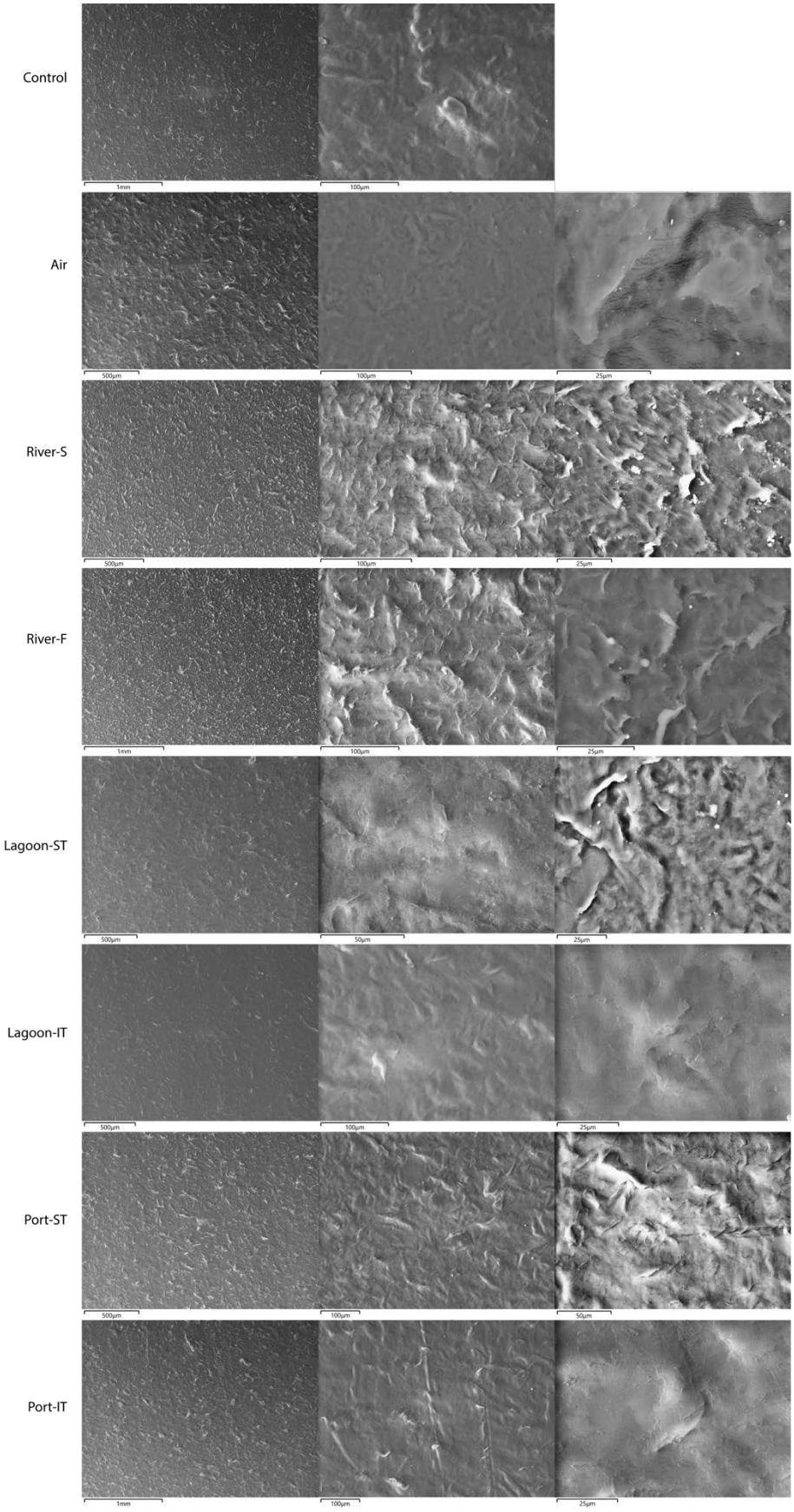
Control
1mm
100µm
Air
500µm
100µm
25µm
River-S
500µm
100µm
25µm
River-F
1mm
100µm
25µm
Lagoon-ST
500µm
50µm
25µm
Lagoon-IT
500µm
100µm
25µm
Port-ST
500µm
100µm
50µm
Port-IT
1mm
100µm
25µm

Figure 76: Example SEM images of LDPE strips. Control strip (row 1) and after environmental exposure of 28 weeks in air (row 2), submerged condition of the river environment (row 3), semi-floating condition of the river environment (row 4), subtidal zone of the lagoon environment (row 5), intertidal zone of the lagoon environment (row 6), subtidal zone of the port environment (row 7) and intertidal zone of the port environment (row 8).

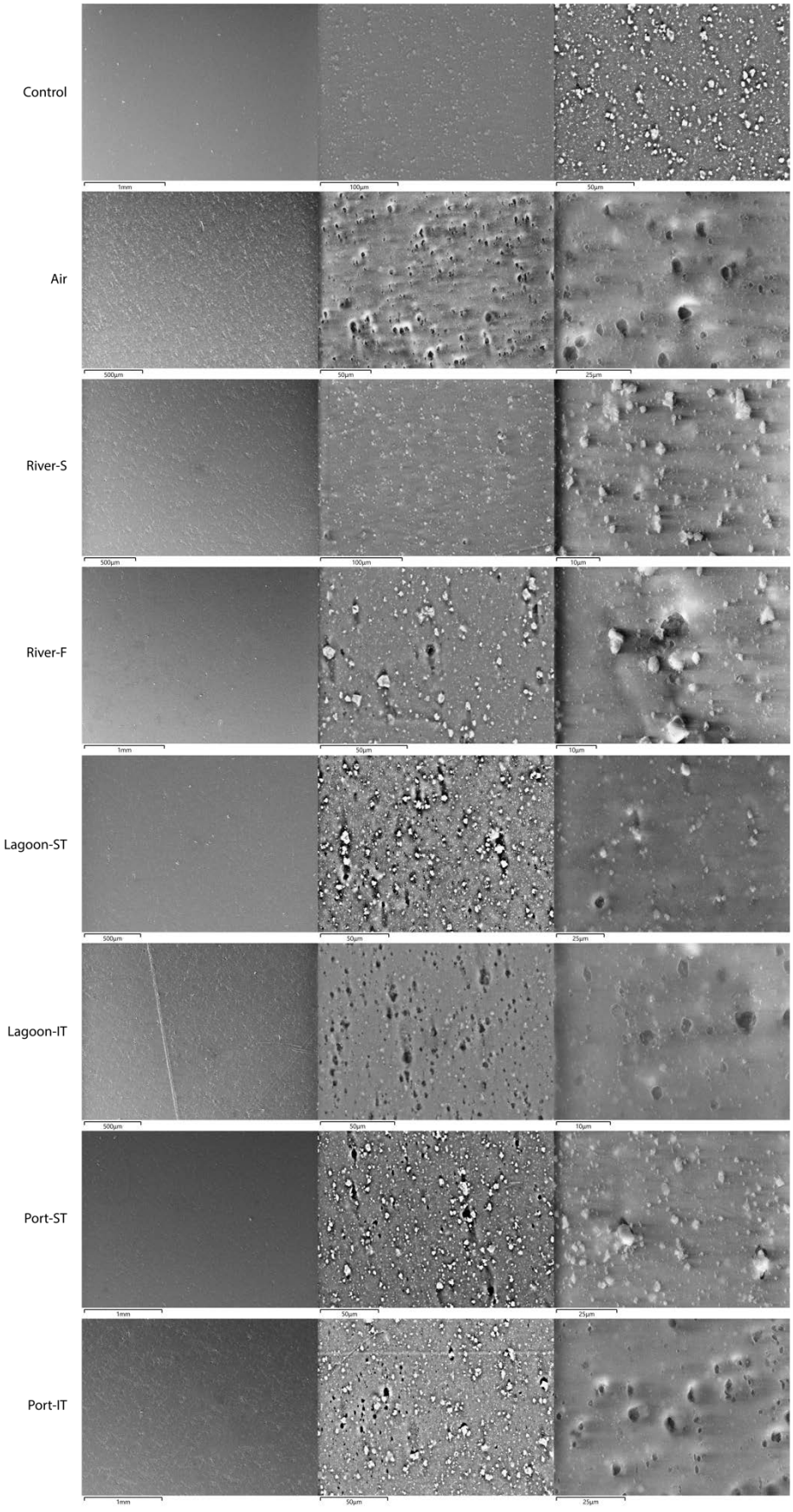
Control
1mm
100µm
50µm
Air
500µm
50µm
25µm
River-S
500µm
100µm
10µm
River-F
1mm
50µm
10µm
Lagoon-ST
500µm
50µm
25µm
Lagoon-IT
500µm
50µm
10µm
Port-ST
1mm
50µm
25µm
Port-IT
1mm
50µm
25µm

Figure 77: Example SEM images of PVC strips. Control strip (row 1) and after environmental exposure of 28 weeks in air (row 2), submerged condition of the river environment (row 3), semi-floating condition of the river environment (row 4), subtidal zone of the lagoon environment (row 5), intertidal zone of the lagoon environment (row 6), subtidal zone of the port environment (row 7) and intertidal zone of the port environment (row 8).

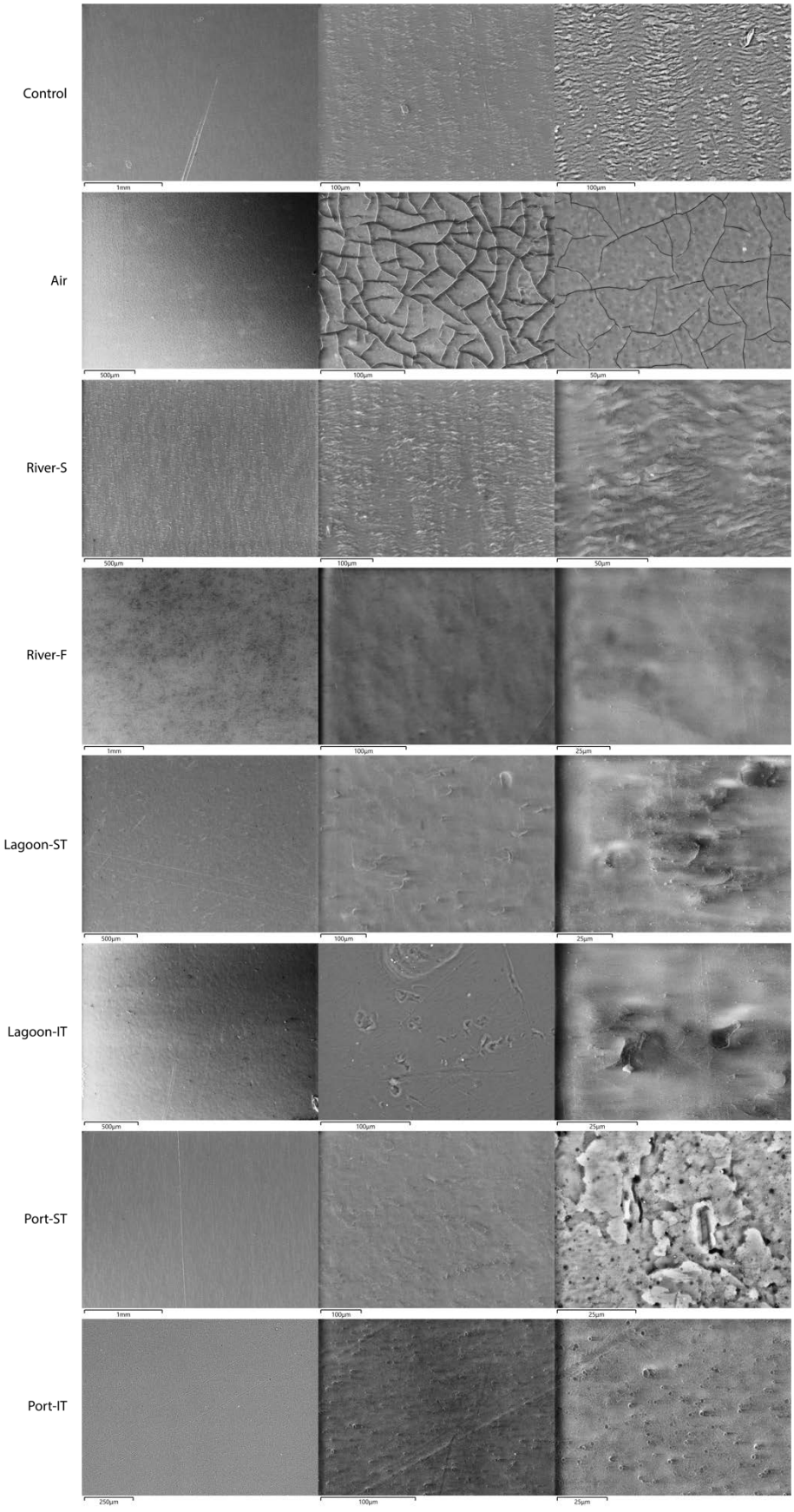
Control
1mm
100µm
100µm
Air
500µm
100µm
50µm
River-S
500µm
100µm
50µm
River-F
1mm
100µm
25µm
Lagoon-ST
500µm
100µm
25µm
Lagoon-IT
500µm
100µm
25µm
Port-ST
1mm
100µm
25µm
Port-IT
250µm
100µm
25µm

Figure 78: Example SEM images of PET strips. Control strip (row 1) and after environmental exposure of 28 weeks in air (row 2), submerged condition of the river environment (row 3), semi-floating condition of the river environment (row 4), subtidal zone of the lagoon environment (row 5), intertidal zone of the lagoon environment (row 6), subtidal zone of the port environment (row 7) and intertidal zone of the port environment (row 8).

Fouling mass

During environmental exposure, all plastic strips exposed in the aquatic environment accumulated fouling consisting of either living organisms (algae, barnacles, mussels, …) and non-living substance, above all sediment.

Figure 79 shows the trend over time of the fouling mass accumulated on the surface of the plastic strips exposed in the river environment. The trends over time of fouling accumulation for each type of plastic, whether exposed in submerged or semi-floating conditions, are similar.

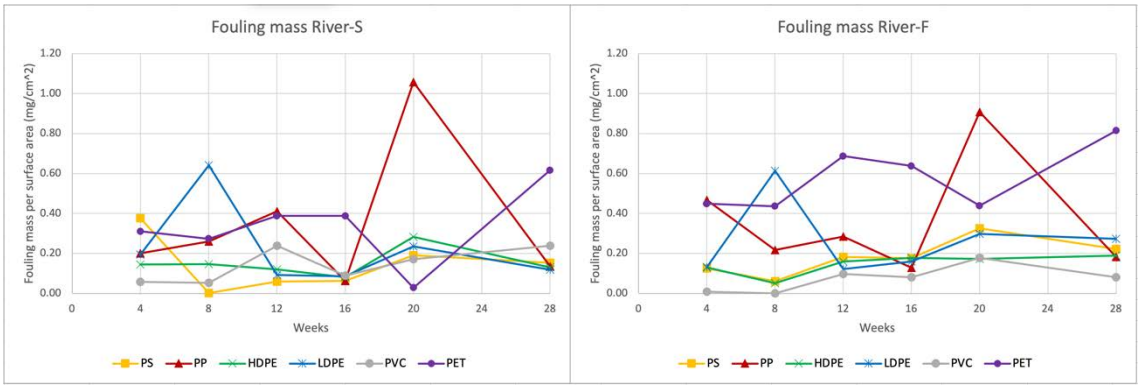

Figure 79: Trends over time of the fouling mass accumulated on the surface of the plastic strips exposed in the river environments.

The fouling mass in the submerged river environment ranged from 0.00 ± 0.03 mg/cm^2 on PS strips at week 8 to 1.06 ± 0.30 mg/cm^2 on PP strips at week 20 and from 0.00 ± 0.01 mg/cm^2 on PVC strips at week 8 to 0.91 ± 0.11 mg/cm^2 on PP strips at week 20 in the semi-floating river environment.

ANOVA, shown in Table 29, identified plastic type (PS, PP, HDPE, LDPE, PVC, PET; $F_{(5,144)}$= 25.49, p < 0.001) as significant predictor of differences in fouling mass accumulation in the river environment (Figure 80). For deployment time (4w, 8w, 16w, 20w, 28w; $F_{(5,144)}$= 5.10, p < 0.001), interaction between deployment time and plastic type ($F_{(5,144)}$ = 7.36, p < 0.001) and interaction between zonation and plastic type ($F_{(5,144)}$ = 3.90, p < 0.001), , the difference was not quite significant at α = 0.05 (Figure 81, Figure 82, Figure 83). Table 30 and Table 31 show the results of the Scheffè's test performed respectively for plastic type and deployment time to integrate the results obtained with ANOVA. The zonation

did not detectably influence the accumulated fouling mass in river environment. This occurred even though there was a greater amount of fouling on the strips exposed for 20 weeks which affected, albeit in different ways, all types of plastics and a slightly different trend based on zonation.

Table 29: Results of the three-way ANOVA analysis of variance for the fouling mass in the river environments.

	SS	Degr. Of Freedom	MS	F	p
Intercept	13.07	1.00	13.07	494.76	0.00
Zonation	0.10	1.00	0.10	3.70	0.06
Deployment time (week)	0.67	5.00	0.13	5.10	0.00
Plastic Type	3.37	5.00	0.67	25.49	0.00
Zonation*Deployment time (week)	0.07	5.00	0.01	0.52	0.76
Zonation*Plastic Type	0.52	5.00	0.10	3.90	0.00
Deployment time (week)*Plastic Type	4.86	25.00	0.19	7.36	0.00
Zonation*Deployment time (week)*Plastic Type	0.48	25.00	0.02	0.72	0.83
Error	3.80	144.00	0.03		

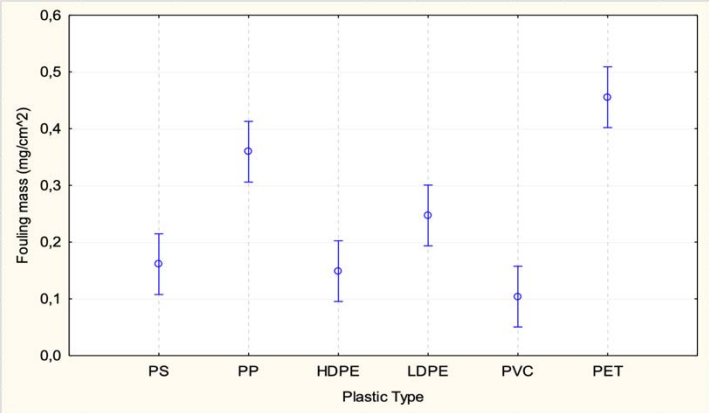

Figure 80: Graphical representation of the ANOVA results. Comparison between the variability of the fouling mass averages for the different types of plastics in the river environment.

Table 30: Results of the post-hoc test, Scheffé's test, of the fouling mass for the types of plastics exposed in the river environment.

Plastic Type	Mean Fouling mass (mg/cm^2)	1	2	3	4
PVC	0.104	****			
HDPE	0.149	****	****		
PS	0.161	****	****		
LDPE	0.247		****	****	
PP	0.359			****	****
PET	0.456				****

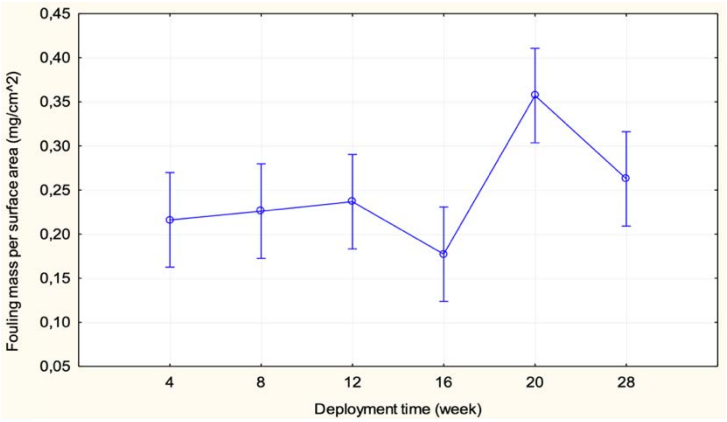

Figure 81: Graphical representation of the ANOVA results: comparison between the variability of the fouling mass averages for the deployment time in the river environment.

Table 31: Results of the post-hoc test, Scheffé's test, of the fouling mass for the deployment time in the river environment.

Deployment time (week)	Mean Fouling mass (mg/cm^2)	1	2
16	0.177	****	
4	0.216	****	
8	0.226	****	
12	0.237	****	****
28	0.263	****	****
20	0.357		****

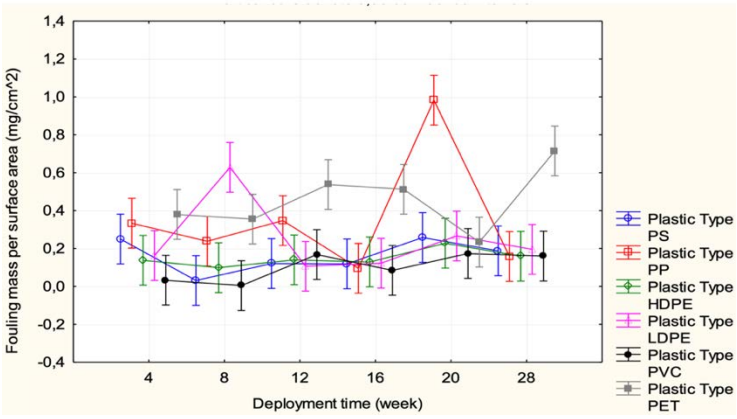

Figure 82: Graphical representation of the ANOVA results: comparison between the variability of the fouling mass averages for the deployment time and for the different types of plastic in the river environment.

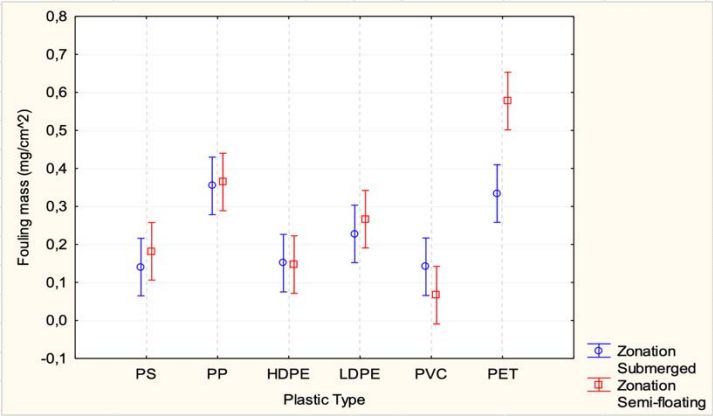

Figure 83: Graphical representation of the ANOVA results: comparison between the variability of the fouling mass averages for the different types of plastics and for the zonation in the river environment.

Figure 84 shows the trend over time of the fouling mass accumulated on the surface of the plastic strips exposed in the lagoon environment. The mass increased with the increase of the exposure time and the trend was similar for the different types of plastics.

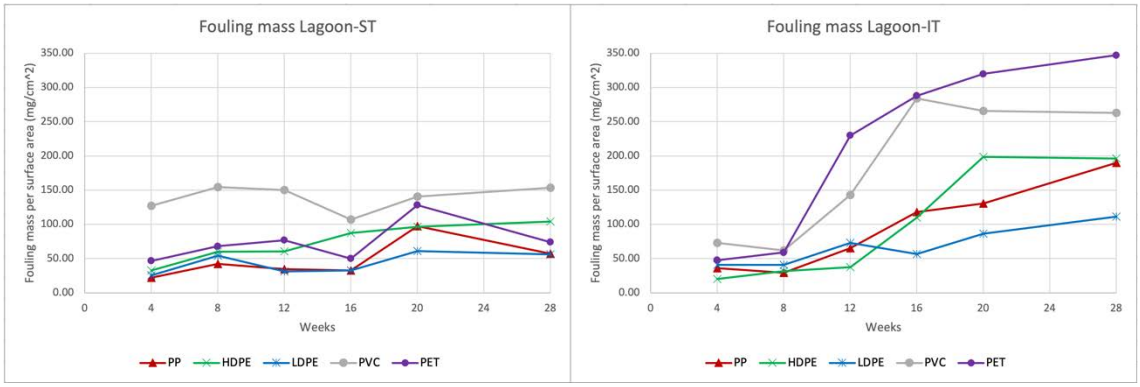

Figure 84: Trends over time of the fouling mass accumulated on the surface of the plastic strips exposed in the lagoon environments.

The accumulation of fouling ranged from 22.21 ± 3.96 mg/cm^2 (PP-4w) to 150.37 ± 21.83 mg/cm^2 (PVC-8w) in the subtidal lagoon environment and from 20.13 ± 0.29 mg/cm^2 (HDPE-4w) to 347.11 ± 65.39 mg/cm^2 (PET-28w) in the intertidal lagoon environment.

ANOVA, shown in Table 32, identified zonation (subtidal or intertidal; $F_{(1,120)} = 131.02$, $p < 0.001$), plastic type (PP, HDPE, LDPE, PVC, PET; $F_{(4,120)} = 70.41$, $p < 0.001$), deployment time (4W, 8W, 16W, 20W, 28W; $F_{(5,120)} = 57.74$, $p < 0.001$) as very significant predictors of differences in fouling mass accumulation in the lagoon environment (Figure 85, Figure

86, Figure 87). Table 33, Table 34 and Table 35 show the results of the Scheffè's test performed respectively for zonation, plastic type and deployment time to integrate the results obtained with ANOVA.

ANOVA identified the interaction between zonation and deployment time ($F_{(5,120)}$ = 30.54, $p < 0.001$) and the interaction between zonation and plastic type ($F_{(4,120)}$ = 19.49, $p < 0.001$) as significant predictors of differences in fouling mass accumulation in the lagoon environment (Figure 88, Figure 89).

Table 32: Results of the three-way ANOVA analysis of variance for the fouling mass in the lagoon environment.

	SS	Degr. Of Freedom	MS	F	p
Intercept	1934405.62	1.00	1934405.62	1777.09	0.00
Zonation	142615.48	1.00	142615.48	131.02	0.00
Deployment time (week)	314249.13	5.00	62849.83	57.74	0.00
Plastic Type	306586.89	4.00	76646.72	70.41	0.00
Zonation*Deployment time (week)	166217.00	5.00	33243.40	30.54	0.00
Zonation*Plastic Type	84857.60	4.00	21214.40	19.49	0.00
Deployment time (week)*Plastic Type	68547.92	20.00	3427.40	3.15	0.00
Zonation*Deployment time (week)*Plastic Type	81122.10	20.00	4056.10	3.73	0.00
Error	130622.75	120.00	1088.52		

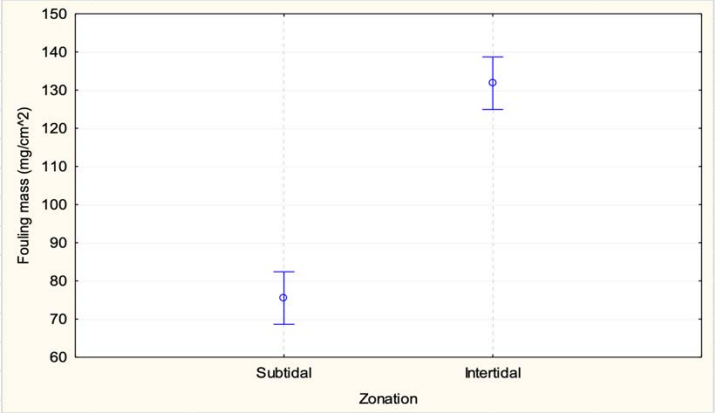

Figure 85: Graphical representation of the ANOVA results: comparison between the variability of the fouling mass averages for zonation in the lagoon environment.

Table 33: Results of the post-hoc test, Scheffé's test, of the fouling mass for the zonation in the lagoon environment.

Zonation	Mean Fouling mass (mg/cm^2)	1	2
Subtidal	75.518	****	
Intertidal	131.814		****

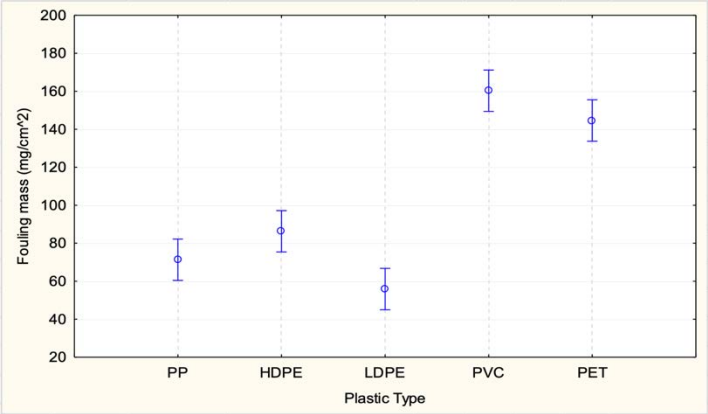

Figure 86: Graphical representation of the ANOVA results: comparison between the variability of the fouling mass averages for the plastic type in the lagoon environment.

Table 34: Results of the post-hoc test, Scheffé's test, of the fouling mass for the plastic type in the lagoon environment.

Plastic Type	Mean Fouling mass (mg/cm^2)	1	2	3
LDPE	55.870	****		
PP	71.309	****	****	
HDPE	86.261		****	
PET	144.607			****
PVC	160.285			****

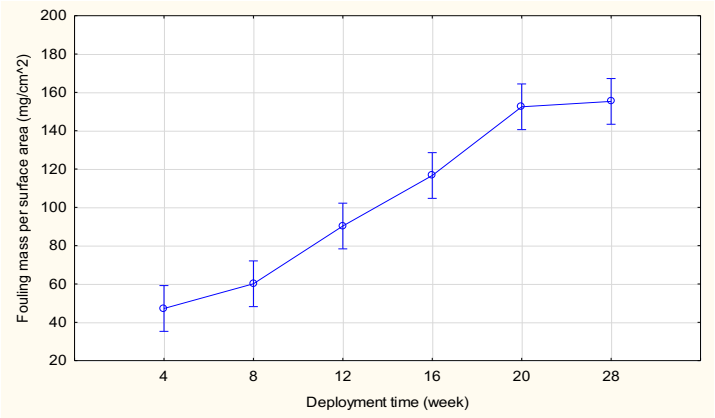

Figure 87: Graphical representation of the ANOVA results: comparison between the variability of the fouling mass averages for deployment time in the lagoon environment.

Table 35: Results of the post-hoc test, Scheffé's test, of the fouling mass for the deployment time in the lagoon environment.

Deployment time (week)	Mean Fouling mass (mg/cm^2)	1	2	3
4	47.227	****		
8	60.122	****		
12	90.262		****	
16	116.636		****	
20	152.478			****
28	155.272			****

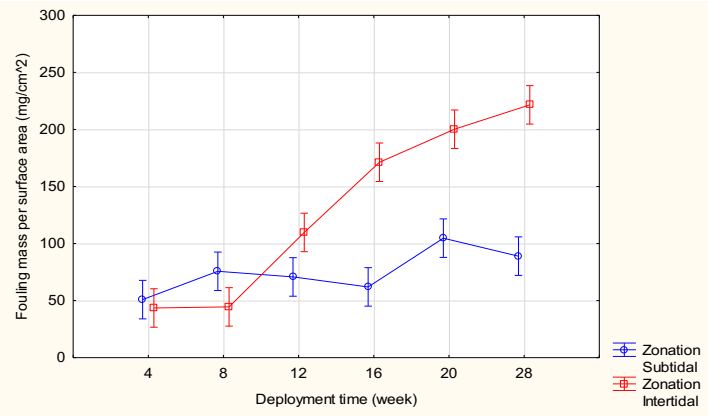

Figure 88: Graphical representation of the ANOVA results: comparison between the variability of the fouling mass averages for deployment time and zonation in the lagoon environment.

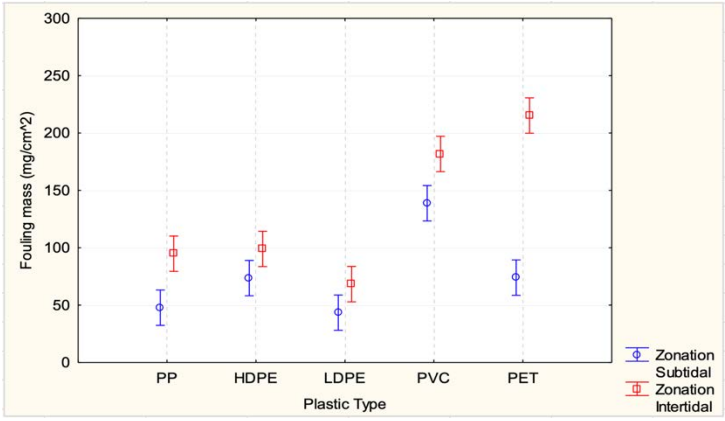

Figure 89: Graphical representation of the ANOVA results: comparison between the variability of the fouling mass averages for plastic type and zonation in the lagoon environment.

Figure 90 shows the trend over time of the fouling mass accumulated on the surface of the plastic strips exposed in the port environment. The trend in the subtidal zone of PS, PP, HDPE and LDPE was very similar. In the intertidal zone, PET was also to these types.

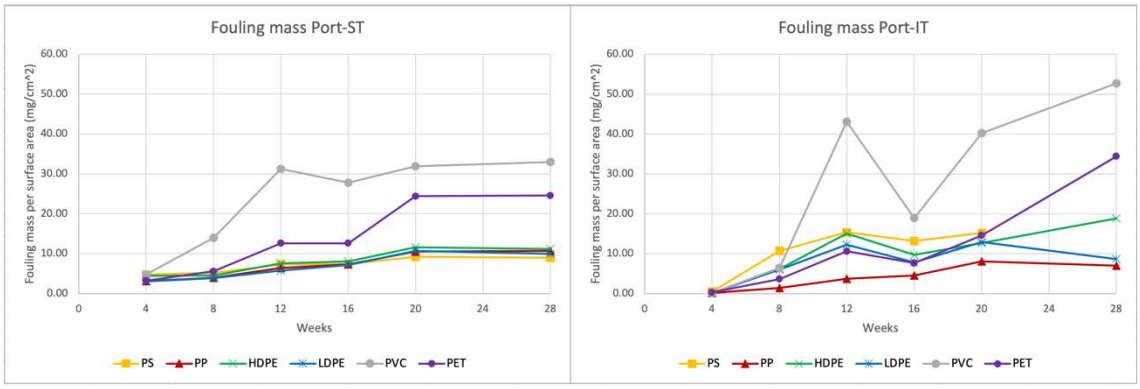

Figure 90: Trends over time of the fouling mass accumulated on the surface of the plastic strips exposed in the port environments.

In the subtidal port environment, the accumulation of fouling mass ranged from 3.08 ± 0.09 mg/cm^2 on LDPE strips at week 4 to 33.01 ± 10.35 mg/cm^2 on PVC strips at week 28, while in the intertidal one it ranged from 0.15 ± 0.03 mg/cm^2 on HDPE strips at week 4 to 52.73 ± 19.25 mg/cm^2 on PVC strips at week 28.

ANOVA, shown in Table 36, identified plastic type (PP, HDPE, LDPE, PVC, PET; $F_{(4,120)}$= 103.20, p < 0.001) and deployment time (4W, 8W, 16W, 20W, 28W; $F_{(5,120)}$ = 73.47, p < 0.001) as very significant predictors of differences in fouling mass accumulation at port environment (Figure 91, Figure 92). Table 37 and Table 38 show the results of the Scheffè's test performed respectively for plastic type and deployment time to integrate the results obtained with ANOVA. For the interaction between plastic type and deployment type ($F_{(20,120)}$ = 10.02, p < 0.001) and between zonation and deployment time ($F_{(5,120)}$ = 5.61, p < 0.001), although with the advancement of the exposure time there was a slightly differential increase between the intertidal and subtidal environment and a greater increase in fouling on the surfaces of PVC and PET, the difference was not quite significant at α = 0.05 (Figure 93, Figure 94). The zonation did not detectably influence the accumulated fouling mass in port environment.

Table 36: Results of three-way ANOVA analysis of variance for fouling mass in the port environment.

	SS	Degr. Of Freedom	MS	F	p
Intercept	26220.45	1.00	26220.45	1202.09	0.00
Zonation	8.00	1.00	8.00	0.37	0.55
Deployment time (week)	8012.41	5.00	1602.48	73.47	0.00
Plastic Type	9004.34	4.00	2251.08	103.20	0.00
Zonation*Deployment time (week)	612.05	5.00	122.41	5.61	0.00
Zonation*Plastic Type	262.01	4.00	65.50	3.00	0.02
Deployment time (week)*Plastic Type	4371.25	20.00	218.56	10.02	0.00
Zonation*Deployment time (week)*Plastic Type	979.44	20.00	48.97	2.25	0.00
Error	2617.48	120.00	21.81		

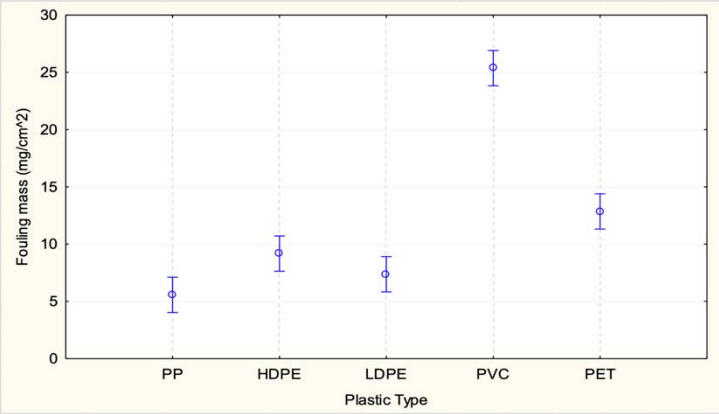

Figure 91: Graphical representation of the ANOVA results: comparison between the variability of the fouling mass averages for the different types of plastics in the port environment.

Table 37: Results of the post-hoc test, Scheffé's test, of the fouling mass for the plastic type in the port environment.

Plastic Type	Mean Fouling mass (mg/cm^2)	1	2	3	4
PP	5.574	****			
LDPE	7.374	****	****		
HDPE	9.176		****		
PET	12.852			****	
PVC	25.370				****

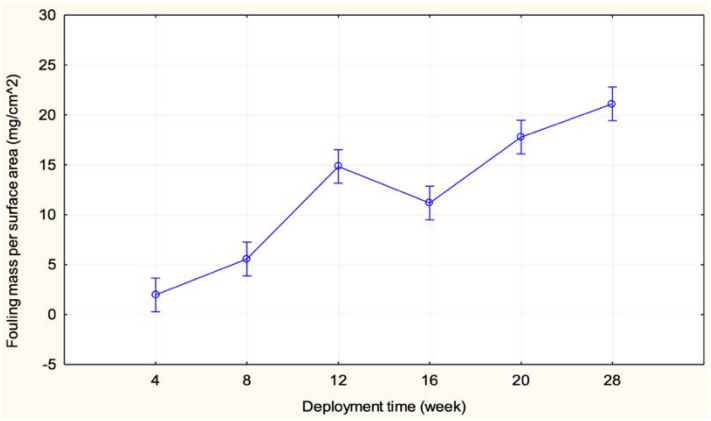

Figure 92: Graphical representation of the ANOVA results: comparison between the variability of the fouling mass averages for the deployment time in the port environment.

Table 38: Results of the post-hoc test, Scheffé's test, of the fouling mass for the deployment time in the port environment.

Deployment time (week)	Mean Fouling mass (mg/cm^2)	1	2	3	4
4	1.965	****			
8	5.564	****			
16	11.172		****		
12	14.833		****	****	
20	17.777			****	****
28	21.105				****

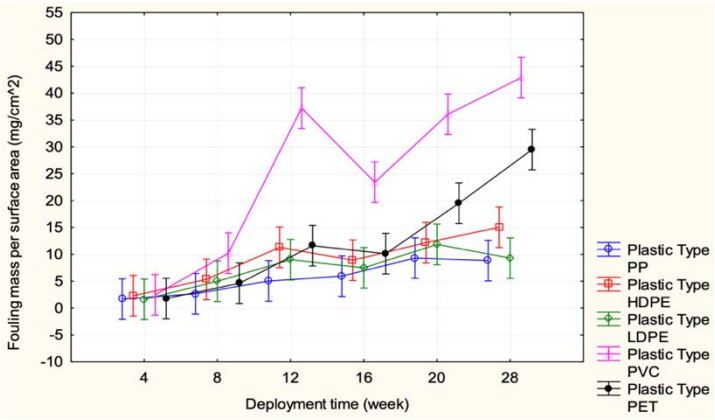

Figure 93: Graphical representation of the ANOVA results: comparison between the variability of the fouling mass averages for the deployment time and for the different types of plastic in the port environment.

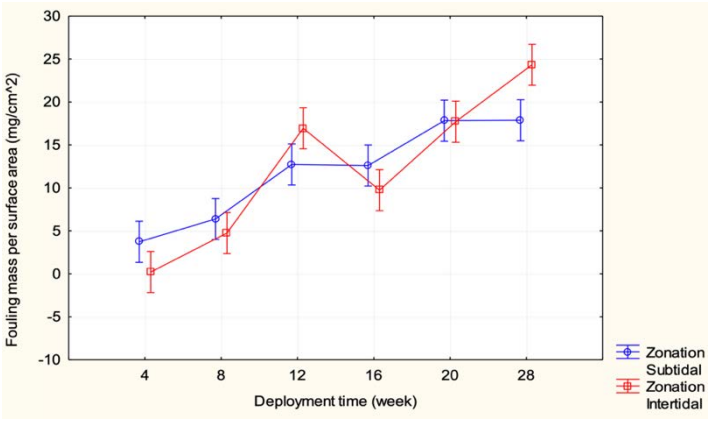

Figure 94: Graphical representation of the ANOVA results: comparison between the variability of the fouling mass averages for deployment time and for zonation in the port environment.

Chlorophyll *a* accumulation

Chlorophyll *a*, measured as a proxy of periphyton accumulation on the plastic strips, accumulated during environmental exposure.

Figure 95 shows the trend of the accumulation of chlorophyll *a* in the plastics exposed in the river environment. A similar trend was seen between the concentration of chlorophyll *a* accumulated on submerged and semi-floating plastics, with an increase in 12 and 28 weeks, even if the two zones had values with different scales.

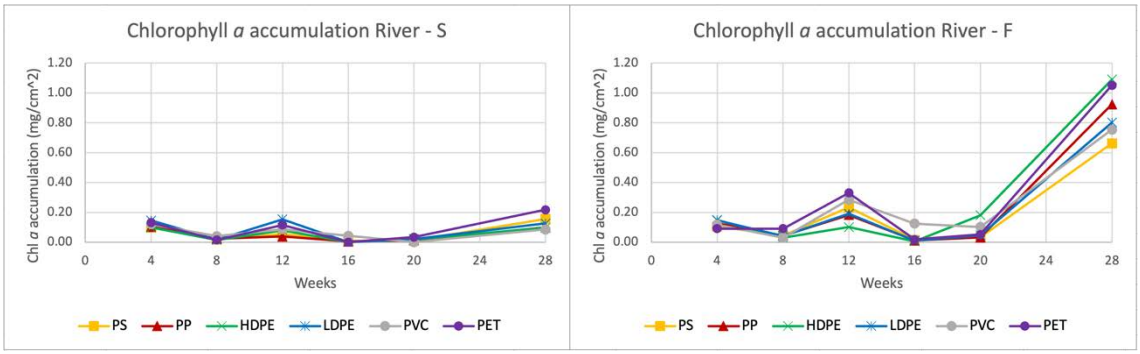

Figure 95: Trends over time of the Chl *a* accumulated on the surface of the plastic strips exposed in the river environment, in submerged (left) and semi-floating (right) condition.

It reached up to 0.22 ± 0.01 mg/cm^2 on PET strips from submerged river environment at week 28, up to 1.09 ± 0.44 mg/cm^2 on HDPE strips from semi-floating environment at week 28.

ANOVA, shown in Table 39, identified zonation (submerged or semi-floating; $F_{(1,144)}$= 129.64, p < 0.001), deployment time (4w, 8w, 16w, 20w, 28w; $F_{(5,144)}$= 104.20, p < 0.001) and interaction between zonation and deployment time ($F_{(5,144)}$= 63.88, p = 0.001) as significant predictors of differences in chlorophyll *a* accumulation at river environment (Figure 96, Figure 97, Figure 98). Table 40 and Table 41 show the results of the Scheffè's test performed respectively for zonation and deployment time to integrate the results obtained with ANOVA. The plastic type did not detectably influence the accumulated chlorophyll *a* in river environment.

Table 39: Results of the three-way ANOVA analysis of variance for chlorophyll *a* in the river environment.

	SS	Degr. Of Freedom	MS	F	p
Intercept	4.58	1.00	4.58	389.71	0.00
Zonation	1.52	1.00	1.52	129.64	0.00
Deployment time (week)	6.12	5.00	1.22	104.20	0.00
Plastic Type	0.06	5.00	0.01	0.99	0.43
Zonation*Deployment time (week)	3.75	5.00	0.75	63.88	0.00
Zonation*Plastic Type	0.06	5.00	0.01	0.95	0.45
Deployment time (week)*Plastic Type	0.35	25.00	0.01	1.20	0.25
Zonation*Deployment time (week)*Plastic Type	0.27	25.00	0.01	0.91	0.59
Error	1.69	144.00	0.01		

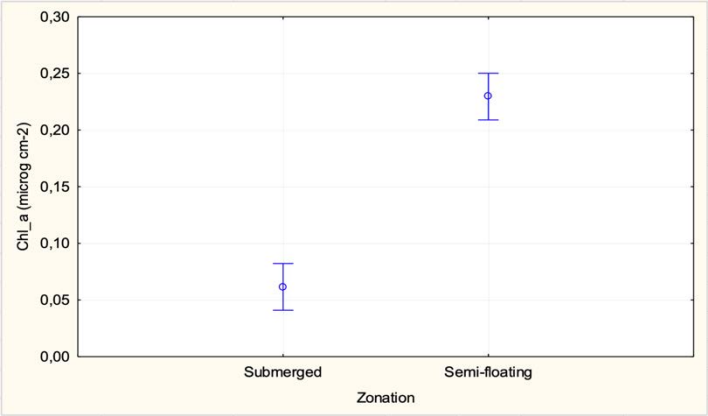

Figure 96: Graphical representation of the ANOVA results: comparison between the variability of the chlorophyll *a* accumulation averages for zonation in the river environment.

Table 40: Results of the post-hoc test, Scheffé's test, of the chlorophyll *a* accumulation for the zonation in the river environment.

Zonation	Mean Chl_a (microg cm-2)	1	2
Submerged	0.062	****	
Semi-floating	0.230		****

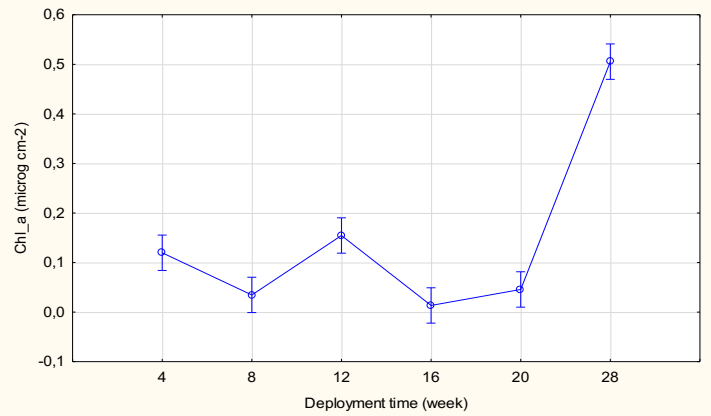

Figure 97: Graphical representation of the ANOVA results: comparison between the variability of the chlorophyll *a* accumulation for deployment time in the river environment.

Table 41: Results of the post-hoc test, Scheffé's test, of the chlorophyll *a* accumulation for the deployment time in the river environment.

Deployment time (week)	Mean Chl_a (microg cm-2)	1	2	3	4
16	0.013	****			
8	0.035	****	****		
20	0.046	****	****		
4	0.120		****	****	
12	0.155			****	
28	0.505				****

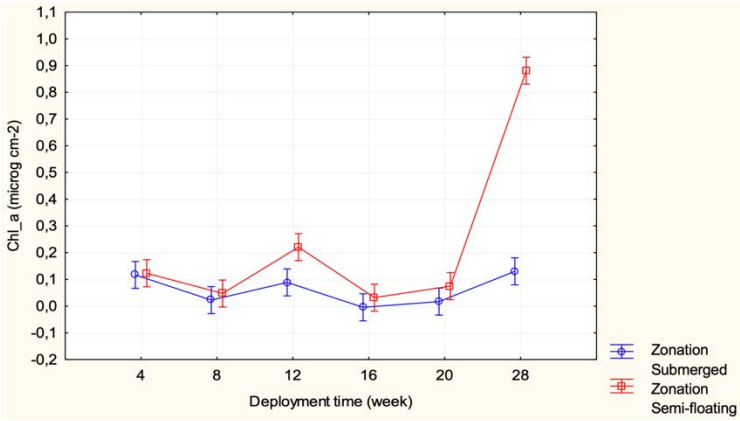

Figure 98: Graphical representation of the ANOVA results: comparison between the variability of the chlorophyll *a* accumulation averages for zonation and deployment time in the river environment.

In the strips of plastic exposed in the lagoon environment, there was a significant difference between the accumulation of chlorophyll *a* in the two areas with almost double values in the intertidal zone compared to the subtidal one. There was an average increase in accumulation in both zones, clearer in the subtidal one than in the intertidal one (Figure 99).

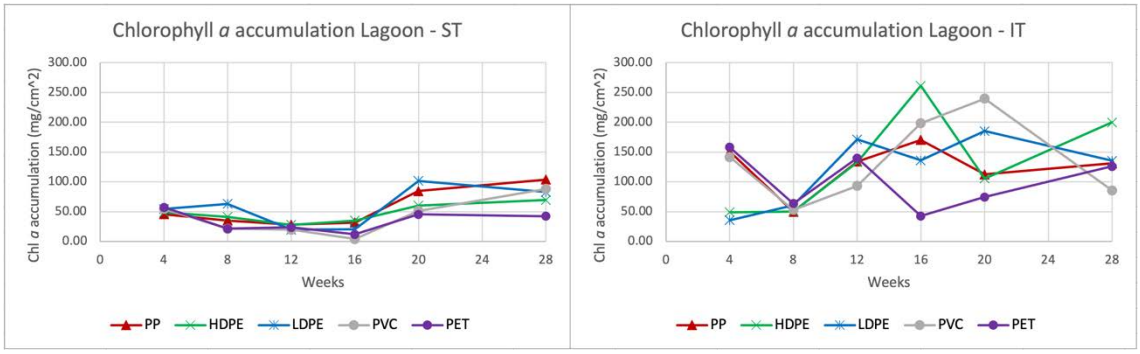

Figure 99: Trends over time of the Chl *a* accumulated on the surface of the plastic strips exposed in the lagoon environment, in subtidal (left) and intertidal (right) zones.

Chlorophyll *a* reached up to 103.90 ± 20.04 mg/cm^2 on PP strips from subtidal lagoon environment at week 28 and up to 261.12 ± 144.86 mg/cm^2 on HDPE strips from intertidal lagoon environment at week 16.

ANOVA, shown in Table 42, identified zonation (subtidal or intertidal; $F_{(1,120)} = 70.78$, $p < 0.001$) as significant predictor of differences in chlorophyll *a* accumulation at lagoon environment (Figure 100). For the deployment time ($F_{(5,120)} = 4.10$, $p < 0.001$) and the interaction between deployment time and zonation ($F_{(5,120)} = 3.81$, $p < 0.001$), albeit showing an increase in chlorophyll *a* with time and more marked for the intertidal environment, the difference was not quite significant at $\alpha = 0.05$ (Figure 101, Figure 102). Table 43 and Table 44 show the results of the Scheffè's test performed respectively for zonation and deployment time to integrate the results obtained with ANOVA. The plastic type did not detectably influence the accumulated chlorophyll *a* in the river environment.

Table 42: Results of the three-way ANOVA analysis of variance for chlorophyll *a* in the lagoon environment.

	SS	Degr. Of Freedom	MS	F	p
Intercept	1291751.82	1.00	1291751.82	347.99	0.00
Zonation	262744.93	1.00	262744.93	70.78	0.00
Deployment time (week)	76093.15	5.00	15218.63	4.10	0.00
Plastic Type	13886.36	4.00	3471.59	0.94	0.45
Zonation*Deployment time (week)	70800.16	5.00	14160.03	3.81	0.00
Zonation*Plastic Type	6659.93	4.00	1664.98	0.45	0.77
Deployment time (week)*Plastic Type	105393.79	20.00	5269.69	1.42	0.13
Zonation*Deployment time (week)*Plastic Type	98288.15	20.00	4914.41	1.32	0.18
Error	445445.76	120.00	3712.05		

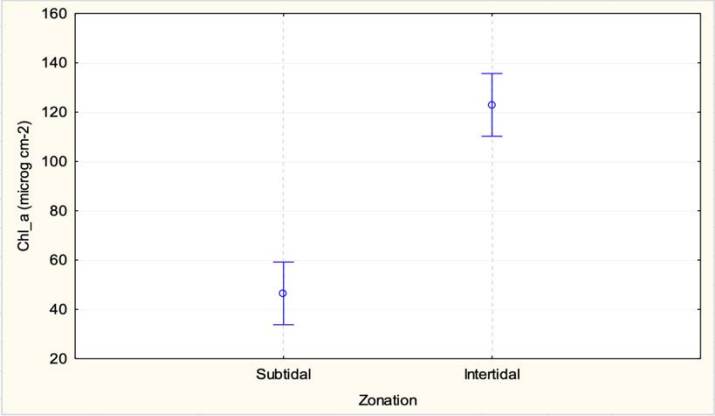

Figure 100: Graphical representation of the ANOVA results: comparison between the variability of the chlorophyll *a* accumulation averages for zonation in the lagoon environment.

Table 43: Results of the post-hoc test, Scheffé's test, of the chlorophyll *a* accumulation for the zonation in the lagoon environment.

Zonation	Mean Chl_a (microg cm-2)	1	2
Subtidal	46.508	****	
Intertidal	122.920		****

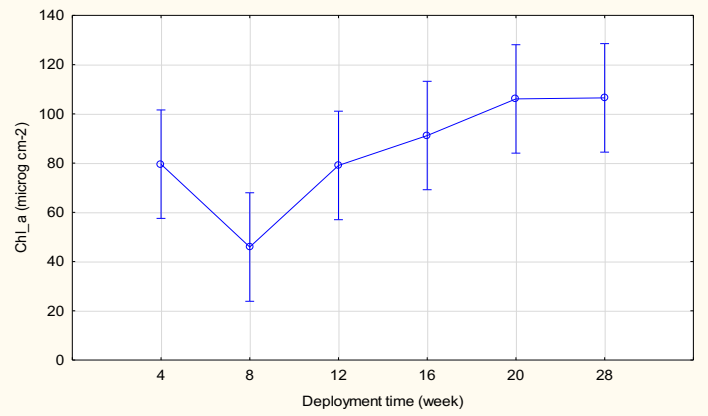

Figure 101: Graphical representation of the ANOVA results: comparison between the variability of the chlorophyll *a* accumulation averages for deployment time in the lagoon environment.

Table 44: Results of the post-hoc test, Scheffé's test, of the chlorophyll *a* accumulation for the deployment time in the lagoon environment.

Deployment time (week)	Mean Chl_a (microg cm-2)	1	2
8	45.913		****
12	79.049	****	****
4	79.561	****	****
16	91.201	****	****
20	106.068	****	
28	106.491	****	

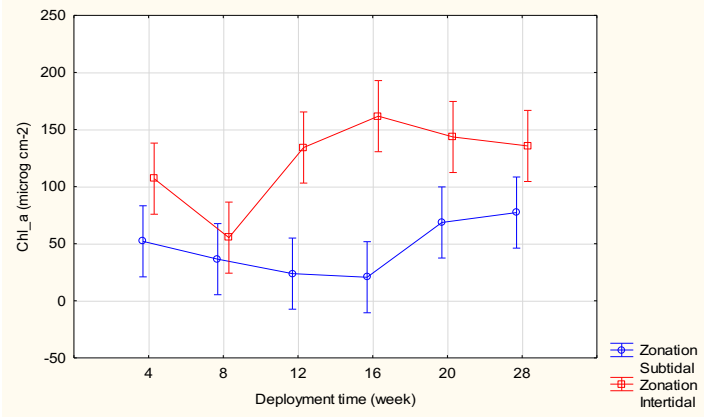

Figure 102: Graphical representation of the ANOVA results: comparison between the variability of the chlorophyll *a* accumulation averages for deployment time and zonation in the lagoon environment.

In the port environment, there was an increase over time of chlorophyll *a* accumulated on the surface of the strips for both zones, however the increase in the accumulation of chlorophyll *a* was more marked for the intertidal zone (Figure 103).

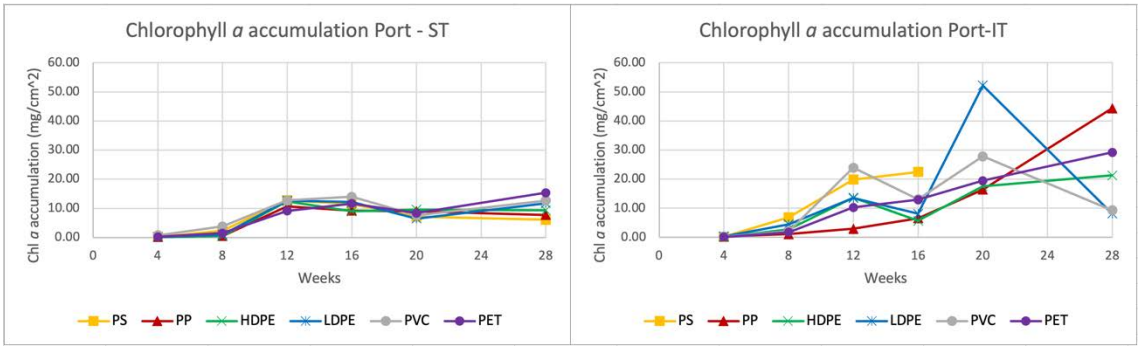

Figure 103: Trends over time of the Chl *a* accumulated on the surface of the plastic strips exposed in the port environment, in subtidal (left) and intertidal (right) zones.

Chlorophyll *a* amounted to 15.37 ± 0.95 mg/cm^2 on PET strips from subtidal port environment at week 28 and to 52.19 ± 17.25 mg/cm^2 on LDPE strips from intertidal port environment at week 20.

ANOVA, shown in Table 45, identified zonation (subtidal or intertidal; $F_{(1,120)}$= 61.13, p < 0.001), deployment time (4w, 8w, 16w, 20w, 28w; $F_{(5,120)}$= 87.36, p < 0.001) and their interaction ($F_{(5,120)}$= 26.21, p < 0.001) as significant predictors of differences in chlorophyll *a* accumulation at port environment (Figure 104, Figure 105, Figure 106). Table 46 and Table 47 show the results of the Scheffè's test performed respectively for zonation and deployment time to integrate the results obtained with ANOVA. The plastic type did not detectably influence the accumulated chlorophyll *a* in port environment.

Table 45: Results of the three-way ANOVA analysis of variance for chlorophyll *a* accumulation in the port environment.

	SS	Degr. Of Freedom	MS	F	p
Intercept	17396.28	1.00	17396.28	944.29	0.00
Zonation	1126.11	1.00	1126.11	61.13	0.00
Deployment time (week)	8047.33	5.00	1609.47	87.36	0.00
Plastic Type	153.23	4.00	38.31	2.08	0.09
Zonation*Deployment time (week)	2413.91	5.00	482.78	26.21	0.00
Zonation*Plastic Type	77.11	4.00	19.28	1.05	0.39
Deployment time (week)*Plastic Type	2820.48	20.00	141.02	7.65	0.00
Zonation*Deployment time (week)*Plastic Type	3414.54	20.00	170.73	9.27	0.00
Error	2210.70	120.00	18.42		

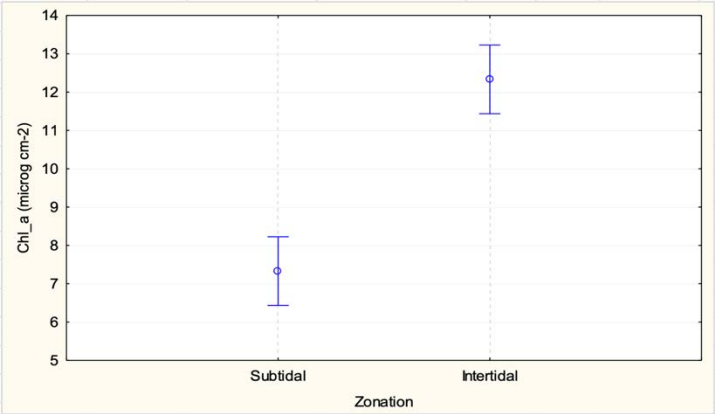

Figure 104: Graphical representation of the ANOVA results: comparison between the variability of the chlorophyll *a* accumulation averages for zonation in the port environment.

Table 46: Results of the post-hoc test, Scheffé's test, of the chlorophyll *a* accumulation for the zonation in the port environment.

Zonation	Mean Chl_a (microg cm-2)	1	2
Subtidal	7.330	****	
Intertidal	12.332		****

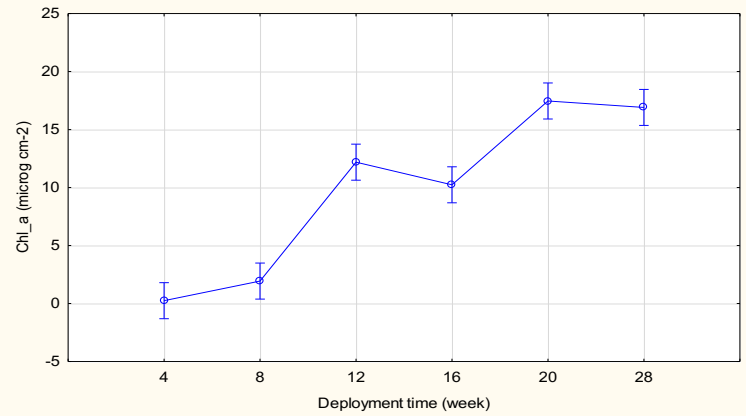

Figure 105: Graphical representation of the ANOVA results: comparison between the variability of the chlorophyll *a* accumulation averages for deployment time in the port environment.

Table 47: Results of the post-hoc test, Scheffé's test, of the chlorophyll *a* accumulation for the deployment time in the port environment.

Deployment time (week)	Mean Chl_a (microg cm-2)	1	2	3
4	0.247	****		
8	1.937	****		
16	10.239		****	
12	12.189		****	
28	16.910			****
20	17.463			****

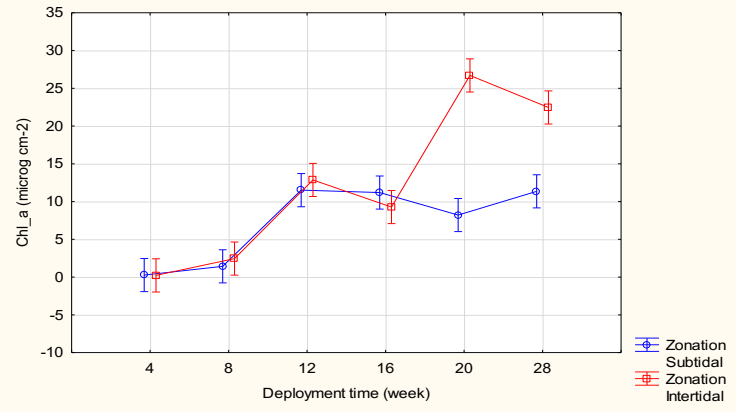

Figure 106: Graphical representation of the ANOVA results: comparison between the variability of the chlorophyll *a* accumulation averages for deployment time and zonation in the port environment.

Chl *a* accumulation and fouling mass were positively correlated (both normalized to plastic surface area) (Figure 107), reflecting that the biofouling was anchored by periphyton. The slope of the relationship was significantly different between environments (m = 0.73 on Port-IT, m = 0.64 on Lagoon-IT, 0.56 on River-F, m = 0.53 on Port-ST, m = 0.49 on Lagoon-ST and m = 0.11 on River-S), indicating that the accumulation of chlorophyll *a* was more related to the fouling mass in the intertidal environment than in the subtidal one.

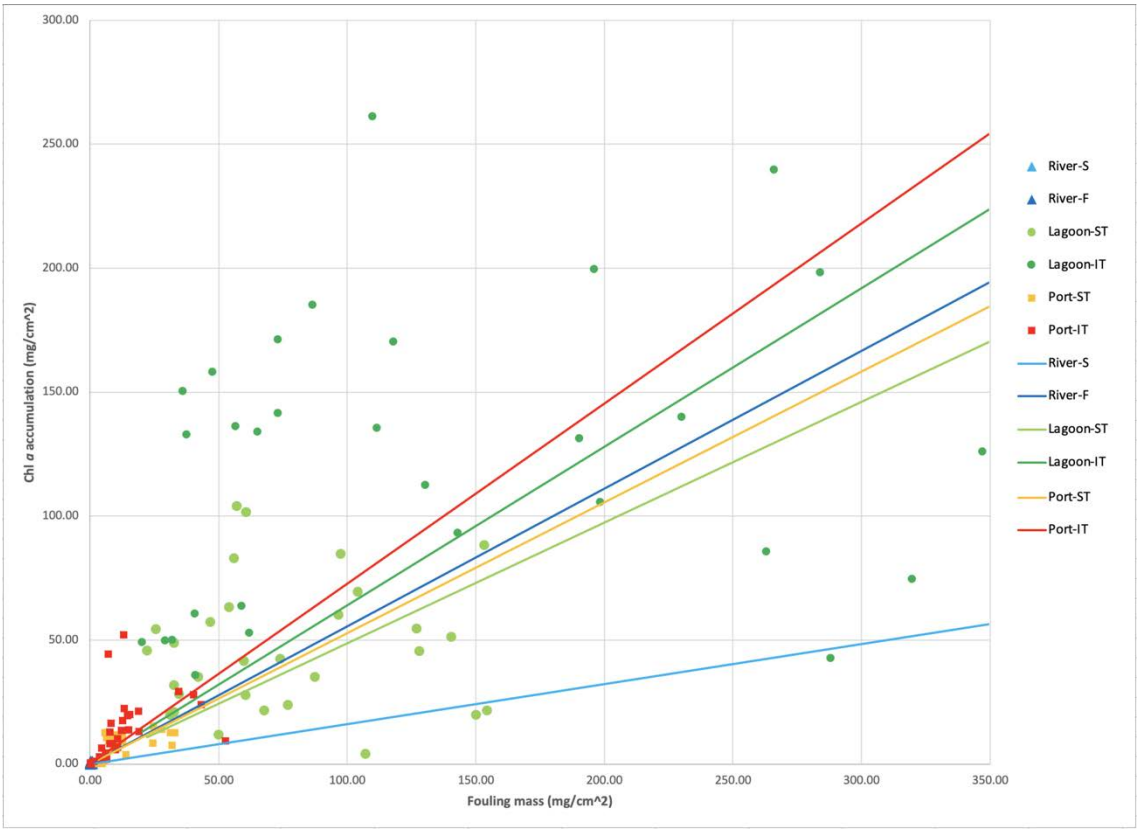

Figure 107: Chl *a* accumulation versus fouling mass, both normalized to plastic surface area, plotted by environments.

Analysis of variance in aquatic environments

Analysis of variance (ANOVA) performed on the entire data set showed an overview of the variation of apparent mass change, fouling mass and chlorophyll *a* in the environments examined with the exception of air.

For the apparent mass change, ANOVA (Table 48) identified location (river, lagoon, port; $F_{(2,236)}$ = 353.35, p < 0.001) and deployment time (4w, 8w, 16w, 20w, 28w; $F_{(5,236)}$ = 135.91, p < 0.001) as very significant predictors of differences in apparent mass change in the three environments examined (Figure 108, **Errore. L'origine riferimento non è stata trovata.**). The zonation (subtidal/submerged or intertidal/semi-floating; $F_{(1,236)}$= 53.18, p < 0.001) and plastic type (PP, HDPE, LDPE, PVC, PET; $F_{(4,236)}$ = 8.59, p < 0.001) were identified as significant predictors of differences in apparent mass change (Figure 110, Figure 111). Table 49, Table 50, Table 51, and Table 52 show the results of the Scheffè's test performed respectively for location, deployment time, zonation and plastic type to integrate the results obtained with ANOVA.

Furthermore, ANOVA identified the interaction between location and deployment time ($F_{(10,236)}$ = 8.40, p < 0.001) as significant predictors of differences in apparent mass change.

Table 48: Results of the four-way ANOVA analysis of variance for apparent mass change in the river, lagoon and port environment.

	SS	Degr. Of Freedom	MS	F	p
Intercept	3.14	1.00	3.14	2176.56	0.00
{1}Location	1.02	2.00	0.51	353.35	0.00
{2}Zonation	0.08	1.00	0.08	53.18	0.00
{3}Deployment time (week)	0.98	5.00	0.20	135.91	0.00
{4}Plastic Type	0.20	4.00	0.05	34.32	0.00
Location*Zonation	0.00	2.00	0.00	1.28	0.28
Location*Deployment time (week)	0.33	10.00	0.03	22.72	0.00
Zonation*Deployment time (week)	0.02	5.00	0.00	2.09	0.07
Location*Plastic Type	0.10	8.00	0.01	8.40	0.00
Zonation*Plastic Type	0.00	4.00	0.00	0.30	0.88
Deployment time (week)*Plastic Type	0.08	20.00	0.00	2.88	0.00
Location*Zonation*Deployment time (week)	0.01	10.00	0.00	0.65	0.77
Location*Zonation*Plastic Type	0.01	8.00	0.00	0.59	0.79
Location*Deployment time (week)*Plastic Type	0.06	40.00	0.00	1.03	0.42
Zonation*Deployment time (week)*Plastic Type	0.01	20.00	0.00	0.29	1.00
1*2*3*4	0.02	40.00	0.00	0.32	1.00
Error	0.34	236.00	0.00		

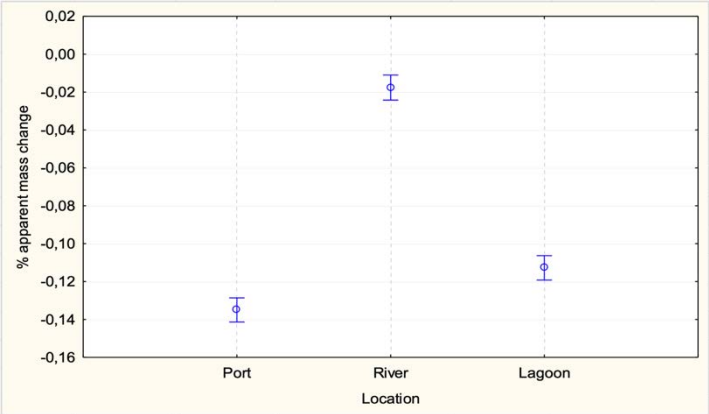

Figure 108: Graphical representation of the ANOVA results: comparison between the variability of the apparent mass change averages for location.

Table 49: Results of the post-hoc test, Scheffé's test, of the apparent mass change for the location tested.

Location	Mean apparent mass change (%)	1	2	3
Port	-0.140	****		
Lagoon	-0.110		****	
River	-0.018			****

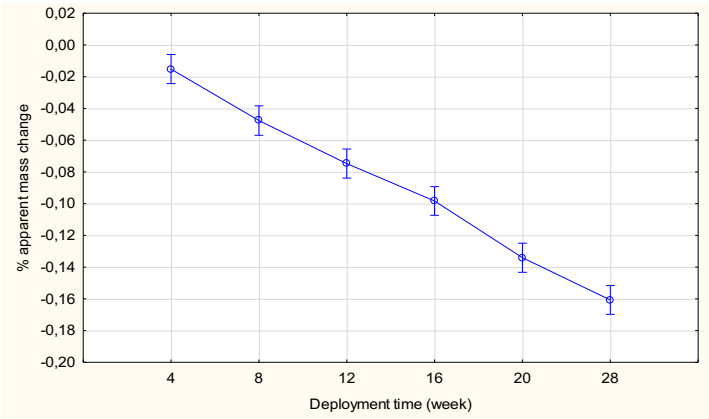

Figure 109: Graphical representation of the ANOVA results: comparison between the variability of the apparent mass change averages for deployment time.

Table 50: Results of the post-hoc test, Scheffé's test, of the apparent mass change for the deployment time in all environments tested.

Deployment time (week)	Mean apparent mass change (%)	1	2	3	4	5	6
28	-0.164	****					
20	-0.137		****				
16	-0.105			****			
12	-0.076				****		
8	-0.050					****	
4	-0.015						****

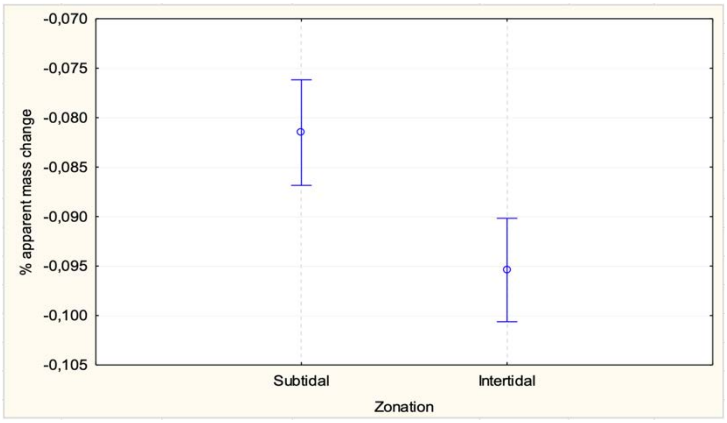

Figure 110: Graphical representation of the ANOVA results: comparison between the variability of the apparent mass change averages for zonation.

Table 51: Results of the post-hoc test, Scheffé's test, of the apparent mass change for the zonation in all environments tested.

Zonation	Mean apparent mass change (%)	1	2
Intertidal	-0.102	****	
Subtidal	-0.080		****

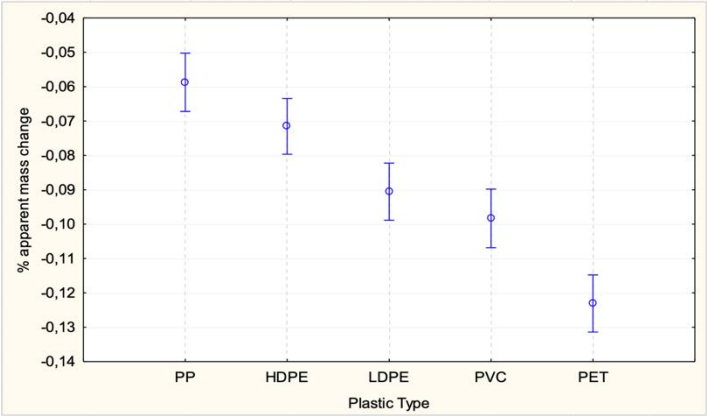

Figure 111: Graphical representation of the ANOVA results: comparison between the variability of the apparent mass change averages for plastic type.

Table 52: Results of the post-hoc test, Scheffé's test, of the apparent mass change for the plastic type in all environments tested.

Plastic Type	Mean apparent mass change (%)	1	2	3
PET	-0.128			****
PVC	-0.099	****		
LDPE	-0.094	****		
HDPE	-0.074		****	
PP	-0.064		****	

For the fouling mass, ANOVA (Table 53), identified location (river, lagoon, port; $F_{(2,360)}$ = 1558, $p < 0.001$), zonation (subtidal/submerged and intertidal/semi-floating; $F_{(1,360)}$= 130.57, $p < 0.001$), plastic type (PP, HDPE, LDPE, PVC, PET; $F_{(4,360)}$ = 91.59, $p < 0.001$) and deployment time (4w, 8w, 16w, 20w, 28w; $F_{(5,360)}$ =74.90, $p < 0.001$) as very significant predictors of differences in fouling mass in the three environments examined (Figure 112, Figure 113, Figure 114, **Errore. L'origine riferimento non è stata trovata.**). Table 54, Table 55, Table 56, and Table 57 show the results of the Scheffè's test performed respectively for location, zonation, plastic type, and deployment time to integrate the results obtained with ANOVA.

Furthermore, ANOVA identified the interaction between location and zonation ($F_{(2,360)}$ = 127.39, $p < 0.001$) as very significant predictors of differences in fouling mass; the interaction between location and plastic type ($F_{(8,360)}$ =60.79, $p < 0.001$), location and deployment time ($F_{(10,360)}$ = 49.62, $p < 0.001$), zonation and deployment time ($F_{(5,360)}$ =

31.78, $p < 0.001$) and zonation and plastic type ($F_{(4,360)} = 18.03$, $p < 0.001$) were identified as significant predictors of differences in apparent mass change.

Table 53: Results of the four-way ANOVA analysis of variance for fouling mass in the river, lagoon and port environment.

	SS	Degr. Of Freedom	MS	F	p
Intercept	807340.20	1.00	807340.20	2181.28	0.00
{1}Location	1153298.32	2.00	576649.16	1558.00	0.00
{2}Zonation	48326.17	1.00	48326.17	130.57	0.00
{3}Deployment time (week)	138610.16	5.00	27722.03	74.90	0.00
{4}Plastic Type	135590.81	4.00	33897.70	91.59	0.00
Location*Zonation	94297.40	2.00	47148.70	127.39	0.00
Location*Deployment time (week)	183652.03	10.00	18365.20	49.62	0.00
Zonation*Deployment time (week)	58810.42	5.00	11762.08	31.78	0.00
Location*Plastic Type	180003.47	8.00	22500.43	60.79	0.00
Zonation*Plastic Type	26692.09	4.00	6673.02	18.03	0.00
Deployment time (week)*Plastic Type	27242.94	20.00	1362.15	3.68	0.00
Location*Zonation*Deployment time (week)	108018.69	10.00	10801.87	29.18	0.00
Location*Zonation*Plastic Type	58428.03	8.00	7303.50	19.73	0.00
Location*Deployment time (week)*Plastic Type	45680.88	40.00	1142.02	3.09	0.00
Zonation*Deployment time (week)*Plastic Type	27124.02	20.00	1356.20	3.66	0.00
1*2*3*4	54977.85	40.00	1374.45	3.71	0.00
Error	133243.72	360.00	370.12		

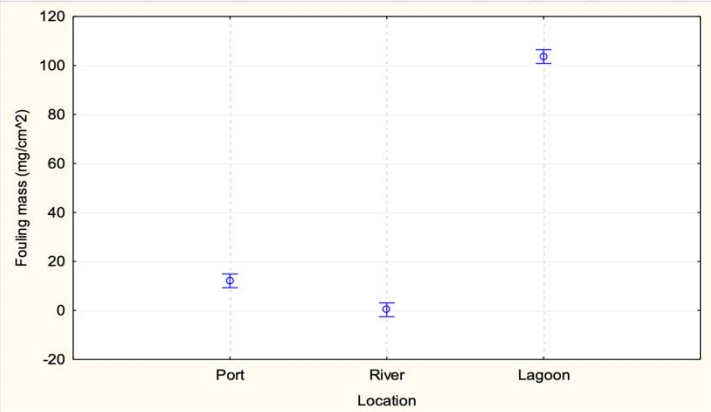

Figure 112: Graphical representation of the ANOVA results: comparison between the variability of the fouling mass averages for location.

Table 54: Results of the post-hoc test, Scheffé's test, of the fouling mass for the location tested.

Location	Mean Fouling mass (mg/cm^2)	1	2	3
River	0.263	****		
Port	12.069		****	
Lagoon	103.666			****

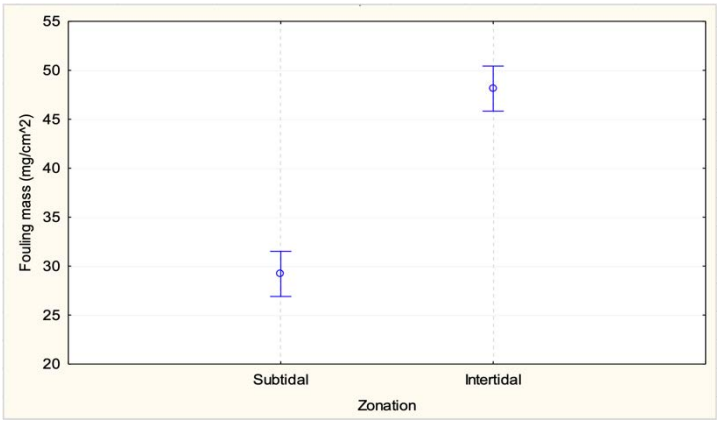

Figure 113: Graphical representation of the ANOVA results: comparison between the variability of the fouling mass averages for zonation.

Table 55: Results of the post-hoc test, Scheffé's test, of the fouling mass for the zonation in all environments tested.

Zonation	Mean Fouling mass (mg/cm^2)	1	2
Subtidal	29.206	****	
Intertidal	48.126		****

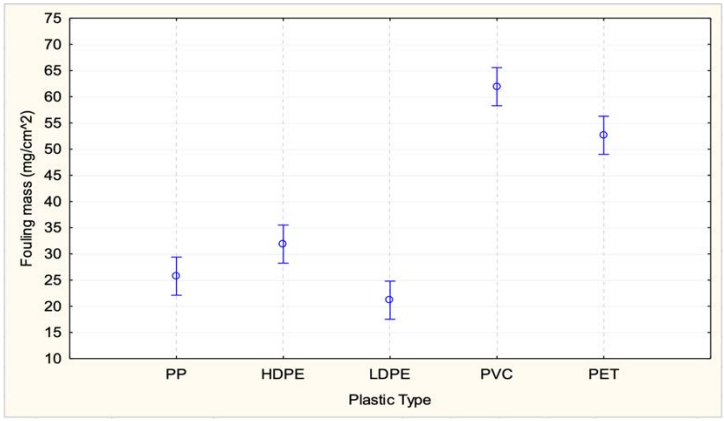

Figure 114: Graphical representation of the ANOVA results: comparison between the variability of the fouling mass averages for plastic type.

Table 56: Results of the post-hoc test, Scheffé's test, of the fouling mass for the plastic type in all environments tested.

Plastic Type	Mean Fouling mass (mg/cm^2)	1	2	3	4
LDPE	21.164	****			
PP	25.747	****	****		
HDPE	31.862		****		
PET	52.638			****	
PVC	61.920				****

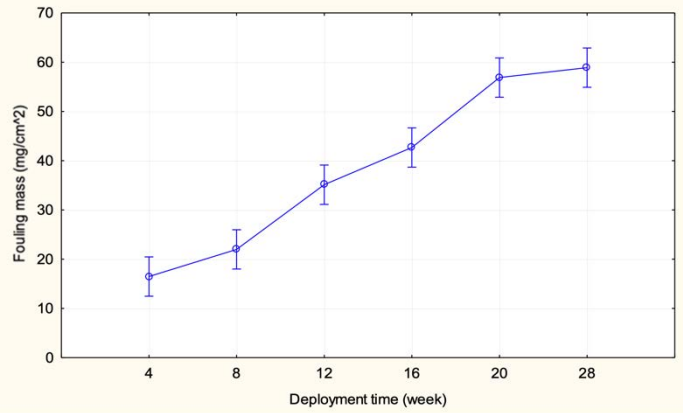

Figure 115: Graphical representation of the ANOVA results: comparison between the variability of the fouling mass averages for deployment time.

Table 57: Results of the post-hoc test, Scheffé's test, of the fouling mass for the deployment time in all environments tested.

Deployment time (week)	Mean Fouling mass (mg/cm^2)	1	2	3
4	16.467	****		
8	21.984	****		
12	35.118		****	
16	42.666		****	
20	56.877			****
28	58.885			****

For the chlorophyll *a* accumulation, ANOVA (Table 58), identified location (river, lagoon, port; $F_{(2,360)} = 310.06$, $p < 0.001$) and zonation (subtidal/submerged and intertidal/semi-floating; $F_{(1,360)} = 80.30$, $p < 0.001$) as very significant predictors of differences in chlorophyll *a* accumulation in the three environments examined (Figure 116, Figure 117). For the deployment time ($F_{(5,360)} = 6.68$, $p < 0.001$), albeit showing an increase in chlorophyll *a* with time, the difference was not quite significant at $\alpha = 0.05$ (**Errore. L 'origine riferimento non è stata trovata.**). Table 59, Table 60, and Table 61 show the results of the Scheffè's test performed respectively for location, zonation, and deployment time to integrate the results obtained with ANOVA. The plastic type did not detectably influence the accumulated chlorophyll *a* in the three environments.

Furthermore, ANOVA identified the interaction between location and zonation ($F_{(2,360)} = 65.95$, $p < 0.001$) as significant predictors of differences in chlorophyll *a* accumulated.

Table 58: Results of the four-way ANOVA analysis of variance for chlorophyll *a* accumulation in the river, lagoon and port environment.

	SS	Degr. Of Freedom	MS	F	p
Intercept	538030.05	1.00	538030.05	432.68	0.00
{1}Location	771122.13	2.00	385561.07	310.06	0.00
{2}Zonation	99856.38	1.00	99856.38	80.30	0.00
{3}Deployment time (week)	41544.43	5.00	8308.89	6.68	0.00
{4}Plastic Type	4500.66	4.00	1125.16	0.90	0.46
Location*Zonation	164016.07	2.00	82008.03	65.95	0.00
Location*Deployment time (week)	42601.54	10.00	4260.15	3.43	0.00
Zonation*Deployment time (week)	22560.54	5.00	4512.11	3.63	0.00
Location*Plastic Type	9538.96	8.00	1192.37	0.96	0.47
Zonation*Plastic Type	1891.65	4.00	472.91	0.38	0.82
Deployment time (week)*Plastic Type	37711.98	20.00	1885.60	1.52	0.07
Location*Zonation*Deployment time (week)	50657.08	10.00	5065.71	4.07	0.00
Location*Zonation*Plastic Type	4845.42	8.00	605.68	0.49	0.87
Location*Deployment time (week)*Plastic Type	70502.61	40.00	1762.57	1.42	0.05
Zonation*Deployment time (week)*Plastic Type	35335.79	20.00	1766.79	1.42	0.11
1*2*3*4	66367.07	40.00	1659.18	1.33	0.09
Error	447658.01	360.00	1243.49		

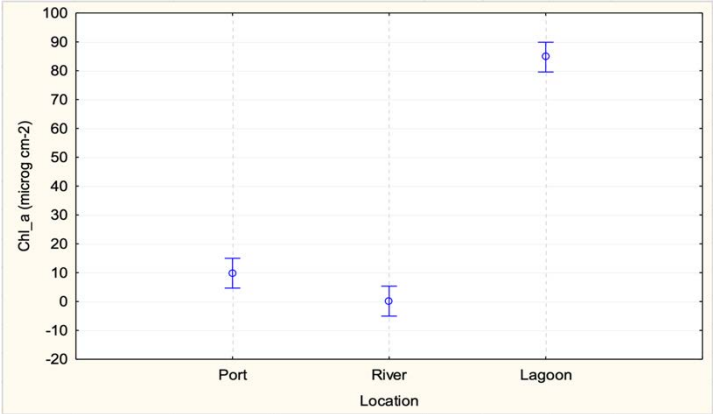

Figure 116: Graphical representation of the ANOVA results: comparison between the variability of the chlorophyll *a* accumulation averages for location.

Table 59: Results of the post-hoc test, Scheffé's test, of the chlorophyll *a* accumulation for the location tested.

Location	Mean Chl_a (microg cm-2)	1	2	3
River	0.151	****		
Port	9.831		****	
Lagoon	84.714			****

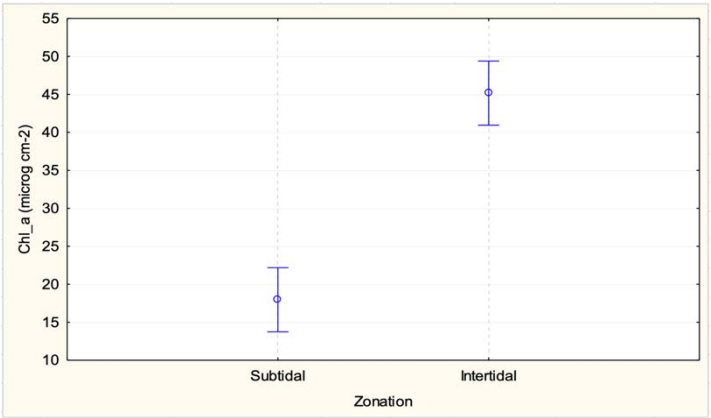

Figure 117: Graphical representation of the ANOVA results: comparison between the variability of the chlorophyll *a* accumulation averages for zonation.

Table 60: Results of the post-hoc test, Scheffé's test, of the chlorophyll *a* accumulation for the zonation in all environments tested.

Zonation	Mean Chl_a (microg cm-2)	1	2
Subtidal	17.967	****	
Intertidal	45.164		****

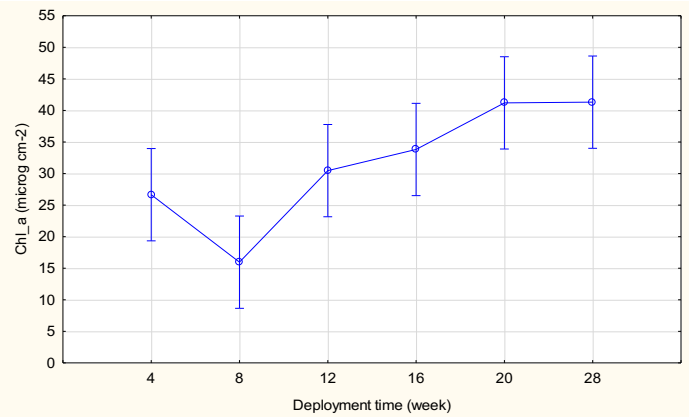

Figure 118: Graphical representation of the ANOVA results: comparison between the variability of the chlorophyll a accumulation averages for deployment time.

Table 61: Results of the post-hoc test, Scheffé's test, of the chlorophyll *a* accumulation for the deployment time in all environments tested.

Deployment time (week)	Mean Chl_a (microg cm-2)	1	2
8	15.962		****
4	26.644	****	****
12	30.465	****	****
16	33.818	****	
20	41.194	****	
28	41.308	****	

Leaching test

The leaching tests were conducted on the plastic strips of both intertidal and subtidal zones deployed in the river, lagoon and port environments, which were exposed for 12 and 28 weeks, in addition to the control strips.

The electrical conductivity (EC) showed for all environments higher values in the leachate obtained from the strips exposed for 28 weeks compared to those obtained from the strips exposed for 12 weeks (Figure 119, Figure 120, Figure 121). In the leachate obtained from the plastic strips exposed for 12 weeks, the EC varied from 0.01 mS/cm to 0.04 mS/cm in the river environment, from 2.4 mS/cm to 8.48 mS/cm in the lagoon environment and from 1.93 mS/cm to 9.02 mS/cm in the port environment; while in that obtained from the strips exposed for 28 weeks it ranged between 0.04 mS/cm and 0.08 mS/cm in the river environment, between 4.00 mS/cm and 13.27 mS/cm in the lagoon environment and from 2.54 mS/cm to 12.3 mS/cm in the port environment.

The EC of the leachate obtained from the strips deployed in semi-floating condition in the river environment (Figure 119) were generally higher than that obtained from the strips exposed in the submerged zone. It ranged from 0.02 mS/cm to 0.08 mS/cm for the strips in semi-floating condition, and from 0.01 mS/cm to 0.06 mS/cm for the strips in submerged condition. Exceptions were leachate from PS strips exposed for 12 weeks and PP strips and PVC strips deployed for 28 weeks which had equal values between those shown in the two zones (respectively 0.04 mS/cm, 0.04 mS/cm and 0.06 mS/cm). In the lagoon and port environments (Figure 120, Figure 121), all the values of the solutions obtained from the subtidal zone were lower than the respective ones of the intertidal zone. For the leachate obtained from strips exposed in the intertidal zones, the EC ranged from 5.82 mS/cm to 13.27 mS/cm in the lagoon environmental and from 1.93 mS/cm to 12.3 mS/cm in the port environmental; while for those obtained from strips exposed in the subtidal zones the EC ranged from 2.40 mS/cm to 8.53 mS/cm in the lagoon environmental and from 2.35 mS/cm to 7.35 mS/cm in the port environmental.

From the analysis of the single anions and cations released in solution, responsible for the EC, the highest values, for the plastics exposed in the river environment (Figure 122), were those of the bicarbonate ion and the calcium ion, that respectively reached up 42.0 mg/l and 10.8 mg/l.

Both in the lagoon (Figure 123) and port environments (Figure 124), instead, the highest values were those of the chloride ion and the sodium ion, that respectively reached up 4967.7 mg/l and 572.3 mg/l in the lagoon environmental and 3200.0 mg/l and 610.0 mg/l in the port environmental.

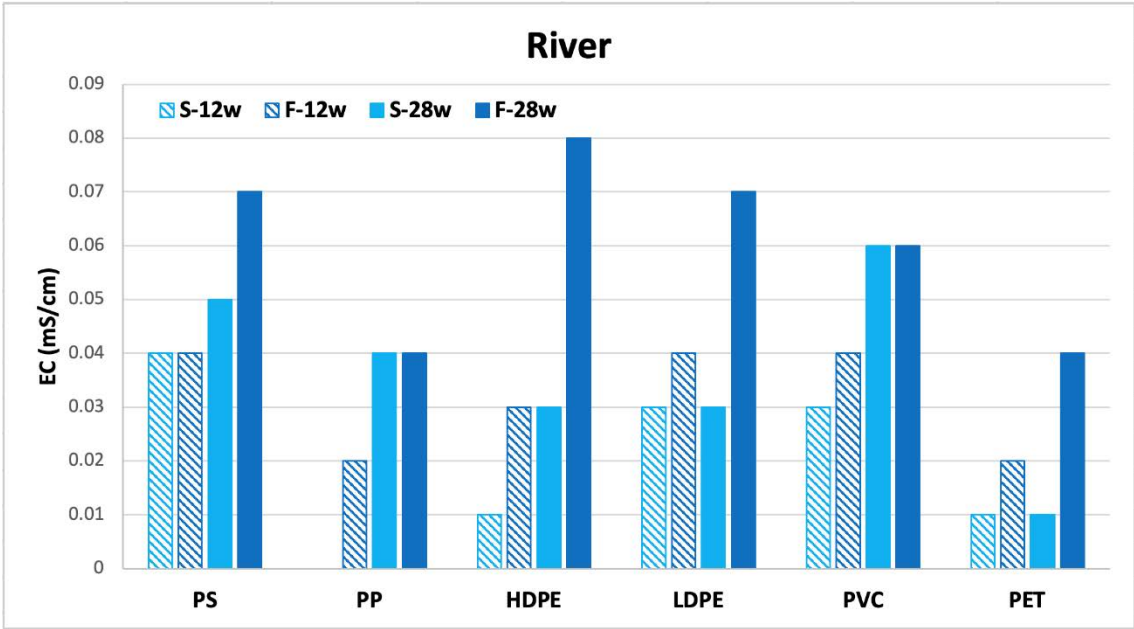

Figure 119: Electric conductivity (EC) values, expressed in milliSiemens per centimeter, measured in the solutions obtained from the leaching tests performed on the plastic strips exposed for 12 and 28 weeks in the submerged and semi-floating zones of the river environment.

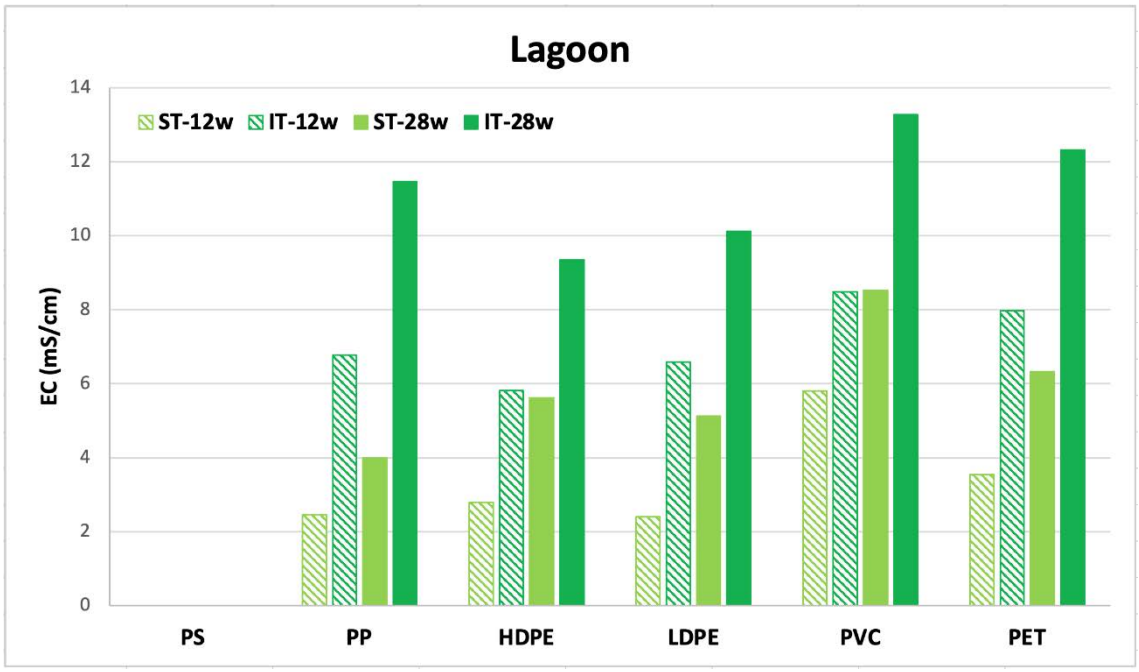

Figure 120: Electric conductivity (EC) values, expressed in milliSiemens per centimeter, measured in the solutions obtained from the leaching tests performed on the plastic strips exposed for 12 and 28 weeks in the subtidal and intertidal zones of the lagoon environment.

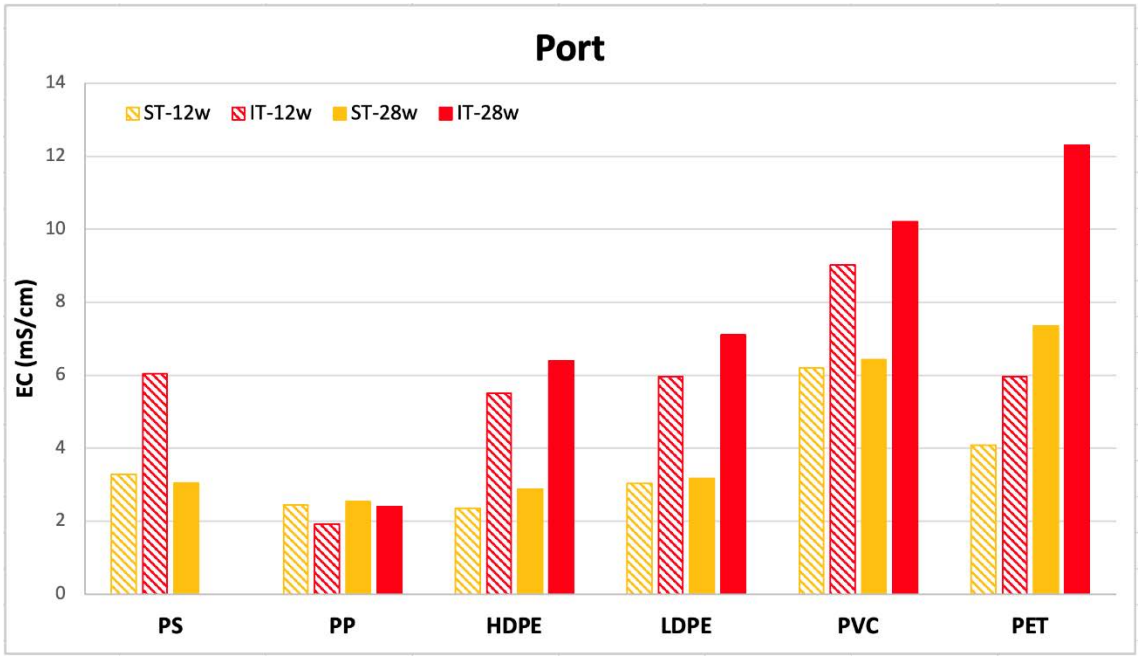

Figure 121: Electric conductivity (EC) values, expressed in milliSiemens per centimeter, measured in the solutions obtained from the leaching tests performed on the plastic strips exposed for 12 and 28 weeks in the subtidal and intertidal zones of the port environment.

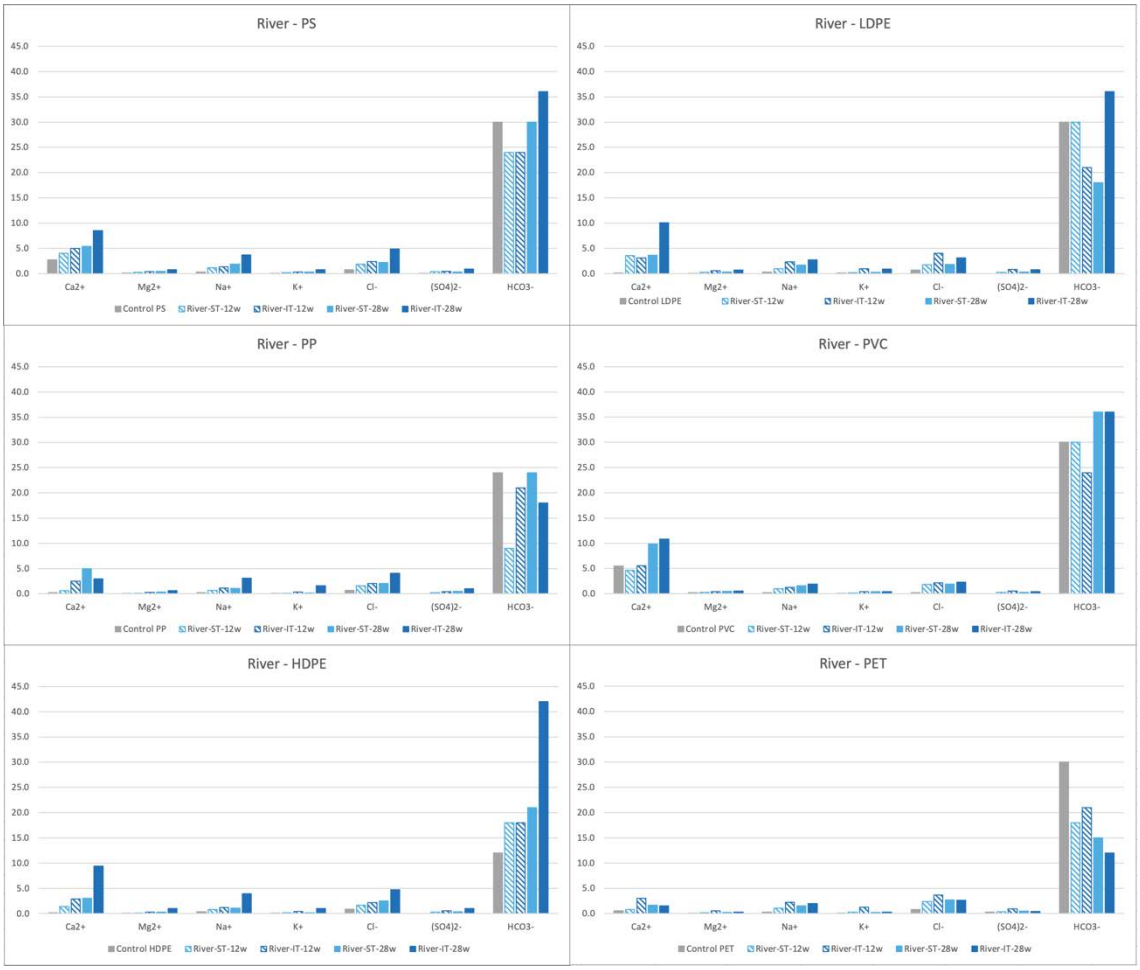

Figure 122: Concentration, expressed in ppm, of the main ions present in the solutions obtained from the leaching tests performed on the plastic strips exposed for 12 and 28 weeks in the submerged and semi-floating zones of the river environment.

Figure 123: Concentration, expressed in ppm, of the main ions present in the solutions obtained from the leaching tests performed on the plastic strips exposed for 12 and 28 weeks in the subtidal and intertidal zones of the lagoon environment.

Figure 124: Concentration, expressed in ppm, of the main ions present in the solutions obtained from the leaching tests performed on the plastic strips exposed for 12 and 28 weeks in the subtidal and intertidal zones of the port environment.

Dissolution

The dissolution of the plastic strips that were exposed for 28 weeks in the port and in the lagoon with the relative fouling were compared with the results of the dissolutions performed on the sediments of the respective exposure environments.

The tests showed that the dissolved material deposited on the strips had a geochemical composition that reflected the composition of the sediment of the respective exposure environments.

In the strips exposed in the lagoon environment, the major concentrations of the main cations were those of Na, Mg, Al, K, Ca and Fe and P, Ti and Mn were present in low concentrations (Figure 125). All plastics exposed in the subtidal zone showed higher values of Mg, Al, K, Ti, Mn and Fe than those in the intertidal zone, while the values of Na, P and Ca were higher in those exposed in the intertidal zone. Exceptions were the Na which was higher in the subtidal zone for LDPE plastic and the Ca which was higher in the subtidal zone for PET.

In the strips exposed in the port environment, the greatest concentration among the main cations was that of Ca, while in low concentrations there were Na, Mg, Al, P and Fe (Figure 126). All plastics exposed in the subtidal zone showed higher values of Mg, Al, P, Ca and Fe than those in the intertidal zone, while the values of Na were higher in those exposed in the intertidal zone. Exceptions were Al, P and Ca which were higher in the intertidal zone for PP, PP and HDPE plastics respectively.

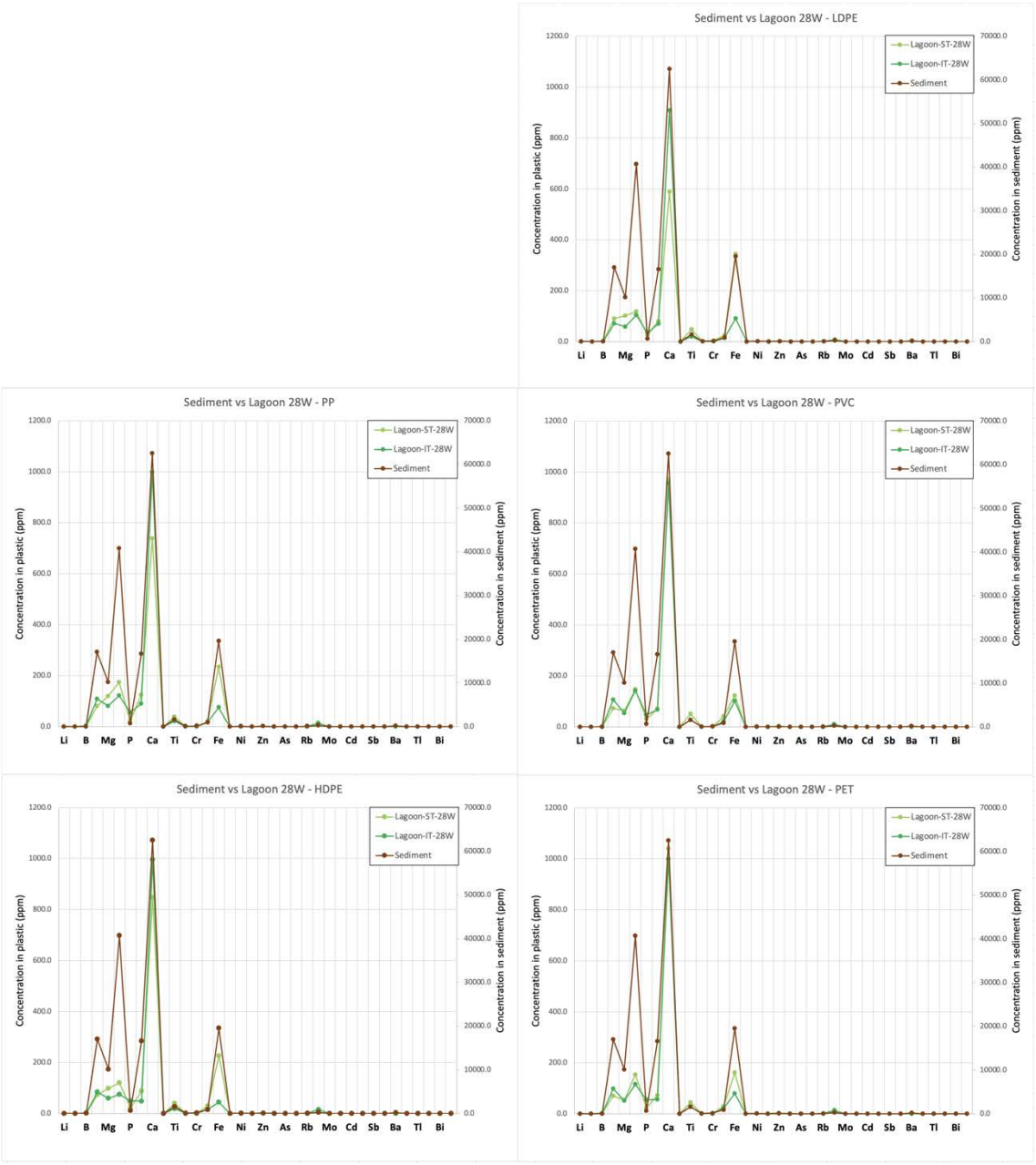

Figure 125: Concentration, expressed in ppm, of the cations obtained from the dissolutions of the plastic strips that were exposed for 28 weeks in the lagoon with the relative fouling compared with the concentration of the cations obtained from the dissolutions performed on the sediments of the exposure environment. NB: the scale on the left of each graph refers to the concentration of ions obtained from the test on plastics, while the scale on the right refers to the concentration of ions obtained from the sediment test.

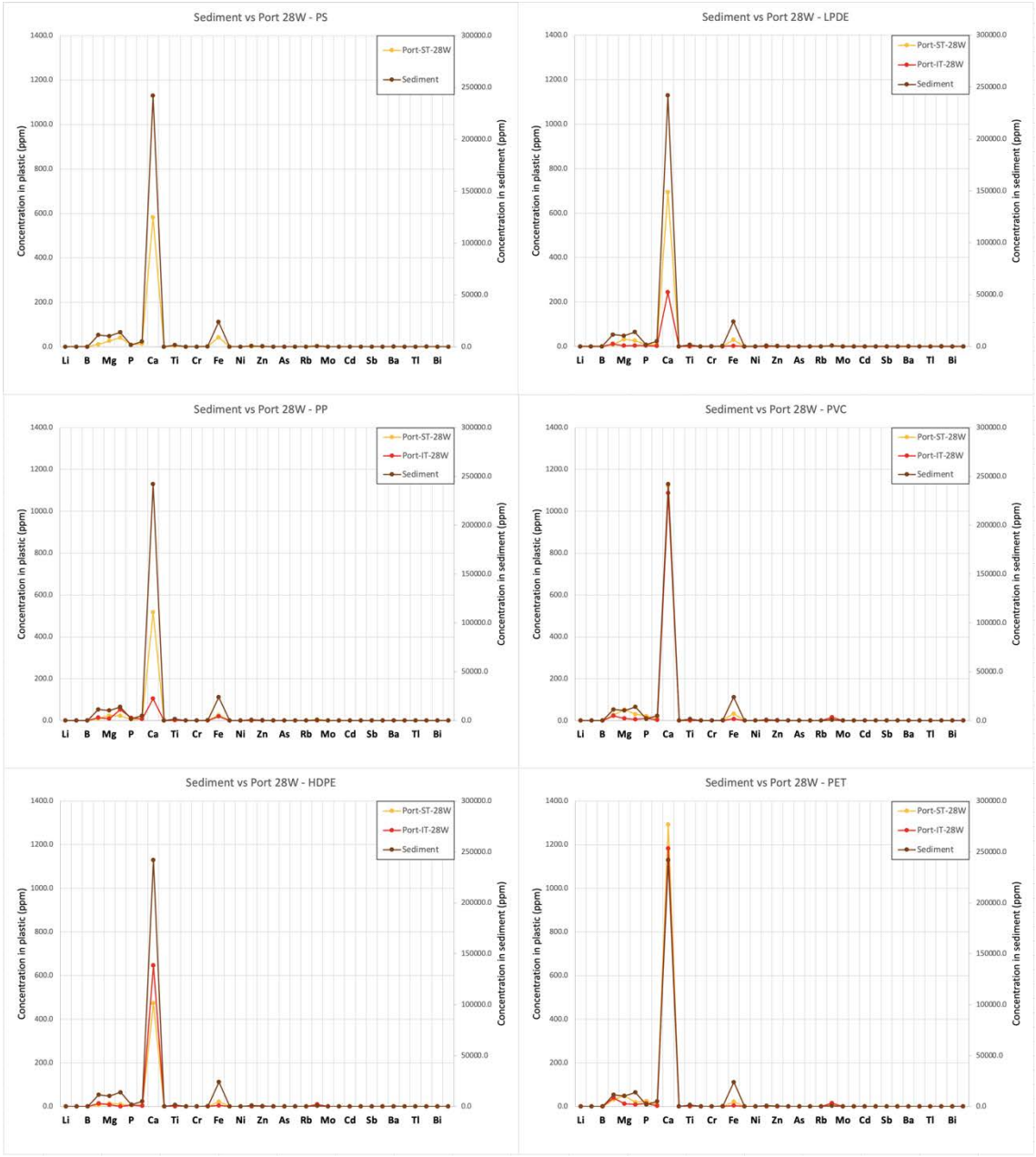

Figure 126: Concentration, expressed in ppm, of the cations obtained from the dissolutions of the plastic strips that were exposed for 28 weeks in the port with the relative fouling compared with the concentration of the cations obtained from the dissolutions performed on the sediments of the exposure environment. NB: the scale on the left of each graph refers to the concentration of ions obtained from the test on plastics, while the scale on the right refers to the concentration of ions obtained from the sediment test.

Discussion

Although chemical and biological inertness are among the key traits that have helped enable the dominance of plastics as a consumer material, their stability has also led to an ubiquity and persistence of plastic debris and microplastics in the environment, a concern which has risen to international attention (Koelmans et al., 2017; Krause et al., 2020). The coastal environment is likely the most important source of microplastics to the marine environment (Andrady, 2011), yet the factors that affect plastic degradation and the production of microplastics in this environment are complex and remain incompletely understood. A better understanding of the rates and controls of plastic degradation in the coastal environment are crucial for developing mitigation strategies and could be useful for establishing priority areas for intensive intervention such as direct removal (Rizzo et al., 2021).

To understand the degradation of plastics in the coastal environment, the river environment, the lagoon environment, and the port environment were selected, to test the degradation of the common consumer polymers PS, PP, HDPE, LDPE, PVC and PET. Strips of these six types of plastics were exhibited for a total of 36 weeks in these three environments under contrasting deployment depths (subtidal/submerged versus intertidal/semi-floating) and in an urban air environment.

This study was preceded by a preliminary experiment carried out in Maryland (USA) in which two types of plastics, PS and HDPE, were tested in a tidal subestuary under contrasting hydrodynamic intensities (depositional versus erosional) and deployment depths (subtidal versus intertidal) (Rizzo et al., 2021). This experiment revealed a significant surface alteration of HDPE within 4 weeks of environmental exposure, observed by SEM. This plastic in fact had numerous grooves and pittings on the surface, while a change in marginal mass was detected. PS strips degraded faster than HDPE strips, as evidenced by the mass loss at 4 weeks and the polymer surface. The hydrodynamic conditions were found to influence the PS alteration and fragmentation rate, with larger cavities and greater mass loss observed among the PS strips exposed to the erosional site compared to the deposition site. The deployment depth was found to

have a complex effect on plastic degradation, but generally the PS strips positioned at intertidal depths were more altered than those at subtidal depths. Both plastic types developed a fouling biofilm, more consistent at subtidal depths, which probably influenced the degradation rates, as it played a protective role. The study was then implemented, adding 4 other types of plastics and differentiating the deployment environments. The new tests were therefore carried out in the lagoon, port, river and air environment.

The study showed that the rate of degradation and the type of degradation strongly depend on the environment to which the plastics were exposed. This result is in accordance with what Biber (2016) found after testing 4 types of polymers deployed in seawater, fresh water and air, for 600 days.

The rate of degradation was also higher in the air environment than in the aquatic environments. Similar results were obtained for all the researches where the air environment was compared with the marine or freshwater one, including Pegram and Andrady (1989), Andrady et al. (1993a, 1993b), Arias-Villamizar and Vázquez-Morillas (2018), Biber et al. (2019). These scholars attribute the cause of greater degradation in air compared to water to higher UV radiation, higher temperatures and the absence of fouling. Other authors, including Gewert et al. (2015), also impute oxygen, which diffuses faster and can be at higher concentration in the air than in water, as the initiating cause of abiotic degradation.

Among the aquatic environments tested in this study, the one that caused the greatest degradation is the port one, followed by the lagoon one and finally the river one as also highlighted by four-way ANOVA and confirmed by Scheffé's post-hoc test. The agents that contributed to the degradation are many: exposure to UV rays, high exposure temperatures, water salinity, accumulation of fouling, oxygen availability, hydrodynamic energy.

As mentioned before, previous studies on this topic demonstrated that the factor that most influences the degradation of plastics is exposure to UV radiation, which mainly causes photooxidation. Regarding the temperature, the literature indicates that a higher

temperature causes a more rapid degradation (Pegram and Andrady, 1989; Andrady et al., 1993b; Min et al., 2020); although according to Gardette et al. (2013) in the absence of sunlight, thermo-oxidative degradation, caused by temperature, does not occur at appreciable rates below 100°C for PE. In this experiment, the exposure data, therefore a higher light intensity and a higher temperature, recorded in the port environment, confirm that higher values of these parameters produce greater degradation. Even higher salinity, as also reported by Arias-Villamizar and Vázquez-Morillas (2018) who tested HDPE exposed to direct weathering in the Caribbean Sea and the Magdalena River, Colombia, in this study promoted a rate of greater degradation; in fact, in the river environment, characterized by fresh water, less degradation was found compared to the lagoon environment, characterized by brackish water, where, in turn, less degradation was recorded compared to the port environment, the one where there was a salinity higher.

Fouling also had effects on the deterioration of the polymers. In the aquatic environment, especially lagoon and port, all the samples showed the accumulation of fouling, as evidenced by macroscopic observation, by ANOVA and by Scheffé's post-hoc test. Accumulation of fouling on plastics in the aquatic environments has also been found in other studies, including Ye and Andrady (1991), Gündoğdu et al. (2017), Pauli et al. (2017), Karkanorachaki et al. (2021). Fouling on the one hand may have caused increasing drag and chronic shear stress, as reported by Biber et al. (2019), exerted mechanical, chemical and enzymatic stresses, eroded the surface and caused depolymerization, as found by Gu (2003), Shah et al. (2008) and Nowak et al. (2011). On the other hand, it may have mitigated the photo-oxidation rate by decreasing the penetration of sunlight, as reported by Pegram and Andrady (1989), O'Brine and Thompson (2010), Andrady (2011), Arias-Villamizar and Vázquez-Morillas (2018). According to the results obtained, the fouling has mainly carried out a protective action as in the lagoon environment, where it has accumulated more, there has not been as much degradation as in the port environment, where the plastic strips have remained mostly uncovered by the fouling.

Considering the depth of deployment, the strips of all types of plastic, albeit differently from the environment, deteriorated more rapidly in the intertidal/semi-floating zone than in the subtidal/submerged zone, as proved by ANOVA and by Scheffé's post-hoc test and also found by Biber et al. (2019) and Rizzo et al. (2021). The greater degradation in the intertidal environment is probably due to a greater exposure to UV radiation, to the greater thermal stress to which the polymers are subjected by emerging and immersing for an average of 12 hours a day, and to the greater hydrodynamic energy of the intertidal zone compared to the subtidal zone.

ANOVA confirmed that the type of plastic influenced the rate of degradation. This differentiation was further verified by Schieffè's post-hoc test. PS was more prone to degradation among all types of plastics tested and in all environments. It fragmented more frequently and more completely than the other plastic strips, limiting its recovery. Where recovered, it also exhibited the greatest loss in weight. The PS strips deployed in the subtidal port environment exhibited a high degree of cavity formation, as was seen through the SEM images. These results confirmed what Restrepo-Flórez et al. (2014) demonstrated, according to which amorphous regions of the plastic are more prone to attack than more crystalline regions. Also in the study by Biber et al. (2019), where it had been tested with PE and PET, PS deteriorated faster than other materials, demonstrating a high sensitivity to light. In the laboratory experiment of Gerritse et al. (2020), on the other hand, PS showed a lower fragmentation rate than PET, but this is probably due to the fact that the exposure conditions between PS and PET were not the same and PS, unlike PET that had sunk, was floating covered with fouling that shielded UV radiation.

In an aquatic environment, PP has been shown to be the least prone to degradation, while, when exposed to air, it has reported a higher rate of degradation relative to PET, PVC, LDPE and HDPE. The in-air result is in line with the experiment of Gijsman et al. (1999), in which PP is compared with PE and other types of polymers that have been exposed to thermo-oxidative agents in the laboratory, and with that of Ojeda et al. (2011), during which HDPE, LLDPE and PP were exposed to natural weathering and PP suffered the most rapid degradation. The result in the aquatic environment is also

reflected in the literature. Artham et al. (2009), in fact, by immersing PC (Polycarbonate), LDPE, HDPE and PP in the Bay of Bengal, found that PP showed the lowest weight loss. The exception occurred in the intertidal port environment where PP had lost more than HDPE, perhaps due to less fouling of the PP strips and therefore greater exposure to UV rays. The lower propensity for fouling accumulation on PP compared to HDPE was proved by Artham et al. (2009), according to which HDPE has higher fouling due to a more hydrophobic surface than PP.

HDPE in the aquatic environment lost less mass compared to PET, PVC and LDPE, while in air it had degraded to a lesser extent than all the other types tested. HDPE has higher degree of crystallinity than LDPE, which gives it greater stability when exposed to UV radiation under laboratory conditions (Craig et al., 2005), and has been shown to be more stable to aging than LDPE (Gulmine et al., 2003). Here I additionally show that this greater stability holds true under a range of environmental conditions.

LDPE has undergone less degradation than PET and PVC in the aquatic environments and more than HDPE and PP. Artham et al. (2009) observed the greatest weight loss of LDPE compared to HDPE and PP when immersed in seawater.

PET showed greater mass loss than PVC, LDPE, HDPE and PP. Chamas et al. (2020) reported that PET undergoes both thermal oxidation, hydrolytic cleavage and photooxidation. Several authors, including Krueger et al. (2015), Wei and Zimmermann (2017) and Amaral-Zettler et al. (2020), argue that polymers with hydrolysable chemical bonds in their backbone, such as PET, are more susceptible to biodegradation than non-hydrolysable ones (PE, PP, PS and PVC). Furthermore, Gerritse et al (2020), in agreement with the results of this study, reported that PET had undergone greater weight loss than PE, PS and PP in a laboratory seawater microcosm.

It was difficult to compare the results obtained for PVC with the existing literature. Most of the studies involved experiments testing only photooxidative degradation. Ito and Nagai (2007) carried out a laboratory study with artificial aging tests, using two instruments. One of these involved simultaneous testing with a xenon lamp and cyclic spray of the distilled water. The surface observations by SEM are very similar to those

obtained in this study. In fact, as a result of aging, voids are visible. They argue that the voids are caused by the solubilization of inorganic components (plasticizer), mainly calcium carbonate, which are added to improve the basic properties of PVC, such as impact resistance (Gilbert and Patrick, 2017).

In the river environment, although ANOVA identified different trends in the degradation rates among the types of plastic, the differences were not so significant.

Dissolutions and leaching tests were performed to evaluate whether the plastics with the relative accumulated fouling could adsorb any inorganic compounds from the surrounding environment, as happens with organic contaminants (Mato et al., 2001; Endo et al., 2005; Ogata et al., 2009), and if, in case of imbalance with a new environment, they could release them again. However, these only highlighted that the plastics retained mainly sediments and ions characteristic of the exposure environment. In fact, by comparing the dissolutions of the plastics with those of the sediments collected in the tested environments, the results showed that the chemical composition between the two is very similar. The leaching tests on the plastic strips have brought to the leachate above all bicarbonate and calcium ions for the plastics exposed in the river environment, and chloride and sodium ions for the plastics exposed in the lagoon and port environment. These ions are characteristic of the geological environment of the test sites and of the waters with which the plastics have been in contact. Dissolution and leaching tests therefore did not yield relevant results.

The degradation therefore showed different characters based on the environment, the type of plastic and the exposure time. In addition, several laboratory studies analyzing the individual factors that cause degradation of certain types of plastics have been confirmed. However, the importance of field experiments is highlighted, which allow us to deepen and understand the interactions between the various factors that influence degradation.

Conclusion

Accumulating evidence is identifying that the coastal zone is a region of particular importance for the accumulation and degradation of plastic debris. But it has not yet been clarified how the environment and environmental factors, in different climatic and geological conditions, affect the degradation of plastics.

For this reason, the study aimed to advance current knowledge on the degradation of the six most commonly used types of plastics, polystyrene (PS), polypropylene (PP), high density polyethylene (HDPE), low density polyethylene (LDPE), polyethylene terephthalate (PET) and polyvinyl chloride (PVC), in a coastal environment.

The degradation of these types of plastic was then tested in different coastal environments by investigating the possible responsible factors and a comparison was provided, through an isochronous exposure, between a lagoon environment, a port environment, a river environment near the mouth and an urban air environment. The degradation was quantified as change in mass following fouling removal and by examination of the polymer surface with scanning electron microscopy.

The following conclusions were drawn from this study:

1. The degradation of plastic is strongly affected by the exposure environment. In fact, the rate of degradation is higher in the air environment than in the aquatic environment and among the aquatic environments tested in this study, the one that caused the greatest degradation is the port one, followed by the lagoon one and finally the river one.
2. The rate of degradation during environmental exposure differs between types of plastics. PS was the most prone to degradation in all environments. In the air environment, there was greater degradation for PP, PET and PVC plastics and minimal degradation for LDPE and HDPE. In the aquatic environment, on the other hand, there was a greater degradation for PET and PVC and gradually decreasing for LDPE, HDPE, and PP.

3. The degree of degradation of the plastic is influenced by the exposure time; the longer the exposure of plastics in the environment lasts, the more mass loss and an increase in degradation found through the SEM images has been recorded.
4. The degradation rate of plastic is affected by the depth of the water. In the intertidal/semi-floating zone, in fact, a greater degradation was found compared to the subtidal/submerged zone.
5. The fouling that accumulates on the plastic negatively affects the deterioration of the polymers. In fact, it plays a photo-protective role by shielding the plastic from UV radiation, which has been found to be the most responsible factor for degradation.

However, it is not excluded that, even if only one of the conditions that occurred during the experiment varied, the result could have changed, due to the potential non-linear interaction of the various factors.

References

ACS.org. American Chemical Society National Historic Chemical Landmarks. Foundations of Polymer Science: Wallace Hume Carothers and the Development of Nylon. https://www.acs.org/content/acs/en/education/whatischemistry/landmarks/carotherspolymers.html

Akdogan, Z., and Guven, B., 2019. Microplastics in the environment: a critical review of current understanding and identification of future research needs. Environmental Pollution 254 (A): 113011. https://doi.org/10.1016/j.envpol.2019.113011

Albertsson, A.C., and Karlsson, S., 1993. Aspects of Biodeterioration of Inert and Degradable Polymers. International Biodeterioration & Biodegradation, 31(3): 161-170. https://doi.org/10.1016/0964-8305(93)90002-J

Amaral-Zettler, L.A., Zettler, E.R., and Mincer, T.J., 2020. Ecology of the plastisphere. Nature Reviews Microbiology, **18:** 139-151. https://doi.org/10.1038/s41579-019-0308-0

Amato, I., 1999. "Time 100: Leo Baekeland". https://web.archive.org/web/20000407201944/http://www.time.com/time/time100/scientist/profile/baekeland.html

Ammala, A., Bateman, S., Dean, K., Petinakis, E., Sangwan, P., Wong, S., Yuan, Q., Yu, L., Patrick, C., and Leong, K.H., 2011. An overview of degradable and biodegradable polyolefins. Progress in Polymer Science, 36 (8): 1015-1049. https://doi.org/10.1016/j.progpolymsci.2010.12.002

Andrady, A.L. 2011. Microplastics in the marine environment. Marine Pollution Bulletin 62 (8): 1596-1605. https://doi.org/10.1016/j.marpolbul.2011.05.030

Andrady, A.L., Pegram, J.E., Song, Y., 1993b. Studies on enhanced degradable plastics. II. Weathering of enhanced photodegradable polyethylenes under marine and freshwater floating exposure. Journal of environmental polymer degradation, 1: 117-126. https://doi.org/10.1007/BF01418205

Andrady, A.L., Pegram, J.E., Tropsha, Y., 1993a. Changes in carbonyl index and average molecular weight on embrittlement of enhanced-photodegradable polyethylene. Journal

of environmental polymer degradation, 1 (3): 171-179. https://doi.org/10.1007/BF01458025

Anfuso, G., Bolívar-Anillo, H.J., Asensio-Montesinos, F., Portantiolo Manzolli, R., Portz, L., Villate Daza, D.A., 2020. Beach litter distribution in Admiralty Bay, King George Island, Antarctica. Marine Pollution Bulletin, 160, 111657. https://doi.org/10.1016/j.marpolbul.2020.111657

Arias-Villamizar, C.A., and Vázquez-Morillas, A., 2018. Degradation of conventional and oxodegradable high density polyethylene in tropical aqueous and outdoor environments. Revista Internacional de Contaminacion Ambiental 34(1): 137-147. https://doi.org/10.20937/RICA.2018.34.01.12

Artham, T., and Doble, M., 2008. Biodegradation of aliphatic and aromatic polycarbonates. Macromolecular Bioscience, 8(1):14-24. https://doi.org/10.1002/mabi.200700106

Artham, T., Sudhakar, M., Venkatesan, R., Madhavan Nair, C., Murty, K.V.G.K., and Doble, M., 2009. Biofouling and stability of synthetic polymers in sea water. International Biodeterioration & Biodegradation, 63 (7): 884-890. https://doi.org/10.1016/j.ibiod.2009.03.003

Assobioplastiche.org http://assobioplastiche.org/mondo.html

ASTM, 2019. D883-19: Standard terminology relating to plastics. American Society for Testing and Materials International.

Athey, S.N., Albotra, S.D., Gordon, C.A., Monteleone, B., Seaton, P., Andrady, A.L., Taylor, A.R., Brander, S.M., 2020. Trophic transfer of microplastics in an estuarine food chain and the effects of a sorbed legacy pollutant. Limnology and Oceanography Letters, 5 (1): 154-162. https://doi.org/10.1002/lol2.10130

Bakir, A., Rowland, S.J., and Thompson, R.C., 2014. Enhanced desorption of persistent organic pollutants from microplastics under simulated physiological conditions. Environmental Pollution, 185: 16-23. https://doi.org/10.1016/j.envpol.2013.10.007

Barnes, D.K.A., Galgani, F., Thompson, R.C., and Barlaz, M., 2009. Accumulation and fragmentation of plastic debris in global environments. Philosophical Transactions of the Royal Society B: Biological Sciences, 364 (1526): 1985–1998. https://doi.org/10.1098/rstb.2008.0205

Bernardini, I., Garibaldi, F., Canesi, L., Fossi, M.C., Baini, M., 2018. First data on plastic ingestion by blue sharks (Prionace glauca) from the Ligurian Sea (North-Western Mediterranean Sea). Marine Pollution Bulletin, 135: 303-310. https://doi.org/10.1016/j.marpolbul.2018.07.022

Bezzi, A., Casagrande, G., Martinucci, D., Pillon, S., Del Grande, C., and Fontolan, G., 2019. Modern sedimentary facies in a progradational barrier-spit system: Goro lagoon, Po delta, Italy. Estuarine, Coastal and Shelf Science, 227: 106323. https://doi.org/10.1016/j.ecss.2019.106323

Bianca, M., Monaco, C., Tortorici, L., and Cernobori, L., 1999. Quaternary normal faulting in southeastern Sicily (Italy): a seismic source for the 1693 large earthquake. Geophysical Journal International, 139 (2): 370-394. https://doi.org/10.1046/j.1365-246x.1999.00942.x

Biber, N.F.A., 2016. Plastic fragmentation in the environment. Doctor of Philosophy Thesis, School of Marine Science and Engineering, Plymouth University. http://hdl.handle.net/10026.1/6568

Biber, N.F.A., Foggo, A., and Thompson, R.C., 2019. Characterising the deterioration of different plastics in air and seawater. Marine Pollution Bulletin, 141: 595-602. https://doi.org/10.1016/j.marpolbul.2019.02.068

Bläsing, M., and Amelung, W., 2018. Plastics in soil: analytical methods and possible sources. Science of the Total Environment, 612: 422-435. https://doi.org/10.1016/j.scitotenv.2017.08.086

Bouhroum, R., Boulkamh, A., Asia, L., Lebarillier, S., Ter Halle, A., Syakti, A.D., Doumenq, P., Malleret, L., and Wong-Wah-chung, P., 2019. Concentrations and fingerprints of PAHs and PCBs adsorbed onto marine plastic debris from the Indonesian Cilacap coast and the North Atlantic gyre. Regional Studies in Marine Science, 29: 100611. https://doi.org/10.1016/j.rsma.2019.100611

Bowden, M.E., 1997. Chemical achievers: the human face of the chemical sciences. Chemical Heritage Foundation. ISBN 9780941901123.

Calderoni G., 1982. Regime anemologico nel Delta del Po alla foce dell'Adige. Vol. Annali dell'Università di Ferrara, 8: 61-69.

Carbone, S., Di Geronimo, I., Grasso, M., Iozzia, S., and Lentini F., 1982. I terrazzi marini quaternari dell'area iblea (Sicilia sud-orientale). Contributi conclusivi per la realizzazione della Carta Neotettonica d'Italia, Pubblicazione n. 506 del Progetto Finalizzato Geodinamica.

Carlisle, R.P., 2004. Scientific American Inventions and Discoveries: all the milestones in ingenuity from the discovery of fire to the invention of the microwave oven. John Wiley & Sons, Inc. ISBN 9780471244103

Carpenter, E.J., and Smith, K.L., 1972. Plastics on the Sargasso Sea surface. Science, 175 (4027): 1240–1241. https://doi.org/10.1126/science.175.4027.1240

Carpenter, E.J., Anderson, S.J., Harvey, G.R., Miklas, H.P., Peck, B.B., 1972. Polystyrene Spherules in Coastal Waters. Science, 178 (4062): 749–750. https://doi.org/10.1126/science.178.4062.749

Catalano, S., De Guidi, G., Romagnoli, G., Torrisi, S., Tortorici, G., and Tortorici, L., 2008. The migration of plate boundaries in SE Sicily: Influence on the large-scale kinematic model of the African promontory in southern Italy. Tectonophysics, 449, 41–62. https://doi.org/10.1016/j.tecto.2007.12.003

Catalano, S., Romagnoli, G., and Tortorici, G., 2010. Kinematics and dynamics of the late quaternary rift-flank deformation in the Hyblean Plateau (SE Sicily). Tectonophysics, 486 (1-4): 1-14. https://doi.org/10.1016/j.tecto.2010.01.013

Chae, Y., Kim, D., Kim, S.W., and An, Y.L., 2018. Trophic transfer and individual impact of nano-sized polystyrene in a four-species freshwater food chain. Scientific Reports, 8: 284. https://doi.org/10.1038/s41598-017-18849-y

Chamas, A., Moon, H., Zheng, J., Qiu, Y., Tabassum, T., Jang, J.H., Abu-Omar, M., Scott, S.L., and Suh, S., 2020. Degradation Rates of Plastics in the Environment. ACS Sustainable Chemistry & Engineering, 8 (9): 3494-3511. https://doi.org/10.1021/acssuschemeng.9b06635

Chiellini, E., Corti, A., D'Antone, S., and Baciu, R., 2006. Oxo-biodegradable carbon backbone polymers – Oxidative degradation of polyethylene under accelerated test conditions. Polymer Degradation and Stability, 91 (11): 2739-2747. https://doi.org/10.1016/j.polymdegradstab.2006.03.022

Ciavola, P., Gonella, M., Tessari, U., and Zamariolo, A., 2000. Contributo alla conoscenza del clima meteomarino della Sacca di Goro: misure correntometriche e mareografiche. Studi Costieri, 2: 153-173.

Cole, M., Lindeque, P., Halsband, C., and Galloway, T.S. 2011. Microplastics as contaminants in the marine environment: A review. Marine Pollution Bulletin, 62 (12): 2588-2597. https://doi.org/10.1016/j.marpolbul.2011.09.025

Colton, J.B., Burns, B.R., and Knapp, F.D., 1974. Plastic particles in surface waters of the northwestern Atlantic: The abundance, distribution, source, and significance of various types of plastics are discussed. Science 185 (4150): 491–497. https://doi.org/10.1126/science.185.4150.491

Compa, M., Alomar, C., Mourre, B., March, D., Tintoré, J., Deudero, S., 2020. Nearshore spatio-temporal sea surface trawls of plastic debris in the Balearic Islands. Marine Environmental Research, 158: 104945. https://doi.org/10.1016/j.marenvres.2020.104945.

Corepla.it http://www.corepla.it/la-storia-della-plastica#

Costa, M.F., Ivar Do Sul, J.A., Silva-Cavalcanti, J.S., Araújo, M.C.B., Spengler, Â., Tourinho, P.S., 2010. On the importance of size of plastic fragments and pellets on the strandline: a snapshot of a Brazilian beach. Environmental Monitoring and Assessment, 168: 299-304. https://doi.org/10.1007/s10661-009-1113-4

Courtene-Jones, W., Quinn, B., Ewins, C., Gary, S.F., and Narayanaswamy, B.E., 2020. Microplastic accumulation in deep-sea sediments from the Rockall trough. Marine Pollution Bulletin, 154: 111092. https://doi.org/10.1016/j.marpolbul.2020.111092

Craig, I.H., White, J.R., Shyichuk, A.V., and Syrotynska, I., 2005. Photo-induced scission and crosslinking in LDPE, LLDPE, and HDPE. Polymer engineering and science, 45 (4): 579-587. https://doi.org/10.1002/pen.20313

Dal Cin, R., 1983. I litorali del Delta del Po e alle foci dell'Adige e del Brenta: caratteri tessiturali e dispersione dei sedimenti, cause dell'arretramento e previsioni sull'evoluzione futura. Bollettino della Società Geologica Italiana, 102: 9-56.

Dal Cin, R., 1994. Lo Scannone di Goro nel Delta del Po: evoluzione morfologica e possibili interventi per conservare l'ambiente della laguna retrostante. Sacca di Goro: studio integrato sull'ecologia: 291-303, Ed. Franco Angeli. ISBN 978-8820481964

Dal Cin, R., and Pambianchi, P., 1991. I sedimenti della Sacca di Goro (Delta del Po). Sacca di Goro: studio integrato sull'ecologia: 253-263, Ed. Franco Angeli. ISBN 978-8820481964.

Del Grande, C., Gabbianelli, G., and Simeoni, U., 1997. Lineamenti evolutivi della moderna Sacca di Goro (Delta del Po). Atti 1° Forum Italiano di Scienze della Terra: 234-235, Bellaria.

Dewey, J.F., Helman, M.L., Knott, S.D., Turco, E., and Hutton, D.H.W., 1989. Kinematics of the western Mediterranean. Geological Society, London, Special Publications, 45 (1): 265-283. http://doi.org/10.1144/GSL.SP.1989.045.01.15

Di Grande, A., and Raimondo, W., 1982. Linee di costa plio-pleistoceniche e schema litostratigrafico del Quaternario siracusano, Geologica Romana, 21: 279-309.

Di Grande, A., Romeo, M., and Raimondo, W., 1982. Il Membro di Gaetanì ed il Membro di Buscemi della Formazione Palazzolo: Facies, distribuzione ed età. Bollettino Della Società Geologica Italiana, 101 (3): 343-372.

Di Stefano, A., 1995. Biostratigrafia a nannofossili calcarei dei sedimenti medio-supramiocenici del settore occidentale del Plateau Ibleo (Sicilia sud-orientale). Bollettino della Società Paleontologica Italiana, 34, 147-162.

EN 13432:2000, Packaging - Requirements for packaging recoverable through composting and biodegradation - Test scheme and evaluation criteria for the final acceptance of packaging.

Endo, S., Takizawa, R., Okuda, K., Takada, H., Chiba, K., Kanehiro, H., Ogi, H., Yamashita, R., and Date, T., 2005. Concentration of polychlorinated biphenyls (PCBs) in beached resin pellets: Variability among individual particles and regional differences. Marine Pollution Bulletin, 50 (10): 1103-1114. https://doi.org/10.1016/j.marpolbul.2005.04.030

Eriksen, M., Mason, S., Wilson, S., Box, C., Zellers, A., Edwards, W., Farley, H., and Amato, S., 2013. Microplastic pollution in the surface waters of the Laurentian great lakes. Marine Pollution Bulletin, 77 (1–2): 177-182. https://doi.org/10.1016/j.marpolbul.2013.10.007

European-bioplastics.org https://www.european-bioplastics.org/bioplastics/

Feldman, D., 2008. Polymer History. Designed Monomers and Polymers 11 (1): 1–15. https://doi.org/10.1163/156855508X292383

Fontolan, G., Covelli, S., Bezzi, A., Tesolin, V., and Simeoni, U., 2000. Stratigrafia dei depositi recenti della Sacca di Goro. Studi Costieri, 2: 65-79.

Free, C.M., Jensen, O.P., Mason, S.A., Eriksen, M., Williamson, N.J., Boldgiv, B., 2014. High-levels of microplastic pollution in a large, remote, mountain lake. Marine Pollution Bulletin, 85 (1): 156-163. https://doi.org/10.1016/j.marpolbul.2014.06.001

Gabbianelli, G., Del Grande, C., Simeoni, U., Zamariolo, A., and Calderoni, G., 2000. Evoluzione dell'area di Goro negli ultimi cinque secoli (Delta del Po). Studi costieri, 2: 45-63.

Garcés-Ordóñez, O., Espinosa, L.F., Cardoso, R.P., Issa Cardozo, B.B., Meigikos dos Anjos, R., 2020. Plastic litter pollution along sandy beaches in the Caribbean and Pacific coast of Colombia. Environmental Pollution, 267: 115495. https://doi.org/10.1016/j.envpol.2020.115495

Gardette, M., Perthue, A., Gardette, J.L., Janecska, T., Földes, E., Pukánszky, B., and Therias, S., 2013. Photo- and thermal-oxidation of polyethylene: Comparison of mechanisms and influence of unsaturation content. Polymer Degradation and Stability, 98 (11): 2383-2390. https://doi.org/10.1016/j.polymdegradstab.2013.07.017

Gasperi, J., Dris, R., Bonin, T., Rocher, V., and Tassin, B., 2014. Assessment of floating plastic debris in surface water along the Seine River. Environmental Pollution, 195: 163–166. https://doi.org/10.1016/j.envpol.2014.09.001

Gerritse, J., Leslie, H.A., de Tender, C.A., Devriese, L.I., and Vethaak, A.D., 2020. Fragmentation of plastic objects in a laboratory seawater microcosm. Scientific Reports, 10: 10945. https://doi.org/10.1038/s41598-020-67927-1

GESAMP, 2015. Sources, fate and effects of microplastics in the marine environment: a global assessment (Kershaw, P. J., ed.). (IMO/FAO/UNESCO-IOC/UNIDO/WMO/IAEA/UN/UNEP/UNDP Joint Group of Experts on the Scientific Aspects of Marine Environmental Protection). Reports and Studies GESAMP No. 90, 96 p. ISSN: 1020-4873

Gewert, B., Plassmann, M.M., and MacLeod, M., 2015. Pathways for degradation of plastic polymers floating in the marine environment. Environmental Science: Processes & Impacts, 17 (9): 1513-1521. https://doi.org/10.1039/C5EM00207A

Geyer, R., Jambeck, J.R., and Law, K.L., 2017. Production, use, and fate of all plastics ever made. Science Advances, 3 (7), e1700782. https://doi.org/10.1126/sciadv.1700782

Ghisetti, F., and Vezzani, L., 1980. The structural features of the Iblean Plateau and of the Mount Judica area (Southeastern Sicily); A microtectonic contribution to the deformational history of the Calabrian Arc. Italian Journal of Geosciences, 99 (1-2): 57-102.

Gigault, J., Halle, A.T., Baudrimont, M., Pascal, P.Y., Gauffre, F., Phi, T.L., El Hadri, H., Grassl, B., and Reynaud, S., 2018. Current opinion: What is a nanoplastic? Environmental Pollution, 235: 1030-1034. https://doi.org/10.1016/j.envpol.2018.01.024

Gijsman, P., Meijers, G., and Vitarelli, G., 1999. Comparison of the UV-degradation chemistry of polypropylene, polyethylene, polyamide 6 and polybutylene terephthalate. Polymer Degradation and Stability, 65 (3): 433-441. https://doi.org/10.1016/S0141-3910(99)00033-6

Gilbert, M., and Patrick, S., 2017. Chapter 13 - Poly(Vinyl Chloride). Brydson's Plastics Materials (Eighth Edition): 329-388. https://doi.org/10.1016/B978-0-323-35824-8.00013-X

Grasso, M., and Lentini, F., 1982. Sedimentary and tectonic evolution of the eastern Hyblean Plateau (Southeast Sicily) during Late Cretaceous to Quaternary time. Paleogeography, Paleoclimatology, Palaeoecology, 39 (3-4): 261-280. https://doi.org/10.1016/0031-0182(82)90025-6

Grasso, M., and Reuther, C.D., 1988. The western margin of the Hyblean Plateau: A neotectonic transform system on the SE Sicilian foreland. Annales Tectonicae, 2(2): 107-120.

Gu, J.D., 2003. Microbiological deterioration and degradation of synthetic polymeric materials: recent research advances. International Biodeterioration & Biodegradation, 52 (2): 69-91. https://doi.org/10.1016/S0964-8305(02)00177-4

Gulmine, J.V., Janissek, P.R., Heise, H.M., and Akcelrud, L., 2003. Degradation profile of polyethylene after artificial accelerated weathering. Polymer Degradation and Stability, 79 (3): 385-397. https://doi.org/10.1016/S0141-3910(02)00338-5

Gündoğdu, S., Çevik, C., and Karaca, S., 2017. Fouling assemblage of benthic plastic debris collected from Mersin Bay, NE Levantine coast of Turkey. Marine Pollution Bulletin, 124 (1): 147-154. https://doi.org/10.1016/j.marpolbul.2017.07.023

Hepburn, C., 1992. Polyurethane Elastomers, 2nd edition. Elsevier Applied Science. ISBN 978-1851665891

Ho, N.H.E., and Not, C., 2019. Selective accumulation of plastic debris at the breaking wave area of coastal waters. Environmental Pollution, 245: 702-710. https://doi.org/10.1016/j.envpol.2018.11.041

IDROSER, Idrorisorse per lo sviluppo dell'Emilia-Romagna, 1984. Piano progettuale per la difesa della costa Adriatica, Emiliano-Romagnola, pp. 636.

IDROSER, Idrorisorse per lo sviluppo dell'Emilia-Romagna, 1996. Progetto di Piano per la Difesa dal Mare e Riqualificazione Ambientale del Litorale della Regione Emilia-Romagna. Relazione Generale, pp. 365.

Im, J., Joo, S., Lee, Y., Kim, B.Y., and Kim, T., 2020. First record of plastic debris ingestion by a fin whale (Balaenoptera physalus) in the sea off East Asia. Marine Pollution Bulletin, 159: 111514. https://doi.org/10.1016/j.marpolbul.2020.111514

International Association of Plastics Distributors. "Amorphous and Semi-Crystalline Engineering Thermoplastics, Module 4". Basic Plastics Education tutorials. International Association of Plastics Distributors. IAPD Education Committee https://www.google.com/url?sa=t&rct=j&q=&esrc=s&source=web&cd=&cad=rja&uact=8&ved=2ahUKEwj51_zotbP0AhU4hv0HHZC9CqwQFnoECAkQAQ&url=https%3A%2F%2Fwww.modernplastics.com%2Fwp-content%2Fuploads%2F2015%2F03%2Fmodule4.ppt&usg=AOvVaw0lOYYC-ji3tYTZJSPl14_e

ISO, 2013. EN ISO 472:2013 Plastics – Vocabulary. International Organization for Standardization.

Ito, M., and Nagai, K., 2007. Analysis of degradation mechanism of plasticized PVC under artificial aging conditions. Polymer degradation and stability, 92 (2): 260-270. https://doi.org/10.1016/j.polymdegradstab.2006.11.003

Jensen, W.B., 2008. The Origin of the Polymer Concept. Journal of Chemical Education, 85 (5): 624. https://doi.org/10.1021/ed085p624.

Kaczmarek, H., Bajer, K., Galka, P., and Kotnowska, B., 2007. Photodegradation studies of novel biodegradable blends based on poly(ethylene oxide) and pectin. Polymer Degradation and Stability, 92(11): 2058-2069. https://doi.org/10.1016/j.polymdegradstab.2007.07.019

Karkanorachaki, K., Syranidou, E., and Kalogerakis, N., 2021. Sinking characteristics of microplastics in the marine environment. Science of The Total Environment, 793: 148526. https://doi.org/10.1016/j.scitotenv.2021.148526

Katija, K., Choy, C.A., Sherlock, R.E., Sherman, A.D., Robison, B.H., 2017. From the surface to the seafloor: How giant larvaceans transport microplastics into the deep sea. Science Advances, 3 (8). https://doi.org/10.1126/sciadv.1700715

Kijchavengkul, T., Auras, R., Rubino, M., Alvarado, E., Camacho Montero, J.R., and Rosales, J.M., 2010. Atmospheric and soil degradation of aliphatic–aromatic polyester films. Polymer Degradation and Stability, 95 (2): 99-107. https://doi.org/10.1016/j.polymdegradstab.2009.11.048

Klempner, D., and Frish K. C., 1991. Handbook of polymeric foams and foam technology. Hanser Publishers. ISBN 978-3446150973

Koelmans, A.A., Besseling, E., Foekema, E., Kooi, M., Mintenig, S., Ossendorp, B.C., Redondo-Hasselerharm, P.E., Verschoor, A., van Wezel, A.P., and Scheffer, M., 2017. Risks of plastic debris: unravelling fact, opinion, perception, and belief. Environtal Science & Technology, 51 (20): 11513–11519. https://doi.org/10.1021/acs.est.7b02219

Krause, S., Molari, M., Gorb, E.V., Kossel, E., and Haeckel, M., 2020. Persistence of plastic debris and its colonization by bacterial communities after two decades on the abyssal seafloor. Scientific Reports, 10, 9484. https://doi.org/10.1038/s41598-020-66361-7

Krueger, M.C., Harms, H., and Schlosser, D., 2015. Prospects for microbiological solutions to environmental pollution with plastics. Applied Microbiology and Biotechnology, 99: 8857-8874. https://doi.org/10.1007/s00253-015-6879-4

Krzan, A., Hemjinda, S., Miertus, S., Corti, A., and Chiellini, E., 2006. Standardization and certification in the area of environmentally degradable plastics. Polymer Degradation and Stability, 91 (12): 2819-2833. https://doi.org/10.1016/j.polymdegradstab.2006.04.034

Kühn, S., van Franeker, J.A., O'Donoghue, A.M., Swiers, A., Starkenburg, M., van Werven, B., Foekema, E., Hermsen, E., Egelkraut-Holtus, M., and Lindeboom, H., 2020. Details of plastic ingestion and fiber contamination in North Sea fishes. Environmental Pollution, 257: 113569. https://doi.org/10.1016/j.envpol.2019.113569

Lambert, S., Sinclair, C., and Boxall, A., 2014. Occurrence, degradation, and effect of polymer-based materials in the environment. Reviews of Environmental Contamination and Toxicology, 227: 1-53. https://doi.org/10.1007/978-3-319-01327-5_1

Lambetti, P., 1998. Opere di Somma urgenza per la movimentazione naturale delle acque all'interno della Sacca di Goro. Progetto esecutivo: relazione idraulica. Amm. Provinciale di Ferrara.

Lechner, A., Keckeis, H., Lumesberger-Loisl, F., Zens, B., Krusch, R., Tritthart, M., Glas, M., and Schludermann, E., 2014. The Danube so colourful: a potpourri of plastic litter outnumbers fish larvae in Europe's second largest river. Environmental Pollution, 188: 177-181. https://doi.org/10.1016/j.envpol.2014.02.006

Lee, J., Hong, S., Song, Y.K., Hong, S.H., Jang, Y.C., Jang, M., Heo, N.W., Han, G.M., Lee, M.J., Kang, D., and Shim, W.J., 2013. Relationships among the abundances of plastic debris in different size classes on beaches in South Korea. Marine Pollution Bulletin, 77 (1-2): 349-354. https://doi.org/10.1016/j.marpolbul.2013.08.013

Lentini, F., Carbone, S., and Catalano, S., 1994. Main structural domains of the central Mediterranean region and their Neogene tectonic evolution. Bollettino di Geofisica Teorica ed Applicata, 36: 141-144.

LIFE13 NAT/IT/000115, Final report, 2021. https://lifeagree.eu/wp-content/uploads/2021/07/LIFE_AGREE-Final-Report.pdf

Lorenzen, C.J., 1967. Determination of chlorophyll and pheo-pigments: spectrophotometric equations. Limnology and Oceanography, 12 (2): 343-346. https://doi.org/10.4319/lo.1967.12.2.0343

Lucas, N., Bienaime, C., Belloy, C., Queneudec, M., Silvestre, F., and Nava-Saucedo, J.E., 2008. Polymer biodegradation: Mechanisms and estimation techniques – A review. Chemosphere, 73 (4): 429-442. https://doi.org/10.1016/j.chemosphere.2008.06.064

Lugauskas, A., Levinskaite, L., and Pečiulyte, D., 2003. Micromycetes as deterioration agents of polymeric materials. International Biodeterioration & Biodegradation, 52 (4): 233-242. https://doi.org/10.1016/S0964-8305(03)00110-0

Mancia, A., Chenet, T., Bono, G., Geraci, M.L., Vaccaro, C., Munari, C., Mistri, M., Cavazzini, A., and Pasti, L., 2020. Adverse effects of plastic ingestion on the Mediterranean small-spotted catshark (Scyliorhinus canicula). Marine Environmental Research, 155: 104876. https://doi.org/10.1016/j.marenvres.2020.104876

Marques, A.T., 2011. Fibrous materials reinforced composites production techniques. Fibrous and Composite Materials for Civil Engineering Applications, Woodhead Publishing Series in Textiles: 191-215. https://doi.org/10.1533/9780857095583.3.191

Mato, Y., Isobe, T., Takada, H., Kanehiro, K., Ohtake, C., and Kaminuma, T., 2001. Plastic Resin Pellets as a Transport Medium for Toxic Chemicals in the Marine Environment. Environmental Science & Technology, 35 (2): 318-324. https://doi.org/10.1021/es0010498

Min, K., Cuiffi, J.D. and Mathers, R.T., 2020. Ranking environmental degradation trends of plastic marine debris based on physical properties and molecular structure. Nature communications, 11:727. https://doi.org/10.1038/s41467-020-14538-z

Minambiente.it. Italian Ministry of the Environment site: https://www.minambiente.it/pagina/elenco-delle-zps

Moore, C.J., Moore, S.L., Leecaster, M.K., and Weisberg, S.B., 2001. A Comparison of Plastic and Plankton in the North Pacific Central Gyre. Marine Pollution Bulletin, 42 (12): 1297-1300. https://doi.org/10.1016/S0025-326X(01)00114-X

Musumeci, G., 1959. Rilevamento geologico delle tavolette 'Noto, Noto Antica e Avola' (F. 277, IV). Bollettino del Servizio Geologico d'Italia, 81(2-3): 371-402.

Nizzetto, L., Futter, M., and Langaas, S., 2016. Are agricultural soils dumps for microplastics of urban origin? Environmental Science & Technology, 50 (20): 10777–10779. https://doi.org/10.1021/acs.est.6b04140

Nowak, B., Pająk, J., Drozd-Bratkowicz, M., and Rymarz, G., 2011. Microorganisms participating in the biodegradation of modified polyethylene films in different soils under laboratory

conditions. International Biodeterioration & Biodegradation, 65 (6): 757-767. https://doi.org/10.1016/j.ibiod.2011.04.007

O'Brine, T., and Thompson, R.C., 2010. Degradation of plastic carrier bags in the marine environment. Marine Pollution Bulletin, 60 (12): 2279-2283, https://doi.org/10.1016/j.marpolbul.2010.08.005

Oertel, G., 1985. Polyurethane Handbook: Chemistry, Raw Materials, Processing, Application, Properties. 2nd edition, Hanser Publishers. ISBN 9783446171985

Ojeda, T., Freitas, A., Birck, K., Dalmolin, E., Jacques, R., Bento, F., and Camargo, F., 2011. Degradability of linear polyolefins under natural weathering. Polymer Degradation and Stability, 96 (4): 703-707. https://doi.org/10.1016/j.polymdegradstab.2010.12.004

Ogata, Y., Takada, H., Mizukawa, K., Hirai, H., Iwasa, S., Endo, S., Mato, Y., Saha, M., Okuda, K., Nakashima, A., Murakami, M., Zurcher, N., Booyatumanondo, R., Zakaria, M.P., Dung, L.Q., Gordon, M., Miguez, C., Suzuki, S., Moore, C., Karapanagioti, H.K., Weerts, S., McClurg, T., Burres, E., Smith, W., Velkenburg, M.V., Lang, J.S., Lang, R.C., Laursen, D., Danner, B., Stewardson, N., and Thompson, R.C., 2009. International Pellet Watch: Global monitoring of persistent organic pollutants (POPs) in coastal waters. 1. Initial phase data on PCBs, DDTs, and HCHs. Marine Pollution Bulletin, 58 (10): 1437-1446. https://doi.org/10.1016/j.marpolbul.2009.06.014

Osservatorio clima di Arpae, 2020. Rapporto IdroMeteoClima Emilia-Romagna Dati 2019. Centro Stampa della Regione Emilia-Romagna.

Painter, P.C., and Coleman, M.M., 2008. Essentials of Polymer Science and Engineering. DEStech Publications Inc. ISBN 9781932078756

Panzera, F., D'Amico, S., Lombardo, G., and Longo, E., 2016. Evaluation of building fundamental periods and effects of local geology on ground motion parameters in the Siracusa area, Italy. Journal of Seismology, 20: 1001-1019. https://doi.org/10.1007/s10950-016-9577-5

Pauli, N.C., Petermann, J.S., Lott, C., and Weber, M., 2017. Macrofouling communities and the degradation of plastic bags in the sea: an in situ experiment. Royal Society Open Science. https://doi.org/10.1098/rsos.170549

Pedley, H. M., 1981. Sedimentology and palaeoenvironment of the southeast Sicilian Tertiary platform carbonates. Sedimentary Geology, 28 (4): 273–291. https://doi.org/10.1016/0037-0738(81)90050-6

Pedley, H. M., Cugno, G., and Grasso, M., 1992. Gravity slide and resedimentation processes in a Miocene carbonate ramp, Hyblean Plateau, southeastern Sicily. Sedimentary Geology, 79 (1-4): 189-202. https://doi.org/10.1016/0037-0738(92)90011-F

Pedley, H. M., Grasso, M., Maniscalco, R., Bencke, B., Di Stefano, A., Giuffrida, S., and Sturiale, G., 2001. The sedimentology and Palaeoenvironment of quaternary temperate carbonates and their distribution around the northern Hyblean Mountains (SE Sicily). Italian journal of geosciences, 120 (2-3): 233-255.

Peeken, I., Primpke, S., Beyer, B., Gütermann, J., Katlein, C., Krumpen, T., Bergmann, M., Hehemann, L., and Gerdts, G., 2018. Arctic Sea ice is an important temporal sink and means of transport for microplastic. Nature Communication 9 (1): 1505. https://doi.org/10.1038/s41467-018-03825-5

Pegram, J.E., and Andrady, A.L., 1989. Outdoor weathering of selected polymeric materials under marine exposure conditions. Polymer degradation and stability, 26(4): 333-345. https://doi.org/10.1016/0141-3910(89)90112-2

Petry, M.V., Araújo, L.D., Brum, A.C., Benemann, V.R.F., and Finger, J.V.G., 2021. Plastic ingestion by juvenile green turtles (Chelonia mydas) off the coast of Southern Brazil. Marine Pollution Bulletin, 167: 112337. https://doi.org/10.1016/j.marpolbul.2021.112337

PlasticsEurope.org https://www.plasticseurope.org/en

PlasticsEurope, 2016. Plastics - The facts: an analysis of European plastics production, demand and waste data. https://plasticseurope.org/wp-content/uploads/2021/10/2016-Plastic-the-facts.pdf

Pojar, I., Kochleus, C., Dierkes, G., Ehlers, S.M., Reifferscheid, G., and Stock, F., 2020. Quantitative and qualitative evaluation of plastic particles in surface waters of the Western Black Sea. Environmental Pollution, 268 A: 115724. https://doi.org/10.1016/j.envpol.2020.115724

Regione Siciliana, 1998. Assessorato Agricoltura e Foreste Gruppo IV – Servizi allo Sviluppo, Unità di Agrometeorologia, 1998. Climatologia della Sicilia. http://www.sias.regione.sicilia.it/pdf/Climatologia_SR.pdf

Regione Siciliana, 2013. Microzonazione Sismica: Relazione Illustrativa MS livello 1. Università degli Studi di Messuna, C.A.R.E.C.I. - Centro Attrazione Risorse Esterne e Creazione d'Impresa. https://www.protezionecivilesicilia.it/tinymce/js/tinymce/source/rischio-sismico/ms_3907/SIRACUSA/SIRACUSA/Relazione%20illustrativa.pdf

Restrepo-Flórez, J.M., Bassi, A., and Thompson, M.R., 2014. Microbial degradation and deterioration of polyethylene – A review. International Biodeterioration & Biodegradation, 88: 83-90. https://doi.org/10.1016/j.ibiod.2013.12.014

Rigo, M., and Barbieri, F., 1959. Stratigrafia pratica applicata in Sicilia. Bollettino del Servizio Geologico d'Italia, 80: 351-441.

Rizzo, M., Corbau, C., Lane, B., Malkin, S.Y., Bezzi, V., Vaccaro, C., and Nardin, W., 2021. Examining the dependence of macroplastic fragmentation on coastal processes (Chesapeake Bay, Maryland). Marine Pollution Bulletin, 169: 112510. https://doi.org/10.1016/j.marpolbul.2021.112510

Rodriguez, F., Gent, A.N., Preston, J., Stevens, M.P., Bierwagen, G.P., and Kauffman, G.B., 2016. Major industrial polymers. Encyclopedia Britannica. https://www.britannica.com/topic/industrial-polymers-468698

Romagnoli, G., Catalano, S., Pavano, F., and Tortorici, G., 2015. Geological map of the Tellaro River Valley (Hyblean Foreland, southeastern Sicily, Italy). Journal of Maps, 11 (1): 66-74. https://doi.org/10.1080/17445647.2014.944878

Romeo, M., and Sciuto, F., 1987. Stratigrafia micropaleontologica delle successioni mioceniche dell'alta valle del Fiume Tellaro (Sicilia sud-orientale). Bollettino della Società Geologica Italiana, 38: 137-154.

Roure, F., Howel, D.G., Müller, C., and Moretti, I., 1990. Late Cenozoic subduction complex of Sicily. Journal of Structural Geology, 12 (2): 259-266. https://doi.org/10.1016/0191-8141(90)90009-N

Rowley, K.H., Cucknell, A.C., Smith, B.D., Clark, P.F., and Morritt, D., 2020. London's river of plastic: high levels of microplastics in the Thames water column. Science of the Total Environment, 740: 140018. https://doi.org/10.1016/j.scitotenv.2020.140018

Roy, P.K., Titus, S., Surekha, P., Tulsi, E., Deshmukh, C., and Rajagopal, C., 2008. Degradation of abiotically aged LDPE films containing pro-oxidant by bacterial consortium. Polymer Degradation and Stability, 93 (10): 1917-1922. https://doi.org/10.1016/j.polymdegradstab.2008.07.016

Sadri, S.S., and Thompson, R.C., 2014. On the quantity and composition of floating plastic debris entering and leaving the Tamar Estuary, Southwest England. Marine Pollution Bulletin, 81 (1): 55-60. https://doi.org/10.1016/j.marpolbul.2014.02.020

Scicchitano, G., and Monaco, C., 2006. Grotte carsiche e linee di costa sommerse tra Capo Santa Panagia e Ognina (Siracusa, Sicilia Sud-Orientale). Il Quaternario, Italian Journal of Quaternary Sciences, 19 (2): 187-194.

Scicchitano, G., Antonioli, F., Castagnino Berlinghieri, E.F., Dutton, A., and Monaco, C., 2008. Submerged archaeological sites along the Ionian coast of southeastern Sicily (Italy) and implications for the Holocene relative sea-level change. Quaternary Research, 70 (1): 26-39. http://doi.org/10.1016/j.yqres.2008.03.008

Sciencehistory.org. Wallace Hume Carothers. Science History Institute. https://www.sciencehistory.org/historical-profile/wallace-hume-carothers

Seymour, R.B., and Kauffman, G.B., 1992. Polyurethanes: A class of modern versatile materials. Journal of Chemical Education. 69 (11): 909. https://doi.org/10.1021/ed069p909

Shah, A.A., Hasan, F., Hameed, A., and Ahmed, S., 2008. Biological degradation of plastics: A comprehensive review. Biotechnology Advances, 26 (3): 246-265, et al, 2008. https://doi.org/10.1016/j.biotechadv.2007.12.005

Sharma, S., and Chatterjee, S., 2017. Microplastic pollution, a threat to marine ecosystem and human health: a short review. Environmental Science and Pollution Research 24: 21530-21547. https://doi.org/10.1007/s11356-017-9910-8

Simeoni U., Brunelli V., Broggio L., Corbau C., Tessari U., Utizi K., Atzeni P., Soldati M., and Letizia P., 2008. Studio sulla previsione dell'evoluzione morfodinamica dello Scanno e

delle bocche della Sacca di Goro. Rapporto Tecnico, Provincia di Ferrara, Maggio 2008, pp. 202.

Simeoni, U., Ciavola, P., Fontolan, G., Mazzini, E., and Tessari, U., 1998. Centennial evolution of recurved spit: a case study from the spit of Goro Lagoon Po Delta (Italy). CIESM Congress Proceeding, Dubrovnik (Croatia), 35: 100-101.

Simeoni, U., Fontolan, G., Ciavola, P., 2000. Morfodinamica delle bocche lagunari della Sacca di Goro. Studi Costieri, 2: 123-138.

Simeoni, U., Fontolan, G., Tessari, U., and Corbau, C., 2007. Domains of spit evolution in the Goro area, Po Delta, Italy. Geomorphology, 86 (3-4): 332-348. https://doi.org/10.1016/j.geomorph.2006.09.006

Staudinger, H., 1920. Über Polymerisation. Berichte der deutschen chemischen Gesellschaft (A and B Series). https://doi.org/10.1002/cber.19200530627.

Teuten, E.L., Rowland, S.J., Galloway, T.S., and Thompson, R.C., 2007. Potential for Plastics to Transport Hydrophobic Contaminants. Environmental Science & Technology, 41 (22): 7759-7764. https://doi.org/10.1021/es071737s

Thiel, M., Luna-Jorquera, G., Álvarez-Varas, R., Gallardo, C., Hinojosa, I.A., Luna, N., Miranda-Urbina, D., Morales, N., Ory, N., Pacheco, A.S., Portflitt-Toro, M., and Zavalaga, C., 2018. Impacts of marine plastic pollution from continental coasts to subtropical gyresdfish, seabirds, and other vertebrates in the SE Pacific. Frontiers in Marine Science, 5 (238). https://doi.org/10.3389/fmars.2018.00238

UK Patent office, 1865. Patents for inventions. Abridgments of Specifications relating to artificial leather, floorcloth, oilcloth, oilskin, and waterproof fabrics: 255.

UNEP, 2018. Single-use plastics: a roadmap for sustainability. ISBN: 978-92-807-3705-9 DTI/2179/JP.

UNI EN 13432:2002, Imballaggi - Requisiti per imballaggi recuperabili mediante compostaggio e biodegradazione - Schema di prova e criteri di valutazione per l'accettazione finale degli imballaggi.

Van Cauwenberghe, L., Vanreusel, A., Mees, J., and Janssen, C.R., 2013. Microplastic pollution in deep-sea sediments. Environmental Pollution, 182: 495-499. https://doi.org/10.1016/j.envpol.2013.08.013

Waller, C.L., Griffiths, H.J., Waluda, C.M., Thorpe, S.E., Loaiza, I., Moreno, B., Pacherres, C.O., and Hughes, K.A., 2017. Microplastics in the Antarctic marine system: an emerging area of research. Science of The Total Environment, 598: 220-227. https://doi.org/10.1016/j.scitotenv.2017.03.283

Wallström, S., Strömberg, E., and Karlsson, S., 2005. Microbiological growth testing of polymeric materials: an evaluation of new methods. Polymer Testing, 24 (5): 557-563. https://doi.org/10.1016/j.polymertesting.2005.02.005

Wei, R., and Zimmermann, W., 2017. Microbial enzymes for the recycling of recalcitrant petroleum-based plastics: how far are we? Microbial biotechnology, 10 (6): 1308-1322. https://doi.org/10.1111/1751-7915.12710

Whinfield, J.R., and Dickson, J.T., 1941. Improvements Relating to the Manufacture of Highly Polymeric Substances, British Patent 578 079, 1946; Polymeric Linear Terephthalic Esters, U.S. Patent 2,465,319, 1949.

Woodall, L.C., Sanchez-Vidal, A., Canals, M., Paterson, G.L.J., Coppock, R., Sleight, V., Calafat, A., Rogers, A.D., Narayanaswamy, B.E., and Thompson, R.C., 2014. The deep sea is a major sink for microplastic debris. Royal Society Open Science, 1: 140317. https://doi.org/10.1098/rsos.140317

Wright, S.L., and Kelly, F.J., 2017. Plastic and human health: a micro issue? Environmental Science & Technology, 51 (12): 6634-6647. https://doi.org/10.1021/acs.est.7b00423

Wyeth, N.C., and Roseveare, R., 1973. Biaxially Oriented Poly(ethylene terephthalate) Bottle. U.S. Patent 3733309A, 1973.

Ye, S., and Andrady, A.L., 1991. Fouling of floating plastic debris under Biscayne Bay exposure conditions. Marine Pollution Bulletin, 22 (12): 608-613. https://doi.org/10.1016/0025-326X(91)90249-R

Yousif, E., and Haddad, R., 2013. Photodegradation and photostabilization of polymers, especially polystyrene: review. SpringerPlus 2, 398. https://doi.org/10.1186/2193-1801-2-398

Zbyszewski, M., and Corcoran, P.L., 2011. Distribution and degradation of freshwater plastic particles along the beaches of Lake Huron, Canada. Water, Air, & Soil Pollution, 220: 365–372. https://doi.org/10.1007/s11270-011-0760-6

Zbyszewski, M., Corcoran, P.L., and Hockin, A., 2014. Comparison of the distribution and degradation of plastic debris along shorelines of the Great Lakes, North America. Journal of Great Lakes Research, 40 (2): 288-299. https://doi.org/10.1016/j.jglr.2014.02.012

Zhang, W., Zhang, S., Zhao, Q., Qu, L., Ma, D., and Wang, J., 2020. Spatio-temporal distribution of plastic and microplastic debris in the surface water of the Bohai Sea, China. Marine Pollution Bulletin, 158: 111343. https://doi.org/10.1016/j.marpolbul.2020.111343

Zhu, C., Li, D., Sun, Y., Zheng, X., Peng, X., Zheng, K., Hu, B., Luo, X., and Mai, B., 2019. Plastic debris in marine birds from an island located in the South China Sea. Marine Pollution Bulletin, 149: 110566. https://doi.org/10.1016/j.marpolbul.2019.110566

Appendix

EGU2020-7442
https://doi.org/10.5194/egusphere-egu2020-7442
EGU General Assembly 2020

Macro-plastic weathering in a coastal environment: field experiment in Chesapeake Bay, Maryland

Marzia Rizzo[1,2], Benjamin Lane[2,3], Sairah Malkin[2], Carmela Vaccaro[1], Umberto Simeoni[1], William Nardin[2], and Corinne Corbau[1,2]

[1]University of Ferrara, Department of Physics and Earth Science, Ferrara, Italy (rizzo.marzia.90@gmail.com)
[2]Horn Point Laboratory, University of Maryland Center for Environmental Science
[3]St. Olaf College

It is now widely recognized that marine plastics, which are strongly resistant to chemical and biological degradation, have become a widespread and massive pollutant in the world's oceans. Despite this resistance, in the environment, larger plastic items fragment and degrade into secondary microplastics which are ingestible by some marine organisms and are therefore a potential threat to aquatic foodwebs. The present study aims to better understand factors that contribute to the weathering of plastics in a coastal marine environment, where most microplastics appear to be generated.

Here we performed a field experiment to test the influence of different coastal conditions on macro-plastic weathering. Strips of commercial grade high-density polyethylene (HDPE) and polystyrene (PS) were mounted in replicate on racks (similar in appearance to keys on a glockenspiel, though all of the same length) and deployed at different treatment depths (subtidal versus intertidal) and different treatment hydrodynamic intensity zones (erosional versus depositional) in a sub-estuary of Chesapeake Bay (Maryland, USA). Strips were collected after environmental exposure of 4, 8 and 43 weeks and were analyzed for mass loss, surface chlorophyll accumulation, and surface appearance via SEM imaging.

We observed the PS strips degraded more quickly than the HDPE strips. The results show minor mass variation, in some samples even a slight mass increase, contrary to expectation. This was probably due to the deposition of clay and the presence of microorganisms into the microstructure of the strips, as observed by SEM. Moreover, the SEM images show different kind of fragmentation, with holes or with desquamations. The fragmentation was most marked for the PS strips located at intertidal depths caused by a more intense hydrodynamic energy. Finally, an increase over time was observed in the concentration of chlorophyll in both subtidal depositional PS strips and in subtidal erosional HDPE strips, associated with a lower hydrodynamic energy compared to the intertidal zones. This appears to confer a greater protection of the plastic which therefore undergoes less weathering.

Abstract 1: Abstract presented at EGU General Assembly 2020.

Interreg Italy - Croatia ECOMAP
EUROPEAN UNION
3rd International Congress
AGE OF NEW ECONOMY AND NEW JOBS - BLUE ECONOMY AND BLUE INNOVATION

Plastic weathering experiment in the Goro Lagoon, northern Adriatic (Italy)

RIZZO M.*, Corbau C., Vaccaro C.

University of Ferrara, Department of Physics and Earth Sciences, 44122 Ferrara, Italy
*e-mail address: marzia.rizzo@unife.it

Plastic, under the action of physical, chemical, and mechanical agents, weathers into smaller particles, that are called secondary microplastics if their dimensions are less than 5 mm. The most common environmental factors that cause weathering of plastics are photodegradation (action of sunlight), mechanical agents (such as abrasion, wave action and turbulence), biodegradation (action of living organisms), thermo-oxidative degradation (slow oxidative breakdown at moderate temperatures) and hydrolysis (reaction with water). Once the plastic has been embrittled due to photo-oxidation, mechanical processes can increase weathering processes. As a result, local environmental conditions such as sunlight, temperature, and oxygen play a critical role in determining the rate of the degradation of plastic, as do coastal processes such as waves and tides action, organic activity and sediment type. However, there is still a need to further understand the factors that regulate the weathering of plastics and their interconnection. Therefore, since the weathering rates of plastics depend on the environmental conditions and the plastic material (polymer), an experiment was performed to further analyze and eventually quantify the weathering, fragmentation and mineralization rates of six types of plastics in a lagoon environment.
In this study, the first preliminary results obtained in the test site of Goro Lagoon are presented. The Goro Lagoon covers an area of about 20 km^2, with an average depth of 1.5 m. The lagoon is separated from the sea by an 8 km long split, which is locally called “Scanno di Goro”. The delta area is characterized by a Mediterranean climate with some continental influence (wet Mediterranean climate). The tidal conditions are mainly semidiurnal (mean tidal range 0,8 m). The bottom of the lagoon presents a flat morphology and is characterized by alluvial sediments. Sand is more abundant near the southern shoreline, whilst sandy mud occurs in the eastern area. For this experiment, it was decided to use high-density polyethylene (HDPE), low-density polyethylene (LDPE), polypropylene (PP), polystyrene (PS), polyvinyl chloride (PVC), polyethylene terephthalate (PET), because results from several studies suggest the most common resins and fibers are HDPE, LDPE, PP, PS, PVC and PET and PUR resins. The design of the structures consists of plastic strips of 15 cm x 2.5 cm exposed to marine conditions, which were placed in such a way that one face is exposed to the sun and one in shadow/semi-darkness conditions. Each strip was anchored in the middle of two slats of raw fir wood measuring 3 cm x 4 cm x 2 m using steel nails with a diameter of 1.9 mm and a length of 5 cm. Once 20 slats with 10 samples of each type of plastics were ready (60 strips for each slat), they were mounted in two galvanized iron frames to group them into 10 frame strips utilizing galvanized bolts and nuts. The installation of the structures in the Goro Lagoon was carried out on 10 July 2020. Two structures were placed: one at intertidal depth and one at subtidal depth so that the intertidal structures are inundated for approximately 12 hours per day, while the subtidal slats are always inundated. Two HOBO sensors were also attached to the structures, one for each structure, to record the temperature and light intensity parameters to which the plastic strips were subjected. The samplings were initially scheduled every 4 weeks and then every 8 weeks. During every sampling, it has proceeded to the sampling of two slats, one intertidal and one subtidal, to the detection of the temperature data recorded by HOBO sensors, to the measurement of pH, conductivity, salinity and TDS through a multiparametric probe and to the sampling of sediment and water. Preliminary results of mass measurements highlight changes before and after exposure, which are related both to the deposition of biofilm and sediment on the strips and the degradation of plastics. Successively the strips will be also analyzed by using the following techniques:
• optical microscopy and scanning electron microscopy to observe the surface modification,
• micro-Raman spectroscopy to identify eventual changes in the spectra caused by the strip’s exposure to environmental conditions,
• UV-Vis spectrophotometry to quantify the concentration of chlorophyll in the biofilm deposited on the strips,
• leaching tests to determine the potential release of pollutants.

Keywords: plastic weathering, environmental conditions, experiment, intertidal depth, subtidal depth, Goro Lagoon

Abstract 2: Abstract presented at the 3rd International Congress - Age of New Economy and New Jobs - Blue Economy and Blue Innovation.

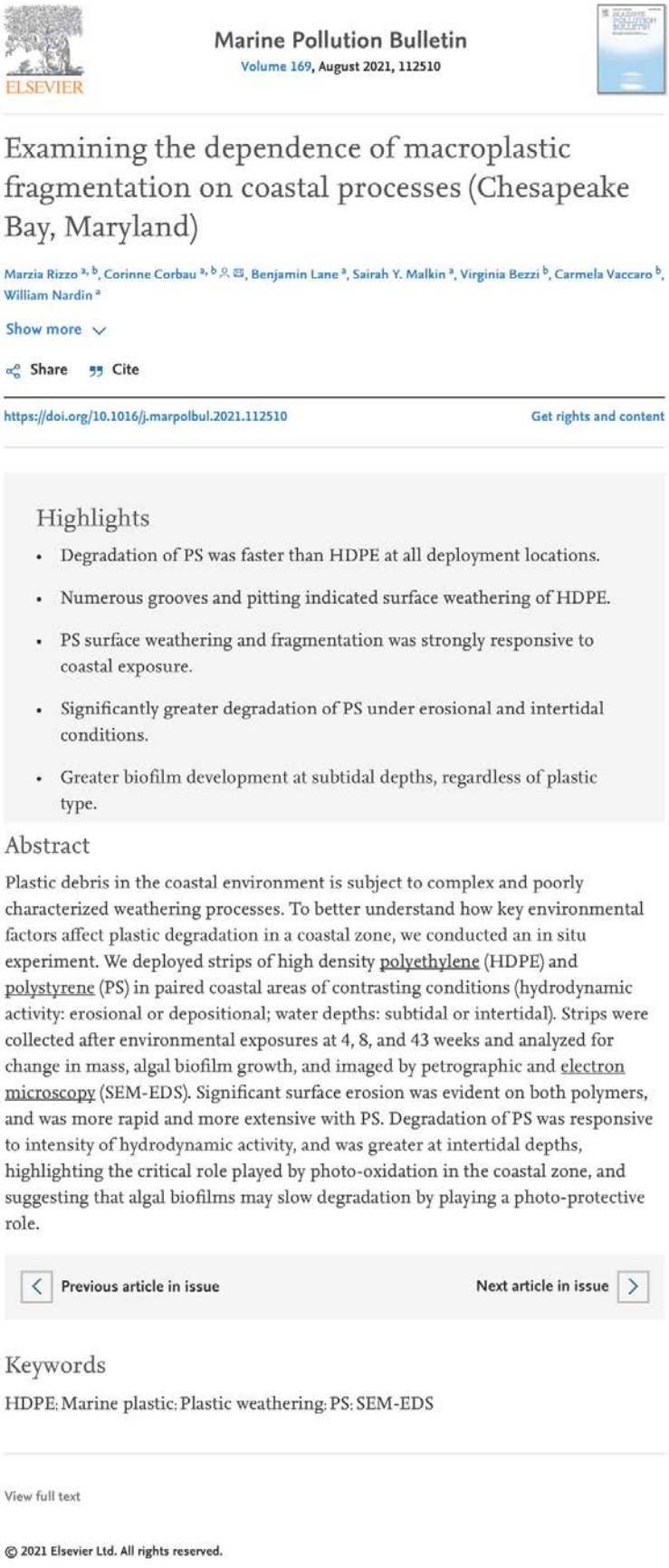

Marine Pollution Bulletin
Volume 169, August 2021, 112510

Examining the dependence of macroplastic fragmentation on coastal processes (Chesapeake Bay, Maryland)

Marzia Rizzo [a, b], Corinne Corbau [a, b], Benjamin Lane [a], Sairah Y. Malkin [a], Virginia Bezzi [b], Carmela Vaccaro [b], William Nardin [a]

Show more

Share Cite

https://doi.org/10.1016/j.marpolbul.2021.112510

Get rights and content

Highlights

- Degradation of PS was faster than HDPE at all deployment locations.
- Numerous grooves and pitting indicated surface weathering of HDPE.
- PS surface weathering and fragmentation was strongly responsive to coastal exposure.
- Significantly greater degradation of PS under erosional and intertidal conditions.
- Greater biofilm development at subtidal depths, regardless of plastic type.

Abstract

Plastic debris in the coastal environment is subject to complex and poorly characterized weathering processes. To better understand how key environmental factors affect plastic degradation in a coastal zone, we conducted an in situ experiment. We deployed strips of high density polyethylene (HDPE) and polystyrene (PS) in paired coastal areas of contrasting conditions (hydrodynamic activity: erosional or depositional; water depths: subtidal or intertidal). Strips were collected after environmental exposures at 4, 8, and 43 weeks and analyzed for change in mass, algal biofilm growth, and imaged by petrographic and electron microscopy (SEM-EDS). Significant surface erosion was evident on both polymers, and was more rapid and more extensive with PS. Degradation of PS was responsive to intensity of hydrodynamic activity, and was greater at intertidal depths, highlighting the critical role played by photo-oxidation in the coastal zone, and suggesting that algal biofilms may slow degradation by playing a photo-protective role.

Previous article in issue Next article in issue

Keywords

HDPE; Marine plastic; Plastic weathering; PS; SEM-EDS

View full text

Abstract 3: Paper published in Marine Pollution Bulletin.